

Comparison of Binary Sorption of Propane and N-Butane on 5A and 13X Zeolites

by

Esam-Al-Deen Zaki Hamad

A Thesis Presented to the

FACULTY OF THE COLLEGE OF GRADUATE STUDIES

KING FAHD UNIVERSITY OF PETROLEUM & MINERALS

DHAHRAN, SAUDI ARABIA

In Partial Fulfillment of the
Requirements for the Degree of

MASTER OF SCIENCE

In

CHEMICAL ENGINEERING

May, 1984

INFORMATION TO USERS

This manuscript has been reproduced from the microfilm master. UMI films the text directly from the original or copy submitted. Thus, some thesis and dissertation copies are in typewriter face, while others may be from any type of computer printer.

The quality of this reproduction is dependent upon the quality of the copy submitted. Broken or indistinct print, colored or poor quality illustrations and photographs, print bleedthrough, substandard margins, and improper alignment can adversely affect reproduction.

In the unlikely event that the author did not send UMI a complete manuscript and there are missing pages, these will be noted. Also, if unauthorized copyright material had to be removed, a note will indicate the deletion.

Oversize materials (e.g., maps, drawings, charts) are reproduced by sectioning the original, beginning at the upper left-hand corner and continuing from left to right in equal sections with small overlaps. Each original is also photographed in one exposure and is included in reduced form at the back of the book.

Photographs included in the original manuscript have been reproduced xerographically in this copy. Higher quality 6" x 9" black and white photographic prints are available for any photographs or illustrations appearing in this copy for an additional charge. Contact UMI directly to order.

U·M·I

University Microfilms International
A Bell & Howell Information Company
300 North Zeeb Road, Ann Arbor, MI 48106-1346 USA
313/761-4700 800/521-0600

Order Number 1355755

**Comparison of binary sorption of propane and n-butane on 5A
and 13X zeolites**

Hamad, Esam-al-Deen Zaki, M.S.

King Fahd University of Petroleum and Minerals (Saudi Arabia), 1984

U·M·I
300 N. Zeeb Rd.
Ann Arbor, MI 48106

COMPARISON OF BINARY SORPTION OF PROPANE AND N-BUTANE
ON 5A AND 13X ZEOLITES

A Thesis Presented to the
FACULTY OF THE GRADUATE SCHOOL
UNIVERSITY OF PETROLEUM & MINERALS
DHAHRAN, SAUDI ARABIA

In Partial Fulfillment of the
Requirements for the Degree
MASTER OF SCIENCE IN CHEMICAL ENGINEERING

by

ESAM-AL-DEEN ZAKI HAMAD

The Library
University of Petroleum & Minerals
Dahran, Saudi Arabia


MAY 1984

UNIVERSITY OF PETROLEUM AND MINERALS

DHAHRAN, SAUDI ARABIA

THE GRADUATE SCHOOL

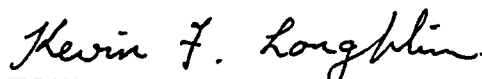
This thesis, written by Esam-Al-Deen Zaki Hamad under the direction of his Thesis Committee, and approved by all its members, has been presented to and accepted by the Dean of the Graduate School, in partial fulfillment of the requirements for the degree of MASTER OF SCIENCE IN CHEMICAL ENGINEERING

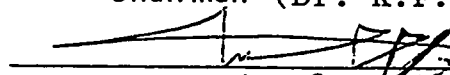

Dean of the Graduate School


Date 9-04/2012


Department Chairman

Thesis Committee


Chairman (Dr. K.F. Loughlin)


Member (Dr. M.A. Hasanain)


Member (Dr. S. Gultekin)

To my parents and my wife

ACKNOWLEDGMENTS

Acknowledgment is due to the University of Petroleum and Minerals for support of this research. I wish to express my appreciation to Dr. K. Loughlin who served as my major advisor. I also wish to thank the other members of my Thesis Committee, Dr. M. Hasanain and Dr. S. Gultekin.

I would like to thank Chemical Engineering Department faculty, staff and technicians particularly Mr. Peter McQue.

My special gratitude to my parents, brothers, sisters and wife whose love and affection is the source of inspiration and encouragement for my studies. I also wish to express my thanks to my friends whose company greatly assisted me throughout my studies.

CONTENTS

<i>Abstract</i>	xii
 <i>Chapter I: INTRODUCTION</i>	 1
Separation By Sorption	1
Zeolite Molecular Sieves	2
Structure And Composition Of Zeolites	4
Scope Of The Present Study	6
 <i>Chapter II: LITERATURE SURVEY</i>	 14
Adsorption Of Binary Mixtures On Zeolites	14
Isotherm Equations	17
Introduction	17
Simple Model Isotherm Equations	19
Henry's Law	19
Freundlich Isotherm	20
Langmuir Model	20
Mobile Adsorbed Phase Film Models	21
Brunauer, Emmet and Teller (B.E.T.) Isotherm	22
Statistical Thermodynamic Formulation	22
Ruthven Isotherm	25
Schirmer Isotherm	26
Ideal Adsorption Solution Theory	27
Vacancy Solution Theory	30
 <i>Chapter III: APPARATUS AND PROCEDURE</i>	 38
Choice of Experimental Method	38
The Apparatus	39
Section One	39
Section Two	40
Procedure	42
Determination of The Dry Weight of Zeolite	42
Calibration of Different Volumes	42
Regeneration of Zeolite	43
Composition Calibration	44
Measurement of Pure Component Equilibrium Data	44
Measurements of Binary Mixture Adsorption Data	45

<i>Chapter IV: PURE COMPONENT ADSORPTION</i>	53
Reproducibility of the Data	53
Non-ideality of the Gas Phase	54
Purity of the Gases	55
Percentage of Binder	55
Experimental Estimation of Henry Constant	56
Pure Components Adsorption Data	57
Comparison with Theoretical Models	58
Experimental Data from Literature	61
Modeling the Data Using the Experimental Henry constants	64
Fitting the Sorption Data	64
 <i>Chapter V: BINARY ADSORPTION</i>	 104
Propane-n-Butane Binary Adsorption	105
 <i>Chapter VI: CONCLUSIONS AND RECOMMENDATIONS</i>	 135
CONCLUSIONS	135
RECOMMENDATIONS	137
 <i>Appendix A: ETHYLENE-CARBON DIOXIDE BINARY MIXTURE</i> . .	 139
 <i>Appendix B</i>	 160
 <i>Appendix C</i>	 167
 <i>Appendix D</i>	 176
 <i>Appendix E</i>	 214
 <i>Appendix F</i>	 217

LIST OF FIGURES

Figure	page
1.1 Adsorption capacity for water vapor of various adsorbents ...	9
1.2 Sodalite cage	10
1.3 Structures of A and X zeolites	11
3.1 Experimental apparatus	49
3.2 Calibration curve	51
4.1 Pure component sorption isotherm for n-butane on 13X zeolite at 423 K	74
4.2 Pure component sorption isotherm for n-butane on 13X zeolite	75
4.3 Virial plot for propane on 5A zeolite	76
4.4 Virial plot for n-butane on 5A zeolite	77
4.5 Virial plot for propane on 13X zeolite	78
4.6 Virial plot for n-butane on 13X zeolite	79
4.7 Van't Hoff plot of Henry constants	80
4.8 Pure component sorption isotherms for propane on 5A zeolite	81
4.9 Pure component sorption isotherms for n-butane on 5A zeolite	82
4.10 Pure component sorption isotherms for propane on 13X zeolite	83
4.11 Pure component sorption isotherms for n-butane on 13X zeolite	84
4.12 Generalized sorption isotherm for n-butane on 5A zeolite	85
4.13 Pure component sorption isotherms for propane on 5A zeolite	86
4.14 Generalized sorption isotherm for propane on 5A zeolite	87
4.15 Pure component sorption isotherms for propane on 5A zeolite	88

4.16	Generalized sorption isotherm for propane on 5A zeolite	89
4.17	Pure component sorption isotherms for n-butane on 5A zeolite	90
4.18	Generalized sorption isotherm for n-butane on 5A zeolite	91
4.19	Pure component sorption isotherms for n-butane on 5A zeolite	92
4.20	Generalized sorption isotherm for n-butane on 5A zeolite	93
4.21	Pure component sorption isotherms for propane on 13X zeolite	94
4.22	Generalized sorption isotherm for propane on 13X zeolite	95
4.23	Pure component sorption isotherms for propane on 13X zeolite	96
4.24	Generalized sorption isotherm for propane on 13X zeolite	97
4.25	Pure component sorption isotherms for n-butane on 13X zeolite	98
4.26	Generalized sorption isotherm for n-butane on 13X zeolite	99
4.27	Pure component sorption isotherms for n-butane on 13X zeolite	100
4.28	Generalized sorption isotherm for n-butane on 13X zeolite	101
5.1	X-Y diagram for the sorption of propane-n-butane binary mixture on 5A zeolite at 498 K and 66.7 kPa	110
5.2	Concentration curves for the sorption of propane-n-butane binary mixture on 5A zeolite at 498 K and 66.7 kPa	111
5.3	X-Y diagram for the sorption of propane-n-butane binary mixture on 5A zeolite at 423 K and 66.7 kPa	112
5.4	Concentration curves for the sorption of propane-n-butane binary mixture on 5A zeolite at 423 K and 66.7 kPa	113
5.5	X-Y diagram for the sorption of propane-n-butane binary mixture on 5A zeolite at 348 K and 66.7 kPa	114

5.6	Concentration curves for the sorption of propane-n-butane binary mixture on 5A zeolite at 348 K and 66.7 kPa	115
5.7	X-Y diagram for the sorption of propane-n-butane binary mixture on 5A zeolite at 498 K and 106.7 kPa	116
5.8	Concentration curves for the sorption of propane-n-butane binary mixture on 5A zeolite at 498 K and 106.7 kPa	117
5.9	X-Y diagram for the sorption of propane-n-butane binary mixture on 5A zeolite at 423 K and 106.7 kPa	118
5.10	Concentration curves for the sorption of propane-n-butane binary mixture on 5A zeolite at 423 K and 106.7 kPa	119
5.11	X-Y diagram for the sorption of propane-n-butane binary mixture on 5A zeolite at 348 K and 106.7 kPa	120
5.12	Concentration curves for the sorption of propane-n-butane binary mixture on 5A zeolite at 348 K and 106.7 kPa	121
5.13	X-Y diagram for the sorption of propane-n-butane binary mixture on 13X zeolite at 498 K and 66.7 kPa	122
5.14	Concentration curves for the sorption of propane-n-butane binary mixture on 13X zeolite at 498 K and 66.7 kPa	123
5.15	X-Y diagram for the sorption of propane-n-butane binary mixture on 13X zeolite at 423 K and 66.7 kPa	124
5.16	Concentration curves for the sorption of propane-n-butane binary mixture on 13X zeolite at 423 K and 66.7 kPa	125
5.17	X-Y diagram for the sorption of propane-n-butane binary mixture on 13X zeolite at 348 K and 66.7 kPa	126
5.18	Concentration curves for the sorption of propane-n-butane binary mixture on 13X zeolite at 348 K and 66.7 kPa	127
5.19	X-Y diagram for the sorption of propane-n-butane binary mixture on 13X zeolite at 498 K and 106.7 kPa	128
5.20	Concentration curves for the sorption of propane-n-butane binary mixture on 13X zeolite at 498 K and 106.7 kPa	129
5.21	X-Y diagram for the sorption of propane-n-butane binary mixture on 13X zeolite at 423 K and 106.7 kPa	130
5.22	Concentration curves for the sorption of propane-n-butane binary mixture on 13X zeolite at 423 K and 106.7 kPa	131
5.23	X-Y diagram for the sorption of propane-n-butane binary mixture on 13X zeolite at 348 K and 106.7 kPa	132

5.24	Concentration curves for the sorption of propane-n-butane binary mixture on 13X zeolite at 348 K and 106.7 kPa	133
A.1	Pure component sorption isotherms for ethylene on 5A zeolite	145
A.2	Pure component sorption isotherms for carbon dioxide on 5A zeolite	146
A.3	X-Y diagram for the sorption of ethylene-carbon dioxide binary mixture on 5A zeolite. Ideal solution	147
A.4	Concentration curves for the sorption of ethylene-carbon dioxide binary mixture on 5A zeolite. Ideal solution.....	148
A.5	X-Y diagram for the sorption of ethylene-carbon dioxide binary mixture on 5A zeolite. Ideal solution.....	149
A.6	Concentration curves for the sorption of ethylene-carbon dioxide binary mixture on 5A zeolite. Ideal solution.....	150
A.7	X-Y diagram for the sorption of ethylene-carbon dioxide binary mixture on 5A zeolite. Ideal solution.....	151
A.8	Concentration curves for the sorption of ethylene-carbon dioxide binary mixture on 5A zeolite. Ideal solution	152
A.9	X-Y diagram for the sorption of ethylene-carbon dioxide binary mixture on 5A zeolite. Non-ideal solution	153
A.10	Concentration curves for the sorption of ethylene-carbon dioxide binary mixture on 5A zeolite. Non-ideal solution ...	154
A.11	X-Y diagram for the sorption of ethylene-carbon dioxide binary mixture on 5A zeolite. Non-ideal solution	155
A.12	Concentration curves for the sorption of ethylene-carbon dioxide binary mixture on 5A zeolite. Non-ideal solution	156
A.13	X-Y diagram for the sorption of ethylene-carbon dioxide binary mixture on 5A zeolite. Non-ideal solution	157
A.14	Concentration curves for the sorption of ethylene-carbon dioxide binary mixture on 5A zeolite. Non-ideal solution	158

ABSTRACT

The objectives of this work are to measure the binary adsorption equilibrium data of propane and n-butane on 5A and 13X zeolites, and to model the behavior of this system. This will provide a basis for the choice of the best conditions for separation of these gases by zeolites.

Data of pure component sorption of propane and n-butane on 5A and 13X zeolites for temperatures of 348, 423 and 498 K is reported. Binary sorption data for these two components at the same temperatures are also reported for total pressures of 66.7 and 106.7 kPa. The pure component data is modelled using the Schirmer et al., Ruthven, vacancy solution and virial models. In general the Schirmer et al. model gives the best fit. The form of the virial model used here presents the pure component data in generalized form.

The binary data is found to be approximately ideal. The selectivity coefficient for propane, which is the reciprocal of the relative volatility, is found to be in the range of 0.08 to 0.40 for the temperatures and pressures studied. The separation increases with decreasing temperature and shows a slight increase with decreasing pressure. The 5A zeolites gives a smaller selectivity coefficient and hence larger separation than the 13X zeolite. However the difference between the selectivities coefficients for the two zeolites is small. The binary data is

modelled using the Schirmer et al., Ruthven et al., vacancy solution and IAST binary models. In general the Schirmer et al. and the ideal adsorption solution theory (IAST) models give the best fit.

ملخص

الهدف من هذا البحث هو قياس ادمصاص الزيوليت ١٥ والزيوليت ١٣ اكس لخليط من البروبان والبيوتان ووصف ادمصاص لنموذج رياضي وبذلك تعرف افضل الظروف لفصل هذين الغازيين باستخدام الزيوليت .

سجلت قياسات ادمصاص لغازين البروبان والبيوتان النقيين على الزيوليت ١٥ والزيوليت ١٣ اكس في درجات الحرارة ٢٤٨ و ٤٢٣ و ٤٩٨ درجة مطلقه كما سجلت القياسات لادمصاص الخليط الثنائي من هذين الغازيين في نفس درجات الحرارة وضغط كلي يساوي ٦٦٧ و ١٠٦٧ كيلوباسكال . وقد استخدم كل من نموذج فيريال وشيرمر وروذن ونظرية المحلول الفراغي في وصف ادمصاص الغازات النقيه ووجد ان نموذج شيرمر يعطى اقرب وصف للقياسات التجريبية كما ان نموذج فيريال المستخدم في هذا البحث يمثل ادمصاص بمنحنى عام لكل درجات الحرارة .

اما بالنسبة لادمصاص الخليط الثنائي فقد وجد انه يمثل تقريبا ادمصاص خليط مثالي ، اما معامل الانتقاء وهو مقلوب قابليه التطاير النسبيه فقد كان بين ٠.٨ و ٤.٠ في مدى الحرارة والضغط المدروسين ، كما لوحظ ان الفصل يزداد بانخفاض الحرارة وتظهر زيادة طفيفة بانخفاض الضغط ، وقد اظهر الزيوليت ١٥ قدره اكبر على الفصل من الزيوليت ١٣ اكس ولكن الفرق ليس بكبير وقد استخدمت نماذج شيرمر وروذن ونظرية المحلول الفراغي ونظرية ادمصاص المحلول المثالي لوصف ادمصاص الخليط الثنائي وقد اعطى نموذج شيرمر ونظرية ادمصاص المحلول المثالي اقرب وصف للنتائج التجريبية

Chapter I
INTRODUCTION

1.1 SEPARATION BY SORPTION

The phenomenon of adsorption has been understood by scientists for over 100 years . However, it is only during the past twenty-five years that it has become established as a major chemical processing technique [1]. While adsorption in some respects is a more complex operation than those like solvent aided separation, it has two potential advantages [2]

1. Adsorbents are much more selective in their affinity for various materials than are any known solvents .
2. Much higher efficiency of transfer of material between fluid and adsorbed phases can be achieved in adsorptive operations than in conventional equipment such as extraction or extractive distillation.

One of the important sorption processes, which is becoming increasingly popular, is pressure swing adsorption [3] . Pressure swing adsorption (PSA) is a short cycle time adsorption / desorption process in fixed beds of adsorbent using gas pressure variation as the principle operating parameter [4] . In the design and optimization of (PSA) processes basic experimental equilibria and rate data at varying temperatures and pressures are required .

An abundance of pure gas equilibria and rate data exist in the literature and good success has been achieved in the correlation of these data . However, the practical application of zeolite molecular sieve adsorbents in PSA processes involve the adsorption of multicomponent mixtures . Available experimental data for such systems are very limited [4] . This shows the importance of getting such data .

1.2 ZEOLITE MOLECULAR SIEVES

One of the key steps in the development of sorption technology was the introduction of synthetic zeolite adsorbents by Union Carbide Corporation scientists in 1954 [1] . Commercial adsorbents which exhibit ultraporosity and which are generally used for the separation of gas and vapor mixtures include the activated carbons, activated clays, inorganic gels such as silicagel and activated alumina, and the crystalline aluminosilicate zeolites [5] .

Activated carbons, activated alumina, and silicagel do not possess an ordered crystal structure and consequently the pores are nonuniform . Hence, all molecular species, with possible exception of high molecular weight polymeric materials, may enter the pores. Zeolite molecular sieves have pores of uniform size which are uniquely determined by the unit structure of the crystal . These pores will completely exclude molecules which are larger than their diameter . The term "molecular sieve" was originated by J. W. McBain to define porous solid materials which exhibit the property of acting as sieves on a molecular scale [5] .

Molecular sieves show strong preference for polar and polarizable molecules . Consequently, the amount of material adsorbed increases rapidly to the saturation value as its concentration increases in the fluid phase . Because of this adsorption mechanism, molecular sieves differ from all other types of adsorbents in that they have an extremely high equilibrium adsorption capacity for polar and polarizable compounds at very low concentrations of these compounds in the fluid phase. This characteristic is illustrated by Fig 1.1 for adsorption of water vapor [6].

Zeolites are basically of two types, mineral zeolites which are available naturally and synthetic zeolites which are manufactured industrially . The insufficient purity of natural zeolite and the small amounts mined have made synthetic production of zeolite necessary. Synthesis involves, in principle mixing aqueous solutions of alkali metal aluminates(especially sodium aluminates) and silicates, heating and slow crystallization [7] .

The first practical use of zeolites probably occurred about 2000 years ago when natural zeolite rock was quarried for use as a building stone [8] . Natural zeolites were first recognized by Cronstedt as a new group of minerals with his discovery of Stilbite in 1756 [5] . Because the mineral exhibited intumescence when heated in blowpipe flame, he called the mineral a zeolite which comes from two Greek words meaning "to boil" and "a stone" . The adsorption of gases by dehydrated zeolites was studied by F. Grandjean in 1909 [5] . The first application of

dehydrated zeolites as a molecular sieve in the separation of gas mixtures was demonstrated by Barrer in 1945 utilizing the zeolite mineral Chabazite [8] .

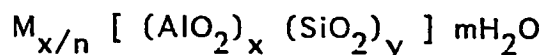
Synthetic zeolites were first introduced and utilized commercially as molecular sieve adsorbents in 1954 [8] . Although only a small number of mineral and synthetic zeolites have reached the commercialization stage, there are about 40 known different zeolite minerals, and over 150 reported synthetic types [9] .

1.3 STRUCTURE AND COMPOSITION OF ZEOLITES

Zeolites are crystalline, hydrated aluminosilicates . Structurally they are "framework" aluminosilicates which are based on an infinitely extending three-dimensional network of AlO_4^- and SiO_4 tetrahedra linked to each other by sharing all the oxygen atoms . The negative charge on the AlO_4^- are neutralized by an equivalent number of cations.

The framework is sufficiently open to accommodate water molecules as well as other sorbed species . This openness imparts characteristic zeolite properties . The water molecules can move easily within the crystals as can the cations with a little more difficulty. These ions therefore, undergo ready exchange with other ions; similarly water molecules can be removed or replaced in a continuous manner and often reversibly [10].

The general composition per unit cell of zeolites is [11]



Where y/x is the molar ratio of Si/Al, and n is the number of positive charges on one cation . The maximum aluminum content possible in tetrahedral aluminosilicates frameworks is a ratio of Si/Al equal to one [9].

The crystal structure of zeolites can be described in terms of larger "secondary building units" . The sodalite unit, shown in Fig 1.2 [12] is one important secondary building unit . It consists of a truncated octahedron with eight hexagonal and six square faces . Each edge represents an oxygen ion located at or near the center of the line, while the small silicon and aluminum ions are located at the corners . The six membered oxygen rings, which make up the hexagonal faces, have a large enough free diameter to admit very small molecules such as water or ammonia but larger molecules can not penetrate the sodalite cage .

The structures of the commercially important A and X zeolites can all be regarded as built up from assemblages of sodalite units . The structure of type A zeolite indicated in Fig 1.3 [12] is obtained by joining the square faces of the sodalite units through 4-membered oxygen bridges to form a cubic cell with sodalite unit at each corner [13] . Zeolite X which is shown also in Fig 1.3 is formed by joining sodalite, in tetrahedral coordinates through the hexagonal faces by means of 6-membered oxygen bridges .

The A type cavity, 1.14 nm in diameter is accessible by six openings which are formed by 8-membered oxygen rings (four from each sodalite unit) . The composition per pseudo cell of the sodium A zeolite is $\text{Na}_{12} [(\text{AlO}_2)_{12} (\text{SiO}_2)_{12}] \cdot 27\text{H}_2\text{O}$ (multiply by 8 for the true cell) [5] . Since the diameter of the inlet neck is .42 nm (4.2 Å) this type of molecular sieve A is termed 4A . Sodium cations may easily be replaced by cations of different metal . When they are replaced by calcium ions, of which only half the number are needed owing to the double charge, the effective neck diameter is widened to roughly .5 nm (.49 nm) ; this calcium form of molecular sieve A is therefore termed 5A . The composition per cell of the fully exchanged 5A zeolite is $\text{Ca}_6 [(\text{AlO}_2)_{12} (\text{SiO}_2)_{12}] \cdot 27\text{H}_2\text{O}$

The X type cavity roughly 1.3 nm in diameter is accessible by four openings composed of 12-membered oxygen rings . The diameter of the opening is .74 nm . The composition per unit cell of the sodium X zeolite is $\text{Na}_{86} [(\text{AlO}_2)_{86} (\text{SiO}_2)_{106}] \cdot 264\text{H}_2\text{O}$ [5]. According to the notation used by the Linde Co., this sieve is termed 13X . Unlike type A molecular sieve, the effective diameter of the necks is decreased when sodium is replaced by calcium to give 10X molecular sieve .

1.4 SCOPE OF THE PRESENT STUDY

The three properties of zeolites which have industrial potential are their capacity [10]

1. to sorb gases, vapors, and liquids;

2. to catalyze reactions; and
3. to act as cation exchangers.

In this work the first property will be used.

The choice of 5A and 13X zeolites is based on their excellent properties which guaranteed their lasting commercial prominence out of more than 150 synthetic zeolites . Their surface is highly selective for water, polar and polarizable molecules. Their pore volumes of nearly $0.5 \text{ cm}^3/\text{cm}^3$ are the highest known for zeolites and give them a distinct economic advantage in bulk separation and purification where high capacity is essential to an economic design . By a judicious selection of cation composition achieved by facile ion exchange reactions, nearly the entire spectrum of known pore sizes in zeolites can be obtained . The pore sizes achieved by cation exchange of types A and X span the entire range from the smallest pore-sized zeolite known, Cs-A at 0.2 nm in size through the 0.3nm potassium A, 0.4 nm sodium A, the 0.5 nm calcium A, to the largest known which is about 0.8 nm in sodium X [9].

This thesis describes the results of the experimental study of the equilibrium sorption of propane and n-butane and their binary mixtures on 5A and 13X zeolites . These gases were selected because they are present in natural gas which may be processed using the PSA technique. Pure component equilibrium adsorption isotherms for propane and n-butane on each zeolite were obtained at three different temperatures 348, 423 and 498 K at pressures up to 1000 torr (133.4 kPa) For the binary mixtures, the measurements were at constant tempera-

ture and total pressure. The pressure chosen are 500 and 800 torr (66.7 and 106.7 kPa) and the temperatures used are the same as for the pure components.

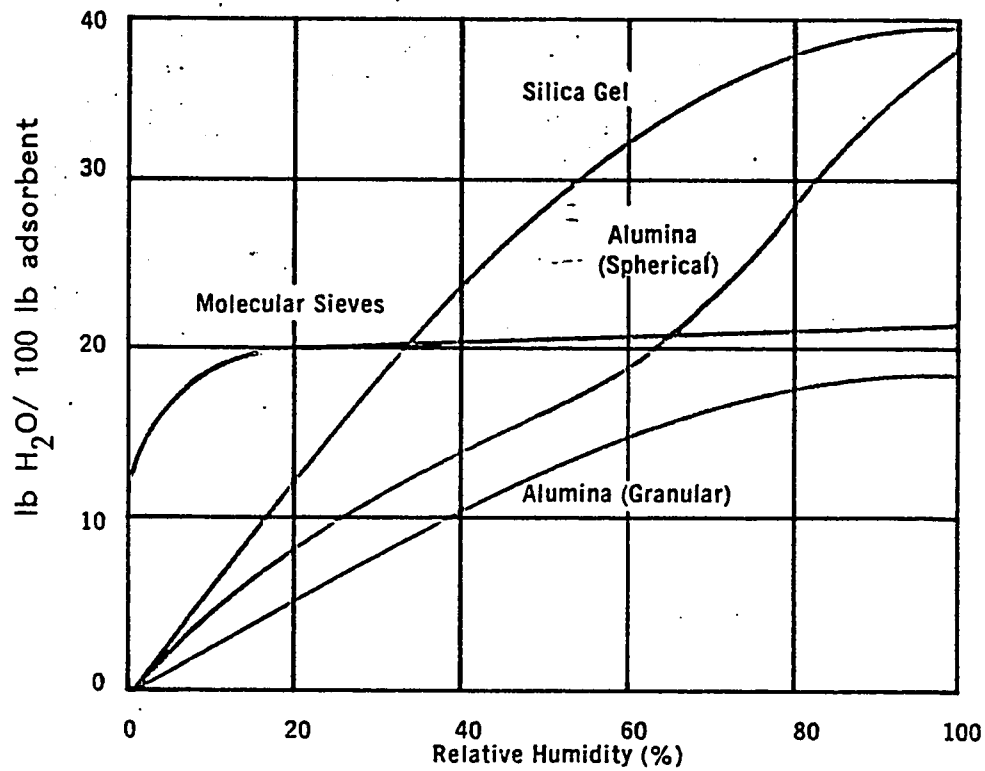


FIGURE 1.1 Adsorption capacity for water vapor of various adsorbents

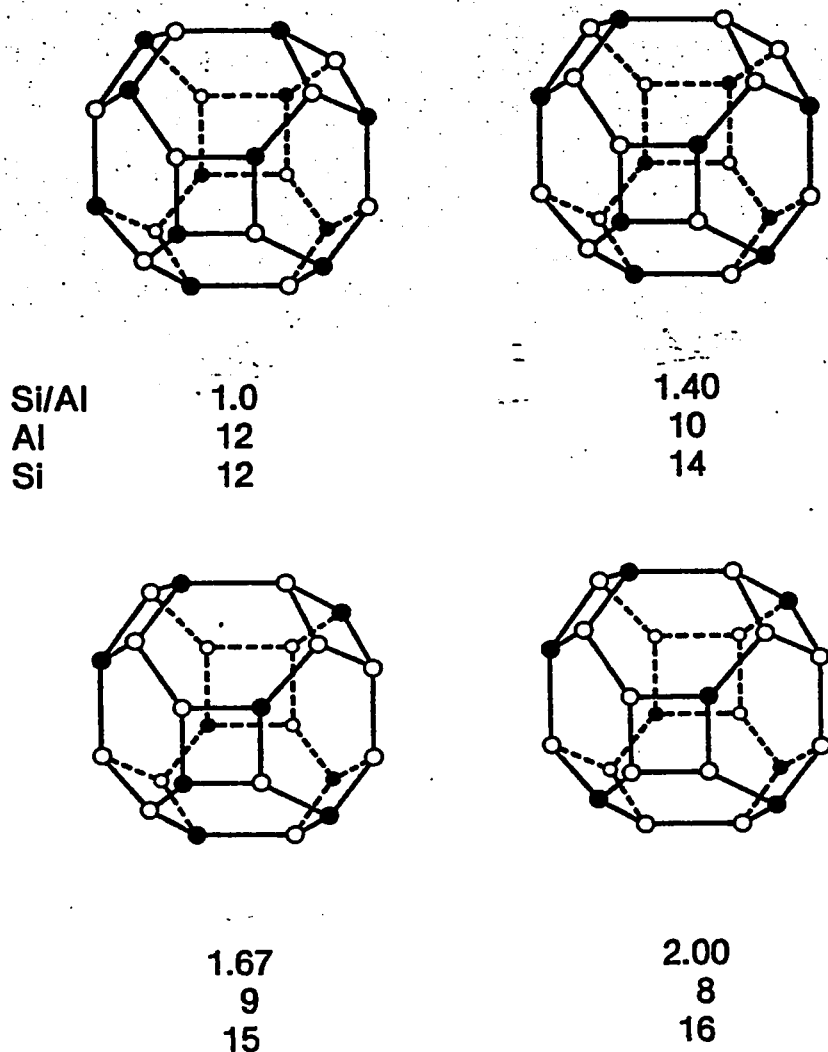


FIGURE 1.2 Sodalite cage. Different arrangements of Si and Al are shown for different Si/Al ratios.

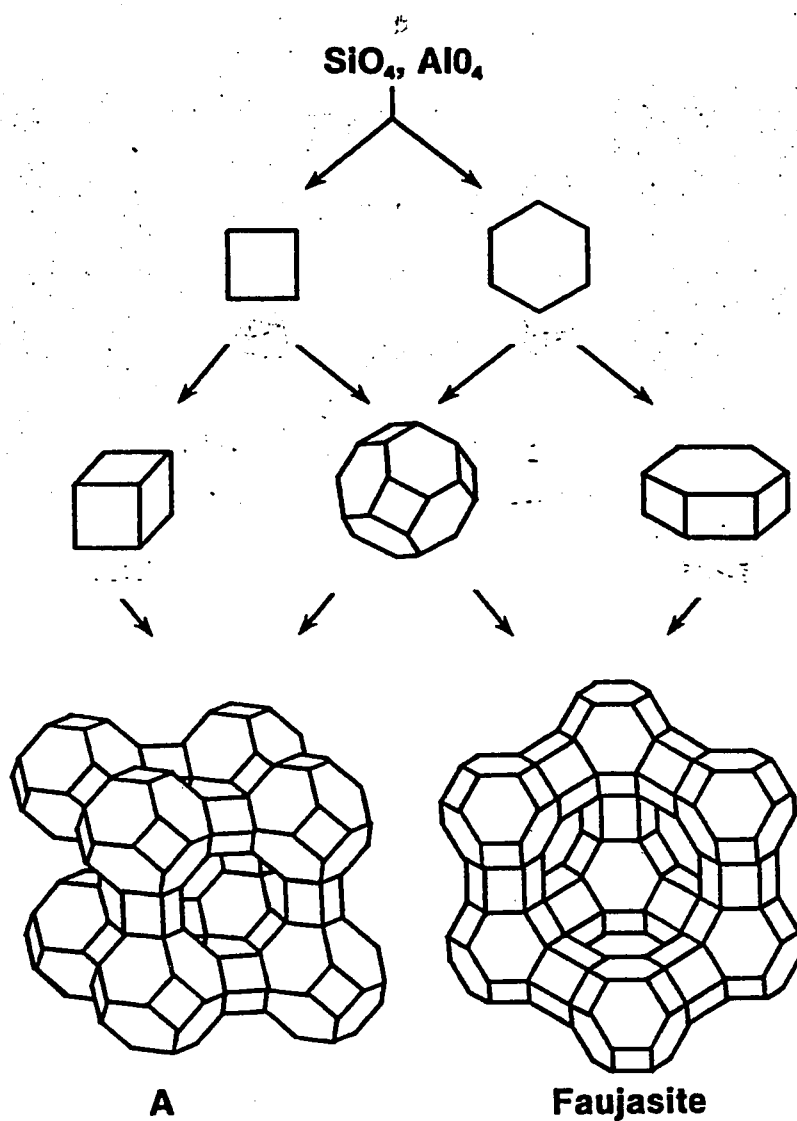


FIGURE 1.3 Structures of A and X (faujasite) zeolites. The figure shows the possible pathways for the formation of these zeolites from SiO_4 and AlO_4 tetrahedra.

REFERENCES

1. Cassidy, D. W. and Holmes, E. S., paper 23 f, presented at AIChE's Golden Jubilee Meeting, Washington, November 1st, (1983)
2. Broughton, D. B. and Gembicki, S. A. paper 23 g, presented at AIChE's Golden Jubilee Meeting, Washington, November 1st, (1983)
3. Fernandez, G. F. and Kenney, C. N., Chem. Eng. Sci., 38 , 827, (1983)
4. Sorial, G. A. , Granville, W. H. and Daly, W. O., Chem. Eng. Sci., 38 , 1517, (1983)
5. Breck, D. W., "Zeolite Molecular Sieves" , John Wiley & Sons, New York, (1974)
6. Davison Molecular Sieves, Trade publication by Davison Chemical, Petroleum Chemicals Department, Division of Grace Chemical Co., PC/ADS-96-1071
7. Ponec, V. , Knor, Z. and Cerny S., "Adsorption on Solids" , Butterworth & Co., London, (1974)
8. Breck, D. W., paper 25, "The Properties and Applications of Zeolites" , Special Publication No. 33, The Chemical Society, London, (1980)
9. Flanigen, E. M., Plenary Paper-Technology "Proceedings of the Fifth International Conference on Zeolites" , Naples, Heyden & Son Ltd., London, 760, (1980)
10. Barrer, R. M. "Zeolites and Clay Minerals as Sorbents and Molecular Sieves" , Academic Press, London, (1978)
11. Stucky, G. D., Preface, ACS Symposium Series No. 218, Washington D. C., (1983)
12. Melchior, M. T., Paper 15, ACS Symposium Series No. 218, Washington D. C., (1983)

13. Holborow, K. A., Ph.D. thesis, University of New Brunswick "Multicomponent Sorption Equilibria of Gases in 5A Zeolite" , (1974)

Chapter II

LITERATURE SURVEY

2.1 ADSORPTION OF BINARY MIXTURES ON ZEOLITES

The behavior of gas mixture on zeolite was first reported by Barrer and Robbins in 1953 [1]. The mixtures H_2 -Ne, H_2 - N_2 and Ne- N_2 were studied at 90 K in mordenite and Ar- O_2 and Ar- N_2 were studied in the mineral chabazite at 90 K. Both components of the mixtures must be capable of entering the intracrystalline channels of the zeolite. If due to a sieving effect, one component of the mixture is excluded, a simple separation occurs. In some instances the pure component may inhibit or prevent the adsorption of the second component. For example, oxygen, as a single component, is readily adsorbed by zeolite A at 90 K and nitrogen is excluded. In an O_2 - N_2 mixture at 90 K nitrogen inhibits the adsorption of oxygen and little total adsorption occurs[1].

Experimentally the usual procedure is to circulate a mixture of the gas through a small bed of adsorbent until equilibrium is established, using a volumetric method (described in chapter 3). The phase rule for adsorption is [2]

$$S(\text{degrees of freedom}) = S(\text{no. of components}) - (\text{no. of phases}) + 3$$

(2.1)

The adsorbent is not counted as a component in Eq. 2.1 . Thus, for binary adsorption equilibria there are 3 degrees of freedom. Unlike the case for vapor-liquid equilibria it is possible to hold two intensive variables constant and vary the composition. Most binary adsorption data reported in the literature are measured at constant temperature and total pressure. In other reported data the temperature and the fluid phase composition are held constant while varying the total pressure. Only one data set has been found in which the total pressure and the fluid phase composition are held constant while varying the temperature[1].

The selectivity factor, defined by the following equation, is the reciprocal of the relative volatility. It gives the affinity of the zeolite to adsorbed component one relative to component two. It is related to the difference in the heats of adsorption of the individual components.

$$S_{1,2} = \frac{x_1/y_1}{x_2/y_2} \quad (2.2)$$

The heats of adsorption are related to the total interaction energy between adsorbate and adsorbent which is itself composed of several individual interaction energy terms. In a system of methane and carbon monoxide, for example, the dispersion and polarization attraction terms are greater for methane. However, the dipole and quadrupole interaction for CO is larger and results in an overall selectivity for CO over CH₄ in the mixture [1].

In the adsorption of hydrocarbon mixtures selectivity depends upon the unsaturated bonds. From measurements of adsorption isotherms of benzene and cyclohexane on zeolite Y over a temperature interval 293-473 K it was found that benzene is much more strongly adsorbed above 423 K [1] (benzene has three unsaturated bonds while all the bonds are saturated in the cyclohexane). In the saturated hydrocarbons two factors affect the selectivity

1. Physicochemical characteristics
2. Packing characteristics

As an example, consider a binary system of n-paraffins. If the paraffins chosen have small number of carbon atoms, then the higher molecular weight paraffin is preferentially adsorbed (see for example C_3 - C_4 system in chapter 4). On the other hand, it has been observed that for long chain paraffins, especially when they are not successive members of the homologous series, that the lower molecular weight paraffin is preferentially adsorbed [3,4] (for example C_8 - C_{10} system [3]). Satterfield and Smeets [4] suggested that the packing characteristics of the higher molecular weight paraffin, rather than its physicochemical characteristic, play a dominant role in the adsorption selectivity on a zeolite [4].

Pure component data is available in the literature for many systems at varying temperatures, but are mostly limited to atmospheric pressure. Some adsorption data at high pressure (up to 180 atm) on 5A and 13X zeolites, especially useful for the design of the PSA process, can be found in a paper by Wakasugi et. al. [5]. A review of high

pressure adsorption methods and data is given by Menon [6]. Pure component adsorption data of propane and n-butane on 5A can be found in many references (for example [1,7,8,9,10]). However, references giving propane and n-butane pure component data on 13X zeolite are not as many as those for 5A [1,10,11]

Since the experimental multicomponent adsorption data are difficult and time consuming to obtain [12], very limited data are available in the literature compared to the number of systems which could be investigated. A selection of binary adsorption data, which has been cited, is shown in Table 2.1 . The text by Breck [1] also has some binary data in it. Only one set of data for propane-n-butane binary mixture was found [13]. However, only the gas phase composition and the total amount adsorbed in mg/100 mg is reported in this work, because the gravimetric method was used in obtaining the data. This does not allow the calculation of the composition of the adsorbed phase. Also only 5A zeolite was used in this study.

2.2 ISOTHERM EQUATIONS

2.2.1 INTRODUCTION

The amount of gas or vapor which is adsorbed by a solid depends on the equilibrium pressure p , the temperature T , the nature of the gas or vapor, and the nature of the solid adsorbent. This is expressed by Eq. 2.3

$$c = f (P,T) \quad (2.3)$$

Table 2.1:
Mixture Sorption Data

MIXTURE	TEMP. C	PRESSURE	ZEOLITE	REFERENCE
Normal Paraffins C ₂ -C ₃ C ₂ -C ₄ C ₃ -C ₄	0	10,25,50, 100,200, 300,400 torr	5A	13
C ₅ -C ₆ C ₆ -C ₇ C ₇ -C ₈ C ₅ -C ₇ C ₅ -C ₈ C ₅ -C ₆ -C ₇ C ₅ -C ₆ -C ₈ C ₅ -C ₇ -C ₈	2-18-30-42	(Liquids)	5A	3
C ₈ -C ₁₀ C ₈ -C ₂₀ C ₈ -C ₃₀	--	(Liquids)	NaY	4
Ethane-Ethylene	25-50	1033.9 torr	13X	27
n-Butane-cis-But-2-en n-Butane-trans-But-2-en n-Butane-But-1-en	30	2.3-10 ⁵ kPa	13X	28
Ethylene-Propane Propane-Cyclopropane Ethylene-Cyclopropane Ethylene-Carbondioxide	-35,0,50	8 torr	5A	20,21,29
i-C ₄ H ₁₀ -C ₂ H ₄ i-C ₄ H ₁₀ -C ₂ H ₆ i-C ₂ H ₄ -CCl ₂	25,50,100	137.8 kPa	13X	30
C ₄ -Kr	-32,-18,-2	97.36 kPa	5A	24,25
CO-N ₂ CO-O ₂ CO ₂ -N ₂	-128.9	101.3 kPa	5A,13X	31
SO ₂ -N ₂ CO ₂ -N ₂ CO ₂ -O ₂ SO ₂ -CO ₂ O ₂ -N ₂	0-100	up to 800 torr	H-mord -enite	33
O ₂ -N ₂	5,20,30	170,440 kPa	5A	32

The nature of this function can be quite complex and generally is not predictable on totally theoretical grounds [1]. The plot of c as a function of P at constant T gives the adsorption isotherm. Increasing the temperature of the gas solid system at a constant pressure will decrease the quantity adsorbed. The process of adsorption involves a decrease in the free energy and the change in enthalpy must be negative since the change in entropy is negative; the adsorption process involves loss in degrees of freedom by the adsorbed molecules and the formation of a more ordered configuration in the adsorbed state. Therefore, the adsorption process is exothermic and heat is evolved.

2.2.2 SIMPLE MODEL ISOTHERM EQUATIONS

Various idealized isotherm models have been proposed. A brief discussion of some of these isotherm equations is now presented.

2.2.2.1 *Henry's Law*

At very low surface coverage a statistical treatment of adsorption gives [14]

$$c = K P \quad (2.4)$$

where K is the Henry's law constant. It can be shown [14] that

$$K = e^{-\Delta G/RT} \quad (2.5)$$

where ΔG is the Gibbs free energy change for the process:

System with adsorbent
and
one adsorbate molecule

----->

adsorbent and one
molecule in the gas
phase at unit fugacity

2.2.2.2 *Freundlich Isotherm*

The following empirical equation was extensively used by Freundlich, and later named the Freundlich isotherm [15]

$$c = k P^{1/n} \quad (2.6)$$

where c is the concentration, P is the pressure and k and n are empirical constants. Thermodynamic consistency of this isotherm was tested by LeVan and Vermeulen [16] with the help of Gibbs adsorption isotherm and it was found that the model is thermodynamically inconsistent when applied to multicomponent sorption.

2.2.2.3 *Langmuir Model*

The Langmuir adsorption isotherm is

$$\theta = \frac{c}{c^*} = \frac{KP}{1 + KP} \quad (2.7)$$

where c^* is the saturation concentration and K is the Henry constant. Implicit in its development are the following assumptions [17]

1. the adsorbate in the bulk gaseous phase behaves as an ideal gas;
2. the amount adsorbed is confined to a monomolecular layer;

3. every part of the surface has the same energy of adsorption;
4. no adsorbate-adsorbate interaction is taken into account, and
5. the adsorbed molecules are localized; i.e., they have definite points of attachment to the surface.

The first two assumptions are acceptable as true for many gas/solid systems, but the second pair are always false. However, the effect of surface non uniformity is to cause the energy of adsorption to decrease with coverage, whereas the effect of adsorbate-adsorbate interaction is to cause it to increase, resulting in partial cancellation of these effects. The success, not always deserved, of the Langmuir equation owes much to this coincidence [17]. LeVan and Vermeulen were able to derive explicit and thermodynamically consistent binary Langmuir isotherms [16].

2.2.3 MOBILE ADSORBED PHASE FILM MODELS

When molecules in the adsorbed phase can move laterally and desorption can take place from any point on the surface, the adsorbed film is said to be mobile. Assuming similarity between adsorbate properties in zeolite and those of a liquid, then the sorbate can be described by an equation of state. The adsorption equation isotherm is then derived by application of Gibbs adsorption isotherm. The ideal gas, Volmer, Van der Waals, Hirschfelder et.al. and the virial equations of state were used to develop adsorption equations [18].

2.2.4 BRUNAUER, EMMET AND TELLER (B.E.T.) ISOTHERM

The B.E.T. equation is derived for multilayer adsorption assuming no lateral interaction among the molecules, and a homogeneous surface.

The resulting equation for m layers

$$\theta = \frac{N}{N_s} = \frac{ax(1 - (m+1)x^m + mx^{m+1})}{(1-x)(1-(1-a)x^m + ax^{m+1})} \quad (2.8)$$

where N is the total number of adsorbed molecules, N_s is the total number of sites, $a = q_1/q_l$ where q_1 and q_l are the partition functions of one molecule in the monolayer and the liquid state respectively and $x = P/P_s$ where P_s is the saturation pressure.

2.2.5 STATISTICAL THERMODYNAMIC FORMULATION

The method of statistical thermodynamic is being applied to describe the results of measuring thermodynamic properties of adsorbate zeolite systems more frequently [19]. The regular pore structure of zeolites makes them convenient for application of statistical mechanics. Since the zeolite adsorbent is an open system (both energy and molecules can be transported across the walls of the system) it is appropriate to use the grand partition function in the derivation. For one-component systems [14]

$$\Xi(V, T, \mu) = \sum_{i=0}^{\infty} Q_i(V, T) \lambda^i \quad (2.9)$$

$$\lambda = e^{\mu/RT}$$

where λ is the absolute activity, μ is the chemical potential, $Q_i(V,T)$ is the canonical partition function, and i is the number of molecules in the system. Q_0 is always equal to one since there is only one energy state of the system, namely the zero energy. For two components

$$\Xi = \sum_{i=0}^M \sum_{j=0}^N Q_{ij}(V,T) \lambda_A^i \lambda_B^j \quad (2.10)$$

$$\lambda_A = e^{\mu_A/RT}$$

$$\lambda_B = e^{\mu_B/RT}$$

For S independent subsystems

$$\Xi = \left[\sum_{i=0}^m Q_i(V,T) \lambda^i \right]^S \quad (2.11)$$

Assuming that the interaction energy between adsorbed molecules in different cavities is negligible, then each cavity can be treated as an independent subsystem.

The average number of molecules in the system is given by

$$\bar{N} = \lambda \left(\frac{\partial \ln \Xi}{\partial \lambda} \right)_{V,T} \quad (2.12)$$

Applying this formula to Eq 2.11 (by taking the logarithm and differentiating with respect to λ gives

$$C = \frac{\bar{N}}{S} = \frac{\sum_{i=1}^m i Q_i \lambda^i}{\sum_{i=0}^m Q_i \lambda^i} \quad (2.13)$$

Similarly for binary systems

$$C_A = \frac{\sum_{i=1}^m \sum_{j=0}^n i Q_{ij} \lambda_A^i \lambda_B^j}{\sum_{i=0}^m \sum_{j=0}^n Q_{ij} \lambda_A^i \lambda_B^j} \quad (2.14)$$

For convenience the quantity $Q_i \lambda^i$ is replaced by $Z_i \xi$ where $\xi = \lambda (2\pi mkT/h^2)^{3/2}$ is the activity which for an ideal gas is P/kT , and Z_i is the configuration integral for the system composing i molecules in one cavity. In the quasi-classical approximation

$$Z_i = \frac{1}{i!} \int_V \exp \left[- \frac{U_i(r_1, \dots, r_i)}{kT} \right] dr_1 \dots dr_i \quad (2.15)$$

where V is the volume of the cavity and U_i is the potential energy of i molecules adsorbed in the cavity. The quantity Z_1/kT is the limiting Henry law constant. The complexity of the physical situation is such that the configuration integral, Z_i can not be evaluated (for $i > 1$) without various simplifications.

2.2.5.1 Ruthven Isotherm

Ruthven [20] introduced the following assumptions

1. The molecules within a given cavity move randomly and independently in the potential field resulting from sorbate-sorbent interactions.
2. The potential is uniform throughout the cavity even when more than molecule is present but that the effective volume of the cavity is reduced.

The configuration integral is then given by $Z_i = Z_1^i (1 - i\beta/V)^i / i!$

Which gives

$$C = \frac{Kp + \sum_{i=2}^m \frac{(Kp)^i}{(i-1)!} (1 - i\beta/V)^i}{1 + Kp + \sum_{i=2}^m \frac{(Kp)^i}{i!} (1 - i\beta/V)^i} \quad (2.16)$$

Where β is the effective covolume of sorbed molecule, V is the volume of a single zeolite cavity and K is the Henry law constant.

Ruthven, Loughlin and Holborow [20,21] extended this model using Eq 2.14 to include binary systems. they got

$$C_A = \frac{K_A P_A + \sum \sum \frac{(K_A P_A)^i (K_B P_B)^j}{(i-1)! j!} (1 - \frac{i\beta_A}{V} - \frac{j\beta_B}{V})^{i+j}}{1 + K_A P_A + K_B P_B + \sum \sum \frac{(K_A P_A)^i (K_B P_B)^j}{i! j!} (1 - \frac{i\beta_A}{V} - \frac{j\beta_B}{V})^{i+j}}$$

$$i + j \geq 2 \quad (2.17)$$

$$\text{and } i\beta_A + j\beta_B \leq V$$

This equation involves the following new assumptions

1. Volumes are additive ($\Delta V^E = 0$). Typical excess volumes of mixing are usually less than 2% [20].
2. Each species is treated equal except for the molecular volume and the Henry constant.

2.2.5.2 Shirmer Isotherm

Shirmer, Fiedler and Stach [22,23] replaced the configuration integral by a finite sum over the different energy levels in the cavity.

$$Q_i \lambda^i = Z_i \xi^i = \left(\frac{P/P_0}{T/T_0} \right)^i \sum_{j=0}^k e^{[i \left(\frac{S_{ij} T - E_{ij}}{RT} \right)]} \quad (2.18)$$

For an energetically homogeneous cavity at a given coverage the number of different energy levels, k is one, while in other cases $k=2$ is found to be sufficient [22].

S_{ij} and E_{ij} are constants representing the standard differences in entropy and energy for one molecule in going from an ideal gas of volume $V_0 = RT_0/P_0$, and temperature T to a cavity which has $(i-1)$ molecules in j different energy levels (on a basis of one mole). Combining Eqs 2.13 and 2.18 Shirmer et.al. got (for $k=1$)

$$c = \frac{\sum_{i=1}^m \left(\frac{P/P_0}{T/T_0} \right)^i \exp\left(i \frac{TS_i - E_i}{RT}\right)}{\sum_{i=0}^m \left(\frac{P/P_0}{T/T_0} \right)^i \exp\left(i \frac{TS_i - E_i}{RT}\right)} \quad (2.19)$$

Loughlin and Roberts extended this model to include multicomponent systems [24,25]. The binary isotherm is

$$C_A = \frac{\sum_{i=1}^m \sum_{j=0}^n i \left(\frac{P_A/P_O}{T/T_O} \right)^i \left(\frac{P_B/P_O}{T/T_O} \right)^j \exp \left[\ell \frac{S_\ell T - E_\ell}{RT} \right]}{\sum_{i=0}^m \sum_{j=0}^n \left(\frac{P_A/P_O}{T/T_O} \right)^i \left(\frac{P_B/P_O}{T/T_O} \right)^j \exp \left[\ell \frac{S_\ell T - E_\ell}{RT} \right]} \quad (2.20)$$

$$S_\ell = \frac{1}{\ell} [i S_{A\ell} + j S_{B\ell} + R \ell n \frac{\ell!}{i!j!} + \Delta S^E]$$

$$E_\ell = \frac{1}{\ell} [i E_{A\ell} + j E_{B\ell} + \Delta E^E]$$

Where $S_{A\ell}$ and $E_{A\ell}$ are the standard difference of entropy and energy for pure A at coverage equivalent to i molecules of A plus j molecules of B. If the binary solution in the adsorbed phase behaves ideally then $S^E = E^E = 0$. In other cases appropriate expressions for the excess entropy and enthalpy need to be included.

2.2.6 IDEAL ADSORPTION SOLUTION THEORY

This theory does not provide a pure component isotherm, rather it uses the pure component equilibrium data (or equation) to predict the behavior of the binary mixture at the same temperature and on the same adsorbent. It was originally proposed by Myers and Prausnitz [2,26]

and applied to adsorption on molecular sieves by Glessner and Myers [20]. By introducing the concept of spreading pressure and assuming that the sorbed mixture forms an ideal solution at constant spreading pressure one may arrive, for binary mixtures, at a set of 7 equations in 9 variables which can be solved if any two variables are known. The concept of spreading pressure is replaced by energy term for microporous sorbents.

The Gibbs adsorption equation for one component is [27]

$$-d\theta + C d\mu + S dT = 0 \quad (2.21)$$

Integration of this expression at constant temperature gives

$$\theta_i = RT \int_0^{P_i^0} \frac{C_i}{P} dP \quad (2.22)$$

Where C_i is the adsorption isotherm for pure component i , and P_i^0 is the equilibrium pressure of pure i . In Eq 2.22 and the derivation to follow, it is assumed that the gas phase obeys the perfect gas law both for the adsorption of the pure gas components and the adsorption of the mixed gas. The pressures of interest in most experimental studies of adsorption are usually less than the atmospheric pressure; therefore, this is usually an excellent approximation. The integral in Eq 2.22 yields two relationships

$$\theta_1 = f(P_1^0) \quad (2.23)$$

$$\theta_2 = f(P_2^0)$$

The equilibrium equation for mixed-gas adsorption

$$Py_i = \gamma_i x_i P_i^0 \quad (2.24)$$

In the case of an ideal solution for which the method is named, the activity coefficient is equal to unity for all values of T, P , and x_i , Eq 2.24 simplifies to

$$Py_1 = x_1 P_1^0$$

$$Py_2 = x_2 P_2^0 \quad (2.25)$$

Since the adsorption takes place at constant energy

$$\theta_1 = \theta_2 \quad (2.26)$$

Also

$$x_1 + x_2 = 1$$

$$y_1 + y_2 = 1$$

(2.27)

There nine unknowns : $\theta_1, \theta_2, P_1^0, P_2^0, P, x_1, x_2, y_1$, and y_2 . Equations 2.23, 2.25, 2.26, 2.27 are seven independent equations. By specifying two independent quantities such as P, y_1 , it is possible to calculate all of the other variables. For the special case when the pure-component adsorption isotherms are given by an analytical equations of the form

$$c_i = f(P_i^0)$$

(2.28)

the procedure described above yields an analytical relationship between P, x_1 , and x_2

$$\int_0^{\frac{Py_1}{x_1}} f(P_1^0) \frac{dP}{P} = \int_0^{\frac{Py_2}{x_2}} f(P_2^0) \frac{dP}{P} \quad (2.29)$$

2.2.7 VACANCY SOLUTION THEORY

This theory was derived by Suwanayuen and Danner in 1980 [12]. It is based on an imaginary entity that is called vacancy. It is defined as the vacuum which acts as the solvent for the system. Thus the VST treats pure-component adsorption as a phase equilibrium between two binary vacancy solutions of different compositions. By equating the chemical potentials of the two phases and using the Gibbs adsorption isotherm one gets

$$P = \left[\frac{C^*}{K} \frac{\theta}{1-\theta} \right] \exp \left[-\int \frac{d \ln \gamma_v^s}{\theta} \right] \lim_{\theta \rightarrow 0} \exp \int \frac{d \ln \gamma_v^s}{\theta} \quad (2.30)$$

is the activity coefficient of the vacancy in the adsorbed phase.

The mole fractions of the vacancy solution are

$$x_i^s = \theta = C_i / C_i^* \quad (2.31)$$

$$x_v^s = 1 - \theta$$

As with pure component adsorption VST treats the binary adsorption as an equilibrium between two vacancy solutions, but this time there are three components, A, B and the vacancy. The general equation, for multicomponent adsorption, with respect to the activity coefficient is [12] (after correcting it as will be explained in chapter five)

$$y_i P = \gamma_i^s x_i \frac{C_m}{C_m^*} \frac{C_i^*}{K_i} \left[\lim_{C_m \rightarrow 0} \frac{1}{\gamma_i^s} \right] \exp \left[\left[\frac{C_i^* - C_m^*}{C_m} - 1 \right] \ln \gamma_v^s x_v^s \right] \quad (2.32)$$

The experimental mole fraction, x_i is on a vacancy free basis. The relationships between the mole fractions are

$$\begin{aligned} x_i^s &= C_m x_i / C_m^* \\ x_v^s &= 1 - C_m / C_m^* \end{aligned} \quad (2.33)$$

Where

$$C_m^* = \sum x_i C_i^* \quad (2.34)$$

Suwanayuen and Danner used the Wilson model for the activity coefficients, but the resulting isotherm fails to explicitly include the effect of temperature in addition to other difficulties.

Later Cochran, Kabel and Danner used the expression for the excess configurational entropy. Since the excess enthalpy is assumed to be zero, the excess Gibbs energy derived by Flory and Huggins [34,35] is given as

$$\frac{G^E}{RT} = \frac{S^E}{RT} = -x_1 \ln \left[x_1 + \frac{v_2}{v_1} x_2 \right] - x_2 \ln \left[x_2 + \frac{v_1}{v_2} x_1 \right] \quad (2.35)$$

By analogy, the excess Gibbs energy for a binary vacancy solution is obtained by replacing v_1 , v_2 , and x_i by a_1 , a_2 and x_i^s respectively where a is the molar area. The equation for the activity coefficient of the vacancy is found from the usual thermodynamic relations to be

$$\ln \gamma_V^s = \frac{\alpha_{1v} \theta}{1 + \alpha_{1v} \theta} - \ln (1 + \alpha_{1v} \theta) \quad (2.36)$$

Where

$$\alpha_{1v} = \frac{a_1}{a_v} - 1 \quad (2.37)$$

By substituting Eq 2.36 into Eq 2.32 the final adsorption isotherm is obtained

$$P = \frac{C^*}{K} \frac{\theta}{1-\theta} \exp \left[\frac{\alpha_{1v}^2 \theta}{1+\alpha_{1v} \theta} \right] \quad (2.38)$$

For multicomponent vacancy solutions

$$\ln \gamma_i^s = \ln \sum_j \frac{x_i^s}{1+\alpha_{ij}} + \left[1 - \left(\sum_j \frac{x_i^s}{\alpha_{ij+1}} \right)^{-1} \right] \quad (2.39)$$

where

$$\alpha_{ij} = \frac{a_i}{a_j} - 1, \quad \alpha_{ii} = 0$$

From Eqs 2.32 and 2.39 the equation for the distribution of gas species i between the adsorbed and gas phases is obtained

$$y_i P = \gamma_i^s x_i \frac{C_m}{C_m^*} \frac{C_i^*}{K_i} \frac{\exp \alpha_{iv}}{1 + \alpha_{iv}} \exp \left[\left[\frac{C_i^*}{C_m} - \frac{C_m^*}{C_m} - 1 \right] \ln \gamma_v^s x_v^s \right] \quad (2.40)$$

To include the temperature dependency of the three parameters contained in the isotherm model, the following equations are proposed

$$K = K_0 \exp(-q/RT) \quad (2.41)$$

$$c^* = c_0^* \exp(-r/T) \quad (2.42)$$

$$\alpha_{1V} = m_1, C_1^* - 1 \quad (2.43)$$

Where K_0 , q , c_0^* , r and are constants (independent of temperature) to be evaluated by regression of multiple isotherms. Equation 2.41 is the only one of the set which has theoretical basis.

REFERENCES

1. Breck, D. W., "Zeolite Molecular Sieves" , John Wiley & Sons , New York , (1974)
2. Myers, A. L. and Prausnitz, J. M., AIChE Journal 11 , 121, (1965)
3. Gupta, R. K., Kunzru, D. and Saraf, D. N., Ind. Eng. Chem. Fundam., 20 , 28, (1981)
4. Satterfield, C. and Smeets, J., AIChE Journal 20 , 618, (1974)
5. Wakasugi, Y., Ozawa, S. and Ogino, J., J. Coll. Interface Sci., 79(2) , 399, (1981)
6. Menon, P. G. Chem. Rev., 68 , 277, (1968); in "Advances in High Pressure Research", Vol. 3 Academic Press, New York , 313, (1980)
7. Loughlin, K. F., Ph.D. thesis, University of New Brunswick "Sorption in 5A Zeolite" , (1970)
8. Ruthven, D. M. and Loughlin, K. F., J.C.S., Far. Trans. I, 68 , 696, (1972)
9. Loughlin, K. F. and Ruthven, D. M., J. Coll. Interfacial Sci., 30(2) , 331, (1972)
10. Linde Data Sheets for Hydrocarbons, Supplied by Linde Div. of Union Carbide Corp., Tarrytown, New York
11. Barrer, R. M. and Sutherland, J. W. Proc. Roy. Soc., Ser A, 237 , 439, (1956)
12. Cochran, R. L., Kable, R. L. and Danner, R. P., paper 6 f, presented at AIChE's Golden Jubilee Meeting, Washington, November 1st, (1983)
13. Veyssiere, M., and Cointot, A., Bulletin De La Societe Chimique De France, No. 5-6 , 1071, (1975)

14. Hill, T. L. "An Introduction to Statistical Thermodynamics" , Addison-Wesley Publishing Company, Inc., Massachusetts, (1960)
15. Khaleeq, M., M. S. thesis, University of Petroleum & Minerals, "Adsorption of Xylenes on Ba-X Zeolite Pellets " , Dhahran, (1984)
16. LeVan, M. and Vermeulen, T., J. Phys. Chem., 85 ,22 ,(1981)
17. Ross, S. and Olivier, T. , "On Physical Adsorption" , John Wiley & Sons, New York, (1964)
18. Barrer, R. M. "Zeolites and Clay Minerals as Sorbents and Molecular Sieves" Academic Press, London ,(1978)
19. Kiselev, A. V., Plenary Paper-Adsorption & diffusion "Proceedings of the Fifth International Conference on Zeolites" , Naples, (1980)
20. Holborow, K. A., Ph.D. thesis, University of New Brunswick "Multicomponent Sorption Equilibria of Gases in 5A Zeolite" , (1974)
21. Ruthven, D. M., Loughlin, K. F. and Holborow, K. A. Chem. Eng. Sci., 28 ,701,(1973)
22. Schirmer, W., Fielder, K. and Stach, H., ACS Symposium Series No. 40 ,303 ,(1977)
23. Stach, H. ,Thamm, K. and Schirmer, W., Workshop "Adsorption of Hydrocarbons in Zeolites" , Vol. 1, 65, (1979)
24. Loughlin, K. F. and Roberts, G. D. ACS Symposium Series No. 135 ,(1980)
25. Roberts, G. D., M. S. thesis, University of New Brunswick "Sorption Equilibrium of Methane-Krypton in 5A Zeolite" , Frederick, N. B., (1978)
26. Myers, A. L. AIChE Journal, 19 ,666,(1973)

27. Alberty, R. A. and Farrington, D., "Physical Chemistry" , John Wiley & Sons, New York, (1980)
28. Danner , R. P. and Edwin, C. F. Ind. Eng. Chem. Fundam., 17 ,248,(1978)
29. Harlfinger, R., Hoppach, D., Quaschik, U. and Quitzsich, K. Chem. Techn., 35 ,413,(1983)
30. Loughlin, K. F., Holborow, K. A. and Ruthven, D. M., Paper presented at the 74th National Meeting of the AIChE, Tulsa, 1974
31. Hyun, S. H. and Danner, R. P. J. Chem. Eng. Data, 27 ,196,(1982)
32. Danner, R. P. and Wenzel, L. A., AIChE Journal, 15 ,515,(1969)
33. Sorial, G. A., Granville, W. H. and Daly, W. O., Chem. Eng. Sci., 38 ,1517,(1983)
34. Joubert, J. I. and Zwiebel, I., paper 56, Advances in Chemistry Series, 102 , American Chemical Society, Washington, D. C., (1971)

Chapter III

APPARATUS AND PROCEDURE

3.1 CHOICE OF EXPERIMENTAL METHOD

The adsorption isotherm is generally determined directly by one of two methods

1. The volumetric method, or
2. The gravimetric method

In the first method, the quantity of gas admitted to the system is determined from measurements of known volumes, pressure and temperature. After exposing this gas to activated adsorbent the pressure drops eventually to a steady state value. From volumetric knowledge of the moles of gas present in the gas phase before and after adsorption, the quantity adsorbed can easily be calculated when equilibrium is attained. The gravimetric method measures the amount of gas or vapor adsorbed by weighing the sample in a closed system on a balance, generally of the quartz spring type. This balance was first used by McBain and is commonly referred to as the McBain adsorption balance [1].

In the gravimetric method, a buoyancy correction must normally be applied which involves the determination of the volume occupied by the sample. In the volumetric method a big amount of adsorbent is used compared to the gravimetric method. This makes the amount of adsorbate in the gas phase much less than that in the sorbed phase.

This introduces a large error in the calculation of the composition of the adsorbed phase from mass balance. In addition it is difficult to provide good mixing in the gas phase and hence the gravimetric method is not suitable for measuring multicomponent adsorption.

For binary adsorption five quantities must be determined (T , P_A , P_B , C_A and C_B). In this work the temperature and the total pressure were maintained at predetermined values. The partial pressures P_A and P_B were obtained by measuring the gas phase composition using a gas chromatograph, and the partial concentrations C_A and C_B were calculated from mass balances over the sorbed and gas phases for each species.

3.2 THE APPARATUS

The apparatus consist of a number of calibrated volumes, one containing the zeolite sample, a mixing chamber, and ancillary equipment. It can be divided into two sections as shown in Fig 3.1. In section one the gas is prepared to be admitted to section two where adsorption takes place.

3.2.1 SECTION ONE

This section is structured from pyrex glassware with high vacuum stop-cocks. In Fig 3.1 A is the original independently calibrated volume (125.0 cc) which was used as a reference for calibrating the volume of the rest of the apparatus. The three chambers B (1236 cc), C (2235 cc), and D (2309 cc) are provided to give flexibility in the amount of gas to be admitted to section two. To assure the dryness of the gases

before entering these volumes they are passed over beds of molecular sieve 4A. The pressure in this part is measured by a mercury manometer. In binary gas adsorption it is necessary to admit two gases, so a vacuum pump is used to evacuate the relevant volumes, before admitting the second gas. The connections in this section are glass tubes (0.75 cm ID).

Propane and n-butane cylinders were supplied by Matheson. The purity on the n-butane cylinder is indicated as 99.5 mole %. When these gases were analyzed with the GC, propane shows only one peak. However, the analysis of the butane shows two peaks in addition to the butane peak. One is very small (about 0.02 %) and the other is 1% . By further testing it was found that the 1% peak is a propane peak. This fact was taken into account in measuring the binary adsorption data. Since the other peak is a very small one it was neglected.

3.2.2 SECTION TWO

The desired gas enters this section through a Balzers control valve, E (type RME 010) connected to Datametrics 1404 valve controller. The control valve is important in controlling the pressure in this section at a fixed predetermined value in binary adsorption. The zeolite chamber (741 cc\$ without zeolite) is made of stainless steel and placed in a furnace with four heating elements. Chamber G (two chambers were used, due to breakage, one was 1248 cc and the other 1275 cc) is the only part made of glass in this section. The reciprocating pump, manufactured by Metal Bellows Corp. (Model MB-118), circulates the bulk gas phase over the sorbent to achieve uniform gas phase composition in

equilibrium with the sorbed phase. The composition of the gas phase is measured by taking a sample through the sampling point to a Gow-Mac Series 150 gas chromatograph (with a thermal conductivity detector Model 69-150). The GC is connected to a Hewlett Packard 3390A integrater. H, a Datametric Inc. differential pressure sensor of the Barocel gauge type 570-D-2N-VIX having a maximum pressure of 1000 torr(133.3 kPa), was employed to measure the pressure in section two, which is the pressure of the gas in equilibrium with the zeolite. The other side is connected to a high vacuum oil diffusion pump, manufactured by Sargent Welch Scientific Co. (Model No. 1400). A Pirani gauge head (Model No. 6) and a Penning gauge head (Model No. 6), both manufactured by Edwards High Vacuum Ltd. were mounted on the line connected to the diffusion pump to trace the pressure in the regeneration step. The signals from these heads were transmitted to their corresponding Edwards High Vacuum Ltd. Pirani and Penning meters respectively. The range of the Pirani gauge was 3 to 10^{-3} torr (0.400 to 1.33×10^{-4} kPa) and the Penning gauge range was 10^{-2} to 10^{-7} torr (1.33×10^{-3} to 1.33×10^{-8} kPa).

In the begining a Furnatrol temperature controller was connected directly to the zeolite chamber, F, but it was found that due to the time lag between the heating elements and the zeolite in the chamber the temperature continues to vary sinusoidally with time. Hence the temperature controler was connected to the heating elements and the temperature of zeolite was monitored by a Beckman multimeter (Model RMS 3030) which read the temperature to within 0.1 K in the range up to 473 C.

The connections in this section are stainless steel tubes and Speedi-vac fittings (about 1.4 cm ID). The valves and fittings are manufactured by Edwards High Vacuum Ltd.

3.3 PROCEDURE

3.3.1 DETERMINATION OF THE DRY WEIGHT OF ZEOLITE

The following steps were followed in determining the dry weight of zeolite

1. The desired amount (approximately) of the zeolite is placed in a round flask. The weight of the zeolite plus the flask is recorded.
2. The flask is put in a furnace and heated to about 623 K under vacuum.
3. After two or three days the flask is taken out from the furnace after sealing, cooled, and weighed.
4. Step 4 is repeated, at shorter intervals of time, until a constant weight is reached.
5. The zeolite is removed from the flask and the weight of the dry zeolite is found by subtracting the final weight of the empty flask from the weight found in the previous step.

3.3.2 CALIBRATION OF DIFFERENT VOLUMES

In studying adsorption by the volumetric method the volumes of different chambers have to be known. A chamber with a known volume is

used to find the volumes of the other chambers. This reference volume, A in Fig. 3.1 was calibrated by filling it with mercury and weighing, and its volume was then found knowing the quantity of mercury needed to fill the chamber and knowing the density of mercury at room temperature. This reference volume was then connected to the rest of section one of the apparatus.

Calibration of chambers B, C, D, G, and F was done by expanding helium, which was negligibly adsorbed at room temperature, into these volumes. To get better accuracy, the electronic manometer was used to measure the atmospheric, initial and final pressures. However this did not allow each volume alone to be calculated; rather a set of five measurements, choosing different combinations of volumes at a time, had to be performed giving five linear independent equations. The volume of each chamber was found by solving these equations simultaneously. This procedure was repeated several times to check the reproducibility.

3.3.3 REGENERATION OF ZEOLITE

Two types of zeolites were used

1. Linde 5A code 69848. The composition is given by Linde as $\text{Ca}_{4.5}\text{Na}_3 [(\text{AlO}_2)_{12} (\text{SiO}_2)_{12}] \cdot 30 \text{H}_2\text{O}$
2. Davison 13X 4-8 mesh beads code 542-08-08-237. This is a NaX faujasite type zeolite. The composition is given by Davison as $\text{Na}_1 [(\text{Al}_2\text{O}_3)_1 (\text{SiO}_2)_{2.8 \pm .2}] \cdot X \text{H}_2\text{O}$

Regeneration is needed to remove any adsorbed molecules on the zeolite. Regeneration was performed by keeping the zeolite chamber at 673 K while applying high vacuum. When the pressure stabilize at about

4×10^{-4} torr (5.33×10^{-5} kPa) the regeneration was considered complete which is consistent with previous studies on these adsorbents.

3.3.4 COMPOSITION CALIBRATION

A calibration curve is needed to find the composition of the gas phase from the area percent found by the integrater connected to the GC. To get the calibration curve section one is filled by propane and n-butane at different ratios (with no zeolite in the system). The gases are mixed by circulating them inside the system for long time. Then a sample of the known composition mixture is taken to the GC where the corresponding area percent is recorded. This data, shown in Table 3.1, is used later in getting the composition from any value of the area percent by Lagrange interpolation. The 1% propane in the butane cylinder was taken into account in calculating the gas phase composition as well as the non-ideality of the mixed gas phase. The data is plotted in Fig 3.2.

3.3.5 MEASUREMENT OF PURE COMPONENT EQUILIBRIUM DATA

Adsorption data of propane and n-butane were obtained at three temperatures 348, 423, 498 K on Linde 5A and Davison 13X zeolites. After regeneration the valve which connects the zeolite chamber to the diffusion pump was closed and the temperature controller was reset to the desired temperature. After that the following procedure was followed

1. Pure gas enters section one (usually chambers A and B only) through the 4A drying bed. When the gas reaches a constant temperature, its pressure is measured using the mercury manometer and hence the initial number of moles is known.

2. When the zeolite temperature reaches 350-320 C the pure gas is admitted to section two. The final pressure in section one is recorded which gives the final number of moles in this section. The difference between the initial and the final number of moles gives the number of moles admitted to section two.
3. When the temperature reaches the desired value and the pressure in section two reaches constant value, the reading of the electronic manometer is recorded. From this pressure reading the number of moles in the gas phase is calculated. The difference between the number of moles in the gas phase and the number of moles admitted to section two is the amount in the adsorbed phase.
4. More gas is admitted to section two and the equilibrium pressure is recorded.
5. Step 4 is repeated until a pressure of about 1000 torr (133 kPa) is reached.

Usually 10 data points are recorded for each isotherm.

3.3.6 MEASUREMENTS OF BINARY MIXTURE ADSORPTION DATA

The procedure for measuring the binary adsorption is as follows

1. After regeneration, pure gas A is admitted to section two through the control valve which controls the pressure in section two at a predetermined value (in this work it is either 66.7 or 106.7 kPa).
2. When equilibrium is established (this can be checked by the fact that no more gas enters section two) the initial

and final pressures in section one are recorded and hence the number of moles of A in section two is known.

3. Chamber G is isolated from the rest of section two and completely evacuated by the vacuum pump connected to section one and the amount of gas left is calculated.
4. The control valve is closed and gas A evacuated from section one. Then gas B is used to purge the relevant volumes from any traces of A through the outlet valve connected to chamber A. This valve is then closed and gas B fills the desired chambers.
5. The control valve allows gas B to enter section two until equilibrium is reached at the desired pressure. The reciprocating pump provides the necessary mixing. Equilibrium is verified by analyzing the gas phase for any change in its composition at intervals of 15 - 30 minutes.
6. The initial and final pressures in section one in addition to the gas phase composition in section two are recorded. The number of moles of B entered section two is calculated from the initial and final pressures in section one. The pressure and composition of the gas phase in section two allow calculating the number of moles of each species in the gas phase. The difference between the amount admitted and the amount left in the gas phase of each species is the amount in the sorbed phase.
7. Steps 3-6 are repeated until the gas phase crosses the

8. To avoid accumulation of error the zeolite is then regenerated and steps 1-7 are repeated starting this time with pure B. In addition to what is mentioned above this step provides a sensitive check on the reproducibility of the data.

The GC was operated at 323 K using a 1.22 m column packed by 20% DC 200 on Chrom.-P. Helium was used as the carrier gas.

It was noticed that equilibrium takes a longer time for the 13X zeolite, even though the micropores of 13X are larger than those of 5A. This can be explained by the difference in the macropore size in the pellets. It is known that the Linde manufactures pellets with larger macropores than Davison [2] and this accounts for the extended time assuming macropore diffusion controls.

**Table 3.1: Calibration Curves for Propane-n-Butane Gas Mixtures
Giving Area Ratio at Different Compositions**

Composition	C_3H_8	Area Ratio
0.000		0.000
0.065		0.062
0.117		0.110
0.335		0.313
0.504		0.466
0.628		0.589
0.800		0.773
0.895		0.878
1.000		1.000

* Area ratio = $A_1 / (A_1 + A_2)$

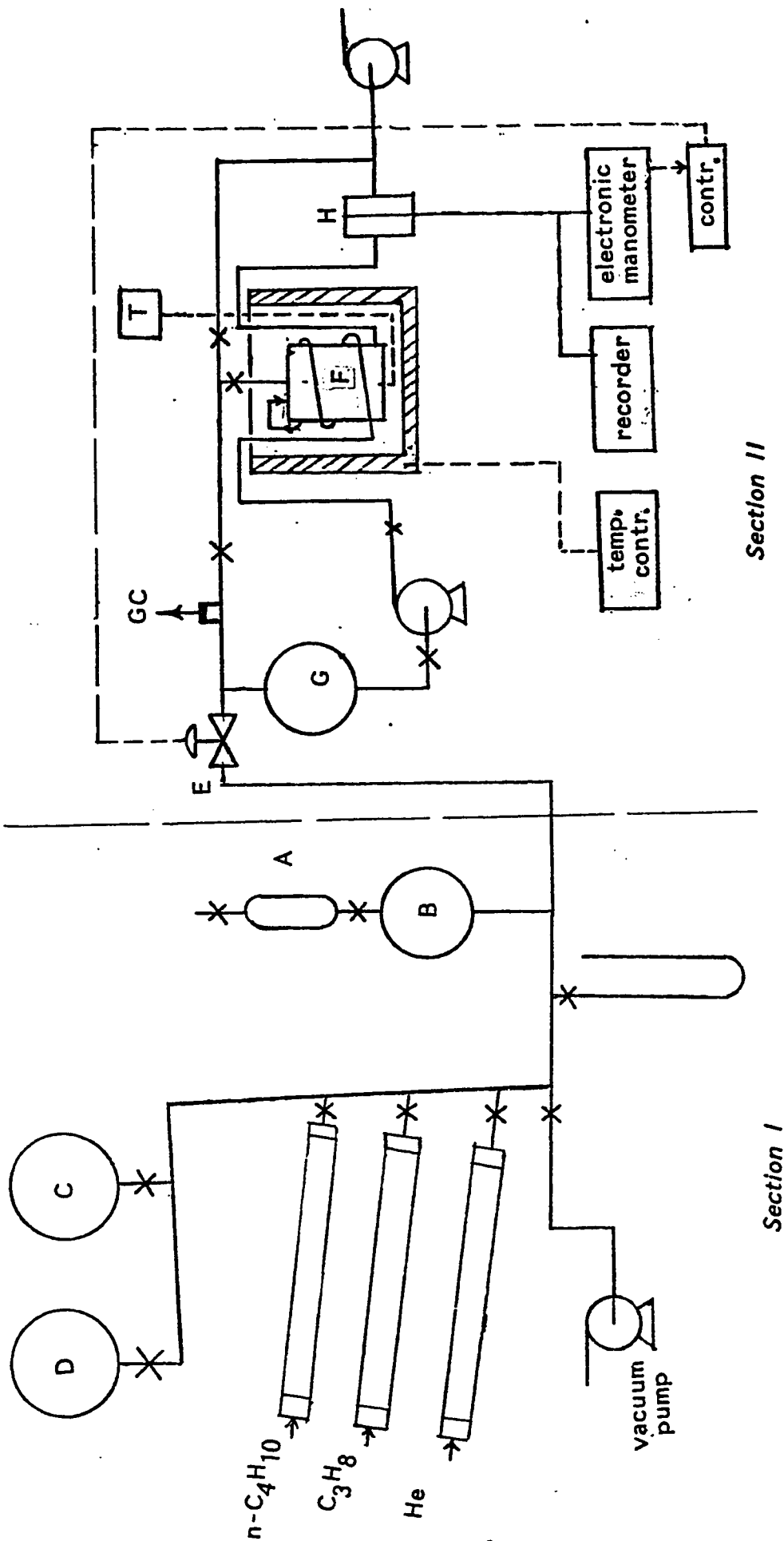


Figure 3.1 Schematic diagram of sorption apparatus.

- A : calibrated volume
 B, C and D : volumes for holding the gas in section I
 E : control valve
 F : zeolite Chamber
 G : glass chamber
 H : Barocel

PLEASE NOTE:

**Page(s) missing in number only; text follows.
Filmed as received.**

U·M·I

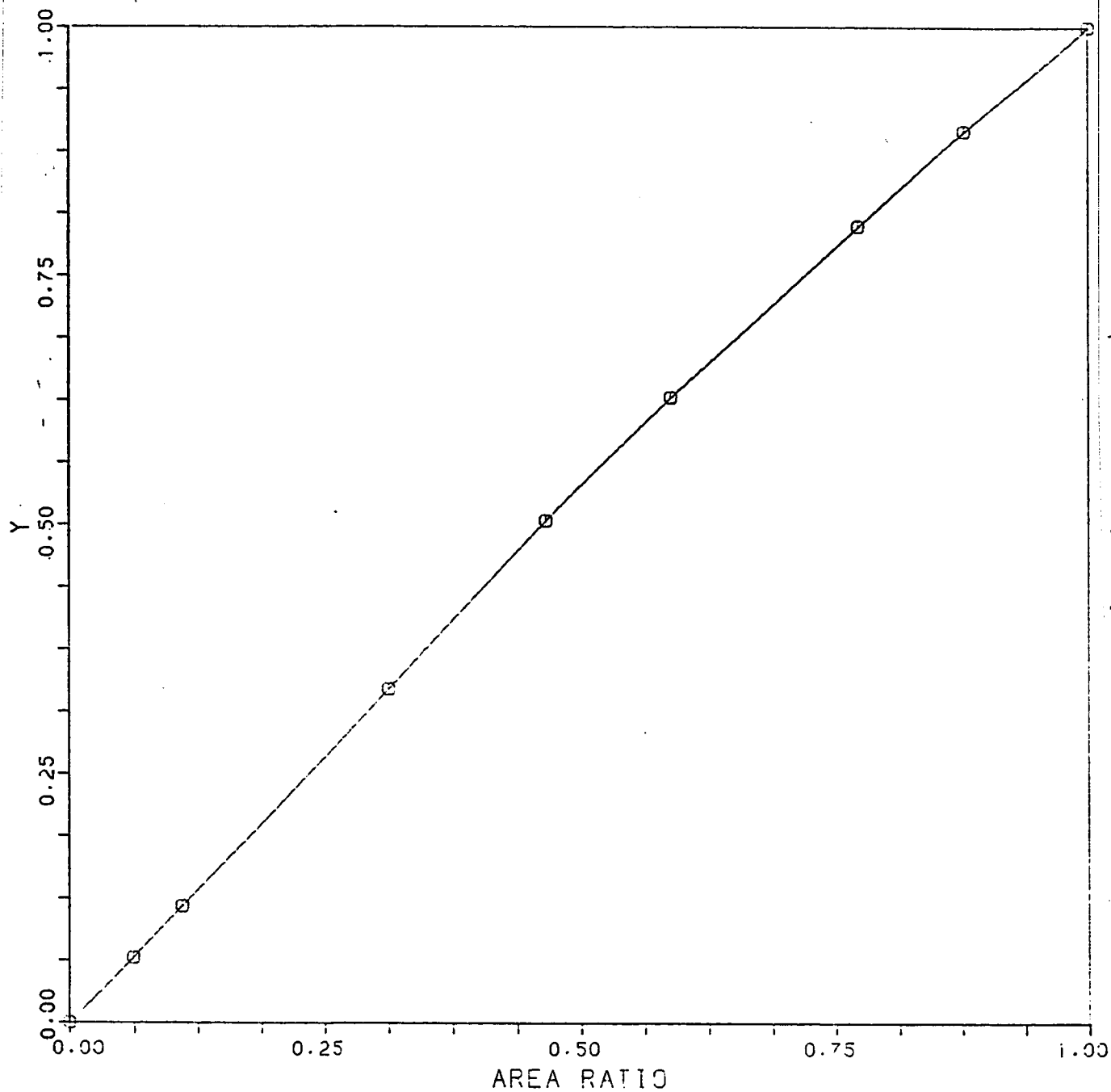


Figure 3.2 TC detector calibration curve for propane-n-butane gas mixture.

REFERENCES

1. Breck, D. W., "Zeolite Molecular Sieves" , John Wiley & sons , New York , (1974)
2. Ruthven, D. M. and Derrah, R. I., The Canadian Journal of Chemical Engineering, 50 , 743, (1972)

Chapter IV

PURE COMPONENT ADSORPTION

The thesis objective is to compare binary data with some models in the literature. However, all of these models use knowledge of pure component isotherms to predict the binary mixture behavior. Therefore, the pure component adsorption data is needed to obtain the parameters for the pure component models.

4.1 REPRODUCIBILITY OF THE DATA

During collection of the data the reproducibility must be carefully verified. The data of propane at 398 K on 5A zeolite was compared with the data of Loughlin [1] which was measured by the gravimetric method. Figure 4.8 shows the good agreement between the two sets of data. Furthermore, the agreement between sorption and desorption measurements and values measured twice using different weights of zeolites as in Figure 4.1 indicates satisfactory reproducibility of the data. Data on the sorption of n-butane on 13X at the commencement of the experiments and at the completion are shown in Fig 4.2 . These data also indicate that good reproducibility is attained.

4.2 NON-IDEALITY OF THE GAS PHASE

The pressure range of the pure and binary data slightly exceeds the atmospheric pressure. To admit the gas to section two of the apparatus a higher pressure is needed in section one. The initial pressure in section one is usually 1.5 times atmospheric. Since the critical temperatures of propane and n-butane are higher than the ambient temperature (370 and 425 K respectively) it is expected that some non-ideality will be exhibited. It was found that the ideal gas law predicts a molar volume which is 2 to 2.5% higher than the real value for propane and 4 to 4.5% higher for n-butane at the conditions mentioned above.

An equation of state is therefore needed to calculate the molar volumes of pure propane and n-butane and their binary mixture. The Chain-of-Rotators equation of state (COR) [2] was chosen because it has been shown to predict successfully the behavior of pure and mixed hydrocarbons including propane and n-butane for a wide range of temperatures and pressures. This equation is described in appendix E. The binary interaction parameter for hydrocarbon mixtures can be calculated fairly accurately by a correlation given by Chien et al.[2]. When the non-ideality of the gas phases in both sections of the apparatus is taken into account, the concentration in the sorbed phase calculated by mass balance increases by 4 to 5% for propane and 9 to 10% for n-butane at the high pressure range.

4.3 PURITY OF THE GASES

As mentioned before it was found that the n-butane cylinder contained 1.0% propane. Unfortunately this was discovered after most of the data had been taken. Since propane and n-butane are both needed for the binary adsorption, the presence of propane as impurity in the butane cylinder can be accounted for easily. However, this is not the case in the pure butane adsorption. Consequently, the adsorption of pure butane on 13X was repeated using another butane cylinder. The purity of this butane is 99.98% as measured by the GC. The results were in agreement with the old data within experimental error, as may be observed in Fig. 4.2 . This suggested that the effect of the 1.0% propane had negligible effect. Hence the adsorption of n-butane on 5A was not repeated.

4.4 PERCENTAGE OF BINDER

When zeolite is manufactured industrially it forms fine crystals (a few microns in diameter). The crystals in this form are like a powder and cause significant pressure drop in packed beds. Therefore, they are usually pelletized using appropriate clay as a binder. In addition the powder form can not sustain the circulation needed for the binary adsorption studies.

The 5A zeolite used is made by Union Carbide, which is known to have 20% binder. The 13X zeolite is made by Davison Company. Parent [3] reported that the percentage of binder can vary from 17 to 20%. To determine the exact percentage the equilibrium adsorption of propane at

298 K and 93.33 kPa (700 torr) was measured and compared with the value reported by Breck [4]. It was found that the percentage of binder was 18%.

4.5 Experimental Estimation of Henry Constant

The Henry constant is defined by

$$K = \lim_{P \rightarrow 0} (C/P) \quad (4.1)$$

At very low pressures all isotherms of adsorption become linear and can be described by Henry's law

$$c = K P \quad (4.2)$$

The slope in the linear region of the isotherm is the Henry constant. However, the pressure required to measure accurate values of the slope is very low and hence other methods are preferred.

Barrer and Lee [9] proposed a virial equation of state to describe the adsorbed phase. When this equation is related to the gas pressure through Gibbs adsorption equation it takes the form

$$P = c/K \exp(A_1 c + A_2 c^2 + A_3 c^3 + \dots) \quad (4.3)$$

where A_i are the virial coefficients and are functions of temperature as a rule. At small concentrations a plot of $\ln(P/c)$ versus c becomes linear with slope of A_1 and intercept of $-\ln(K)$.

4.6 PURE COMPONENTS ADSORPTION DATA

Pure component adsorption data of propane and n-butane on 5A and 13X zeolites were obtained at 398 , 423 , and 498 K and at pressures up to about 133 kPa (1000 torr). The data is tabulated in appendix B. One additional isotherm for propane on 5A was obtained at 398 K to compare this data with data of Loughlin [1]. Henry constant values obtained for each isotherm using the virial isotherm are shown in Figures 4.3 to 4.6 . The K values obtained are tabulated in Table 4.1 . For comparison the Henry constants obtained by Ruthven and Loughlin [5] are shown in Table 4.2 .

The temperature dependence of Henry's law constant is given by

$$K = A e^{\frac{\Delta S_0 T - \Delta H_0}{RT}} = K_0 e^{-q_0/RT} \quad (4.4)$$

where S_0 and H_0 are the entropy and enthalpy changes of adsorption at zero coverage (independent of temperature). To find the values of K_0 and q_0 the values of the Henry constant at various temperatures obtained in this work plus the values given by Ruthven and Loughlin [5] were plotted on a similogarithmic graph versus $1/T$ as shown in Figure 4.7 . The values of K_0 and q_0 obtained by linear least-squares regression are presented in Table 4.1 .

4.7 COMPARISON WITH THEORETICAL MODELS

One of the ultimate aims in gas adsorption is to provide a reliable model which can be used for design applications. In order to verify the reliability of a model it has to be compared with experimental data over wide ranges of temperature and pressure and various sorbate- sorbent systems.

In this work four pure component models were studied. These are

1. Schirmer et al. model [6]
2. Ruthven model [7]
3. Vacancy solution theory [8]
4. Virial model [9]

The details of these models have been given in chapter II. The Schirmer et al. model has $2n$ constants to be evaluated, where n is the maximum number of molecules a cavity can accommodate. One half of the constants represent the entropy change of adsorbate in going from the gas phase to the adsorbed phase and the other half represents the energy change as illustrated in chapter II. For the adsorption of propane and n-butane the heat of adsorption on 5A zeolite is fairly constant (independent of coverage). Therefore, the energy constants are taken to be equal ($E_1 = E_2 = \dots = E_n$)

The entropy constants should be restricted to have an order $S_1 > S_2 > \dots > S_n$ on the basis of thermodynamic considerations[10]. Schirmer et. al. [6] indicate that these constants can be derived from physical or statistical thermodynamic considerations, but do not advise

this procedure since theoretical calculations of molecules adsorbed on zeolites are, at present, at least only approximate, and it is in practice more convenient to determine the constants by matching the theoretical equations to experimental isotherms [10].

The Ruthven isotherm has two parameters. The Henry constant K , and the molecular volume . In this work the molecular volume is assumed to be a linear function of temperature

$$\beta = a + bT \quad (4.5)$$

The dependence of the Henry constant on temperature is given in Eq 4.4

In the virial model Barrer and Lee [9] assumed that the virial coefficients are linear functions of temperature. Here it is assumed that they are independent of temperature. This implies that the heat of adsorption is independent of concentration and temperature and equal to the heat of adsorption at zero coverage. This can be seen from the equation relating the heat of adsorption to the isotherm equation

$$\left(\frac{\partial \ln P}{\partial (1/T)} \right)_c = \frac{q_{ISO}}{R}$$

The virial equation is a special case of the general equation

$$P = f(c)/K = f(c)/ [K_0 \exp(-q_0/RT)] \quad (4.6)$$

and hence

$$q^{iso} = q_0 \quad (4.7)$$

As mentioned before the heat of adsorption of propane and n-butane is fairly constant which means that this assumption is good for the systems studied. In fitting the virial isotherm to the experimental data it was found that two virial coefficients are sufficient. In some cases they give a better fit than three coefficients. The form of the virial coefficients as a linear function of temperature suggested by Barrer and Lee was tried on propane on 5A and 13X. However, compared to taking the virial coefficients as temperature independent, the fit was as good for 5A and slightly better for 13X.

The constants in these models are non-linear and often cannot be linearized, i. e. they cannot be put in the form

$$Y = a_1 f_1 + a_2 f_2 + \dots + a_i f_i \quad (4.8)$$

Therefore, evaluation of these constants from experimental isotherms requires non-linear multivariable least squares regression techniques. This is usually carried out by using an optimization subroutine which minimizes an objective function that reflects the difference between the experimental and theoretical values. In this work a subroutine called BSOLVE was used [11,12]. It was developed specifically for non-linear least squares fitting. It combines the Newton-Raphson method which converges rapidly for a good initial guess and the gradient method which converges for a poor initial guess.

Different objective functions have been used in this work since the explicit variable is not the same for all models. The Schirmer et al. and Ruthven models are explicit in concentration while the vacancy and virial models are explicit in pressure. The objective functions used can be written in the form

$$O.F. = \sum_{i=1}^N \left(1 - \frac{g_{i, \text{exp}}}{g_{i, \text{theo}}}\right)^2 \quad (4.9)$$

where N is the number of data points, $g = c$ for Schirmer et al. and Ruthven models $g = \ln(P)$ for the vacancy model, and $g = \ln(P/c)$ for the virial model. The choice of $g = \ln(P/c)$ for the virial model linearizes the constants in this case.

4.8 EXPERIMENTAL DATA FROM LITERATURE

In testing the models it is desirable to have data for a wide range of temperature and pressure, and hence it was decided to include data from the literature. However, in adsorption on zeolites one has to check for the consistency of the data since the adsorption capacity of a zeolite may be affected by two factors :

1. The origin of the zeolite. Duplication of results in synthesizing zeolites is difficult [13]. This affects the capacity of different samples prepared at different laboratories as reported by Ruthven and et. al. [14]. The same behavior is reported for samples of natural zeolites obtained from different places [15].

2. The percentage and type of binder used, because the binder may participate in sorption and hence alter the capacity and heat of adsorption [16]

To check the consistency, the data of this work along with other sets from literature was plotted on the same graph in Figures 4.8 to 4.11. The data is then fitted to the virial model and plotted as c versus (KP) . If the data fall on the same curve then the data is consistent. The data of each study was compared with the data obtained in this work. Examples of inconsistency of the isotherms from literature are

1. Some isotherms at different temperatures cross each other as in
 - a. The isotherms at 308 and 323 K for n-butane on 5A zeolite.
 - b. The isotherms at 398 and 412 K for n-butane on 5A zeolite.
 - c. The isotherms at 303 and 328 K for n-butane on 13X zeolite.
2. Some isotherms at lower temperature come below others at higher temperature, as in
 - a. The isotherm at 298 K (of Breck) comes below the isotherm at 308 K for propane on 13X.
 - b. The isotherm at 303 K comes below the isotherm at 313 K for n-butane on 13X.

3. Some isotherms at the same temperature show noticeable difference, and some at different temperatures fall on each other, as in
 - a. The isotherms at 298 K for n-butane on 13X show noticeable difference
 - b. The isotherms at 348 and 358 K for n-butane on 5A fall on each other

The fact that the isotherms from different laboratories are not always consistent does not necessarily mean that the data from a particular laboratory is not consistent in itself. For example Figure 4.12 shows the consistency of the Loughlin data [1].

After testing some data from the literature it was found that the only data which is consistent with the data obtained here is the Loughlin data for propane on 5A [1]. The data used in the least squares fitting are

1. Propane on 5A : nine isotherms at eight different temperatures. Five isotherms are from Loughlin data and four from this work.
2. Propane on 13x : the three isotherms measured in this work.
3. n-Butane on 5A : the three isotherms measured in this work.
4. n-Butane on 13X : the three isotherms measured in this work.

4.8.1 MODELING THE DATA USING THE EXPERIMENTAL HENRY CONSTANTS

One of the parameters in the Ruthven , vacancy and the virial models is the Henry constant. In the Schirmer et al. the Henry constant is derived from the first entropy and energy constants. Hence all the models can be related to K_0 and q_0 through the Van't Hoff equation. If K_0 and q_0 are treated as adjustable constants then each model gives a different set of values. However, this is not true physically since the Henry constant reflects the sorbate sorbent interactions and is independent of the model. A more sound test of the models is to fix the value of the Henry constant equal to the experimental value and optimize the other parameters.

The values of K_0 and q_0 are found by plotting the experimental values of the Henry constant versus $1/T$ on a semilogarithmic plot as shown in Figure 4.7 . The values of Henry constant for propane and n-butane on 5A given in Ruthven and Loughlin [5] were used in addition to the values obtained in this work to find K_0 and q_0 . The values of K_0 and q_0 obtained are shown in Table 4.1 .

4.8.2 FITTING THE SORPTION DATA

For each system two sets of parameters were obtained. One with the experimental Henry constant or the heat of adsorption in the case of Schirmer et al. isotherm and the other with the optimized values. In all cases except for the Ruthven and the vacancy models for propane on 13X the optimized values of K_0 and q_0 give better fit as can be seen from Figures 4.13 to 4.28 and Table 4.2. The parameters found from

least squares fitting are given in Tables 4.4 to 4.7 For the virial model the data are plotted in the generalized form (all the isotherm as one curve).

Since a non-linear optimization is involved local minima may exist, and therefore, several initial guesses were tried to ensure that the global minimum is found. The heat of adsorption for n-butane on 5A and 13X zeolites is the same. For propane a small difference was observed. This consistency may be explained by the fact that these gases are non-polar and their interactions with the zeolite are mostly with the oxygen rings. If the sorbates were polar then the heats of adsorption would have been different since the two zeolites have different cations.

In general the best fit is obtained for the Schirmer et al. isotherm. The other models show good fit in one place and not as good in others. The fit for propane in general is better than that for n-butane. This may be due to the fact that n-butane has a higher critical temperature and hence exhibits more non-ideality in the sorbed phase. Among the four systems studied the best fit is found for propane on 13X.

The Schirmer et al. and Ruthven models show a better fit for the 5A zeolite with the exception of the Ruthven model for n-butane when the experimental Henry constant is used where it shows a better fit for the 13X zeolite. This is consistent with the assumption in these models that each cavity is independent of the others. The 13X zeolite has a

more open structure which allow for more interactions between molecules in different cavities.

The form of the virial equation presented here is successful for the systems studied here. It provides a good method for testing the consistency of isotherms at different temperatures. In addition it gives a better generalized form of the data than Polanyi in which the data fall within a band rather than on one curve. It can be extended to systems in which the heat of adsorption is a function of concentration and still give the generalized form.

TABLE 4.1

VALUES OF HENRY CONSTANT AND HEAT OF ADSORPTION OBTAINED IN
THIS WORK

sorbate	sorbent	T	Henry Constant	$K_0 \times 10^6$	q_0
propane	5A	498	0.021	5.2	35.4
		423	0.133		
		398	0.263		
propane	13X	498.	0.016	6.8	32.2
		423.	0.064		
		348.	0.466		
n-butane	5A	498.	0.118	3.5	44.4
		423.	4.507		
		348.	22.07		
n-butane	13X	498.	0.0461	1.1	44.4
		423.	0.379		
		348.	4.811		

T in K

K in molecules/cavity/kPa

K_0 in molecules/cavity/kPa

q_0 in J/mole

TABLE 4.2

VALUES OF HENRY CONSTANT AND HEAT OF ADSORPTION FROM REF [5]

sorbate	temp./K	K /(molecule/cavity Torr)	K_0 /(molecule/cavity Torr)	q_0 /kcal
C_3H_8	273	3.96 (4.39)	1.24×10^{-6}	8.1
	273	3.82 (4.43)		
	323	0.321 (0.375)		
	358	0.117 (0.136)		
	358	0.123 (0.143)		
	398	0.033 (0.037)		
	323	6.24	8.6×10^{-7}	10.2
	323	10.29		
	358	1.87		
	358	3.11		
n- C_4H_{10}	398	0.369		
	398	0.374		
	423	0.175		
	498	0.0176		
	308	12.43		
	318	6.53		
	328	3.87		

TABLE 4.3

AVERAGE DEVIATION IN FITTING THE MODELS *

system	Schirmer		Ruthven		vacancy		virial	
	q_{opt}	q_{exp}	K_{opt}	K_{exp}	K_{opt}	K_{exp}	K_{opt}	
propane on 5A	.039	.059	.057	.066	.091	.125	.071	.097
propane on 13X	.030	.065	.082	.085	.023	.020	.043	.053
n-butane on 5A	.032	.044	.053	.155	.113	.118	.134	.150
n-butane on 13X	.054	.070	.097	.121	.091	.148	.119	.146

*average deviation = $(O.F./N)^{1/2}$

O.F. is the minimum value of the objective function

N is the number of data points

N = 82 for propane on 5A

N = 30 for propane on 13X

N = 29 for n-butane on 5A

N = 60 for n-butane on 13X

K_{opt} :SS for optimized Henry constant

K_{exp} :SS for experimental Henry constant

TABLE 4.4

ENTROPY AND ENERGY CONSTANTS FOR THE SCHIRMER ET AL. MODEL

system		$-S_1$	$-S_2$	$-S_3$	$-S_4$	$-S_5$	$-S_6$	
propane on 5A	q_{opt}	51.28	55.54	60.01	66.17	73.94	82.28	31613
	q_{exp}	58.25	64.39	68.81	75.60	84.32	93.21	35400
propane on 13X	q_{opt}	52.24	55.26	59.11	62.10	66.22	74.10	30130
	q_{exp}	56.90	59.64	63.75	67.02	71.65	78.84	32200
n-butane on 5A	q_{opt}	56.32	64.99	72.39	84.01	118.19	-	40819
	q_{exp}	63.48	72.25	80.28	92.57	130.00	-	44400
n-butane on 13X	q_{opt}	68.26	71.18	75.58	82.76	95.65	-	42423
	q_{exp}	72.28	75.84	79.79	87.41	100.29	-	44400

S in J/mole/K

E in J/mole

TABLE 4.5
CONSTANTS FOR THE RUTHVEN MODEL

system		$K_0 \times 10^6$	$-q_0$	a	$b \times 10^3$
propane on 5A	K_{opt}	5.09	35957.	.1362	0.0000
	K_{exp}	5.26	35400.	.1363	0.0000
propane on 13X	K_{opt}	4.780	34350.	.1214	0.0012
	K_{exp}	6.800	32200.	.0946	0.0000
n-butane on 5A	K_{opt}	2.090	44266.	.1338	0.0893
	K_{exp}	3.500	44400.	.1290	0.1006
n-butane on 13X	K_{opt}	2.170	43414.	.1470	0.0243
	K_{exp}	1.100	44400.	.1533	0.0026

K_0 in molecules/cavity/kPa

q_0 in J/mol

a in nm^3

b in nm^3/K

volume of the 5A zeolite cavity = $.776 \text{ nm}^3$

volume of the 13X zeolite cavity = $.822 \text{ nm}^3$

TABLE 4.6
CONSTANTS FOR THE VACANCY SOLUTION MODEL

system		$K_0 \times 10^6$	$-q_0$	c_0^*	r_1	m_1
propane on 5A	K_{opt}	34.65	28756.	3.92	116.5	0.0077
	K_{exp}	5.26	35400.	3.41	145.4	0.0027
propane on 13X	K_{opt}	6.21	32470.	4.85	00.0	0.1603
	K_{exp}	6.80	32200.	4.86	00.0	0.1905
n-butane on 5A	K_{opt}	4.79	39747.	3.95	17.6	0.0075
	K_{exp}	3.50	44400.	3.37	00.0	1.1540
n-butane on 13X	K_{opt}	0.65	47081.	3.60	38.9	0.0659
	K_{exp}	1.10	44400.	3.99	00.0	0.1146

K_0 in molecules/cavity/kPa

q_0 in J/mol

c_0^* in molecules/cavity

r_1 in K

m_1 in cavities/molecule

TABLE 4.7
CONSTANTS FOR THE VIRIAL MODEL

system		$K_0 \times 10^6$	$-q_0$	A_1	A_2
propane on 5A	K_{opt}	3.50	35430.	-0.1863	0.2705
	K_{exp}	5.26	35400.	0.0271	0.2430
propane on 13X	K_{opt}	4.07	33380.	-0.1500	0.1460
	K_{exp}	6.80	32200.	0.0168	0.1094
n-butane * on 5A	K_{opt}	2.63	39533.	-0.6139	0.5204
	K_{opt}	0.049	57348.	-0.7564	0.7580
	K_{exp}	3.50	44400.	1.2030	0.1243
n-butane on 13X	K_{opt}	0.44	45673.	-0.8518	0.4733
	K_{exp}	1.10	44400.	-0.3712	0.3754

K_0 in molecules/cavity/kPa

q_0 in J/mol

A_1 in cavities/molecule

A_2 in (cavities/molecule)²

* data of Loughlin [1]

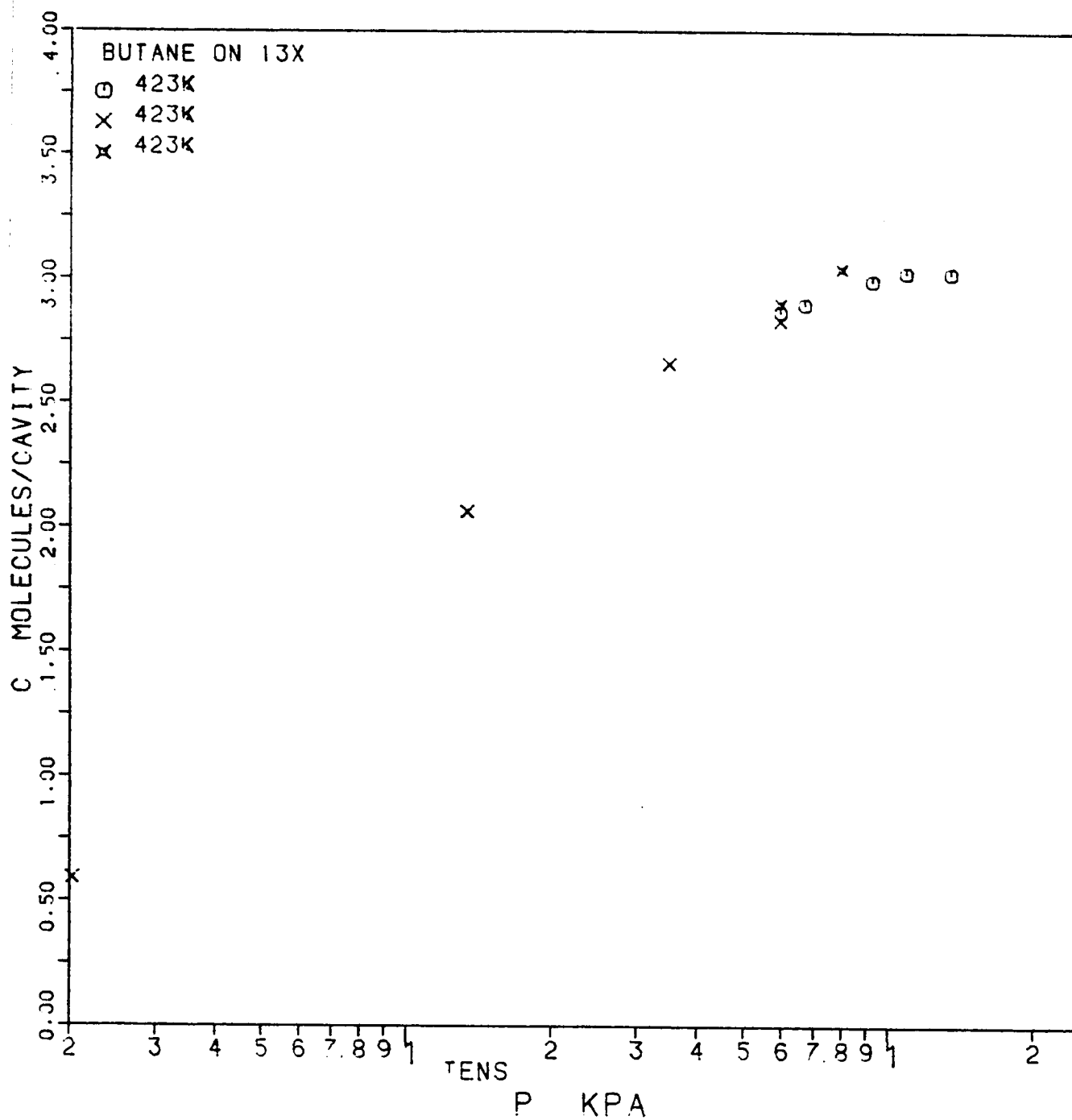


FIGURE 4.1 Pure component sorption isotherm for n-butane on 13X zeolite at 423 K. Run 1 (⊙), run 2(X) and desorption data (x)

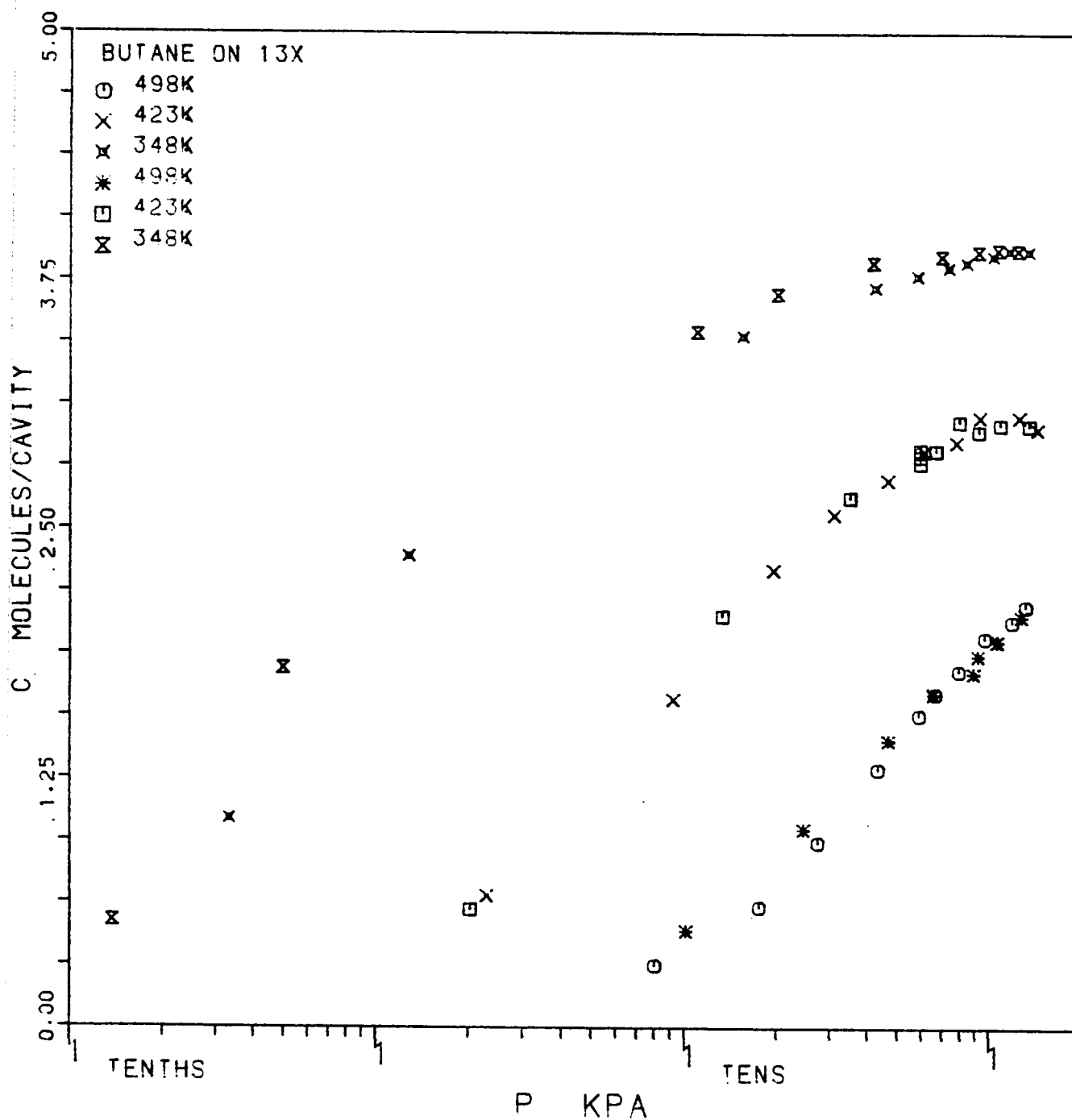


FIGURE 4.2 Pure component sorption isotherm for n-butane on 13X zeolite. Pure n-butane(○ × ✕) and n-butane containing 1% propane(* □ ⦿)

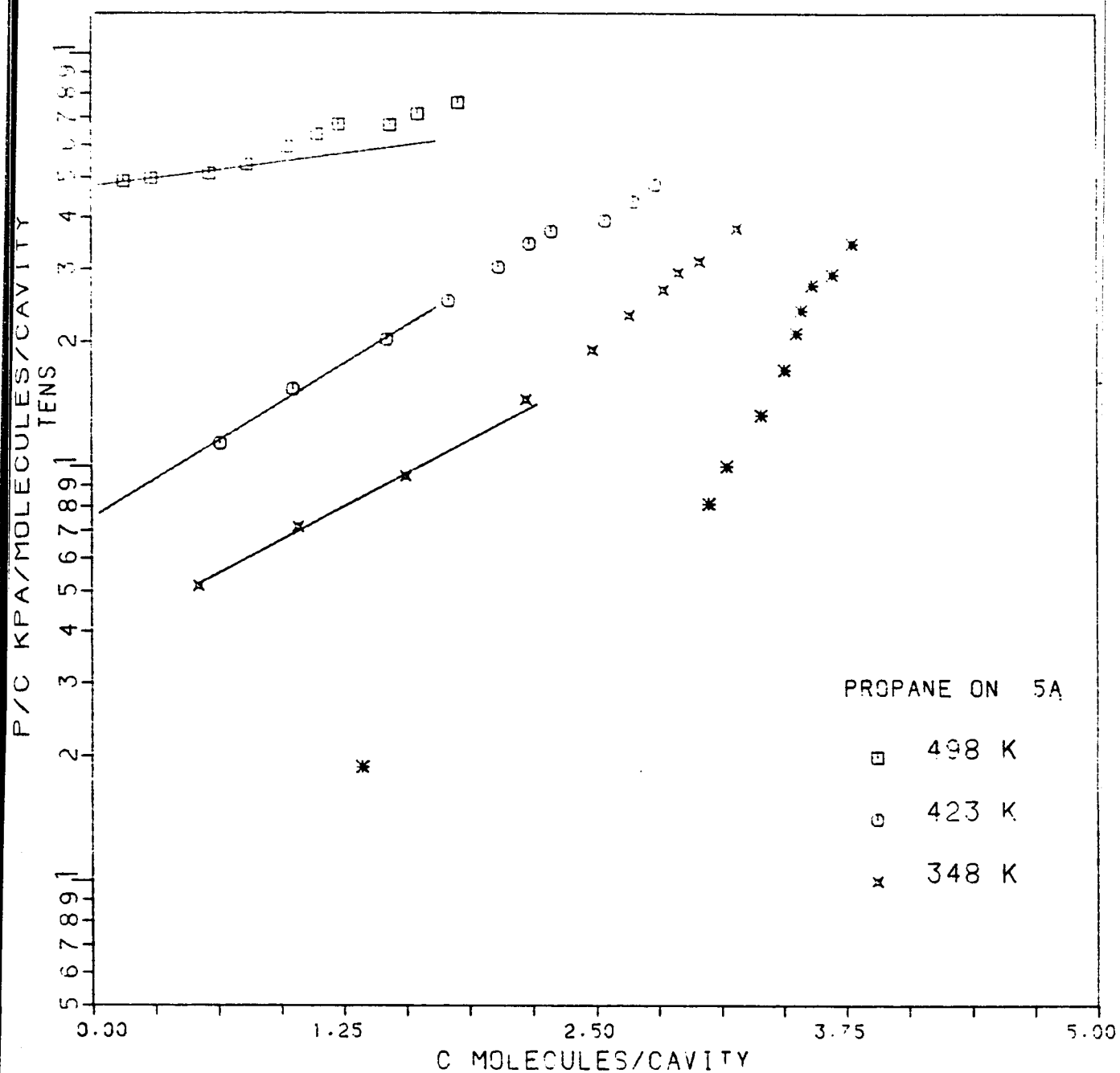


FIGURE 4.3 Virial plot for propane on 5A zeolite.

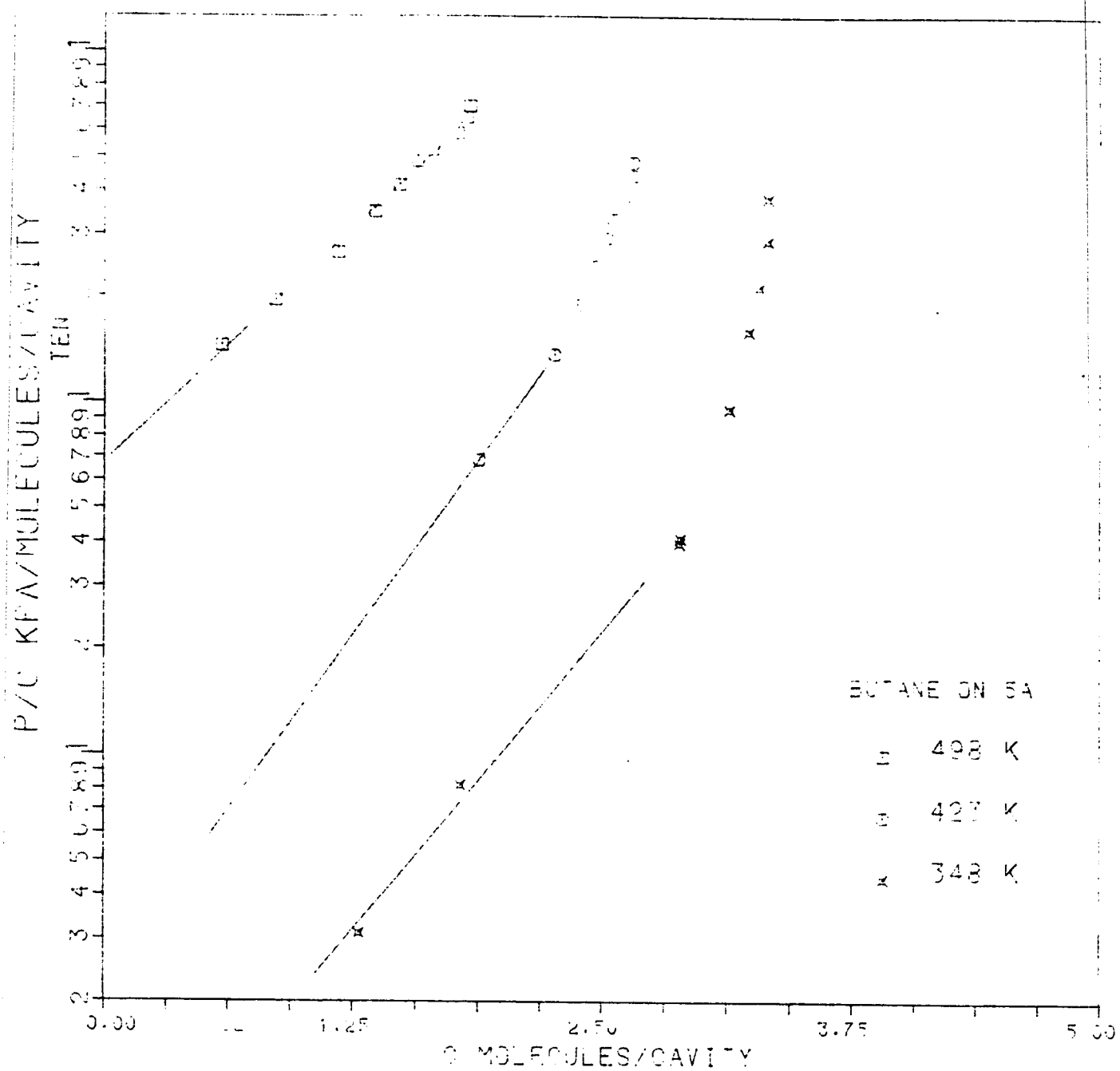


FIGURE 4.4 Virial plot for n-butane on 5A zeolite.

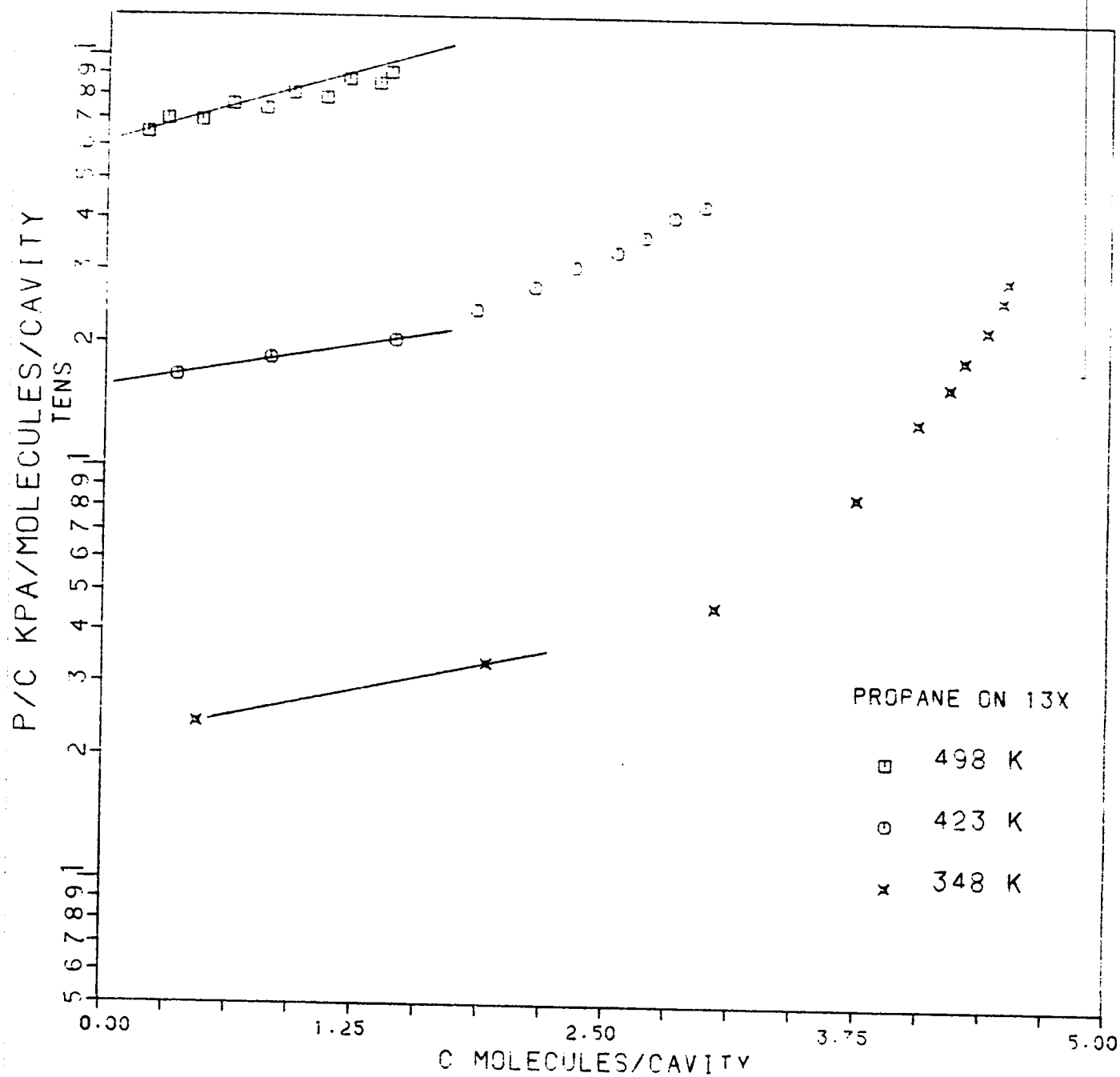


FIGURE 4.5 Virial plot for propane on 13X zeolite.

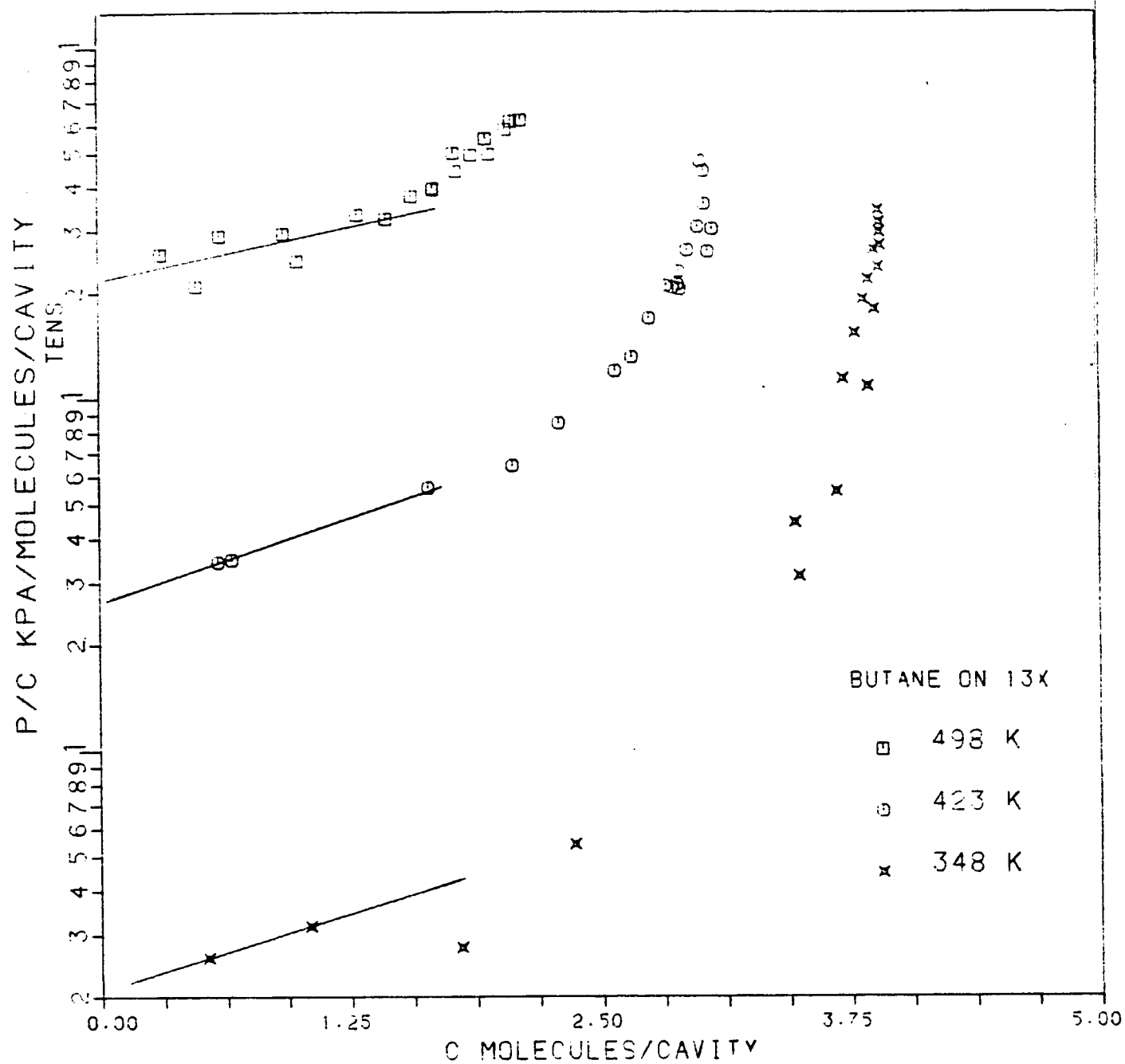


FIGURE 4.6 Virial plot for n-butane on 13X zeolite.

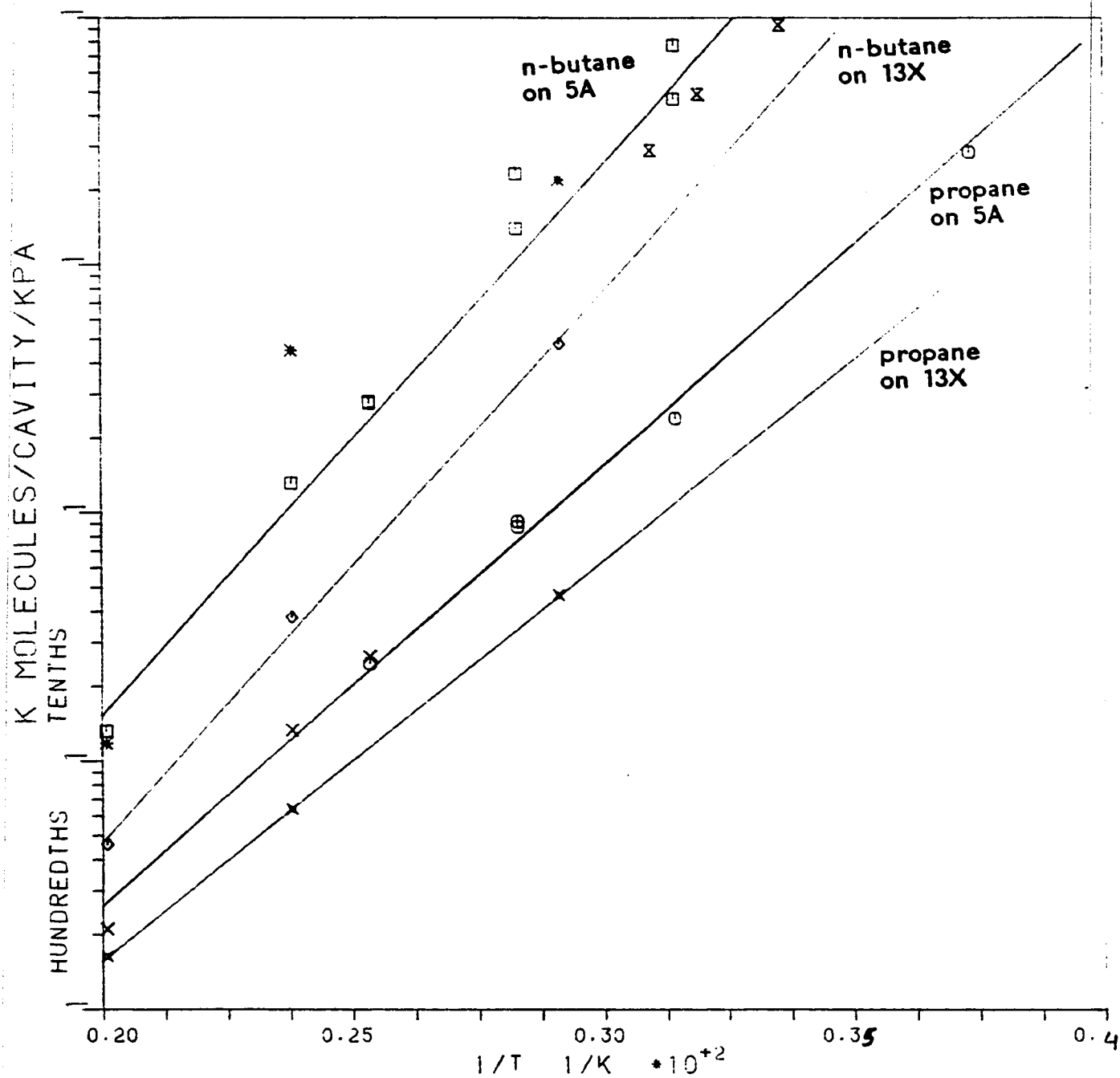


FIGURE 4.7 Van't Hoff plot of Henry constants. Data of this work ($\times \times \circ \ast$), Ruthven et al. ($\square \ominus$) and Glessner (\times).

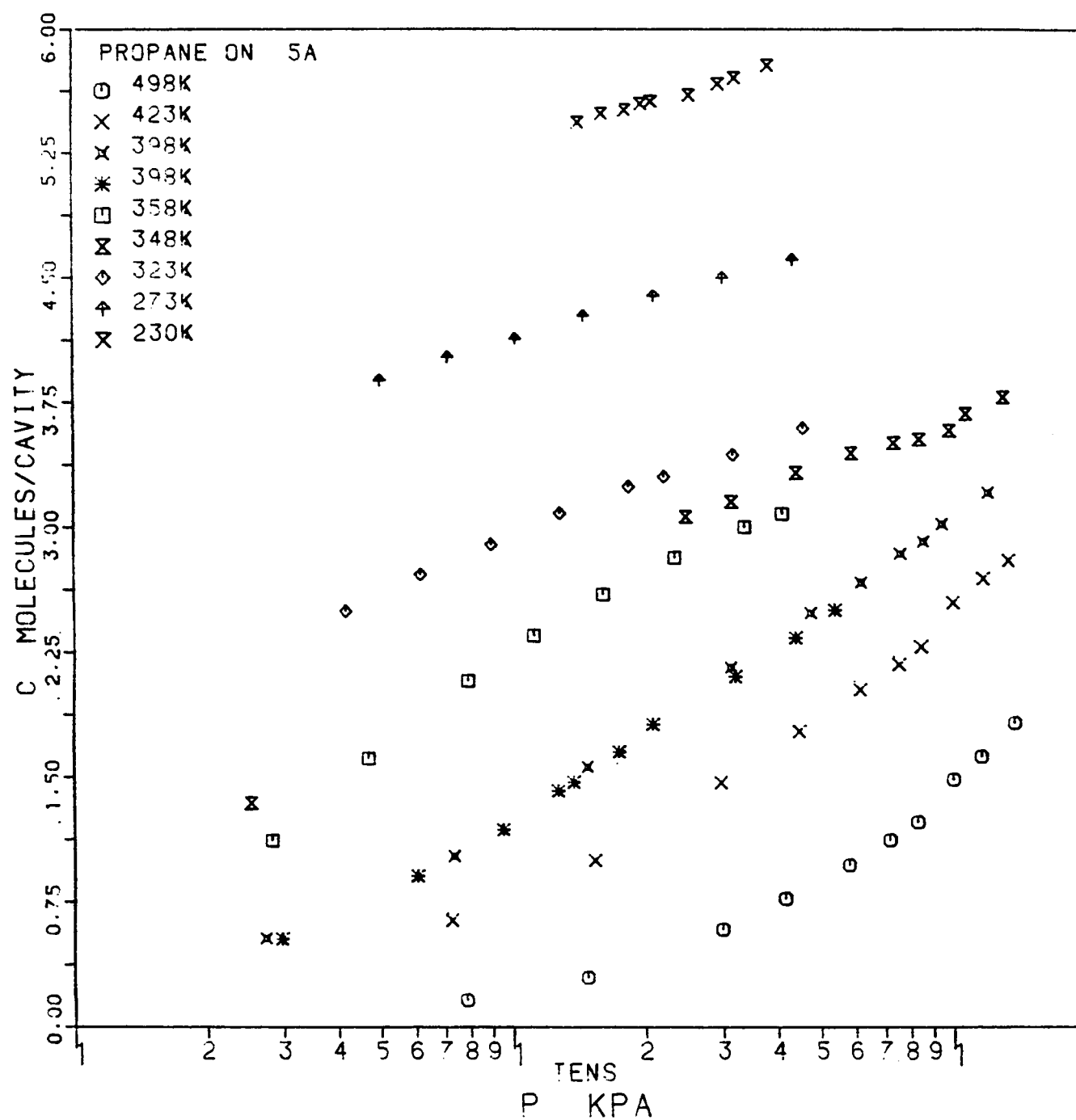


FIGURE 4.8 Pure component sorption isotherms for propane on 5A zeolite. Data of this work (○ × × ×) and Loughlin (* □ ◇ † ×) [1].

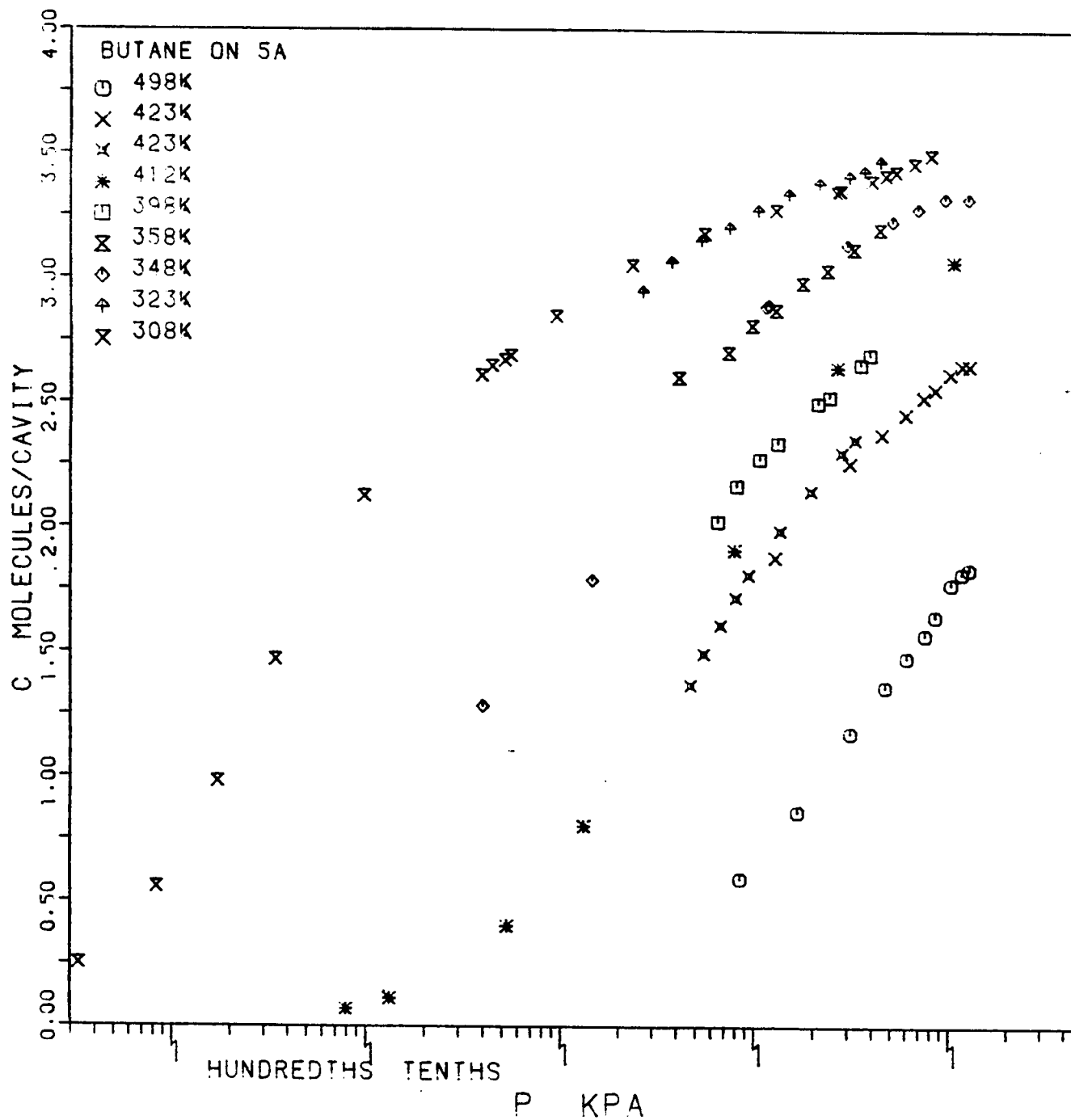


FIGURE 4.9 Pure component sorption isotherms for n-butane on 5A zeolite. Data of this work (○ × ◇), Loughlin (⊗ ⊗ □ ⬢) [1], Glessner (⊗) [20] and Anderson (*) [21].

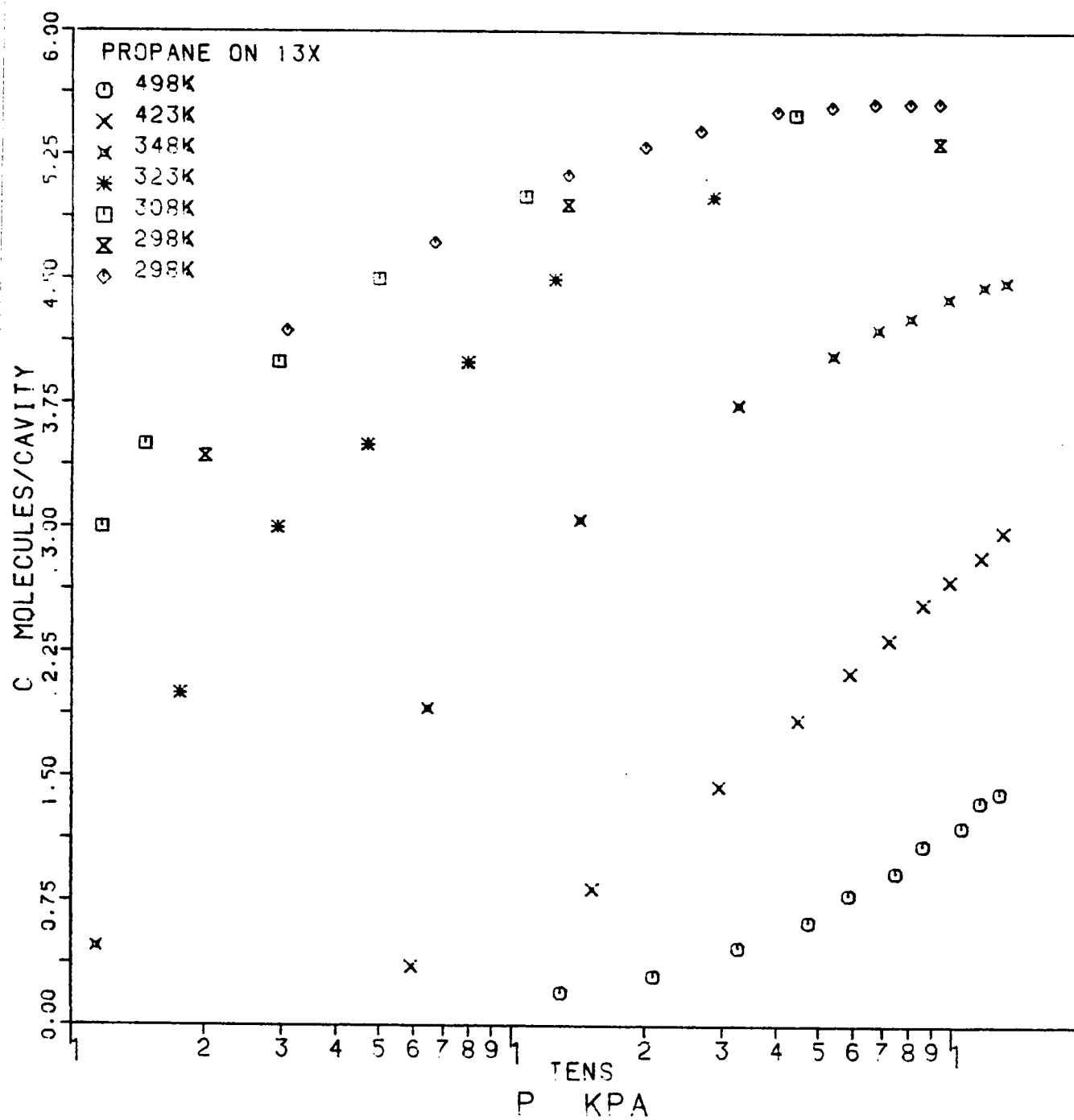


FIGURE 4.10 Pure component sorption isotherms for propane on 13X zeolite. Data of this work (○ × *), Barrer (* □) [18], Breck (⊗) [4] and Linde data sheet (◇) [19]

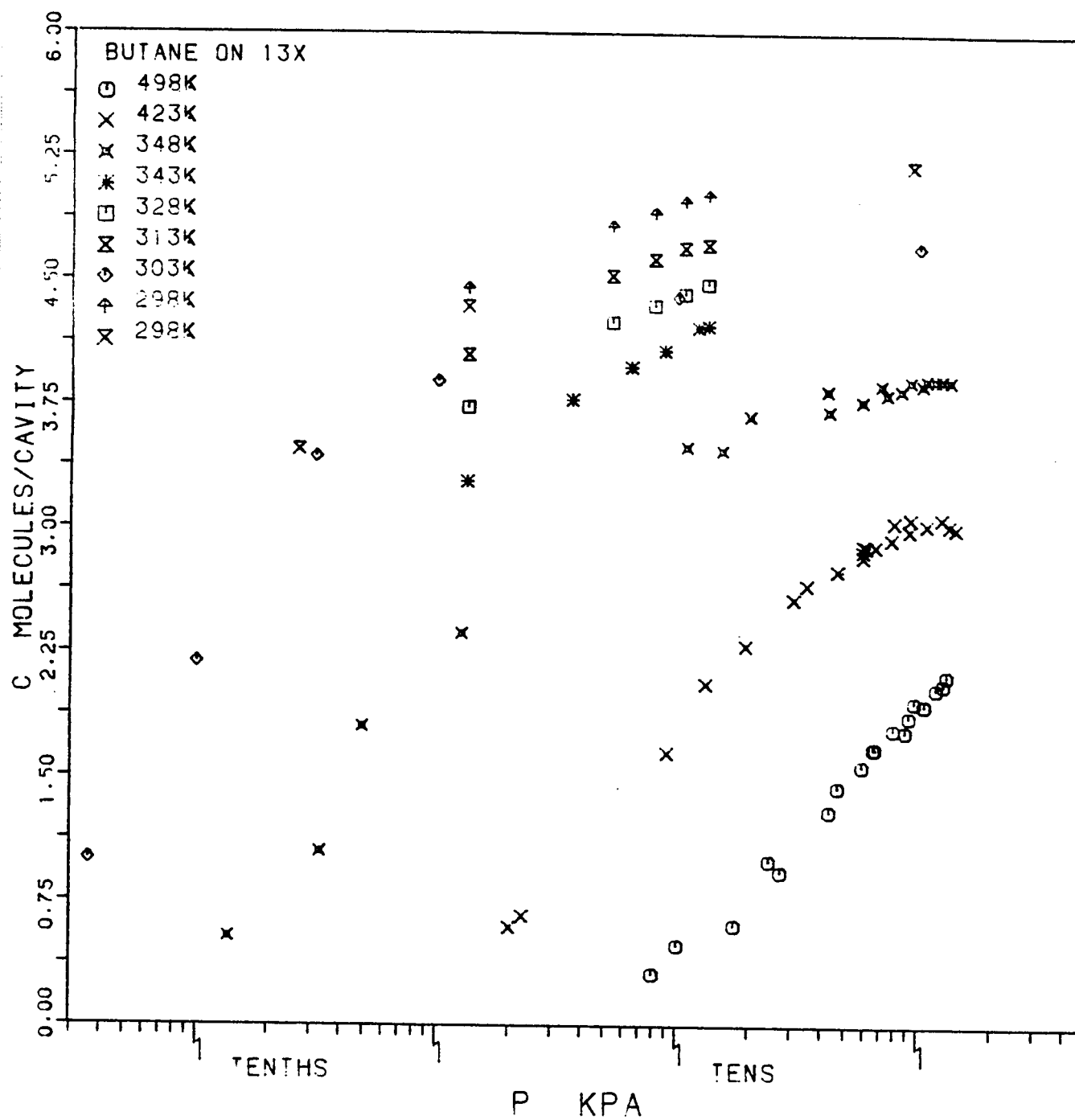


FIGURE 4.11 Pure component sorption isotherms for n-butane on 13X zeolite. Data of this work (○ × ⊗), Barrer (* □ ⊗ ⊕) [16], Breck (⊗) [4] and Harlfinger (◇) [17]

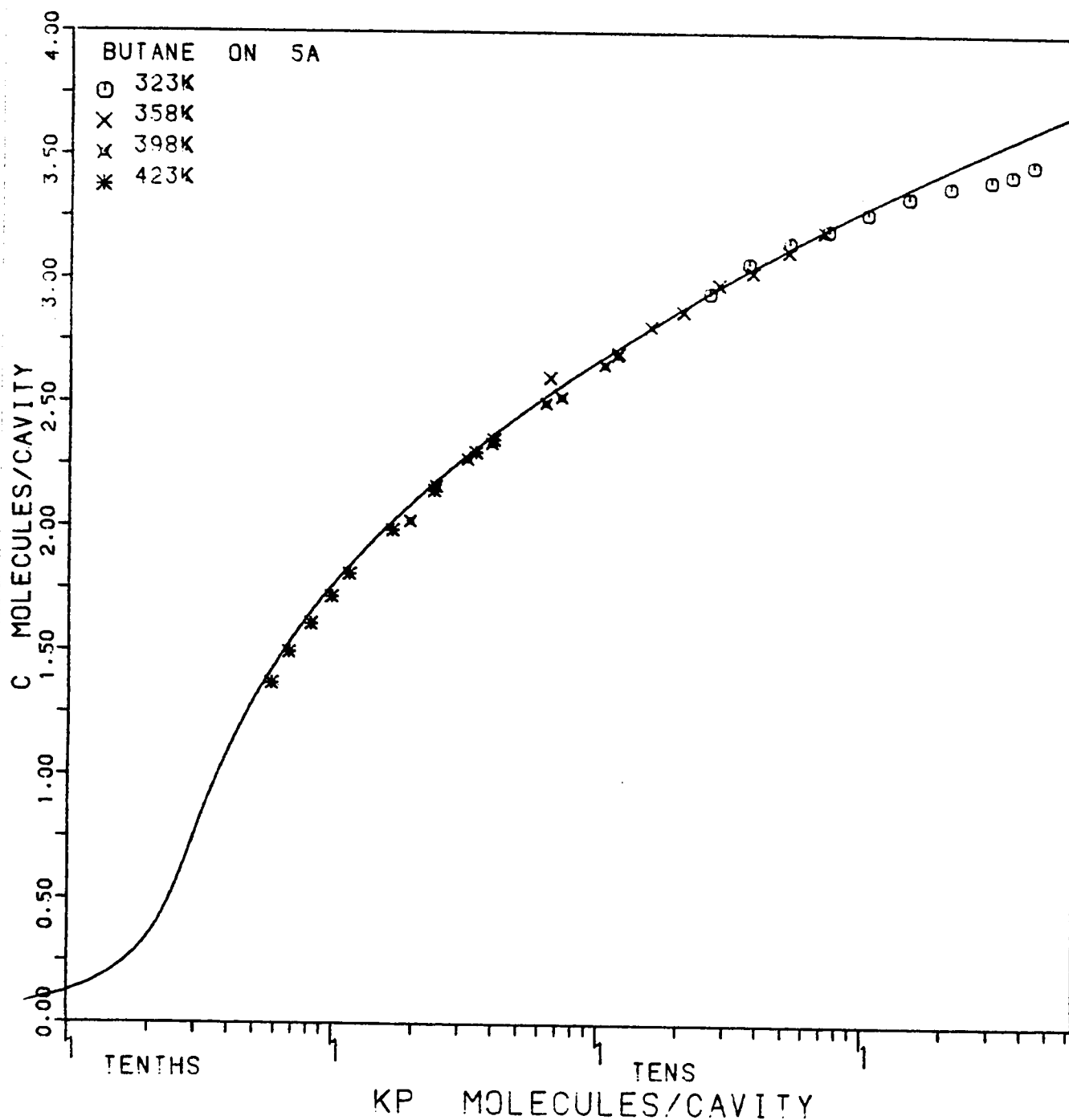


FIGURE 4.12 Generalized sorption isotherm for n-butane on 5A zeolite. Data of Loughlin [1]. Curve from virial model. Calculated using the constants in Table 4.7

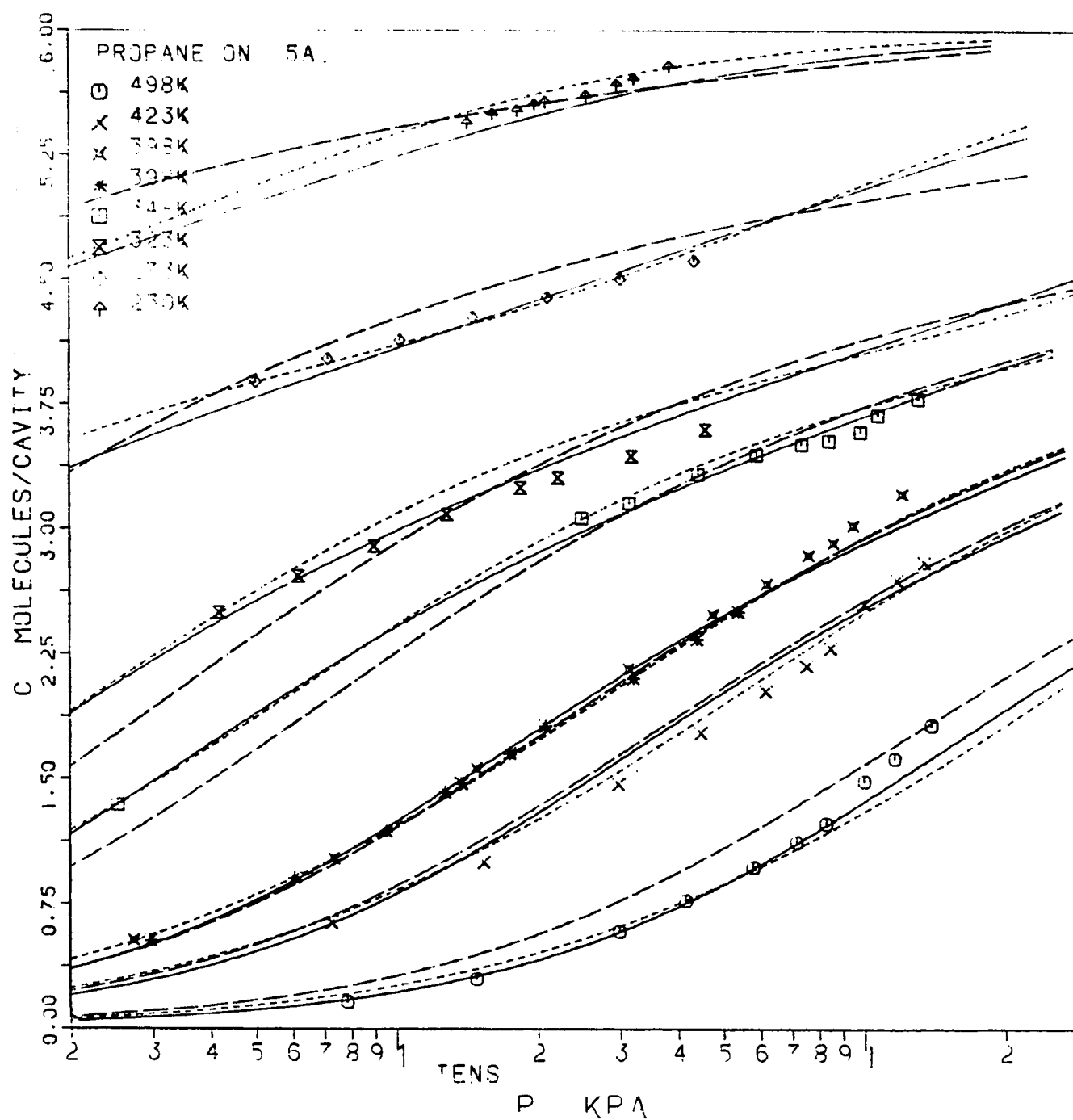


FIGURE 4.13 Pure component sorption isotherms for propane on 5A zeolite. Data of this work (○ × ⊠) and Loughlin (* □ ⊠ ◇ △) [1]. Curves from Schirmer et al. (—), Ruthven (---) and vacancy (---) models. Optimized Henry constant.

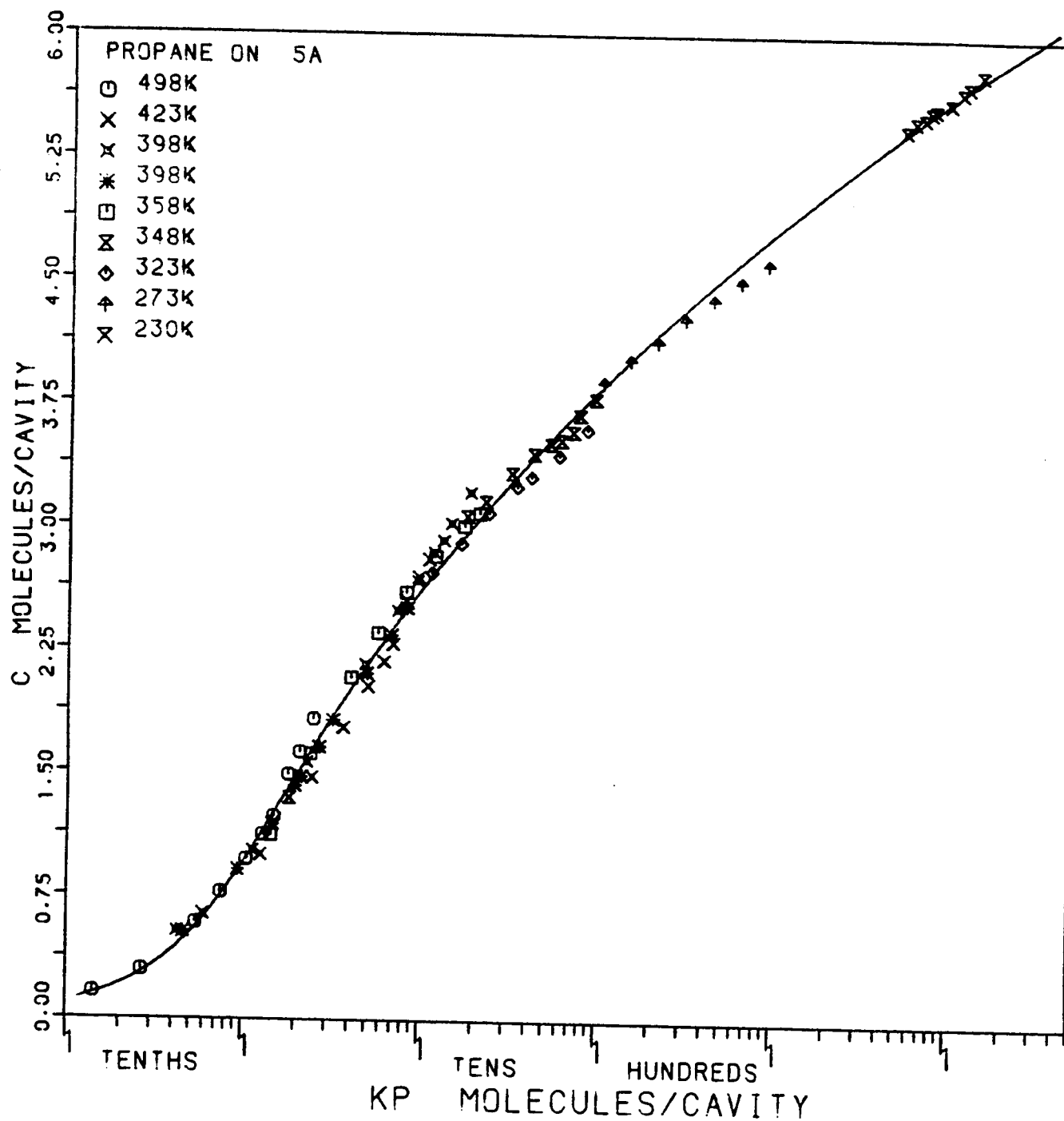


FIGURE 4.14 Generalized sorption isotherm for propane on 5A zeolite. Data as in Fig 4.8. Curve from virial model. Optimized Henry constant.

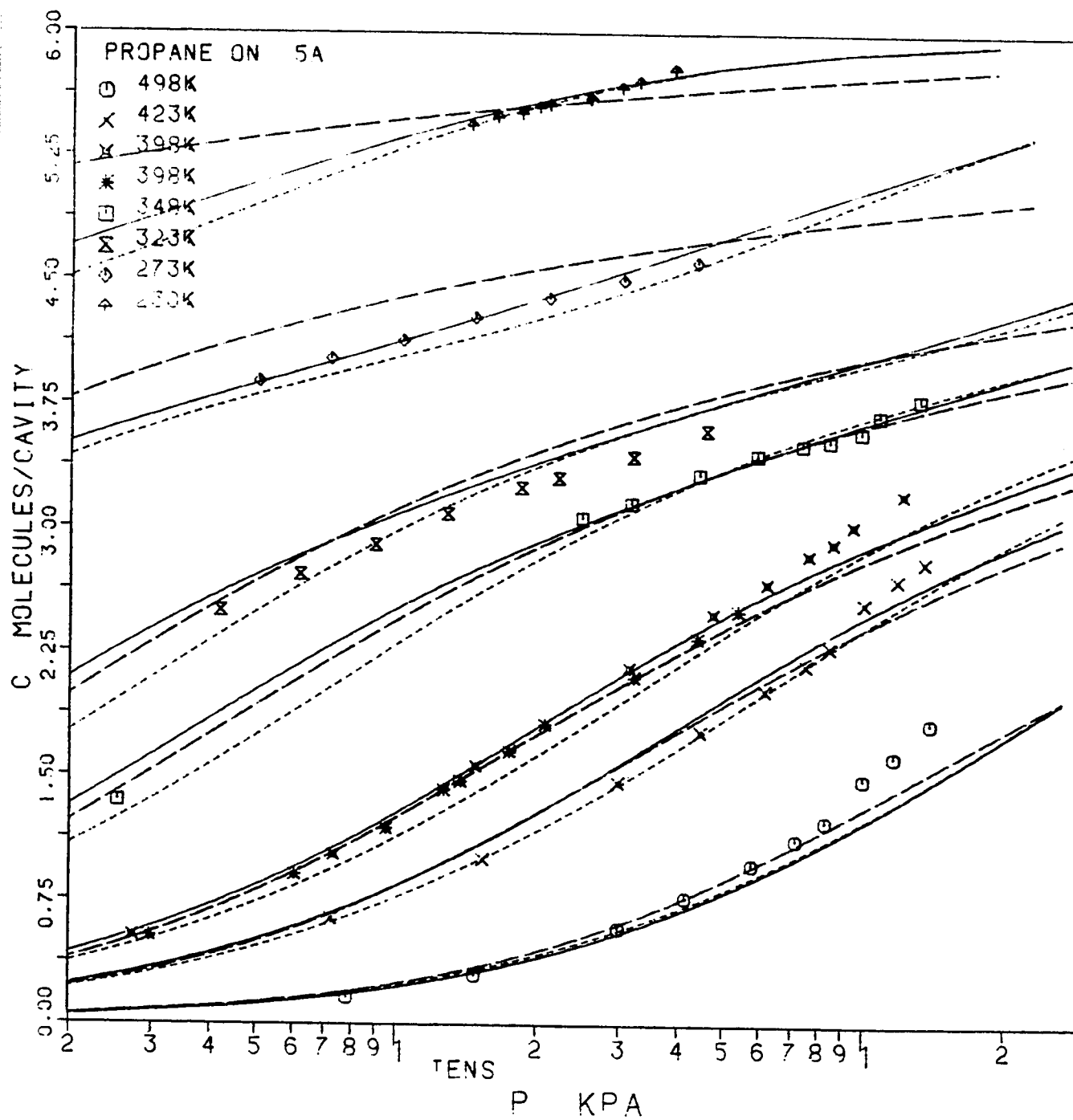


FIGURE 4.15 Pure component sorption isotherms for propane on 5A zeolite. Data and curves as in Fig 4.13. Experimental Henry constant.

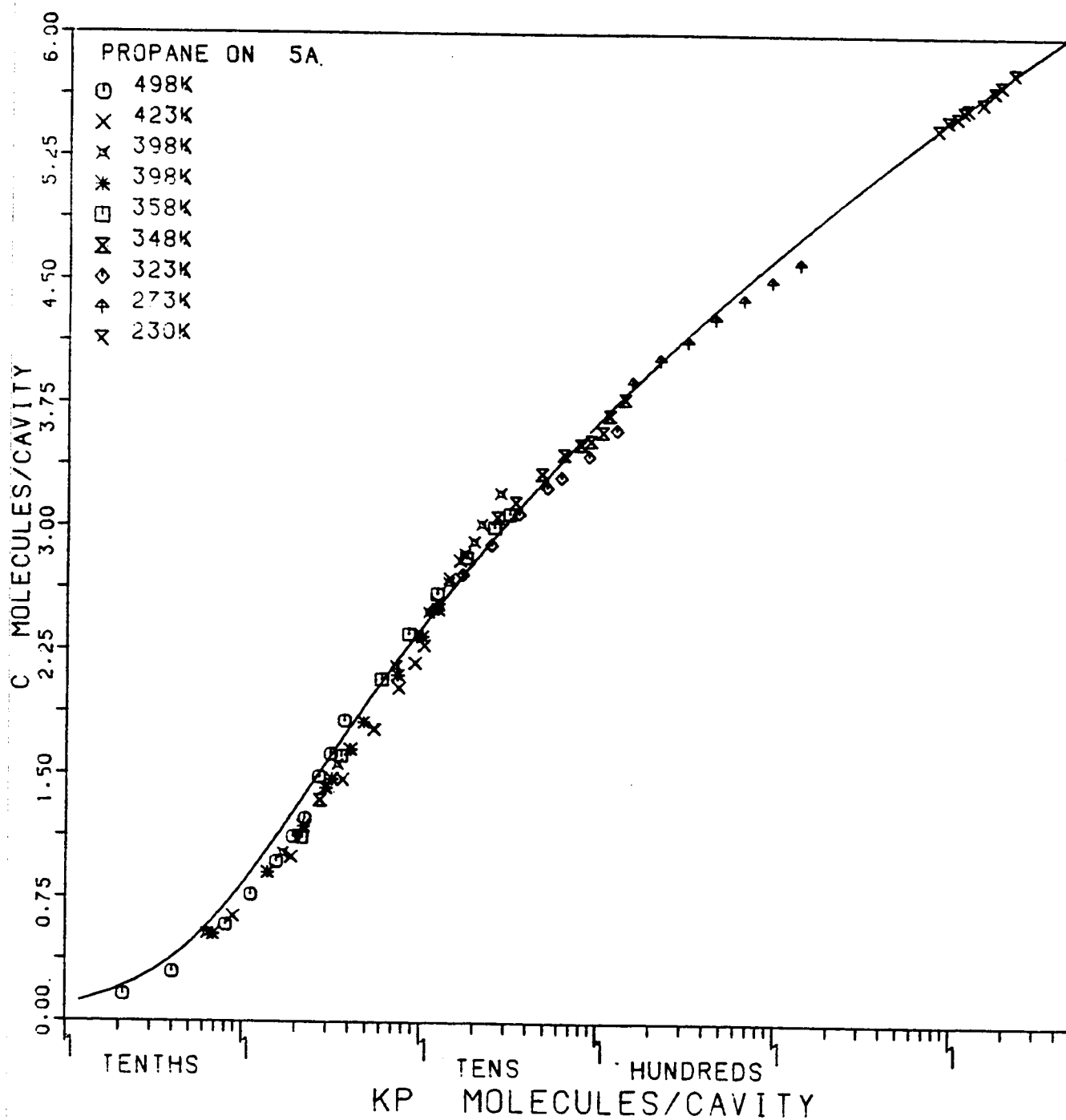


FIGURE 4.16 Generalized sorption isotherm for propane on 5A zeolite. Data as in Fig 4.8. Curve from virial model. Optimized Henry constant.

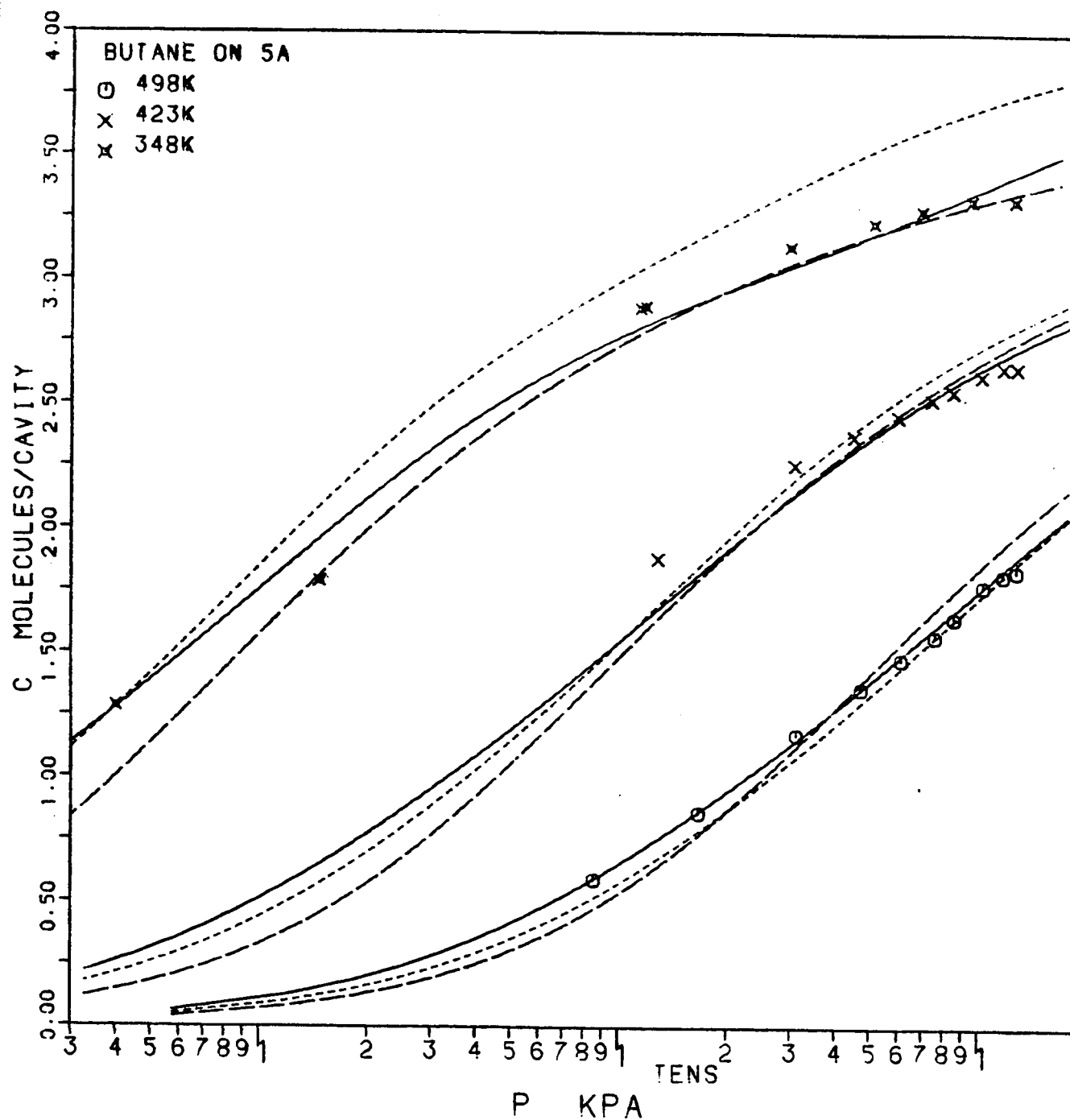


FIGURE 4.17 Pure component sorption isotherms for n-butane on 5A zeolite. Data of this work. Curves as in Fig 4.13. Optimized Henry constant.

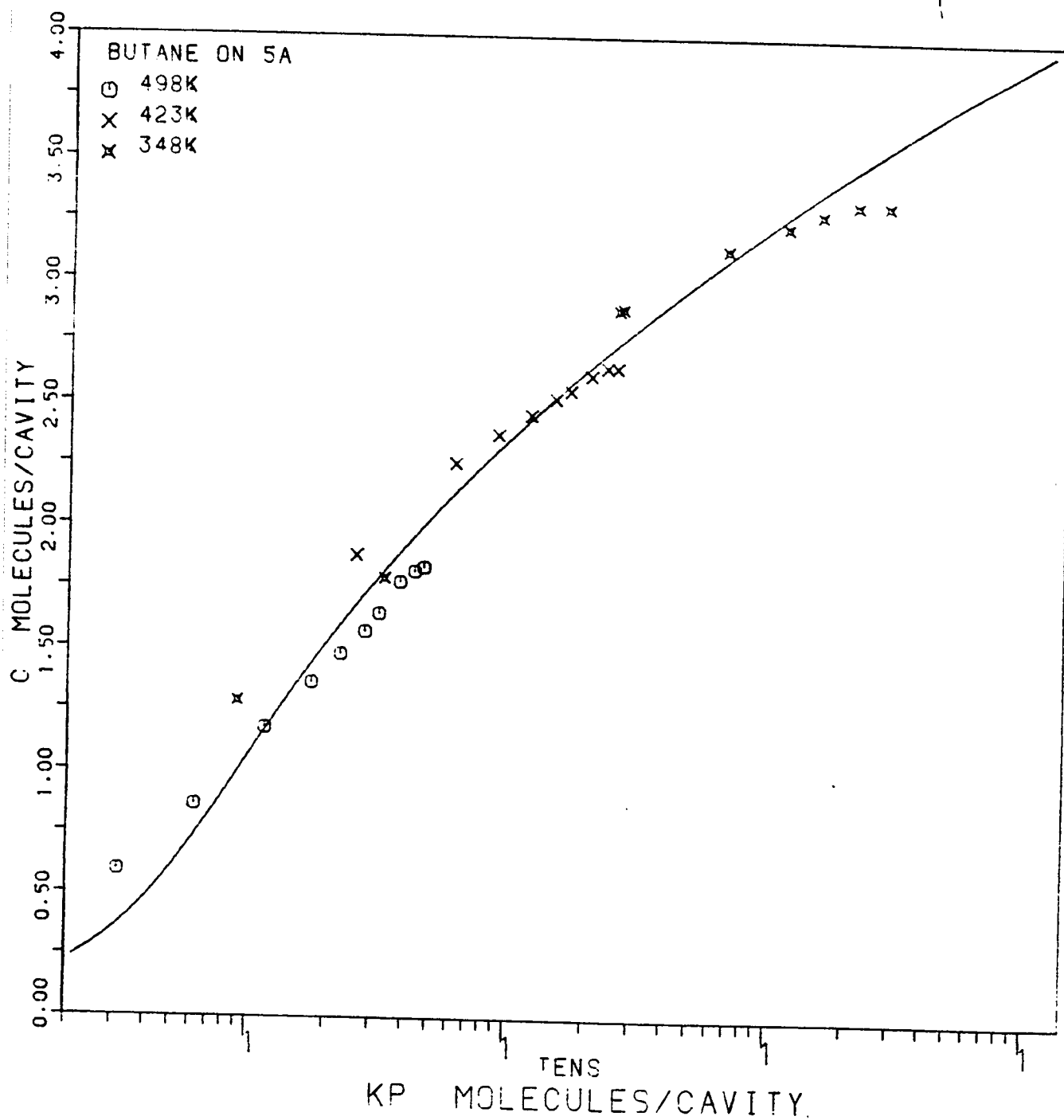


FIGURE 4.18 Generalized sorption isotherm for n-butane on 5A zeolite. Data of this work. Curve from virial model. Optimized Henry constant.

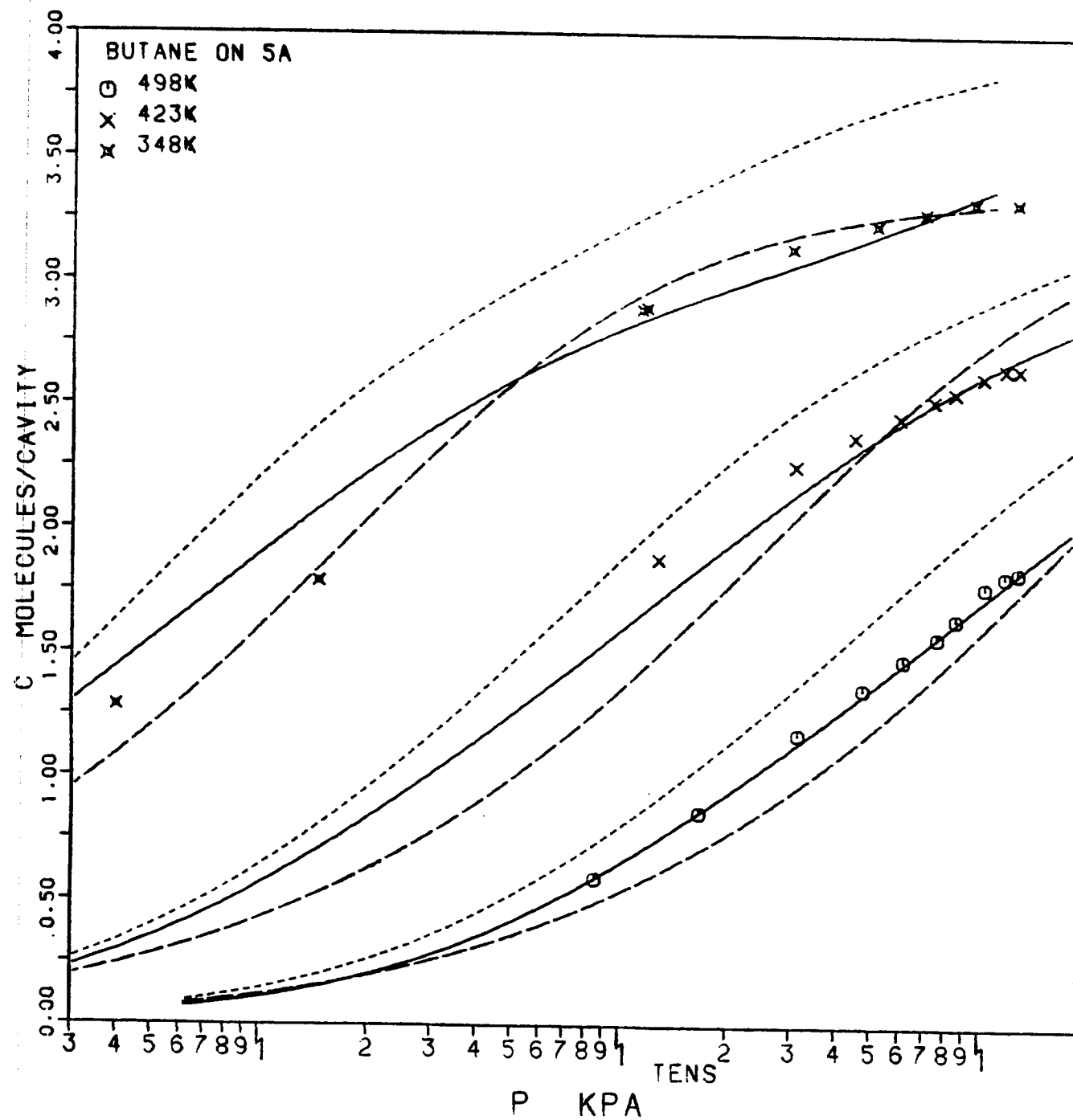


FIGURE 4.19 Pure component sorption isotherms for n-butane on 5A zeolite. Data of this work. Curves as in Fig 4.13. Experimental Henry constant.

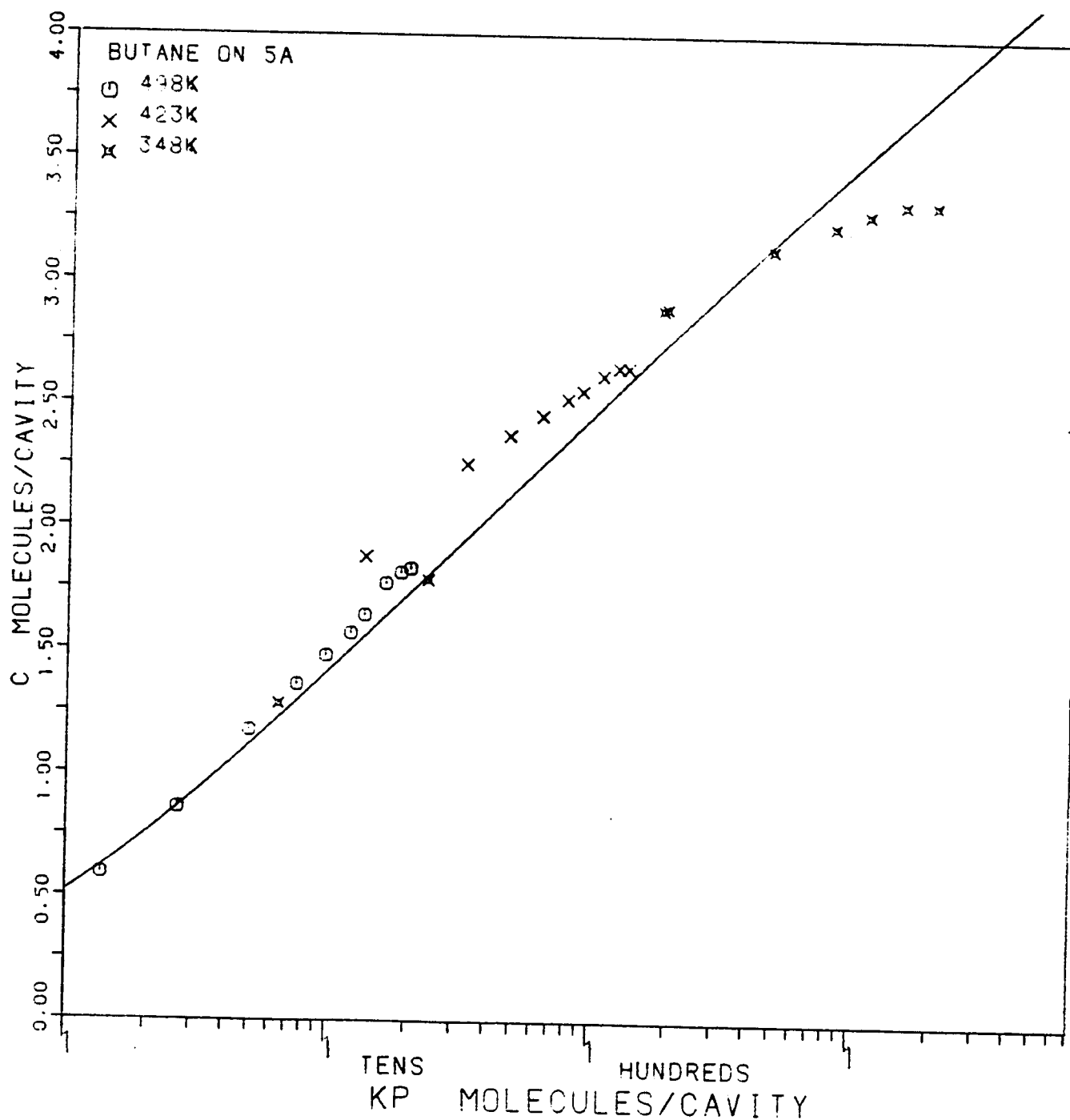


FIGURE 4.20 Generalized sorption isotherm for n-butane on 5A zeolite. Data of this work. Curve from virial model. Experimental Henry constant.

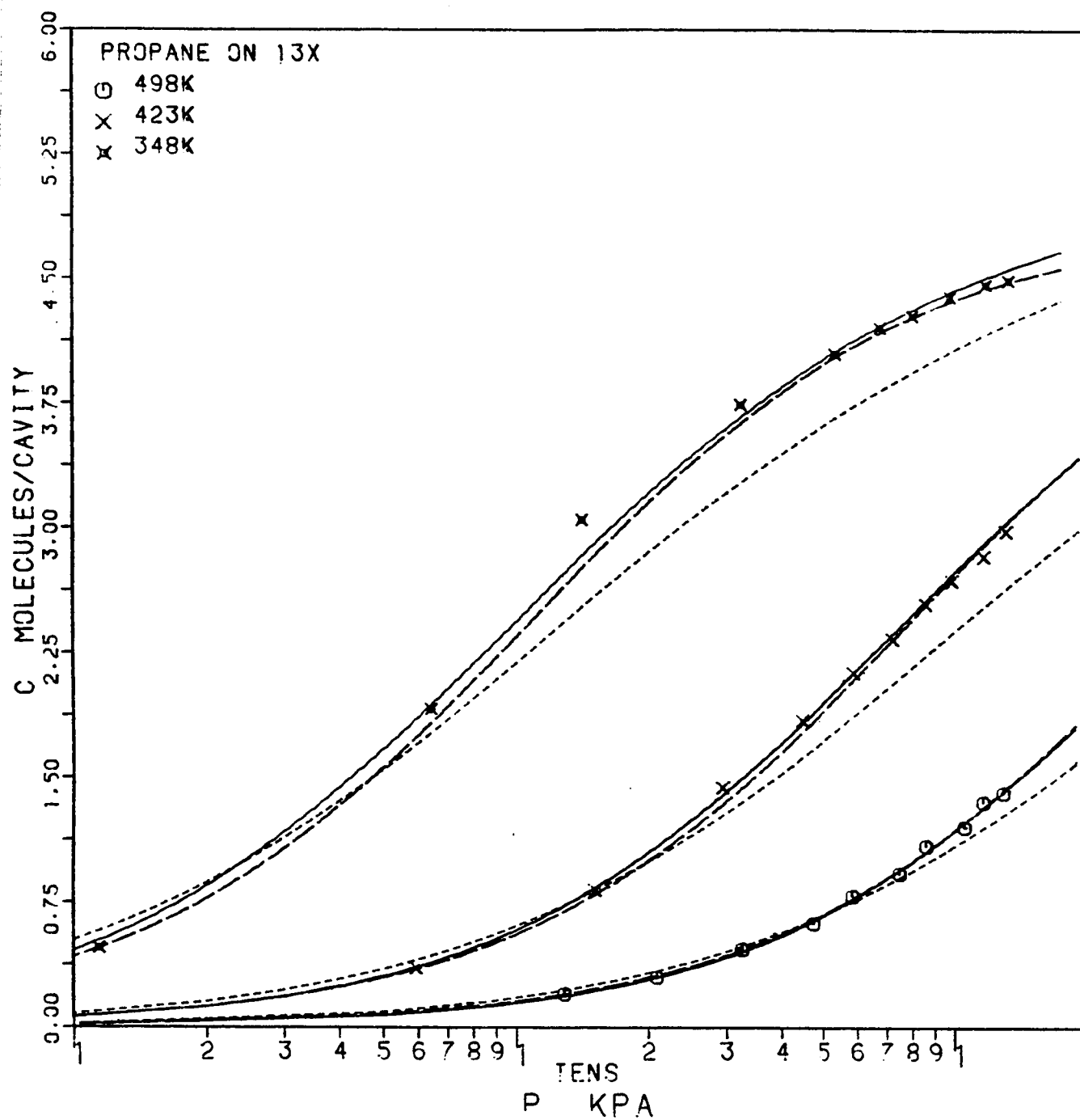


FIGURE 4.21 Pure component sorption isotherms for propane on 13X zeolite. Data of this work. Curves as in Fig 4.13. Optimized Henry constant.

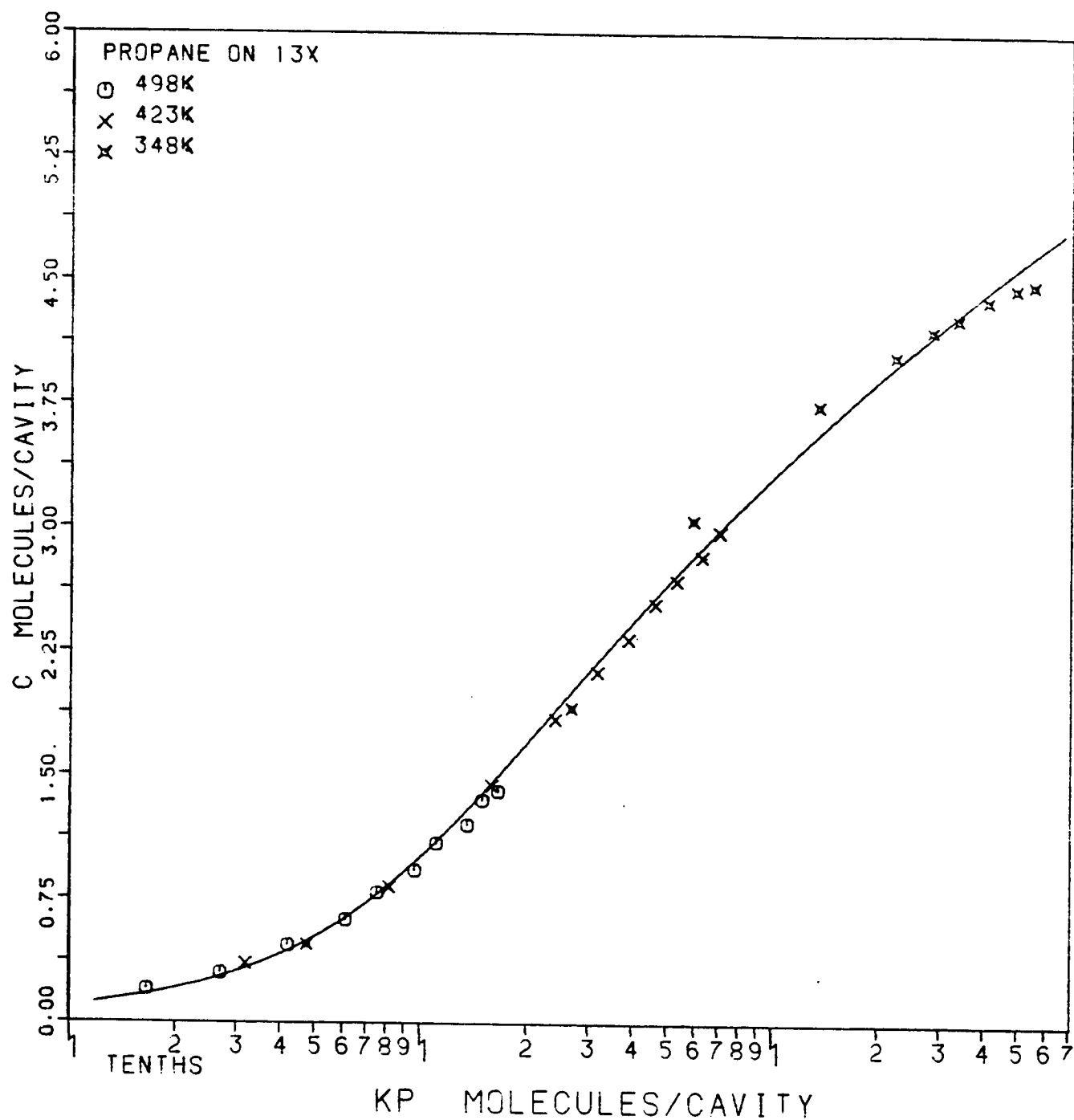


FIGURE 4.22 Generalized sorption isotherm for propane on 13X zeolite. Data of this work. Curve from virial model. Optimized Henry constant.

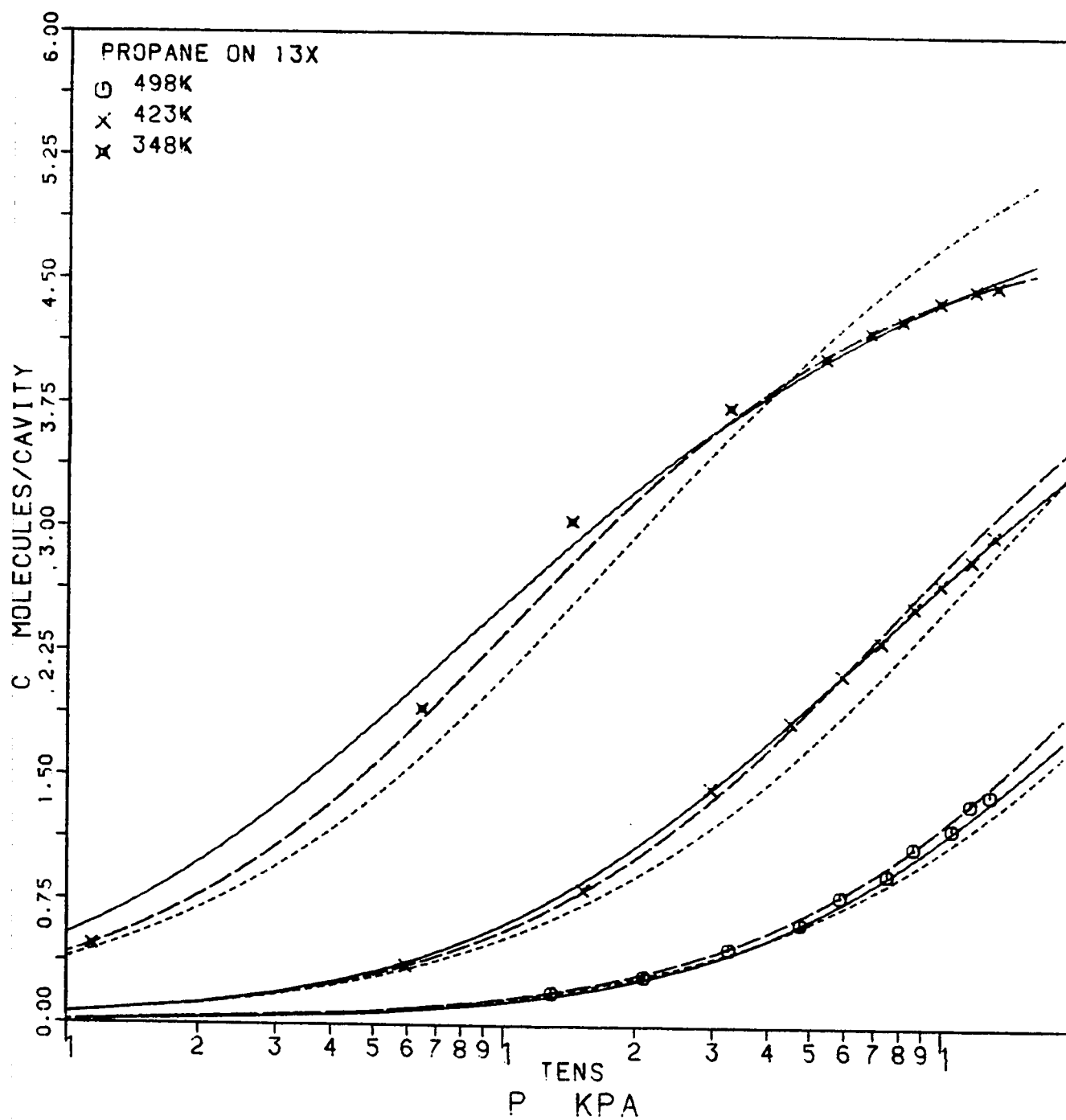


FIGURE 4.23 Pure component sorption isotherms for propane on 13X zeolite. Data of this work. Curves as in Fig 4.13. Experimental Henry constant.

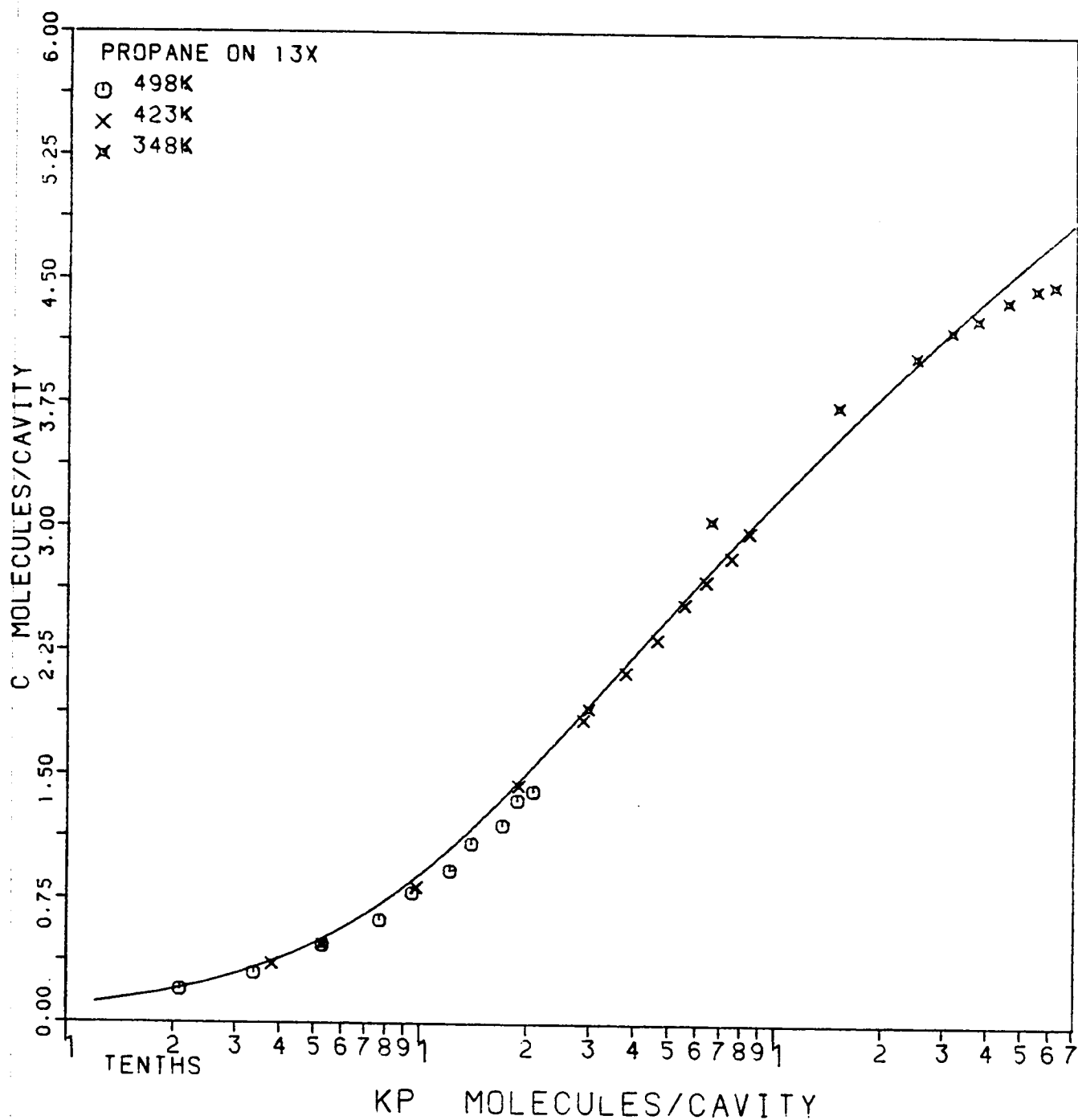


FIGURE 4.24 Generalized sorption isotherm for propane on 13X zeolite. Data of this work. Curve from virial model. Experimental Henry constant.

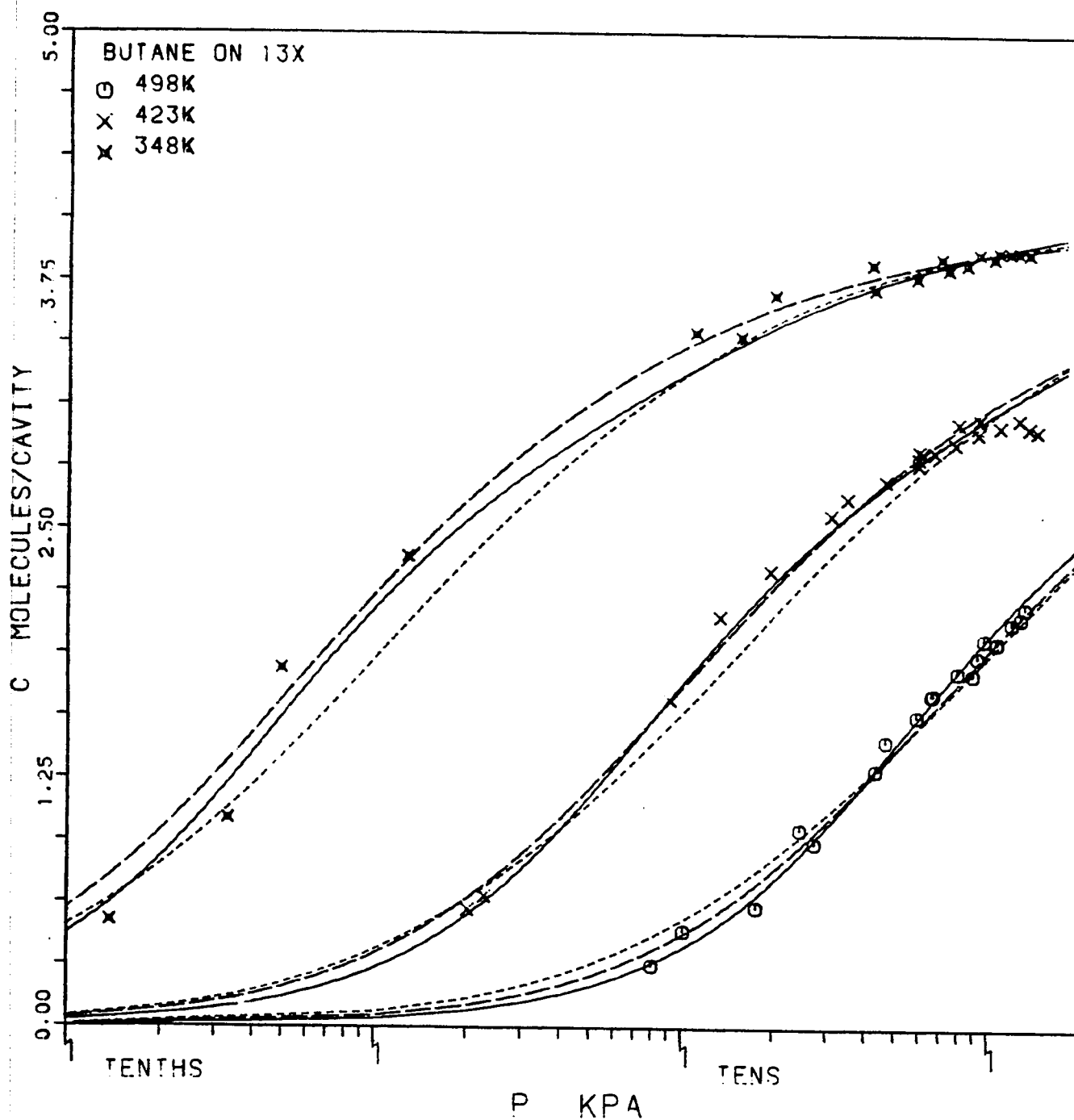


FIGURE 4.25 Pure component sorption isotherms for n-butane on 13X zeolite. Data of this work. Curves as in Fig 4.13. Optimized Henry constant.

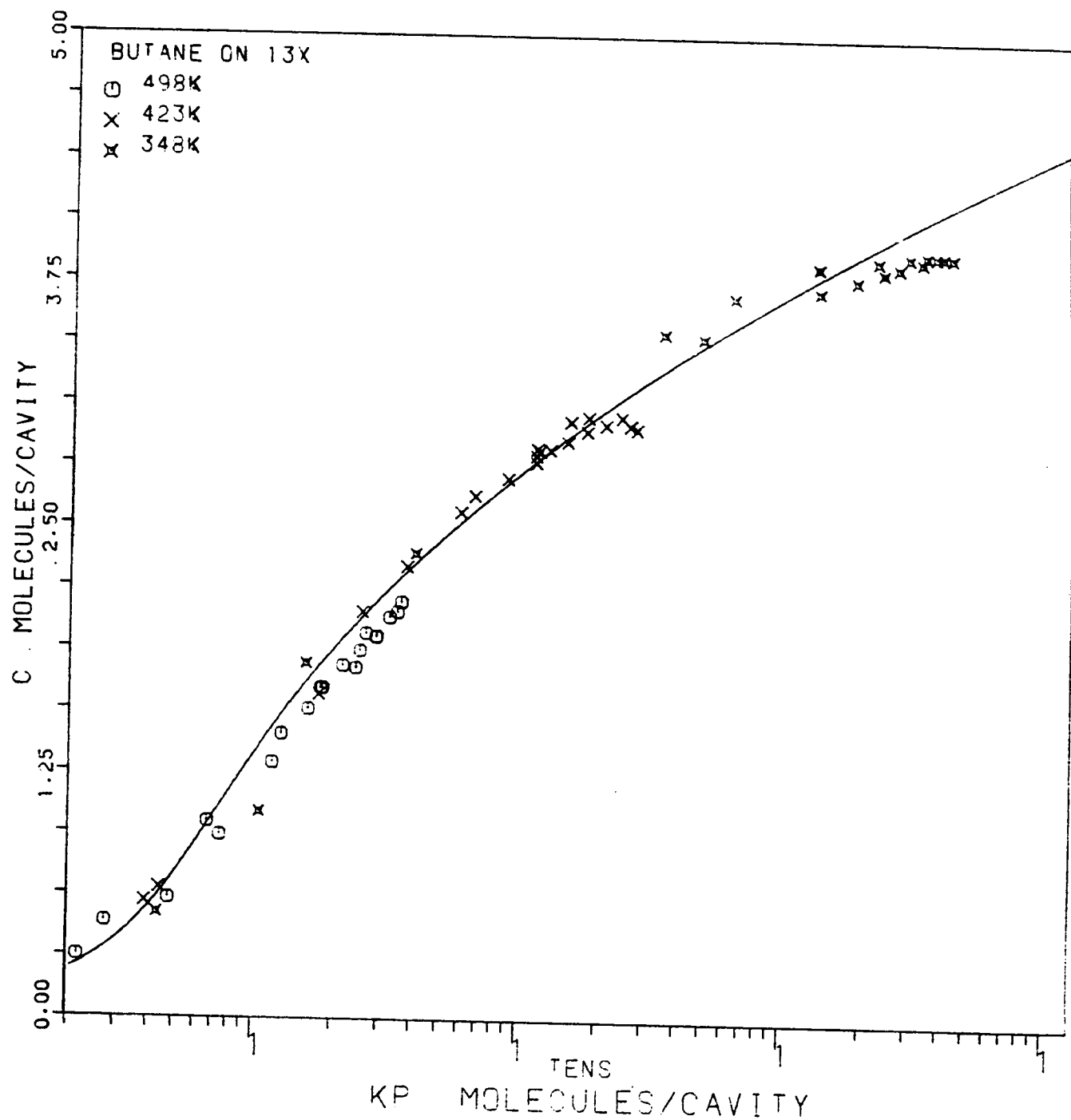


FIGURE 4.26 Generalized sorption isotherm for n-butane on 13X zeolite. Data of this work. Curve from virial model. Optimized Henry constant.

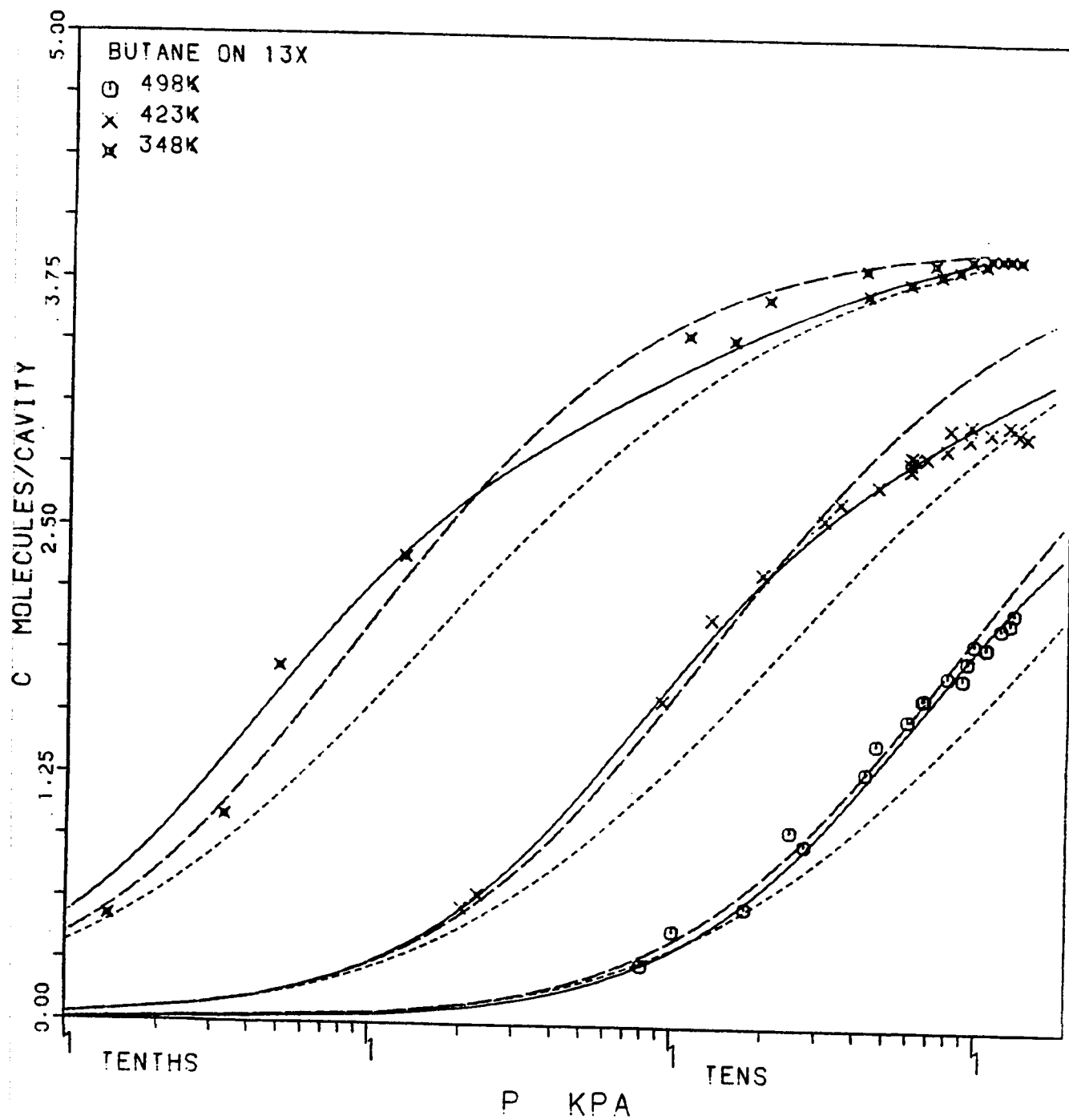


FIGURE 4.27 Pure component sorption isotherms for n-butane on 13X zeolite. Data of Hamad. Curves as in Fig 4.13. Experimental Henry constant.

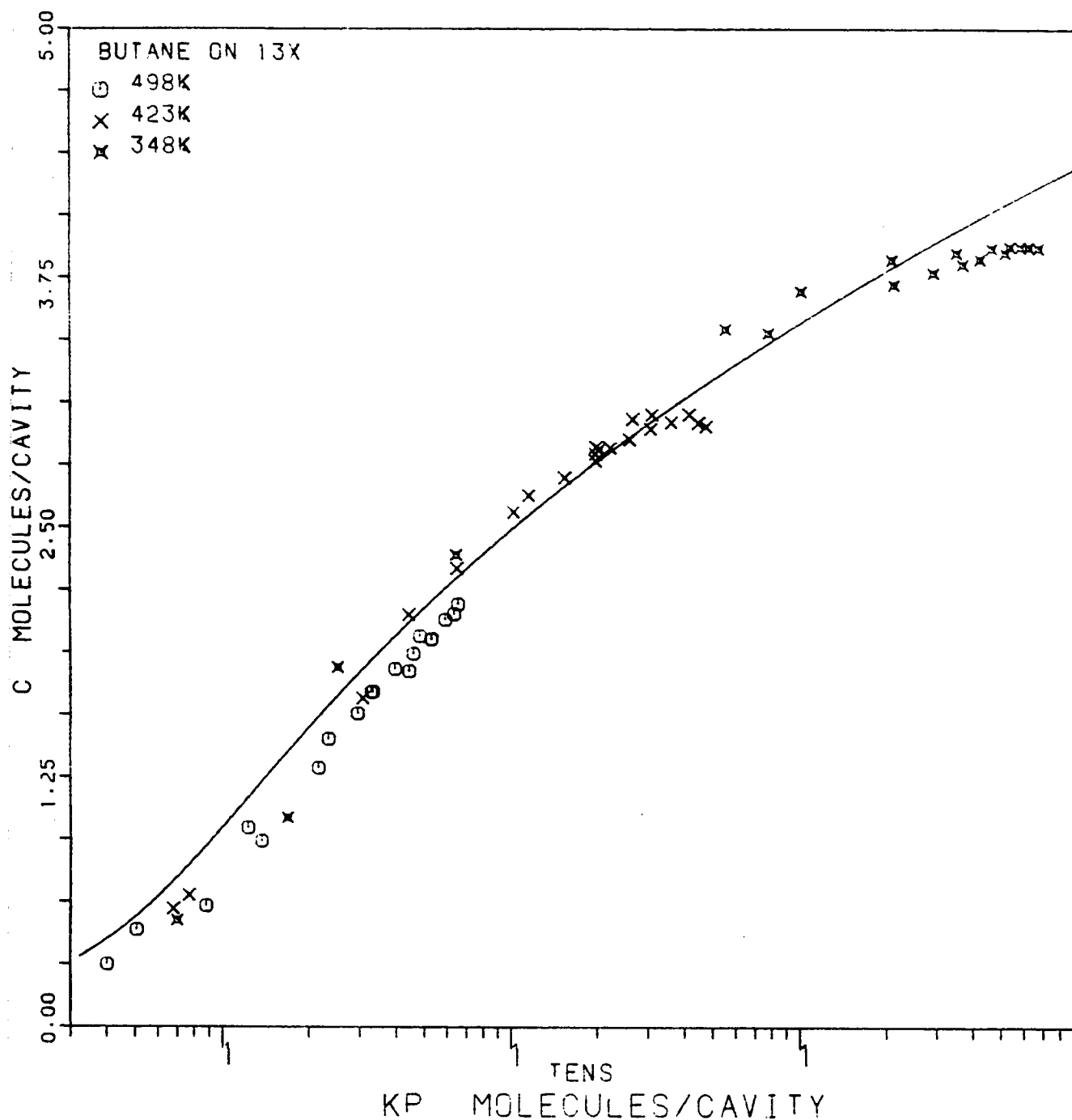


FIGURE 4.28 Generalized sorption isotherm for n-butane on 13X zeolite. Data of this work. Curve from virial model. Experimental Henry constant.

REFERENCES

1. Loughlin, K. F., Ph.D. thesis, University of New Brunswick "Sorption in 5A Zeolite" . (1970)
2. Chien, C. H., Greenkorn, R. A. and Chao, K. C.. AIChE J. 29 , 560, (1983)
3. Parent, Personal communication, March 1984.
4. Breck, D. W., "Zeolite Molecular Sieves" , John Wiley & sons, New York, (1974)
5. Ruthven, D. M. and Loughlin, K. F., J.C.S., Far. Trans. I, 68 , 696, (1972)
6. Schirmer, W., Fielder, K. and Stach, H., ACS Symposium Series No. 40 ,303, (1977)
7. Ruthven, D. M., Loughlin, K. F. and Holborow, K. A. Chem. Eng. Sci., 28 , 701, (1973)
8. Cochran, R. L., Kable, R. L. and Danner, R. P., paper 6 f, presented at AIChE's Golden Jubilee Meeting, Washington, November 1st, (1983)
9. Barrer, R. M. "Zeolites and Clay Minerals as Sorbents and Molecular Sieves" , Academic Press, London, (1978)
10. Loughlin, K. F. and Roberts, G. D. ACS Symposium Series No. 135 , (1980)
11. Kuester, J. L. and Mize, J. H., "Optimization Techniques with FORTRAN" , McGraw-Hill, New York , (1973)
12. Marquardt, D. M., J of the Society for Industrial and Applied Math., 11 , ,431, (1963)
13. Sand, L. B., Plenary Paper-Synthesis "Proceedings of the Fifth International Conference on Zeolites" ,Naples, Heyson & Son Ltd., London, (1980)

14. Ruthven, D. M., Alaisdar, M. G. and Vavlitis, A. "Proceedings of the Fifth International Conference on Zeolites" ,Naples, Heyden & Son Ltd., London (1980)
15. David, T. H. and Lee, J. C. AIChE Symposium Series No. 230, 79, ,67, (1980)
16. Khaleeq, M., M. S. thesis, University of Petroleum & Minerals, "Adsorption of Xylenes on Ba-X Zeolite Pellets " , (1984)
17. Harlfinger, R., Hoppach, D., Quaschik, U. and Quitzs, K. Chem. Techn., 35 ,413, (1983)
18. Barrer, R. M. and Sutherland, J. W. Proc. Roy. Soc., Ser A, 237 ,439, (1956)
19. Linde Data Sheets for Hydrocarbons, Supplied by Linde Div. of Union Carbide Corp., Tarrytown, New York
20. Glessner, A. J. and Myers, A. L., C.E.P. Symposium Series, 65 , 73, (1969)
21. Anderson, R. B., Eagan, J. D. and Kindl, B., AIChE Symposium Series No. 134, 69, ,39 , (19..)

Chapter V

BINARY ADSORPTION

Binary adsorption data for the propane-n-butane system were obtained at temperatures of 498, 423 and 348 K at total pressures of 106.7 and 66.7 kPa (800 and 500 torr) on 5A and 13X zeolites. The experimental data is tabulated in appendix C. Four models were compared to the experimental data : the binary form of the Schirmer model[1,2], Ruthven et al.'s model[3], the vacancy solution model[4] and the ideal adsorbed solution theory (IAST) [5].

If the solution is assumed to be ideal in the sorbed phase, then these models predict the binary behavior using pure component parameters only. For non-ideal behavior, appropriate mixing expressions can be introduced in the Schirmer model as can be seen from Eq 2.20 . The IAST has been adapted to non-ideal behavior by Glessner and Myers [6]. They used a two constant Redlich-Kister equation to find expressions for the activity coefficients. The vacancy model has been applied to such systems without introducing additional binary parameters. The model of Ruthven et al. has not been extended to non-ideal systems. An example of the non-ideal behavior is the sorption of ethylene- carbon dioxide mixture on 5A zeolite reported by Holborow [7].

5.1 PROPANE-N-BUTANE BINARY ADSORPTION

The X-Y and the concentration diagrams for the sorption of propane-n-butane binary mixtures on 5A and 13X zeolites are shown in Figures 5.1 to 5.24. The pure component parameters used in the calculations are given in Tables 4.4 to 4.7. Four curves are plotted on each figure. They represent the four models studied.

In adsorption work, a selectivity coefficient has been defined [5] (see Eq 2.2). The selectivity coefficient $s_{1,2}$ for component 1 is greater than unity if component 1 is the more strongly adsorbed. The experimental data show a selectivity coefficient less than unity for propane which implies that propane is the less adsorbed component as expected. From appendix C a small gas-phase composition dependence for selectivity can be seen. The 5A zeolite show a smaller selectivity coefficient for propane than 13X zeolite which implies that better separation is obtained using 5A zeolite.

The experimental data also show an appreciable increase in selectivity with decreasing temperature. This is known to happen in such systems. It forms the basis for operating sorption processes as in the PSA at ambient temperature. The pressure has a small effect on selectivity. The selectivity decreases weakly with increasing pressure at the same temperature. This is clearer for the data on 13X. These facts are reported in the literature [8,9]. Myers [9] states as a generalization on the behavior of mixture adsorption equilibria

"The selectivity of the adsorbent for the more strongly adsorbed component decreases both with increasing pressure and with increasing temperature."

In principle the IAST prediction should be based on the experimental isotherms. However this requires pure component data at very low and very high concentrations. To predict the binary behavior at the two total pressures studied pure component data at higher pressures are also needed. As an alternative one can use (with less accuracy) an equation fitted to the experimental data along with Equation 2.29 . Since Schirmer et al. model gives the best fit for the pure component data it is selected for the IAST calculations.

The binary equation for the vacancy solution given in [4] does not predict the same concentration as the pure model at $x = 0$ and 1 . The inconsistency between the binary and the pure component models has been checked by trying to reduce the binary model analytically to the pure component model when $y_1=x_1=1$ and $x_2=0$, but with no success. Cochran et al. state that the pure component and gas mixture adsorption models are consistent. However they do not show this. There is the possibility that some equations are mistyped. It can be shown that the binary equations are not correct in [4] and an exponential is missing. The corrected equations are shown in chapter two.

The predictions of Schirmer and IAST models are very close. In general one can see that the Schirmer and the IAST give the best fit

for both the X-Y and the concentration diagrams. The Ruthven et al. isotherm show better prediction for 5A zeolite at 348. K and 66.7 kPa . The vacancy model does not predict the binary behavior correctly for the 5A zeolite. It shows an azeotrop in th X-Y diagram, (it is not shown in the graphs) For 13X zeolite the prediction is satisfactory,

The unsatisfactory prediction of the binary data for 5A may be due to the big difference in the value of $(\alpha+1)$ which is defined as the ratio of the molar volume of sorbate to the molar volume of vacancy. Since the model is based on Flory and Huggins equation in which the non-ideality comes from the difference between the molar volumes of the pure components, then it is expected that α has a big effect on the binary prediction. For the 13X zeolite the values of $(\alpha+1)$ obtained are 0.926 and 0.459 for propane and n-butane respectively at 423 K. Assuming that the molar volume of the vacancy is the same for the adsorption of both gases then the ratio of the molar volume of propane to the molar volume of n-butane is $0.926/0.459 = 2.0$ which is physically not correct, but the prediction is correct. For 5A zeolite the $(\alpha+1)$ values are 0.0132 and 3.89 for propane and n-butane, and the ratio of molar volumes is 0.0034 which is very small.

There is a possibility that the value of α is affected by the value of r_1 which gives the dependence of the molar volume on temperature. If the experimental data is given for a small range of temperature, as Cochran et al.[4] noticed, then r_1 will converge to zero. The author found that the value of α is sometimes affected by r_1 and

hence by the temperature range. For sorption on 5A zeolite the propane data is at wide range of temperature and the n-butane data is at smaller range. While in the case of sorption on 13X the ranges are the same and a better result is obtained. As a check the propane data obtained only in this work which gives the same range of temperature for n-butane was optimized to see if there is any change in the value of α . A small increase was found which does not correct the prediction.

Table 5.1 shows the average values of the selectivity coefficients at the various temperatures and pressures studied. The values of the selectivity coefficients indicate that the separation increases with decreasing temperature and shows a slight increase with decreasing pressure. In addition a better separation is obtained for the 5A zeolite. The values of the reciprocal of the relative volatility for VLE are also shown to compare with.

TABLE 5.1
AVERAGE SELECTIVITY COEFFICIENTS

P = 66.7 kPa

P = 106.7 kPa

T in K	5A zeolite	13X zeolite	5A zeolite	13X zeolite
348.	0.132	0.184	0.185	0.219
423.	0.197	0.193	0.256	0.241
498.	0.262	0.318	0.289	0.349

For vapor-liquid equilibrium of propane and n-butane

T = 233 K P = 101.3 kPa $1/\alpha = 0.143$

T = 233 K P = 1379. kPa $1/\alpha = 0.250$

T = 273 K P = 1379. kPa $1/\alpha = 0.250$

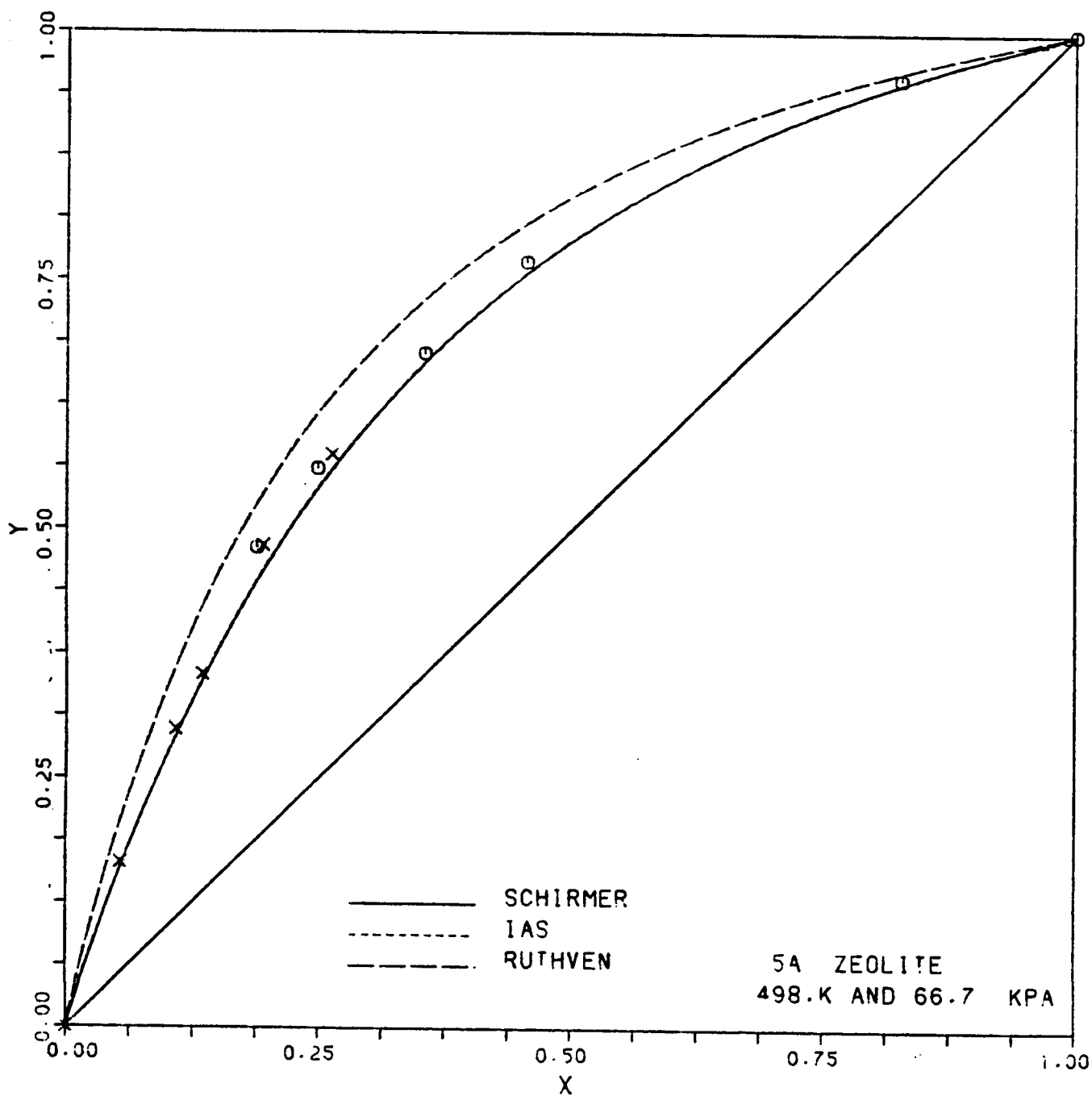


FIGURE 5.1 X-Y diagram for the sorption of propane-n-butane binary mixture on 5A zeolite.

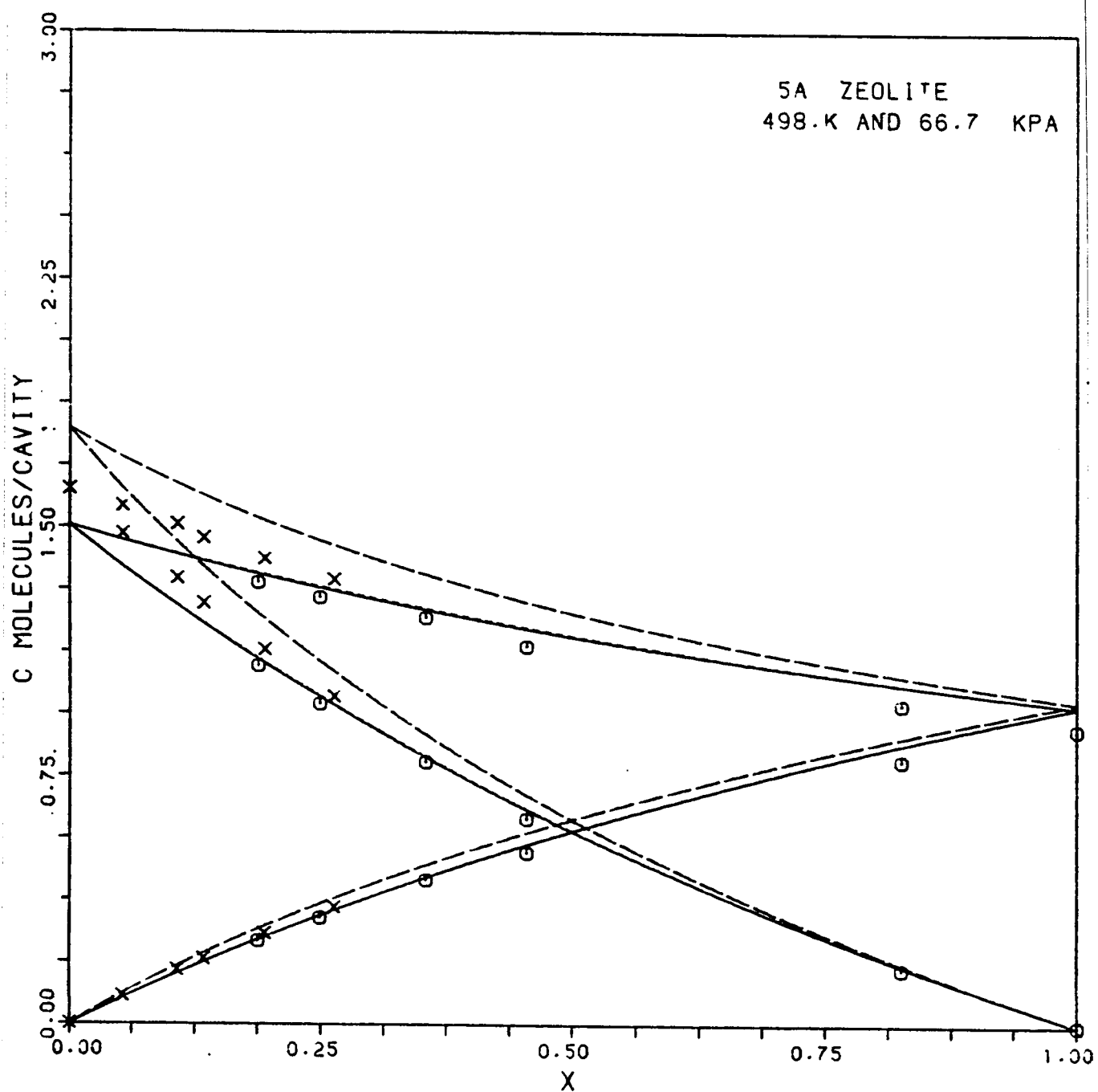


FIGURE 5.2 Concentration curves for the sorption of propane-n-butane binary mixture on 5A zeolite. Curves as in Fig 5.1 .

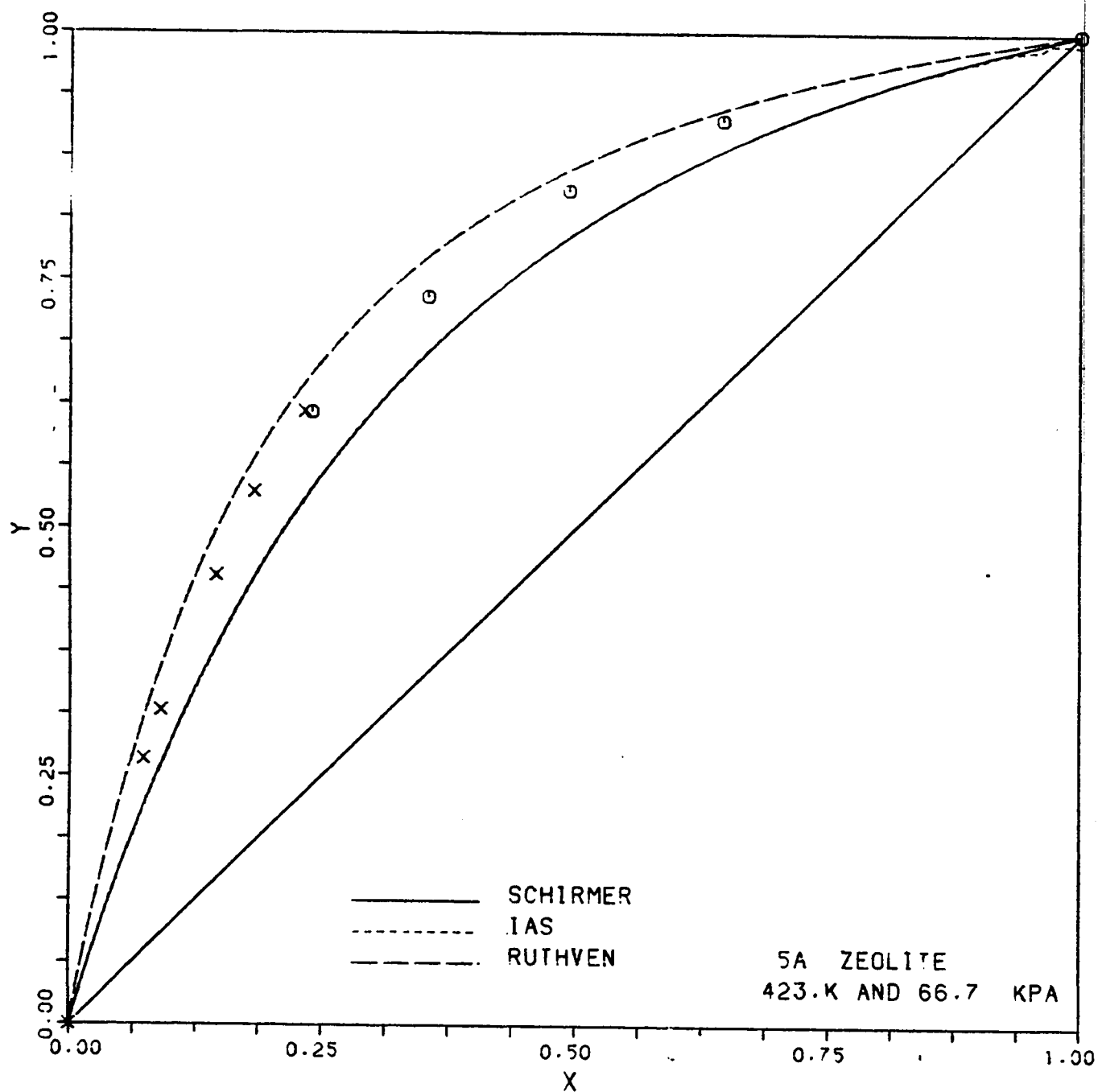


FIGURE 5.3 X-Y diagram for the sorption of propane-n-butane binary mixture on 5A zeolite.

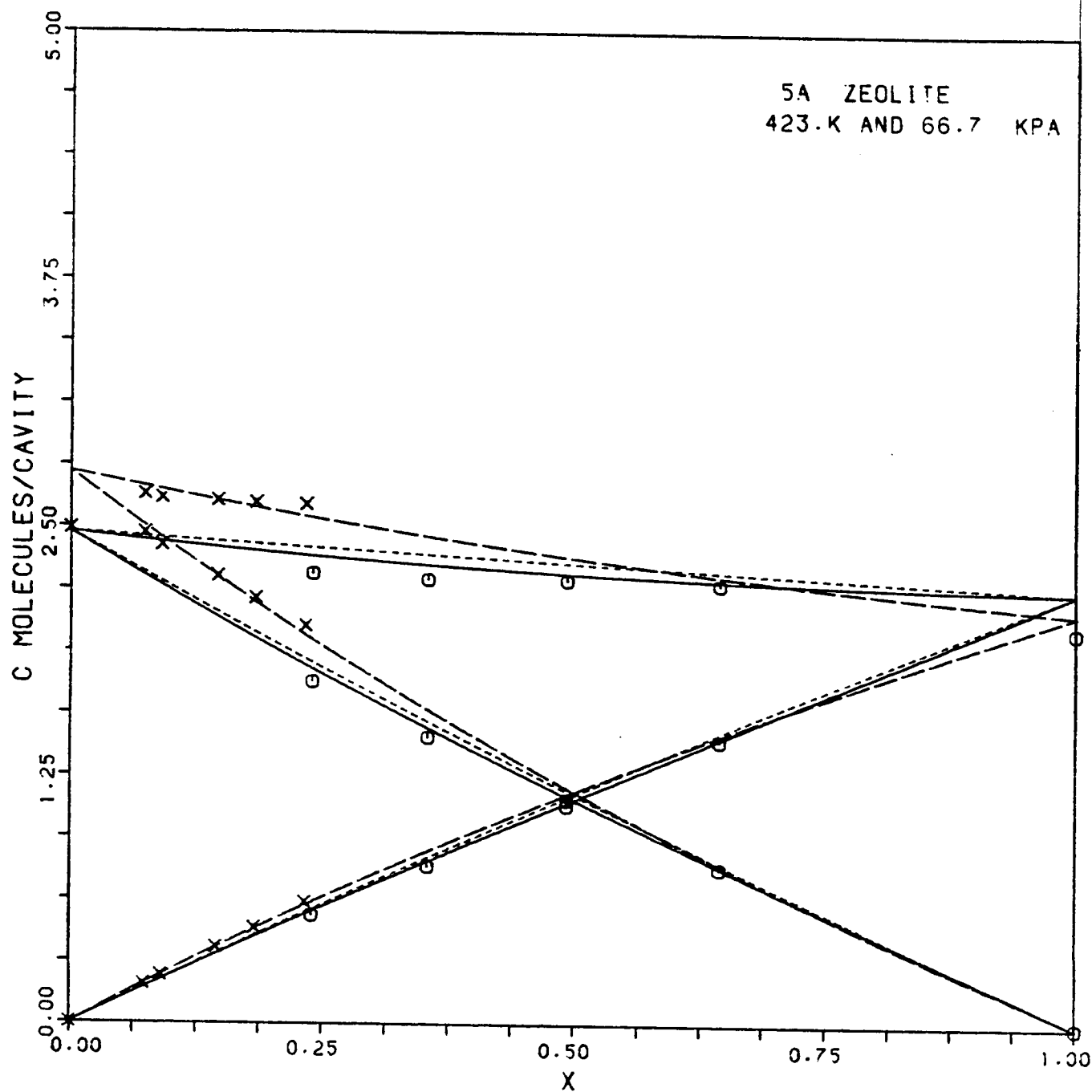


FIGURE 5.4 Concentration curves for the sorption of propane-n-butane binary mixture on 5A zeolite. Curves as in Fig 5.3 .

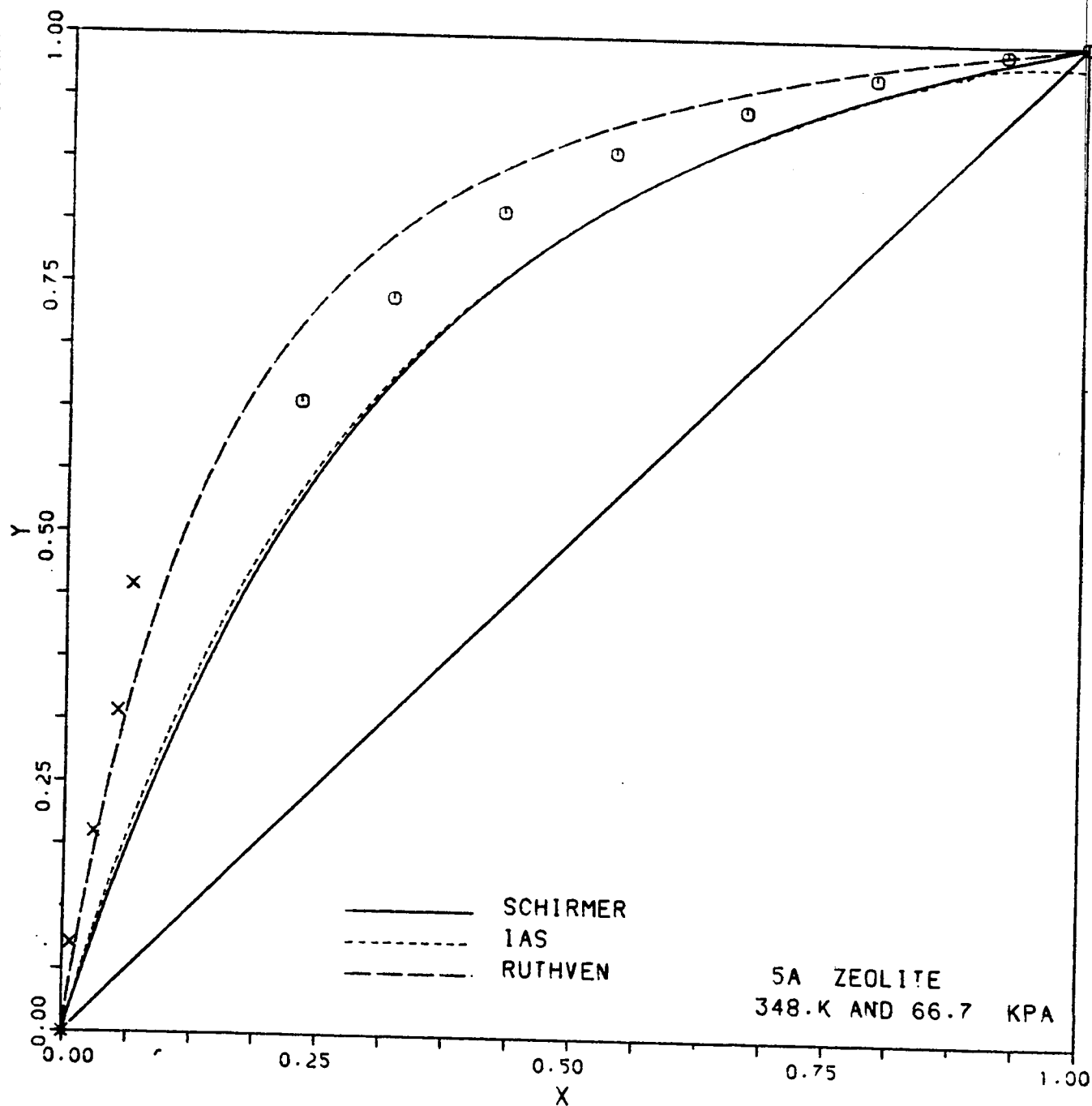


FIGURE 5.5 X-Y diagram for the sorption of propane-n-butane binary mixture on 5A zeolite.

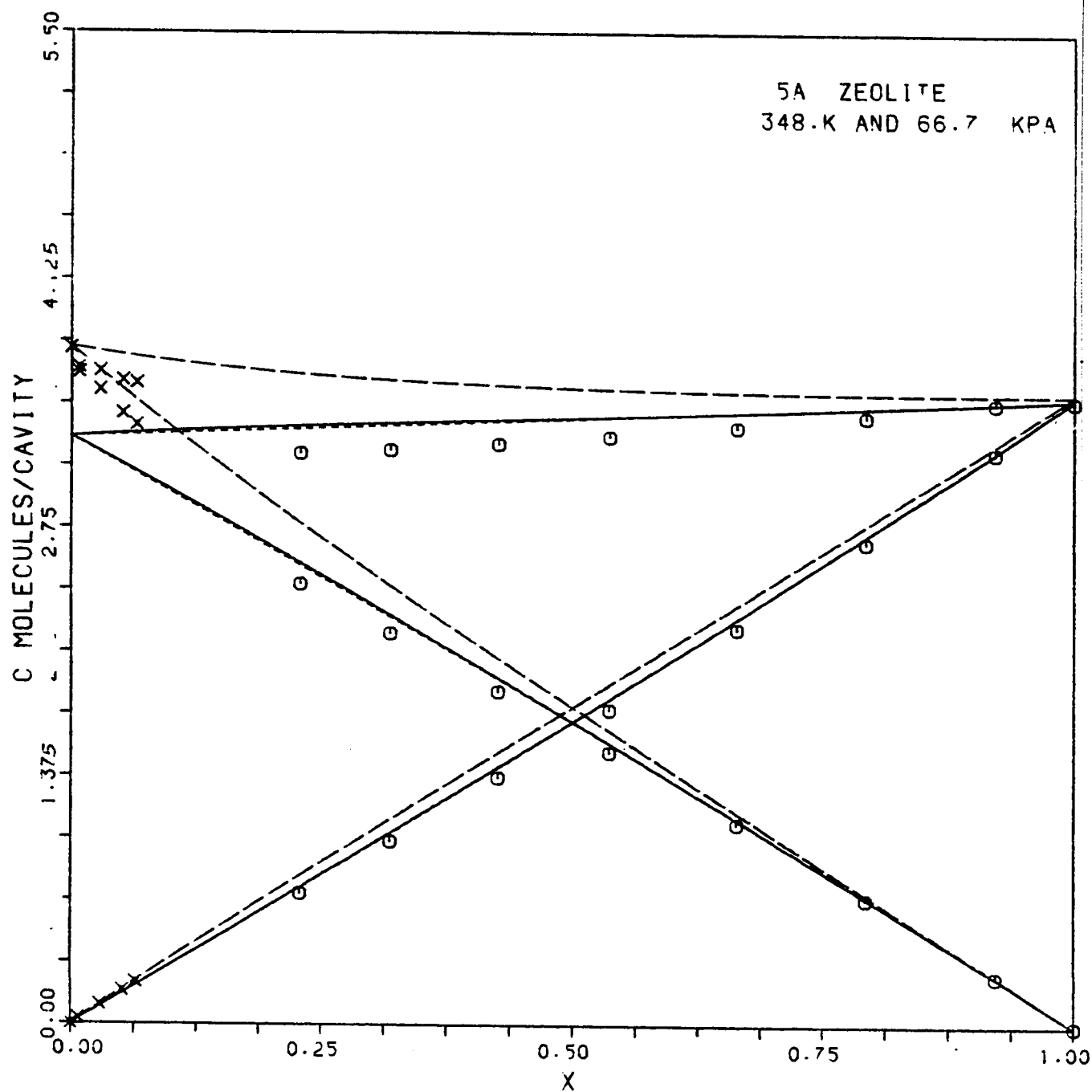


FIGURE 5.6 Concentration curves for the sorption of propane-n-butane binary mixture on 5A zeolite. Curves as in Fig 5.5 .

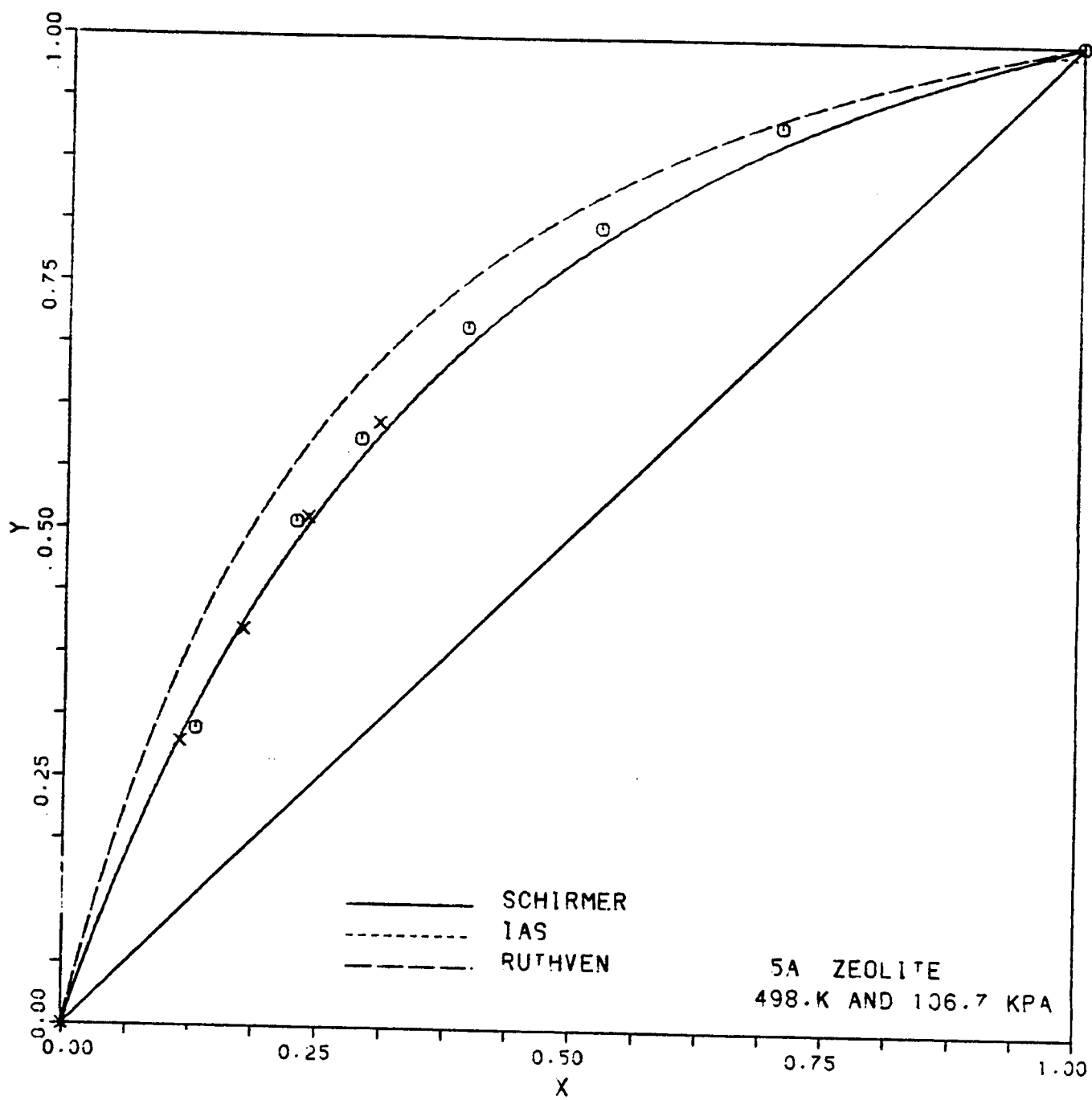


FIGURE 5.7 X-Y diagram for the sorption of propane-n-butane binary mixture on 5A zeolite.

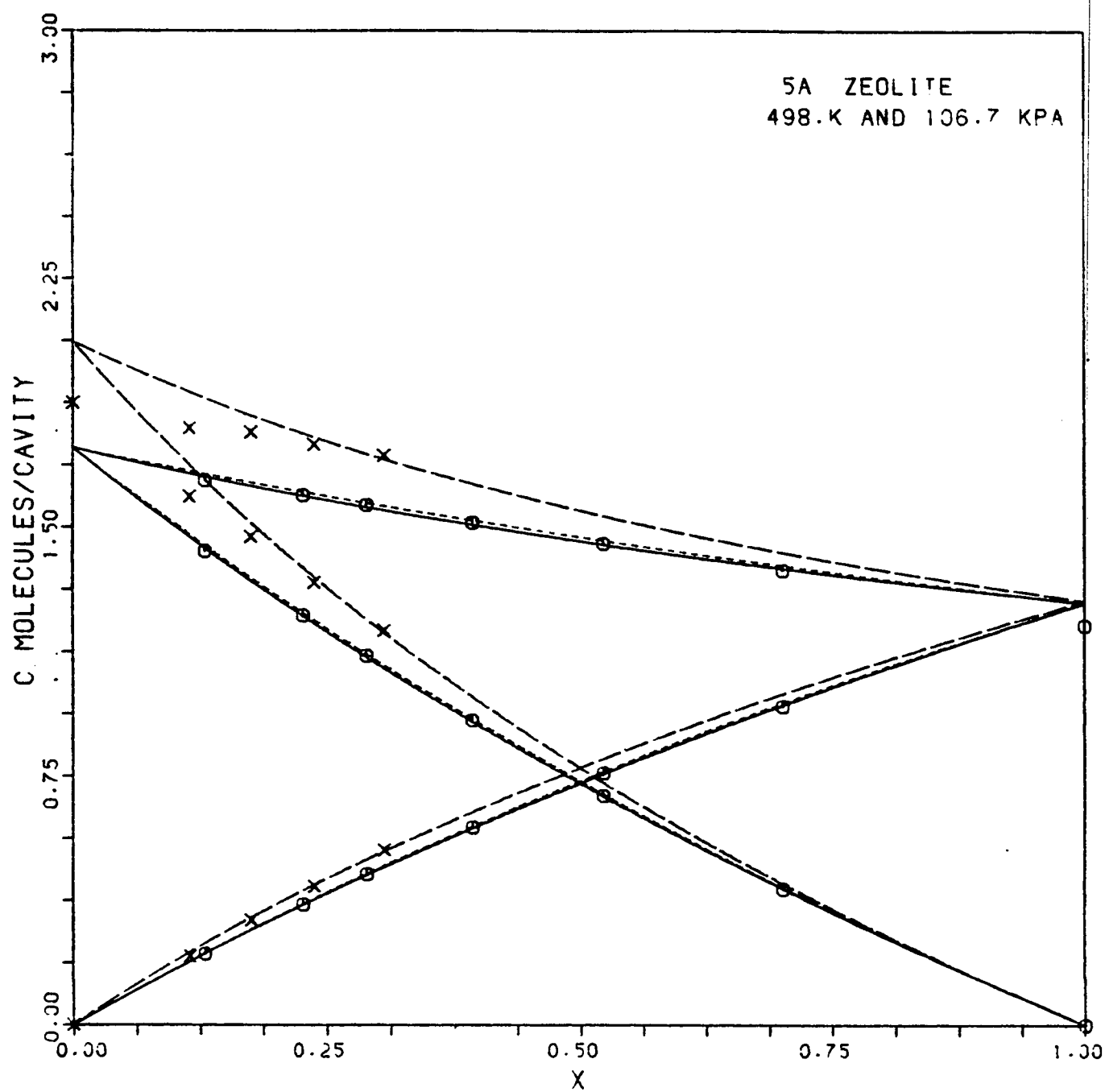


FIGURE 5.8 Concentration curves for the sorption of propane-n-butane binary mixture on 5A zeolite. Curves as in Fig 5.7 .

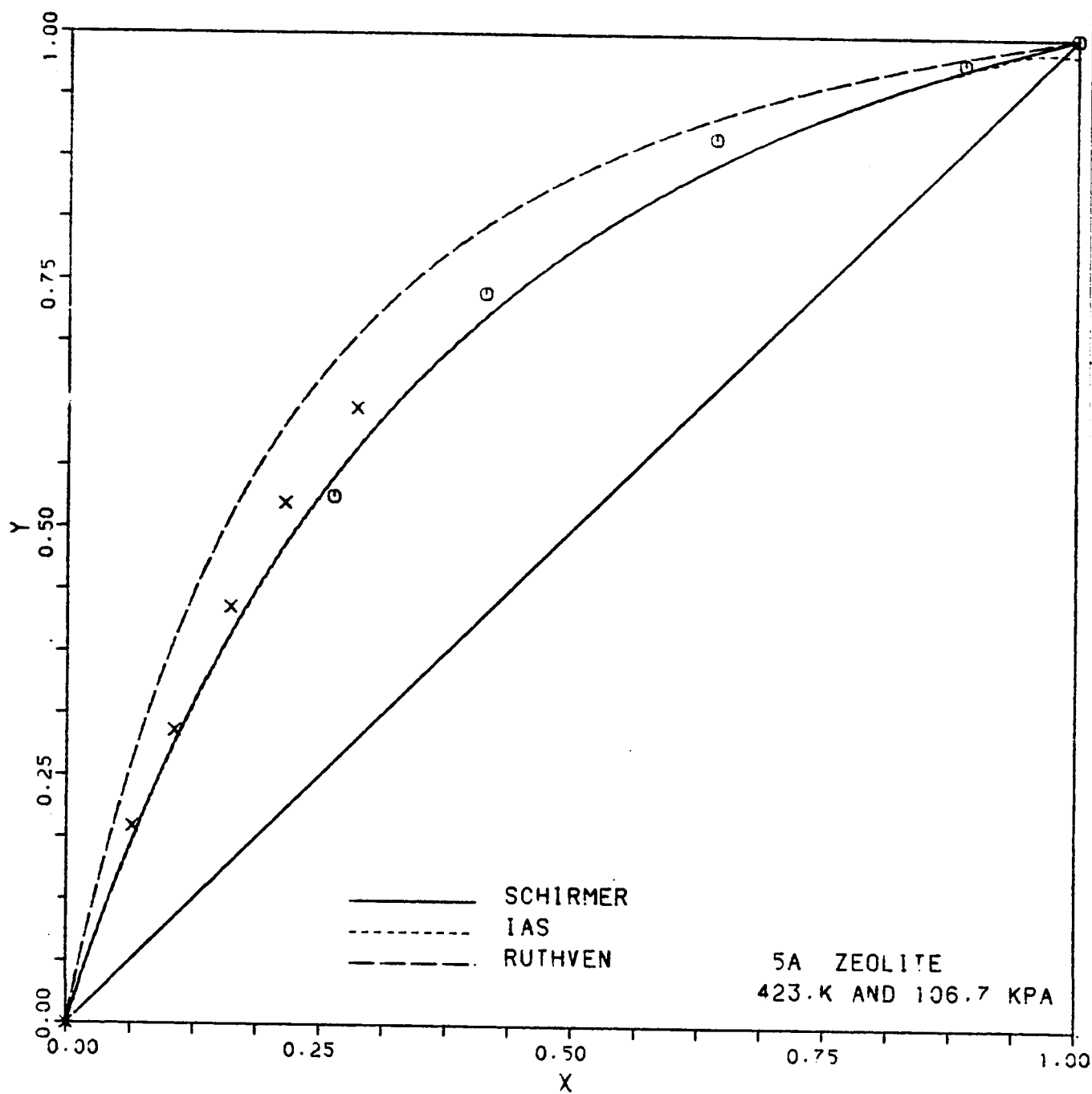


FIGURE 5.9 X-Y diagram for the sorption of propane-n-butane binary mixture on 5A zeolite.

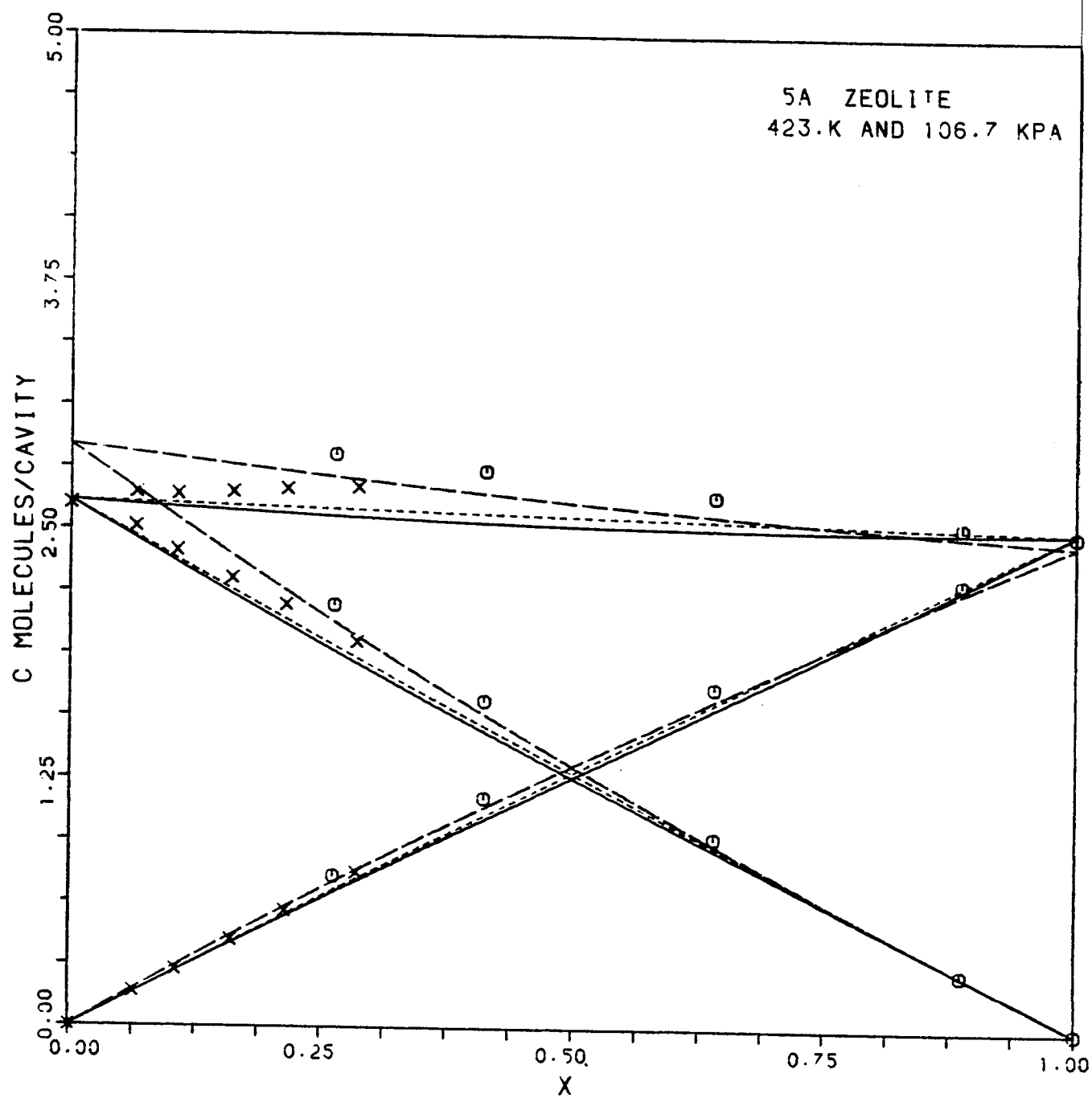


FIGURE 5.10 Concentration curves for the sorption of propane-n-butane binary mixture on 5A zeolite. Curves as in Fig 5.9 .

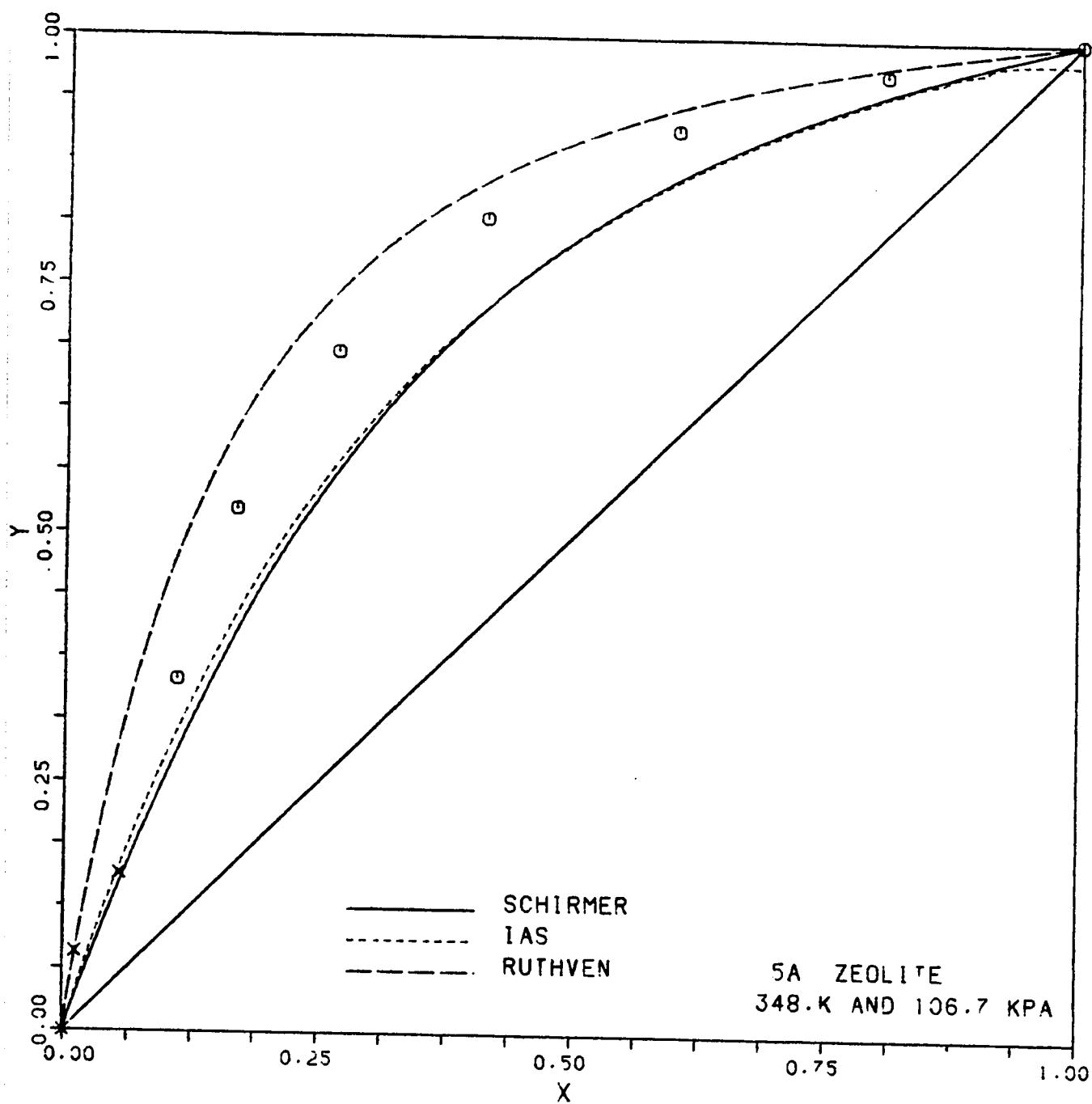


FIGURE 5.11 X-Y diagram for the sorption of propane-n-butane binary mixture on 5A zeolite.

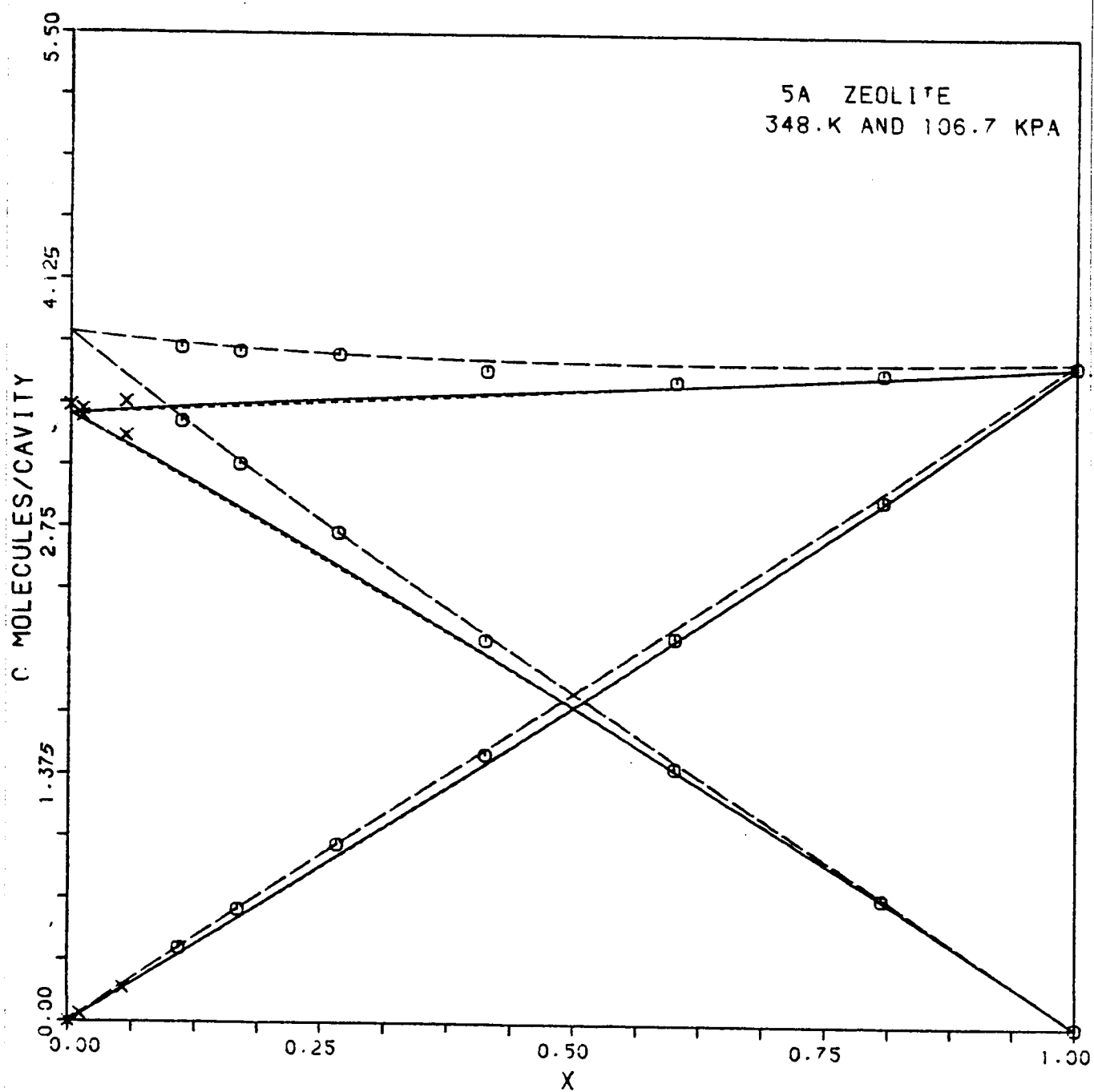


FIGURE 5.12 Concentration curves for the sorption of propane-n-butane binary mixture on 5A zeolite. Curves as in Fig 5.11 .

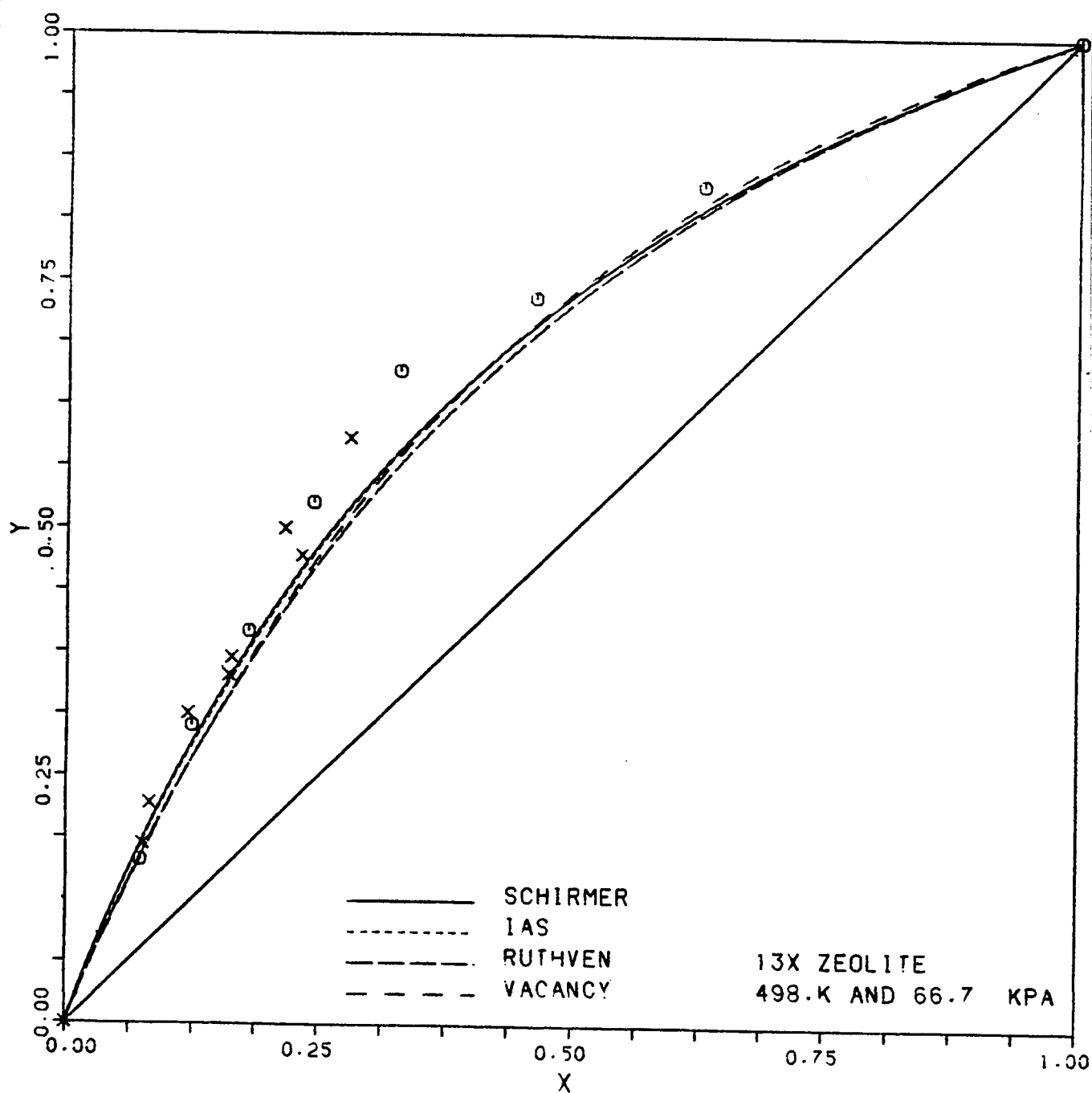


FIGURE 5.13 X-Y diagram for the sorption of propane-n-butane binary mixture on 13X zeolite.

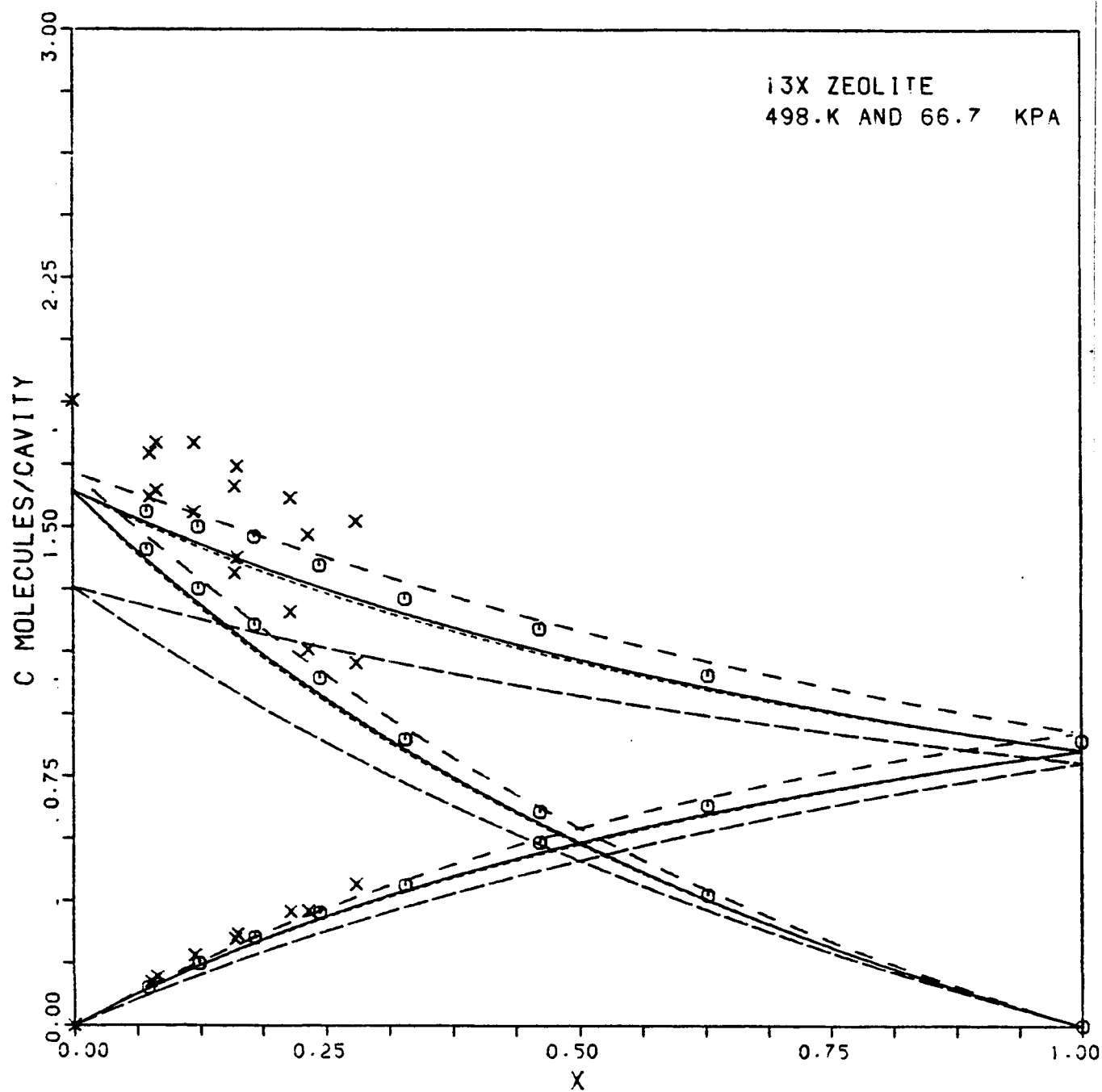


FIGURE 5.14 Concentration curves for the sorption of propane-n-butane binary mixture on 13X zeolite. Curves as in Fig 5.13.

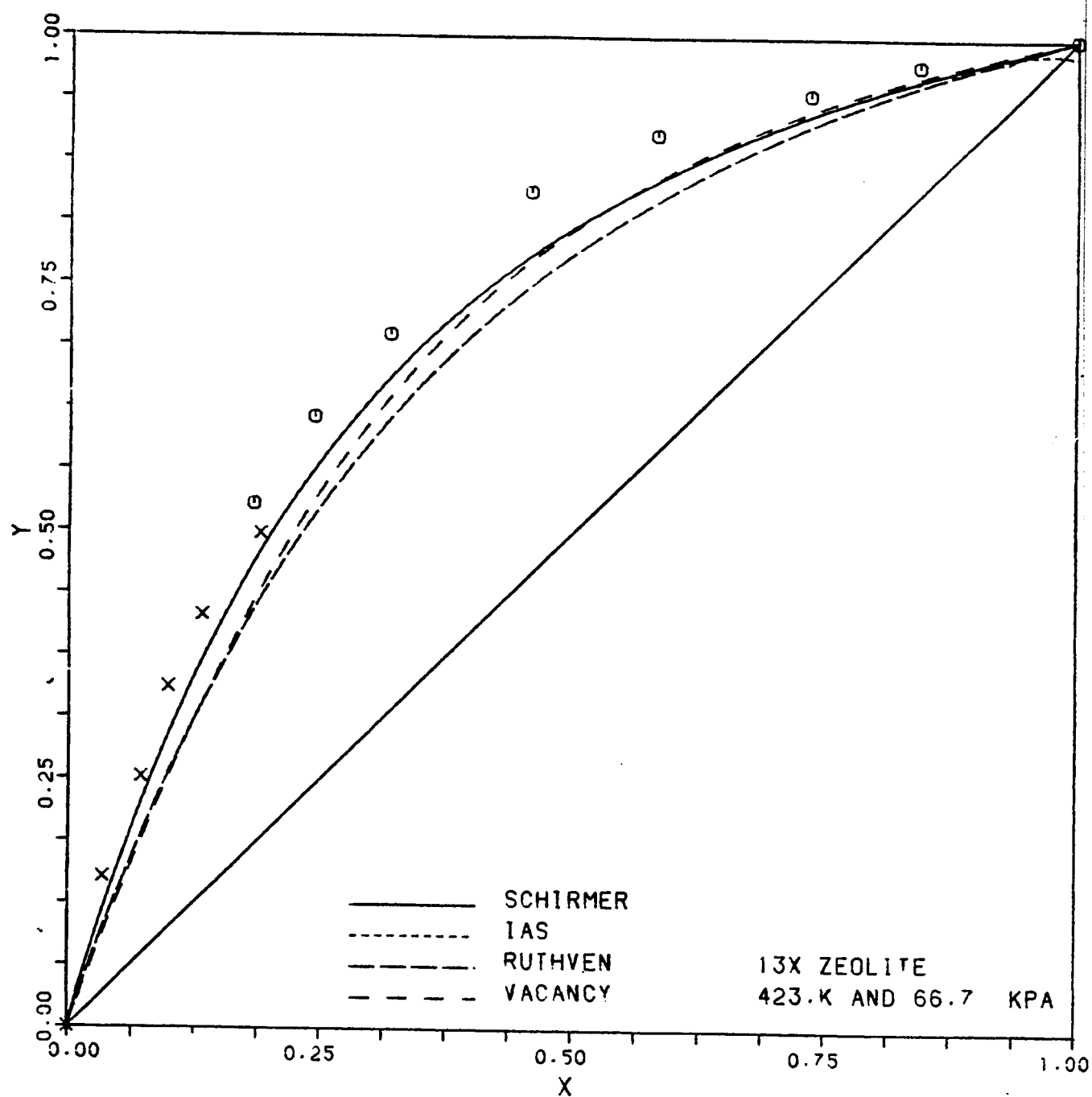


FIGURE 5.15 X-Y diagram for the sorption of propane-n-butane binary mixture on 13X zeolite.

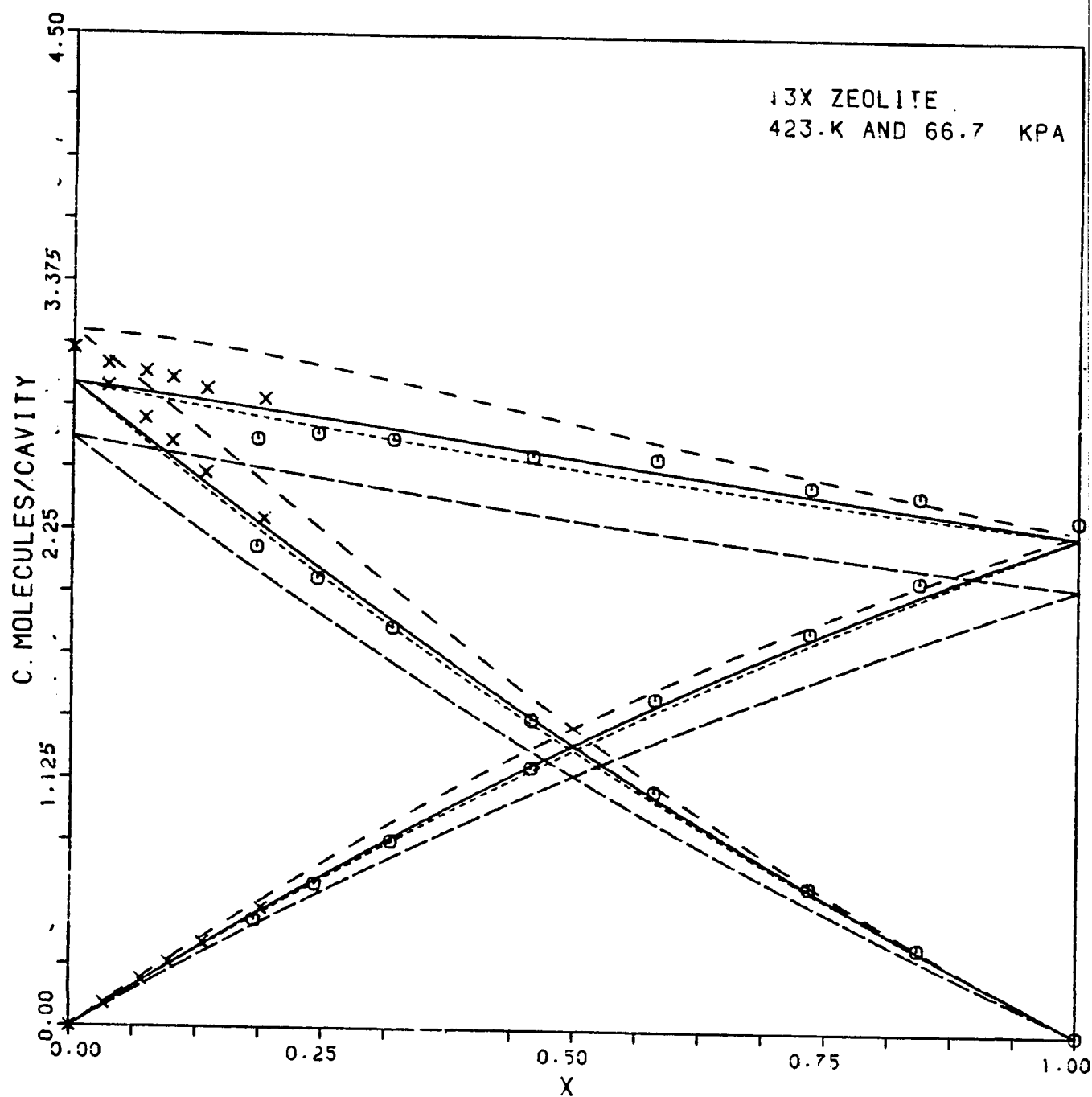


FIGURE 5.16 Concentration curves for the sorption of propane-n-butane binary mixture on 13X zeolite. Curves as in Fig 5.15.

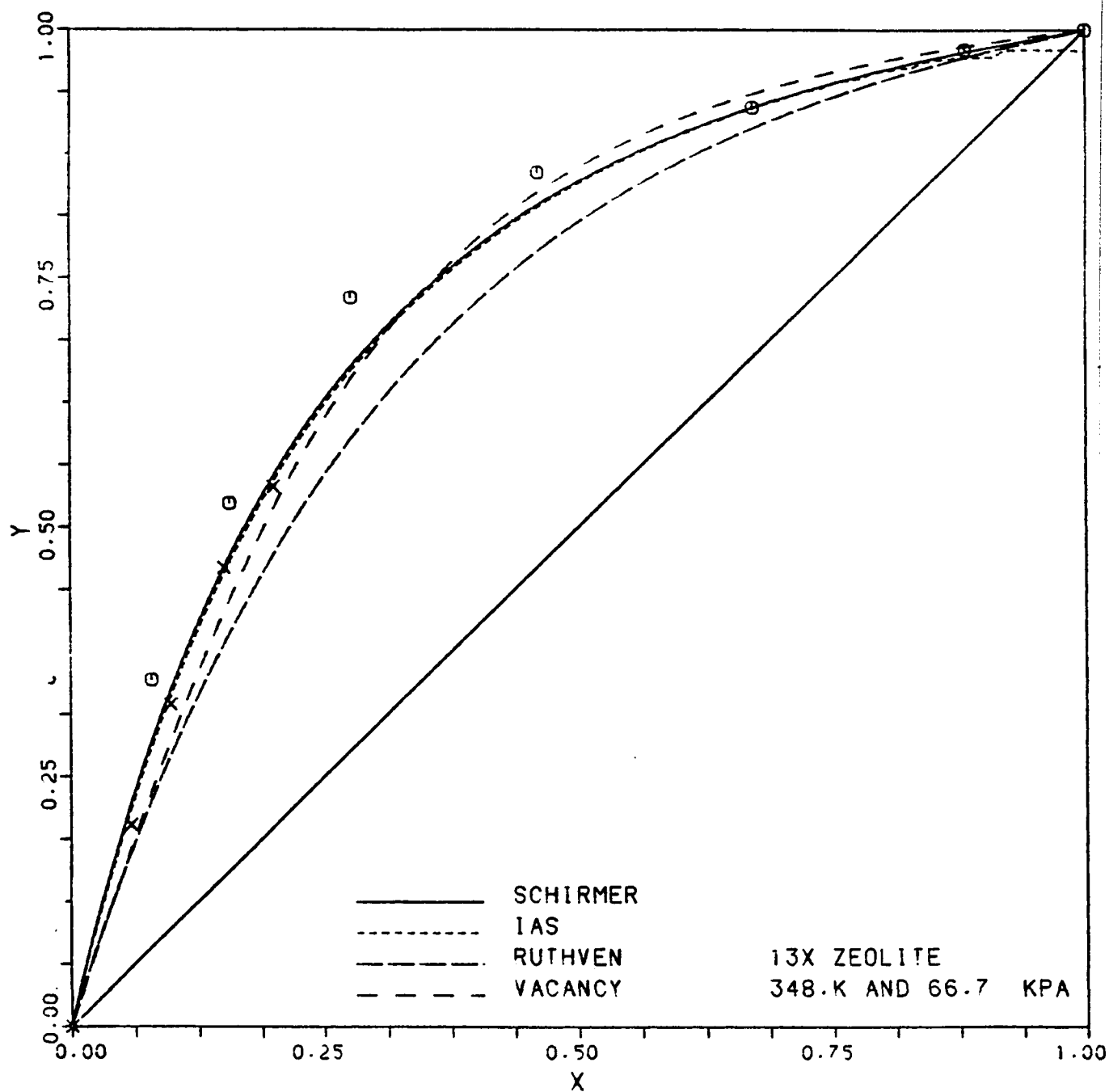


FIGURE 5.17 X-Y diagram for the sorption of propane-n-butane binary mixture on 13X zeolite.

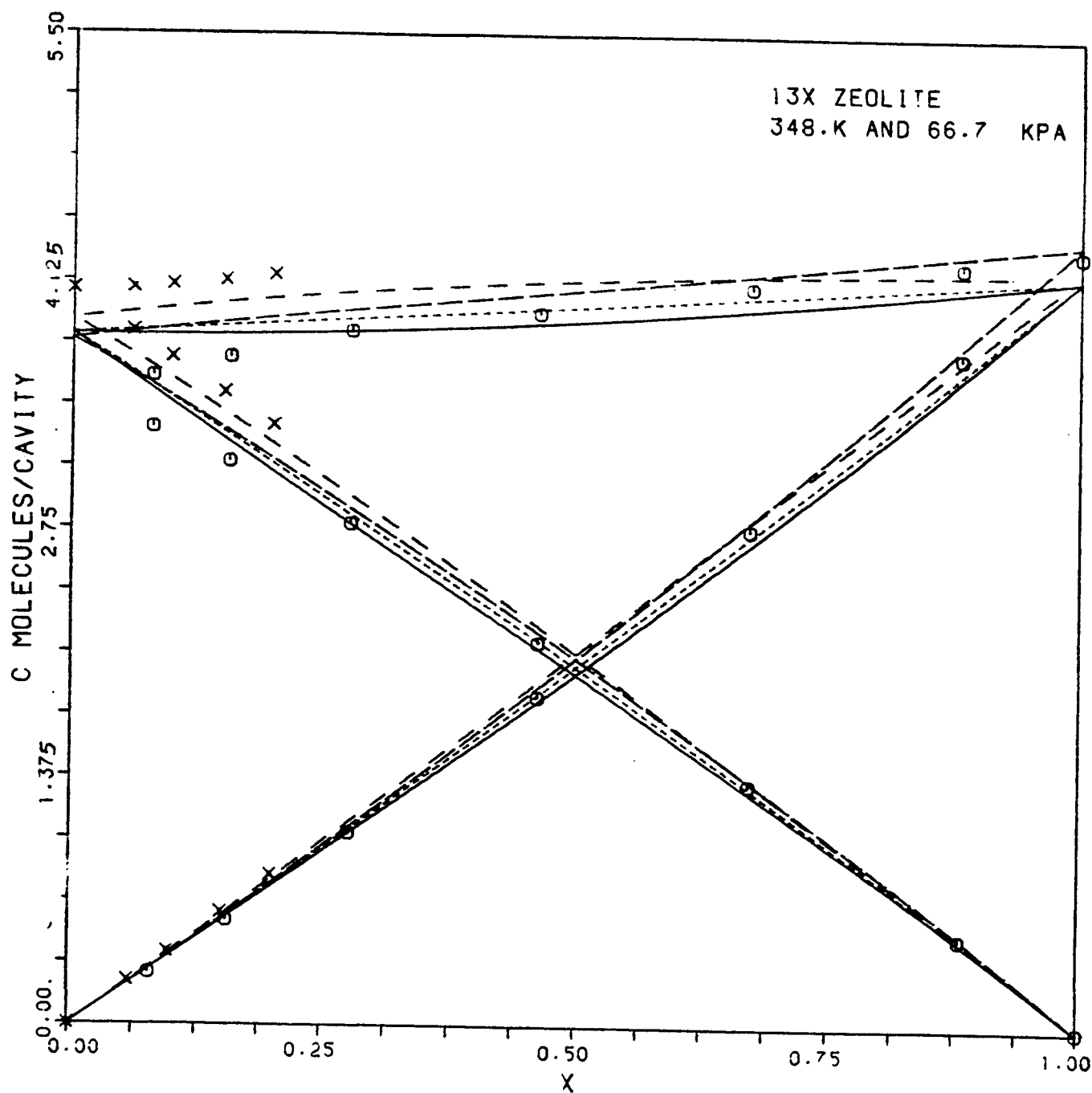


FIGURE 5.18 Concentration curves for the sorption of propane-n-butane binary mixture on 13X zeolite. Curves as in Fig 5.17.

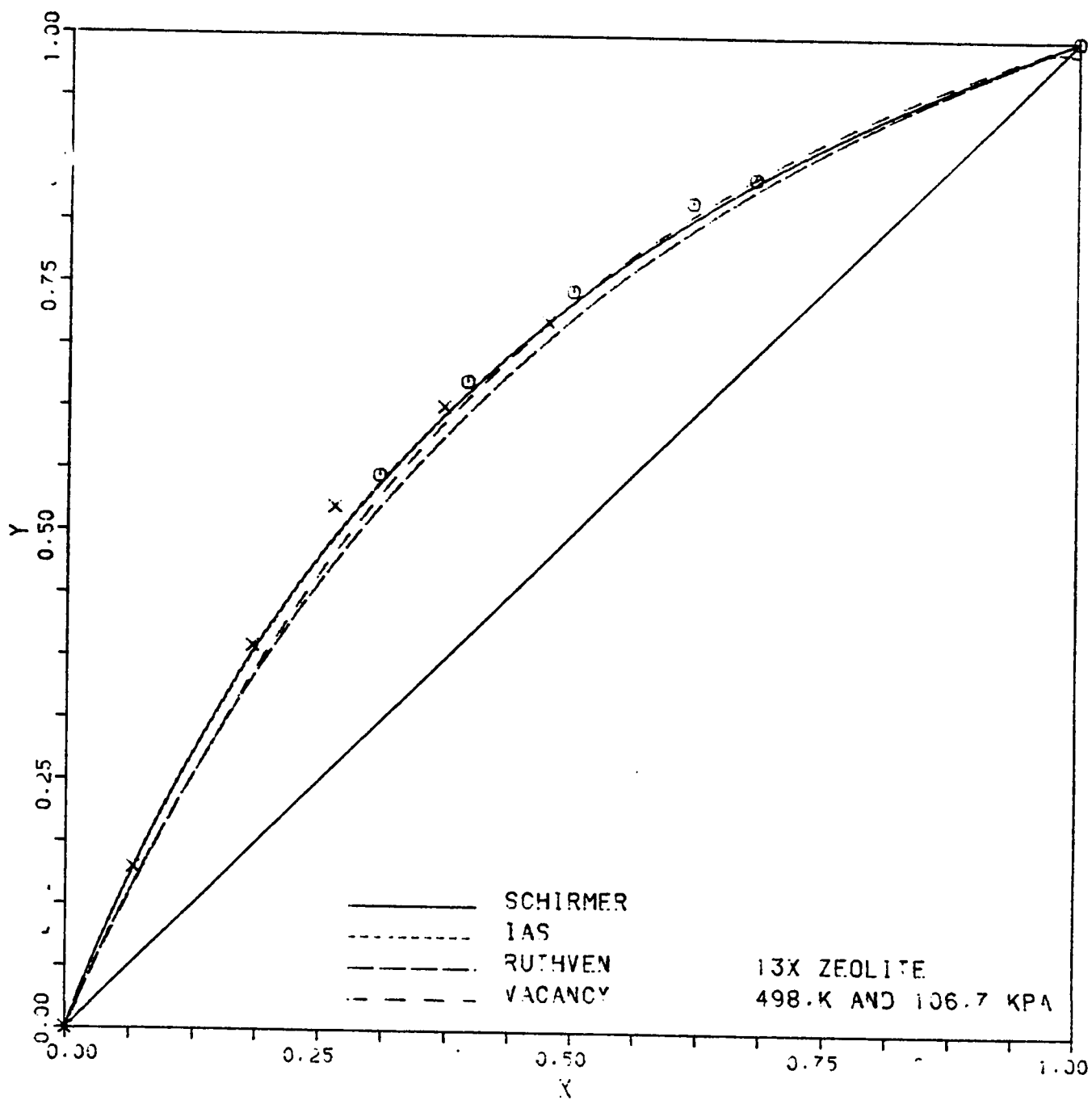


FIGURE 5.19 X-Y diagram for the sorption of propane-n-butane binary mixture on 13X zeolite.

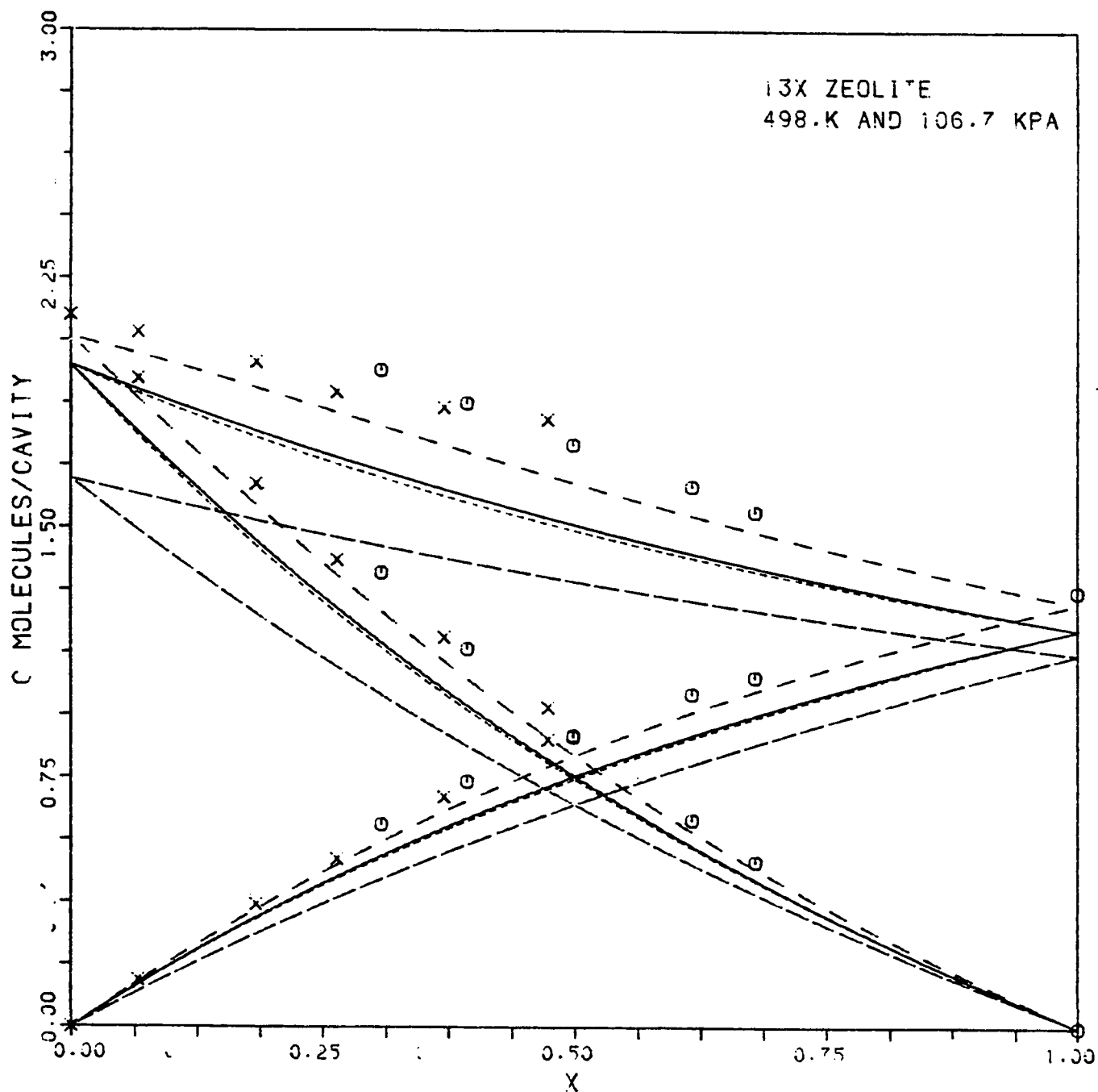


FIGURE 5.20 Concentration curves for the sorption of propane-n-butane binary mixture on 13X zeolite. Curves as in Fig 5.19.

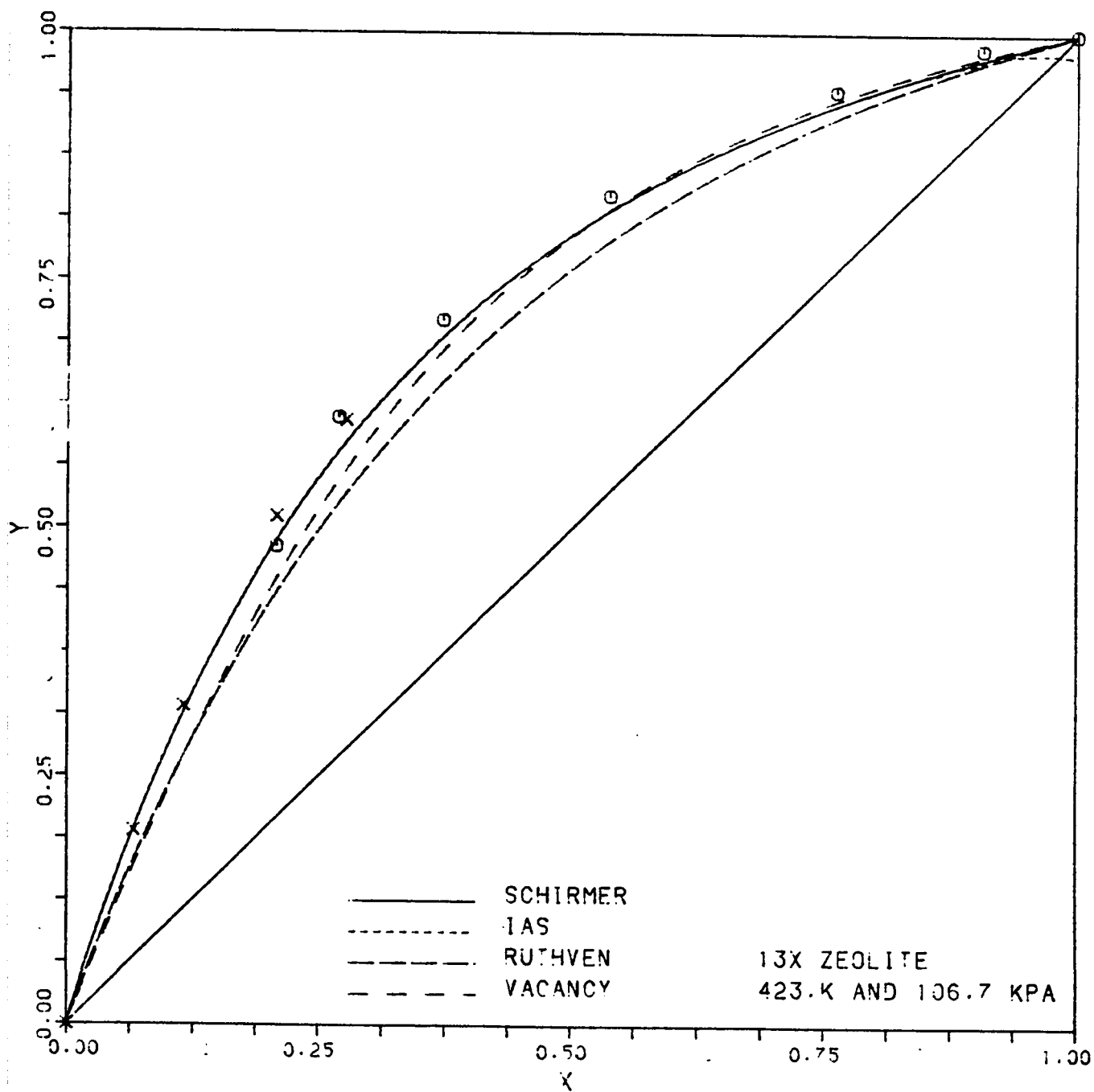


FIGURE 5.21 X-Y diagram for the sorption of propane-n-butane binary mixture on 13X zeolite.

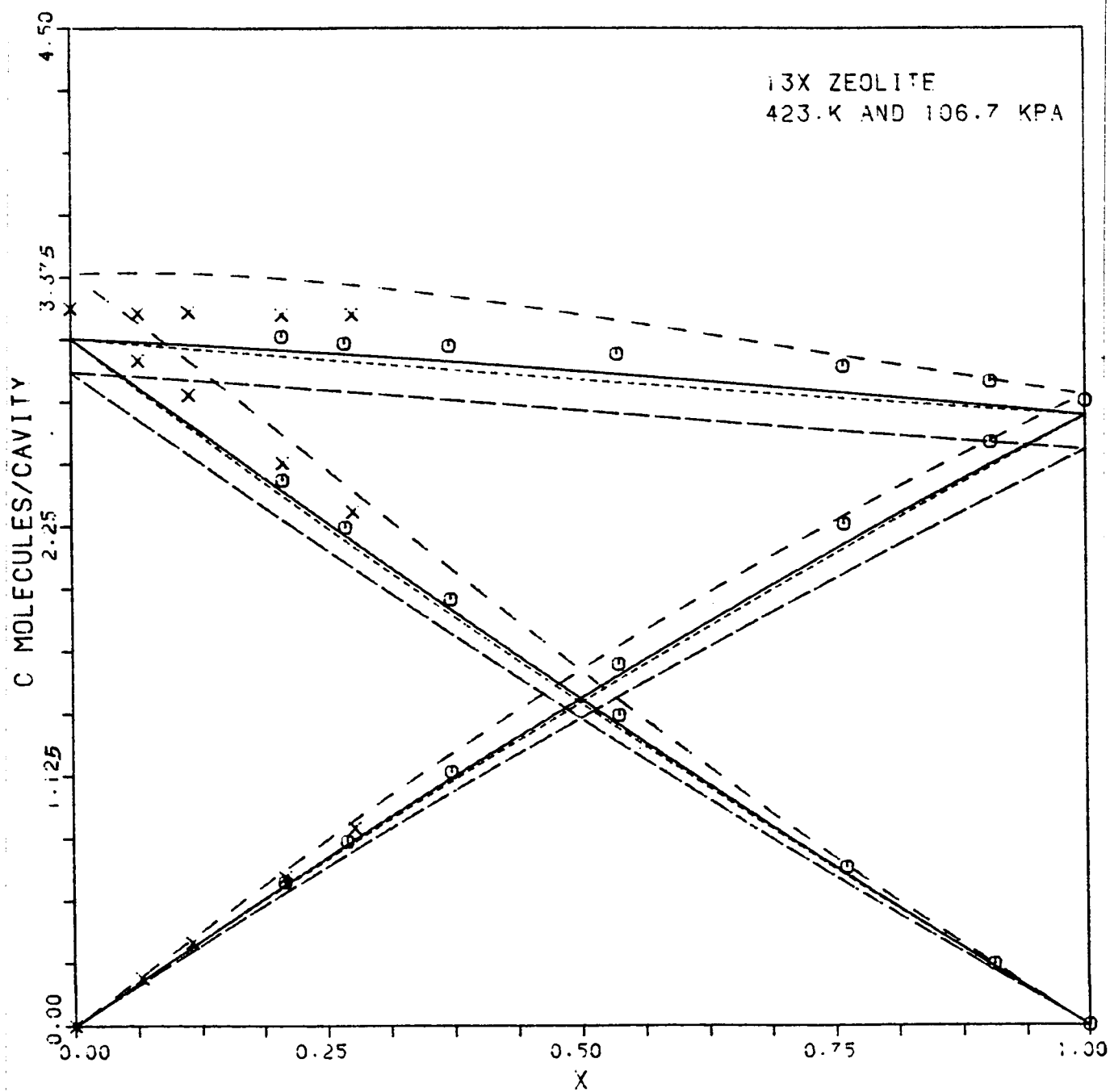


FIGURE 5.22 Concentration curves for the sorption of propane-n-butane binary mixture on 13X zeolite. Curves as in Fig 5.21.

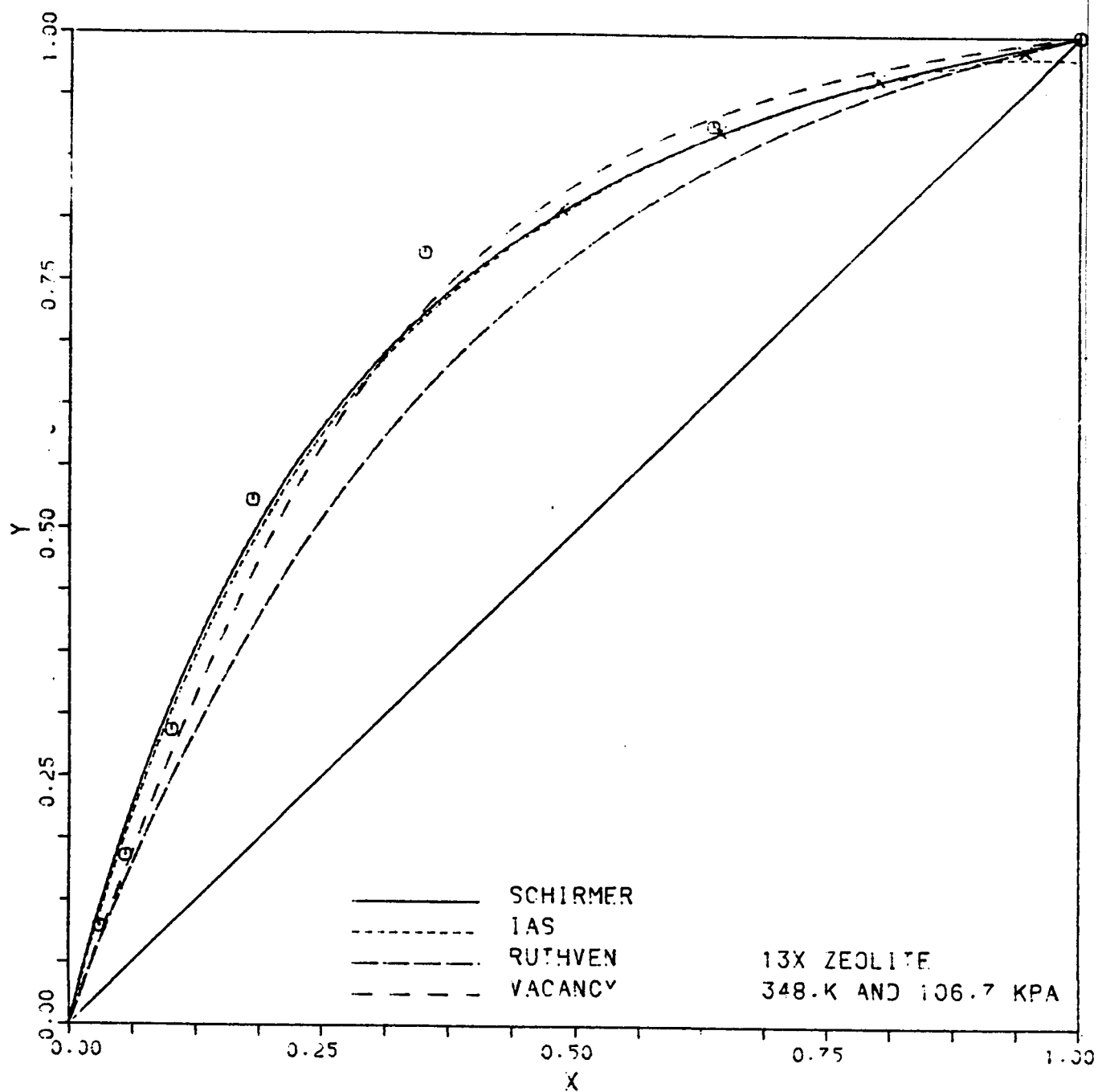


FIGURE 5.23 X-Y diagram for the sorption of propane-n-butane binary mixture on 13X zeolite.

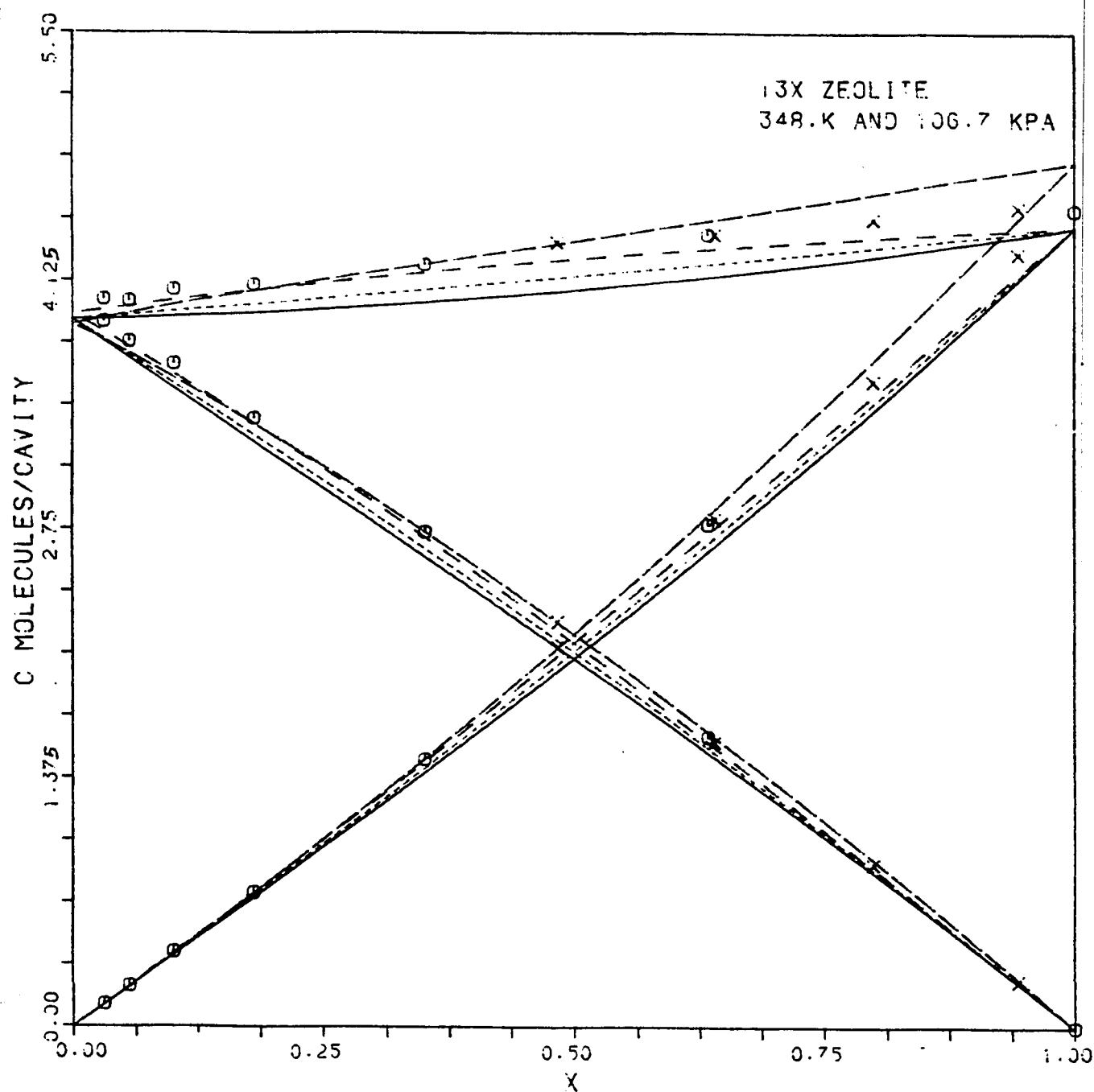


FIGURE 5.24 Concentration curves for the sorption of propane-n-butane binary mixture on 13X zeolite. Curves as in Fig 5.23.

REFERENCES

1. Loughlin, K. F. and Roberts, G. D. ACS Symposium Series No. 135 , (1980)
2. Roberts, G. D., M. S. thesis, University of New Brunswick "Sorption Equilibrium of Methane-Krypton in 5A Zeolite" , (1978)
3. Ruthven, D. M., Loughlin, K. F. and Holborow, K. A. Chem. Eng. Sci., 28 , 701, (1973)
4. Cochran, R. L., Kable, R. L. and Danner, R. P., paper 6 f, presented at AIChE's Golden Jubilee Meeting, Washington, November 1st, (1983)
5. Myers, A. L. and Prausnitz, J. M., AIChE J. 11 , 121, (1965)
6. Glessner, A. J. and Myers, A. L., C.E.P. Symposium Series, 65 , 73, (1969)
7. Holborow, K. A., Ph.D. thesis, University of New Brunswick "Multicomponent Sorption Equilibria of Gases in 5A Zeolite" , (1974)
8. Myers, A. L. AIChE J., 19 , 667, (1973)
9. Myers, A. L. Ind. Eng. Chem. , 60 , 45, (1968)

Chapter VI

CONCLUSIONS AND RECOMMENDATIONS

6.1 CONCLUSIONS

The adsorption of propane and n-butane on 5A and 13X pellets of 5A and 13X zeolites is studied and the Henry constants and the limiting heat of adsorption are evaluated. The limiting heat of adsorption is the same for n-butane on 5A and 13X zeolites and a small difference is found in the case of propane.

Four models were studied for the pure component adsorption namely: Schirmer, Ruthven, Vacancy and Virial models. The Schirmer model shows the best fit in general. Schirmer and Ruthven models show better fit for the 5A zeolite than for 13X zeolite. This is consistent with the assumption utilized to derive these models which states that each cavity is independent subsystem. The 13X framework is more open and hence allow for more interactions between different cavities.

Both Ruthven and Schirmer models are base on statistical thermodynamic considerations. The better fit obtained for Schirmer model is probably due to the fact that in Schirmer model the canonical partition function is evaluated from experimental data in nearly its exact form. While in Ruthven model it is approximated on the basis of crude assumptions.

The form of the virial equation used here shows a good representation of the data in the generalized form. The vacancy solution theory does not give good results as obtained by the original authors. When the experimental Henry constant or the experimental heat of adsorption in the case of Schirmer model are used in the models less accurate fit is obtained in general which shows some weaknesses in the models.

For the binary data it was found that a better separation is obtained for lower temperature and pressure. The temperature has a pronounced effect on the separation while the pressure has a weak effect. The 5A zeolite gives a smaller selectivity factor than 13X zeolite and hence a better separation. However the difference is small. This can be explained by the fact that the gases are non-polar and hence most of the interactions are with the oxygen rings. If they were polar the two zeolites may show much different selectivities since they contain different cations.

The small value for the selectivity coefficient indicates a good separation which gives more opportunity for the success of the PSA process for such systems. The separation is expected to be even more for members of the homologous series which have a difference of more than one carbon atom such as methane and propane.

Regarding model fits the general trends found for the pure component are repeated. The Schirmer and the IAS give in general the best fit. The Ruthven isotherm was not too bad. In fact in one or two cas-

es it gives the best fit. The vacancy solution theory does not success in predicting the binary behavior as was expected.

The models suggested here for predicting the non-ideal behavior of ethylene-carbon dioxide mixture using Schirmer binary model were not very successful. However, the unsatisfactory fit for the pure component does not allow a final conclusion. There was a slight improvement over the ideal case, but it does not give the right behavior at all temperatures.

6.2 RECOMMENDATIONS

The pure component models need more testing for other sorbate-sorbent systems especially the vacancy solution model which does not show good predictions as in the original work in which it appears. Since the virial model used here shows in general a good representation of the data in the generalized form, it is recommended to extend it, in the generalized form, to cases with variable heat of adsorption.

It seems that the application of the PSA process to the separate of light straight chain normal paraffines will be successful because of the large selectivity found, and hence a detailed study is recommended. The pure component and mixture sorption data and column studies at higher pressures and ambient temperature is needed. Sorption data on other commercial zeolites are needed to determine the most suitable zeolite to perform the best separation.

A detailed study of the behavior of non-ideal mixtures in the sorbed phase is recommended to be used in predicting the mixture behavior from the least amount of experimental data. The IAS and Schirmer models are examples where this study will be very useful. A good fit for the pure component data has to be established before going to the mixture. A system with non-ideal behavior, but with constant heat of adsorption and larger molecules for both components is recommended since it is not easy to fit the pure component Schirmer et al. model with large number of constants.

Finally Schirmer and vacancy binary models need to be tested more since they only appear recently in the literature. They need to be tested by other workers at other conditions to get a clear idea about their goodness.

Appendix A

ETHYLENE-CARBON DIOXIDE BINARY MIXTURE

To apply the Schirmer model to $C_2H_4-CO_2$ -5A system which exhibits non-ideality, excess properties are needed. Assuming that the molecular interactions do not alter the arrangement of the molecules in the solution, then the excess entropy can be set equal to zero. If we further assume that the excess enthalpy is equal to Bx_1x_2 , where B is a constant independent on temperature, then we have a regular solution. Hildebrand et al. [1] defined regular solutions as those made up of non associating components. For $C_2H_4-CO_2$ it is not expected that they will form association complexes. Prigogine and Defay state that [2]

" We shall only expect to encounter these complexes in solutions containing molecules which have considerable electric charge near the surface of the molecules, such as in molecules containing the groups, NH_2 , OH ,"

The value of B was optimized from the binary data. B was found to be = -40340 J/mol. This value is high for a regular solution. If the interactions are strong enough to give this value then they will alter the arrangement of molecules [2]. Prigogine and Defay suggested that for the excess entropy to be zero B has to be of the order of the thermal energy (about 2500 J/mol at normal temperatures).

As an alternative the Wilson equation for the excess Gibbs energy can be used. The excess entropy and enthalpy in Eq. 2.20 can be combined to give

Wilson suggested the following equation for the Gibbs energy of mixing for binary mixture

$$G^E = -RT[x_1 \ln(x_1 + G_{12}x_2) + (x_2 \ln(G_{21}x_1 + x_2))] \quad (A.2)$$

where $G_{ij} = V_j/V_i \exp(-a_{ij}/RT)$ where a_{ij} reflects the difference between the interaction of pure i molecules and the interactions of i and j molecules. a_{ij} are taken to be temperature and concentration independent for a limited temperature range[3]. The values of a_{12} and a_{21} are optimized from the binary data using BSOLVE. It was found that $a_{12} = -6899$. and $a_{21} = 90160$ J/mole.

Ethylene and carbon dioxide pure component data from literature was used to fit the Schirmer model. For carbon dioxide it is reported that the heat of adsorption varies with concentration. The author tried to fit the Schirmer et al. model to the data allowing the energy constants to vary with coverage. However, the large number of constants to be regressed (24 constants since the 5A cavity can hold up to 12 CO₂ molecules) results in values which are physically unacceptable.

As a result the energy constants were set equal to the experimental heat of adsorption at the corresponding concentrations. Data of Khvoshchev et al. [4] was used. The constants for ethylene and carbon dioxide are given in Table A.1 . The prediction of the pure component behavior is shown in Figures A.1 and A.2 . The prediction is not satisfactory and hence it does not give a good representation of the binary behavior. The binary predictions are shown for completeness.

The author tried to fit the vacancy model to the pure component data of ethylene and carbon dioxide, but with no success especially for ethylene where the lowest average deviation obtained is 0.958 (.330 for CO_2). Therefore, no binary calculations were done for this model. Holborow used a modified form of the Ruthven et al. model to predict his data.

The prediction of the binary data by Schirmer and IAST models based on ideal solution is shown in Figs A.3 to A.8 . When the regular solution and the Wilson equation are used a little improvement is observed(Fig A.9 to A.14). A slightly better fit was obtained when the Wilson was used (the average deviation is 0.287 for the regular solution and 0.172 for the Wilson equation). However, the fit is still poor. A better fit can be obtained if each temperature alone is fitted. However, this approach is not recommended since it does not allow the prediction of the system at other temperatures and pressures. In addition, the regular solution constant B , cannot be a function of temperature from the thermodynamic point of view[5]. For Wilson equation the assumption that a_{ij} are independent of temperature does not appear adequate.

The excess properties derived from Redlich-Kwong and COR [6] equations of state have been tested, but also with little success. In fact this approach is not expected to work since it is known that the presence of the adsorbate alter the interactions between the two sorbed

species. A study on the behavior of mixtures in the sorbed state is recommended to further clarify this situation.

TABLE A.1

PURE COMPONENT CONSTANTS FOR THE SCHIRMER ET AL. MODEL

	Ethylene		Carbon dioxide	
	-S	-E	-S	-E
1	53.08	32818.	96.04	48200.
2	61.93	32818.	97.18	46000.
3	63.36	32818.	100.29	44900.
4	68.83	32818.	100.92	44600.
5	71.10	32818.	104.46	43800.
6	78.01	32818.	104.64	41700.
7	83.30	32818.	104.81	40500.
8	90.59	32818.	104.84	40000.
9			104.84	40000.
10			106.26	40000.
11			109.60	40000.
12			111.68	40000.

S in J/mole/K

E in J/mole

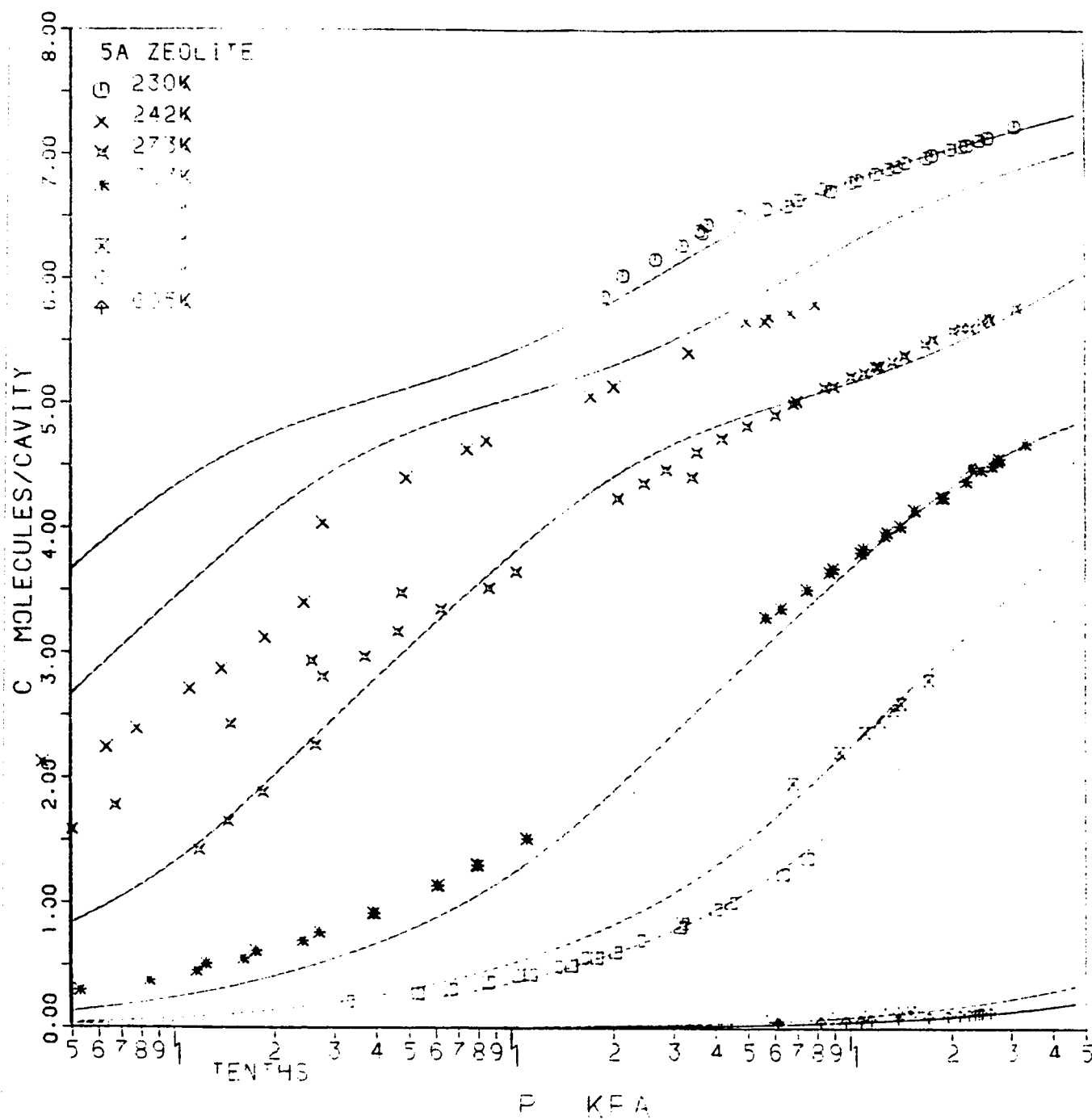


FIGURE A.1 Pure component sorption isotherms for ethylene on 5A zeolite. Curves from Schirmer et al. model.

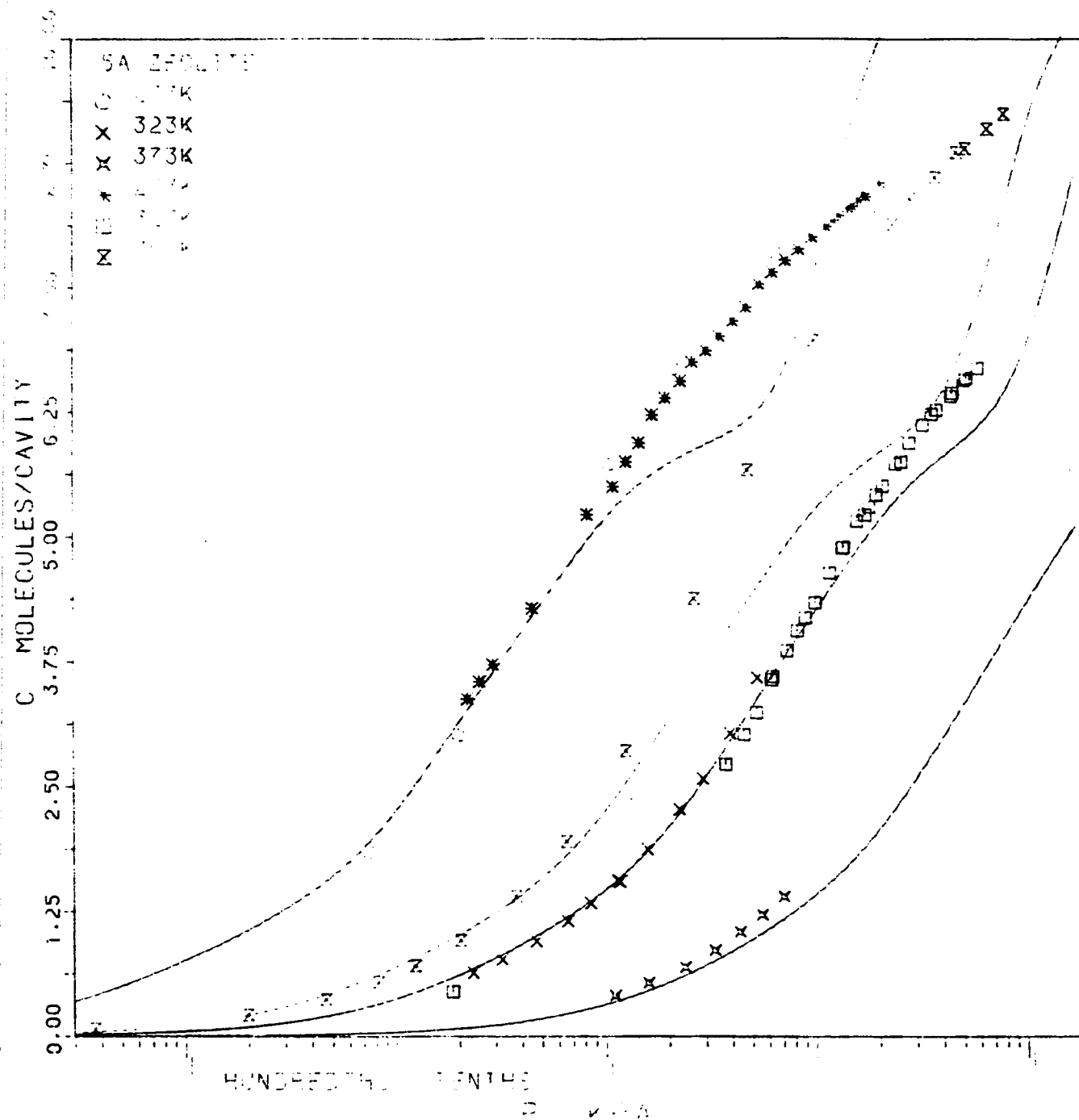


FIGURE A.2 Pure component sorption isotherms for carbon dioxide on 5A zeolite. Curves from Schirmer et al. model.

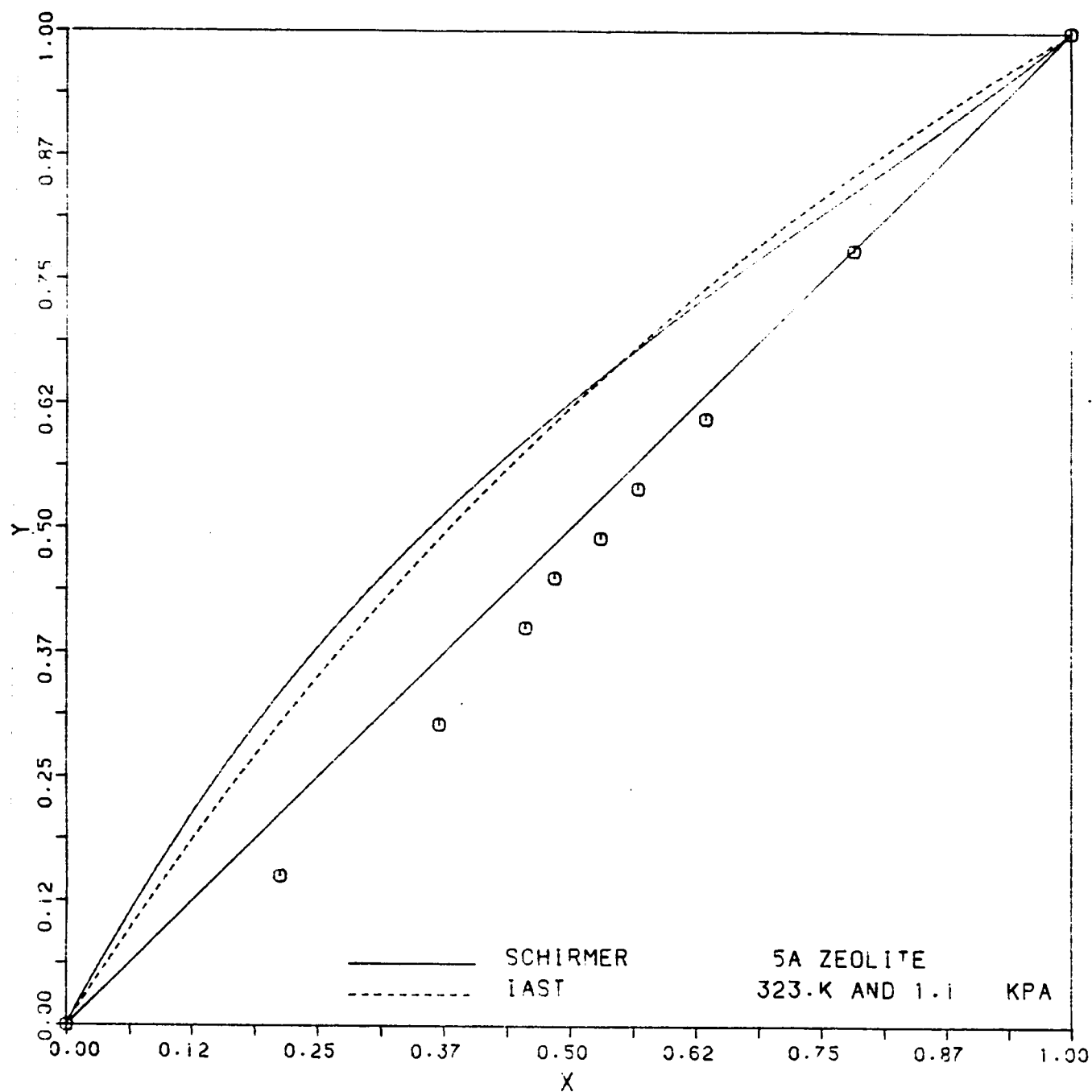


FIGURE A.3 X-Y diagram for the sorption of ethylene-carbon dioxide binary mixture on 5A zeolite. Ideal solution

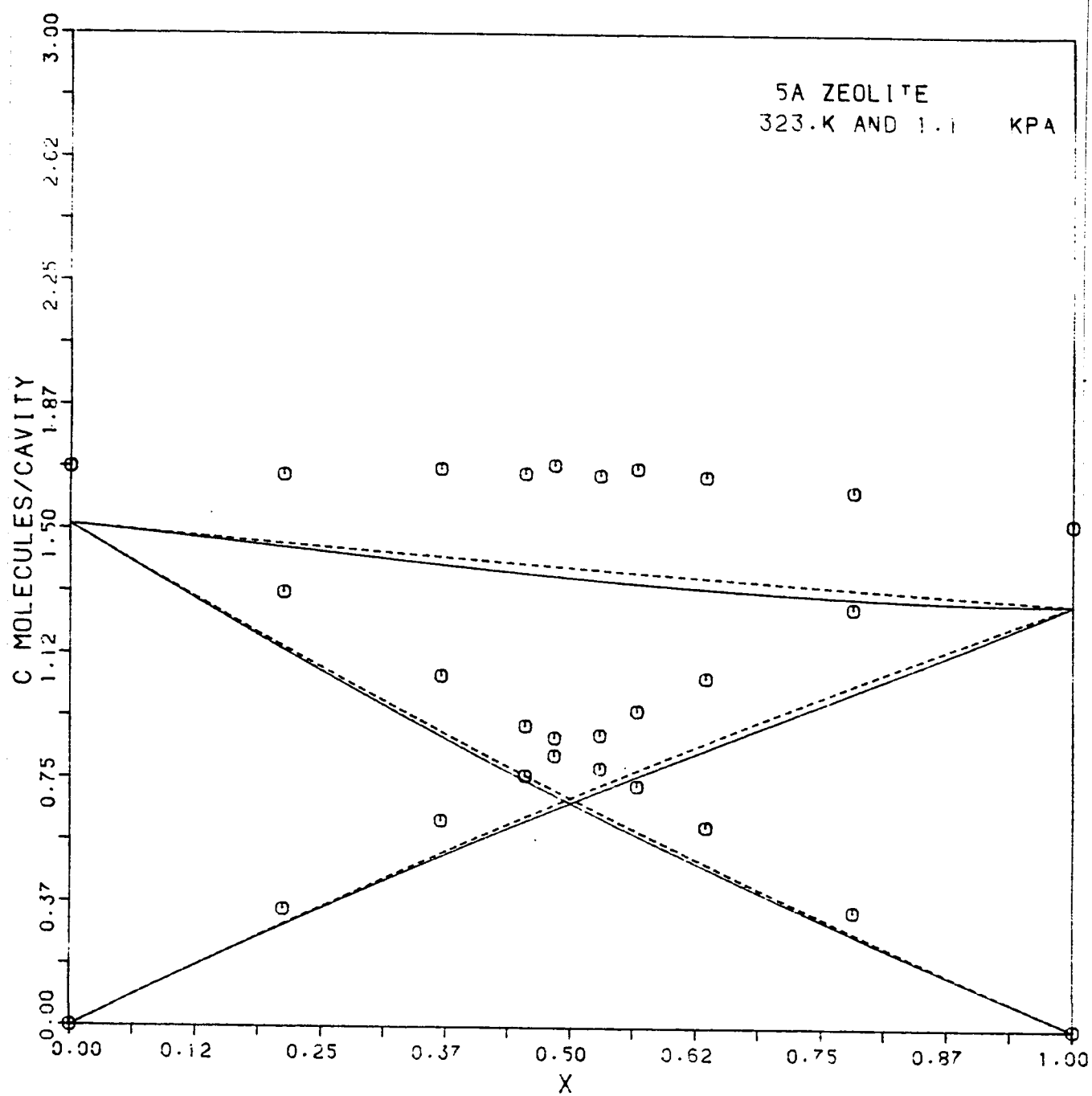


FIGURE A.4 Concentration curves for the sorption of ethylene-carbon dioxide binary mixture on 5A zeolite. Ideal solution

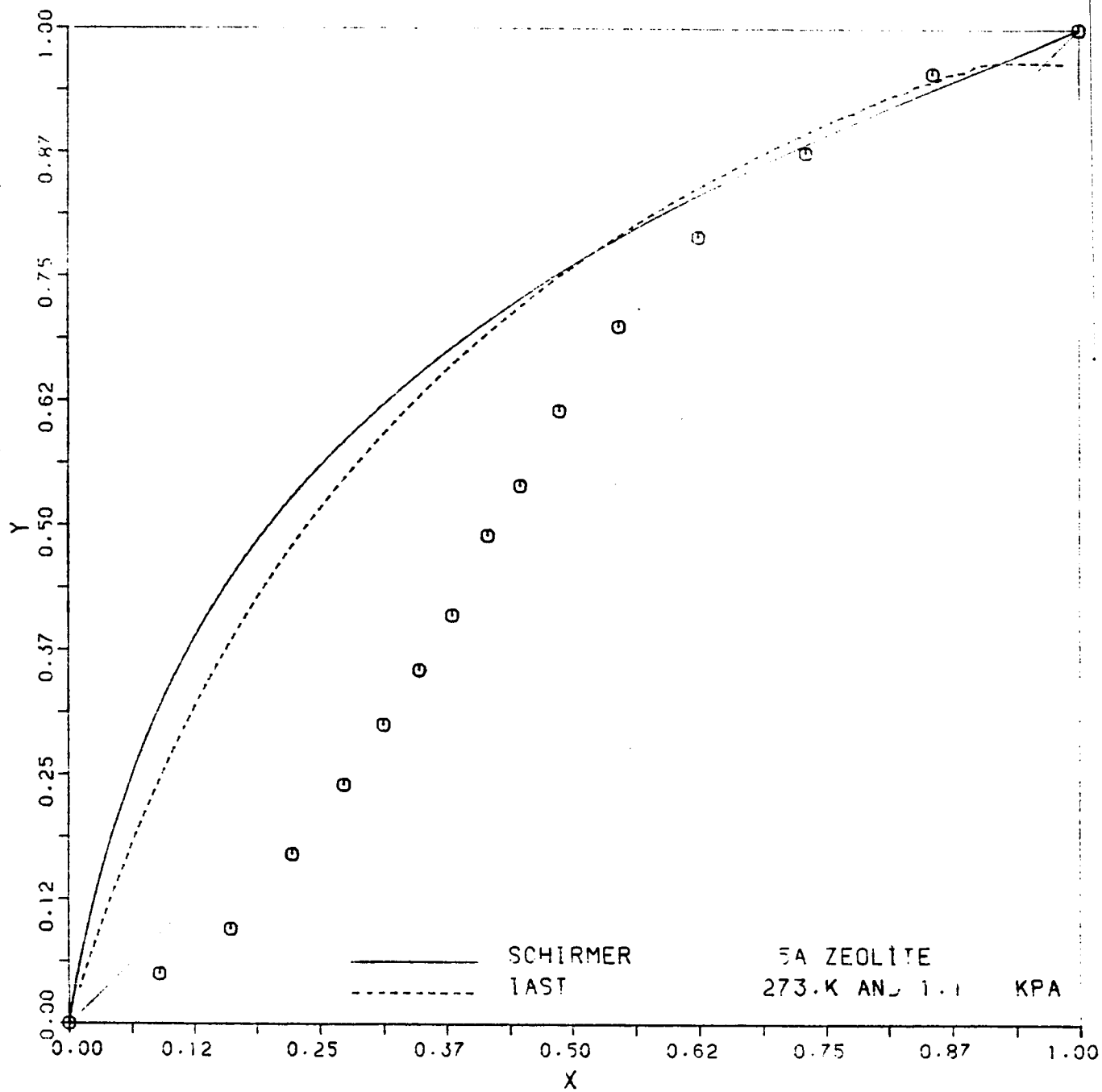


FIGURE A.5 X-Y diagram for the sorption of ethylene-carbon dioxide binary mixture on 5A zeolite. Ideal solution

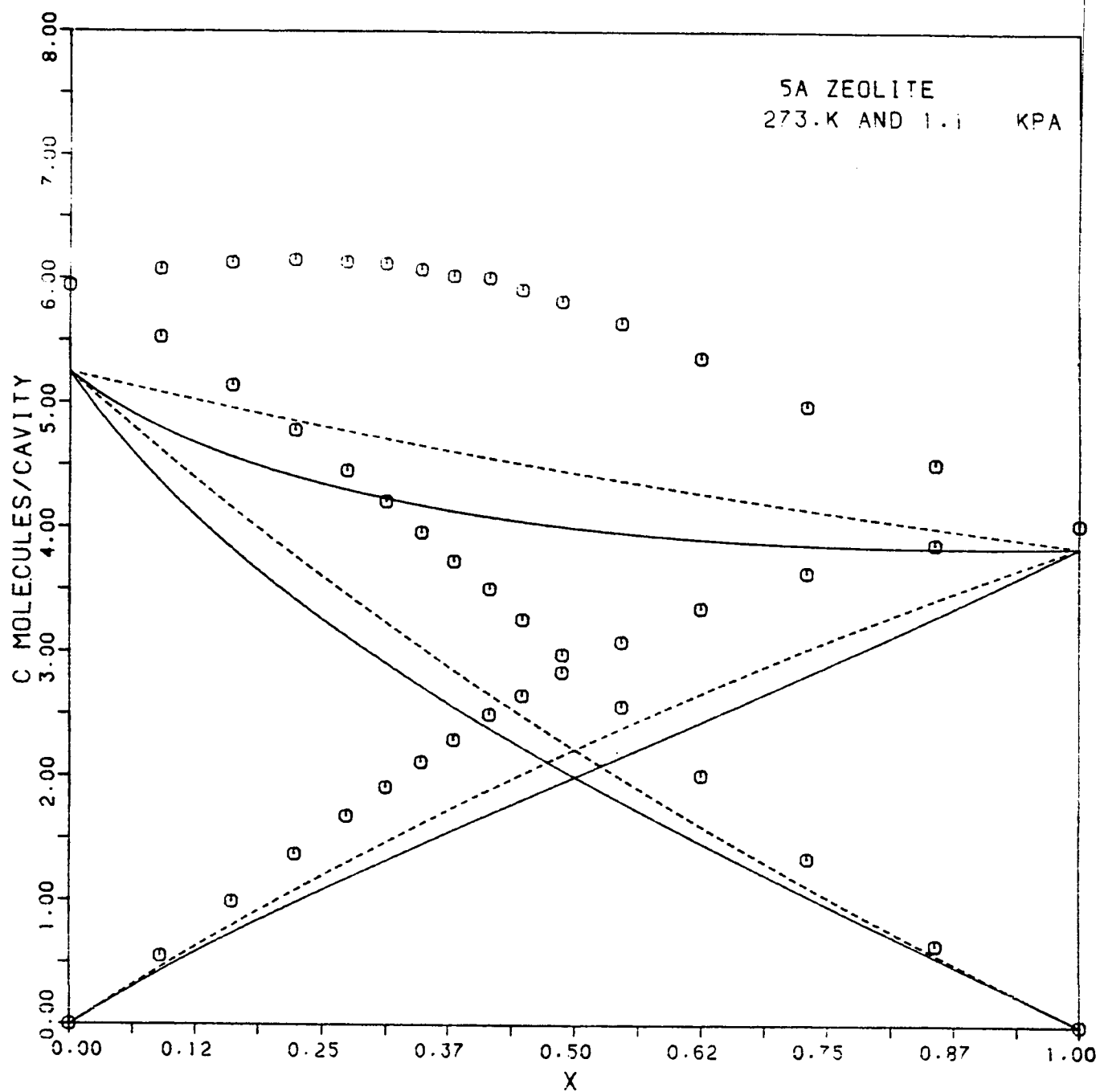


FIGURE A.6 Concentration curves for the sorption of ethylene-carbon dioxide binary mixture on 5A zeolite. Ideal solution

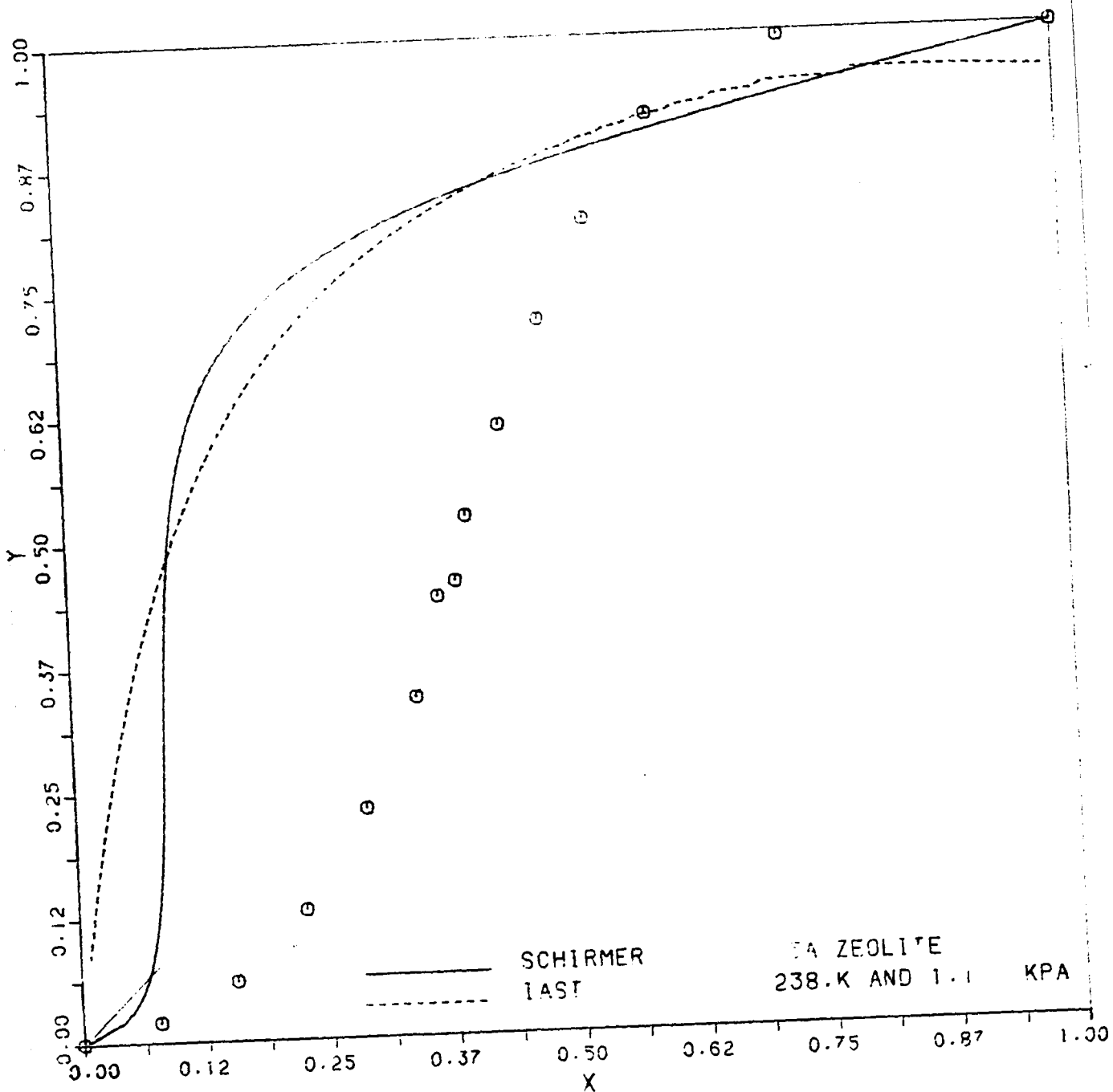


FIGURE A.7 X-Y diagram for the sorption of ethylene-carbon dioxide binary mixture on 5A zeolite. Ideal solution

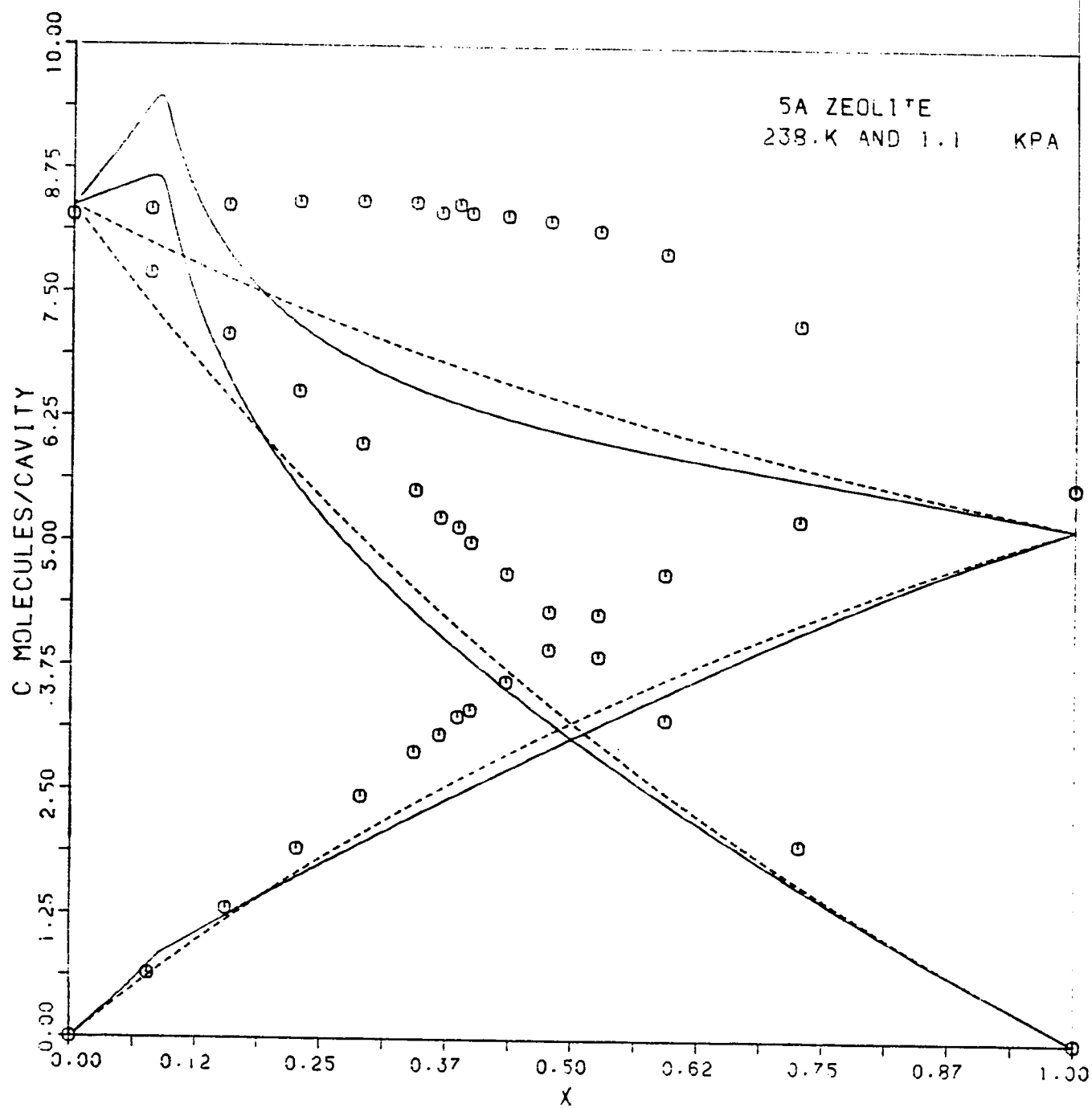


FIGURE A.8 Concentration curves for the sorption of ethylene-carbon dioxide binary mixture on 5A zeolite. Ideal solution

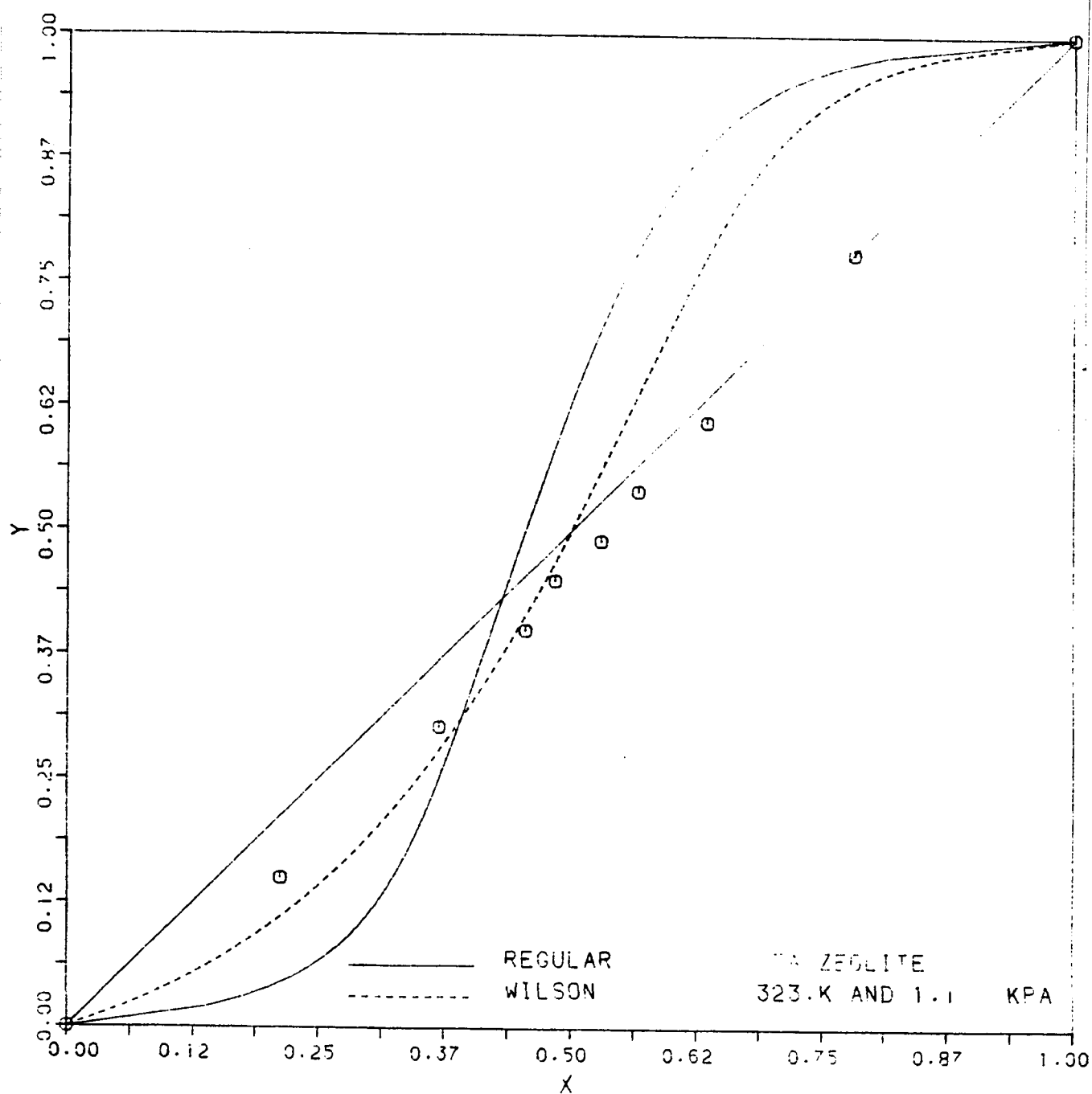


FIGURE A.9 X-Y diagram for the sorption of ethylene-carbon dioxide binary mixture on 5A zeolite. Non-ideal solution

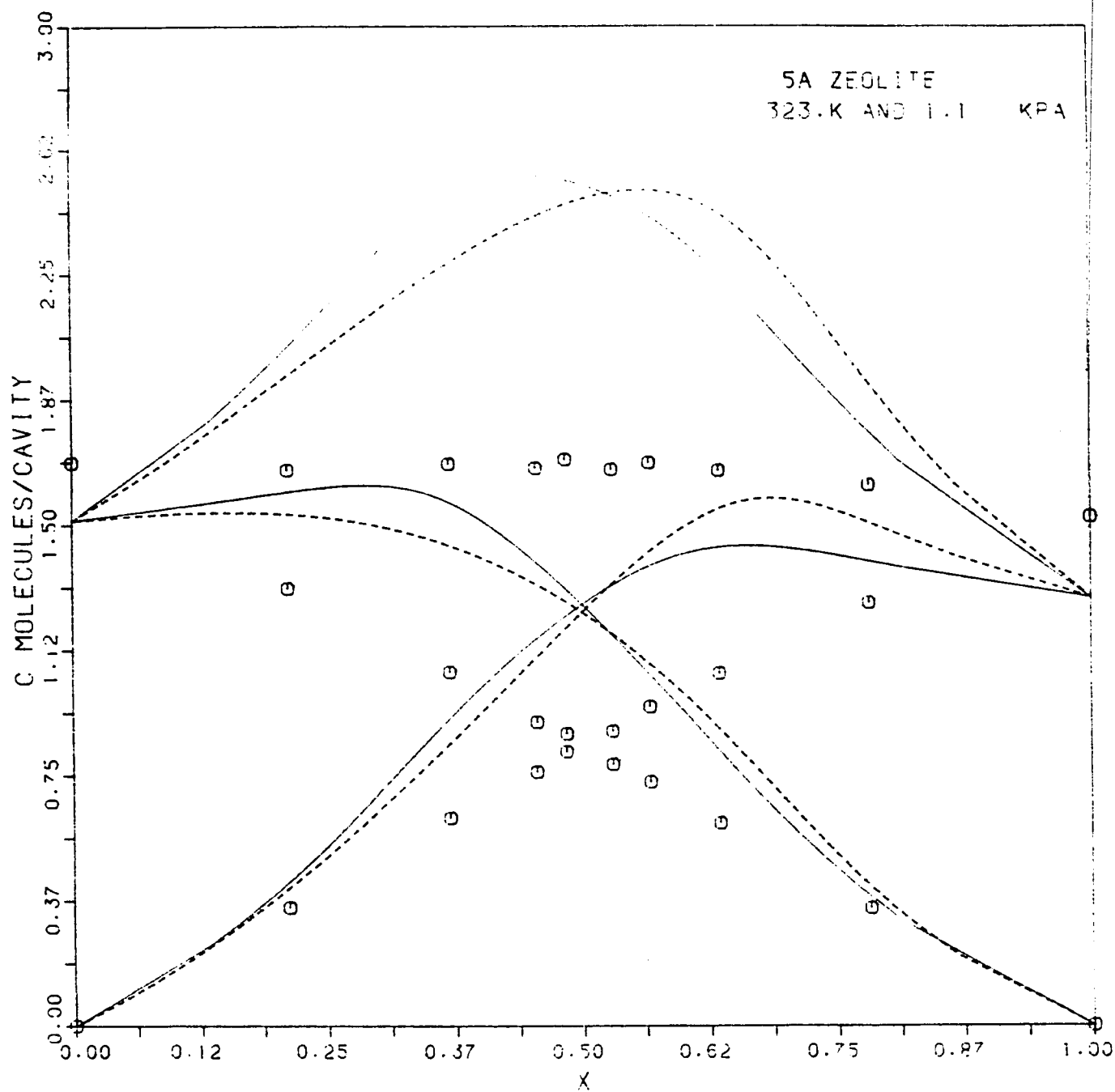


FIGURE A.10 Concentration curves for the sorption of ethylene-carbon dioxide binary mixture on 5A zeolite. Non-ideal solution

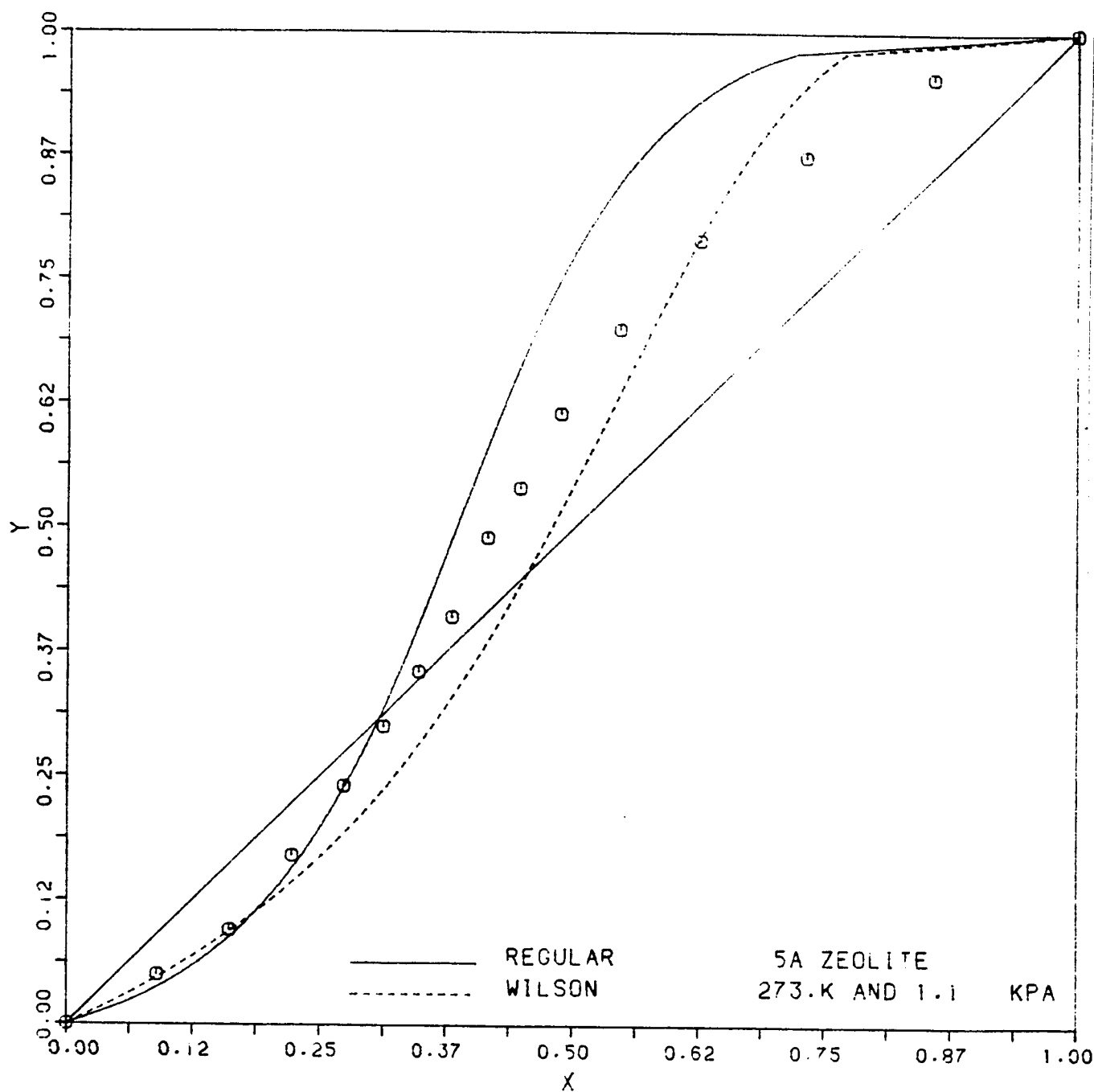


FIGURE A.11 X-Y diagram for the sorption of ethylene-carbon dioxide binary mixture on 5A zeolite. Non-ideal solution

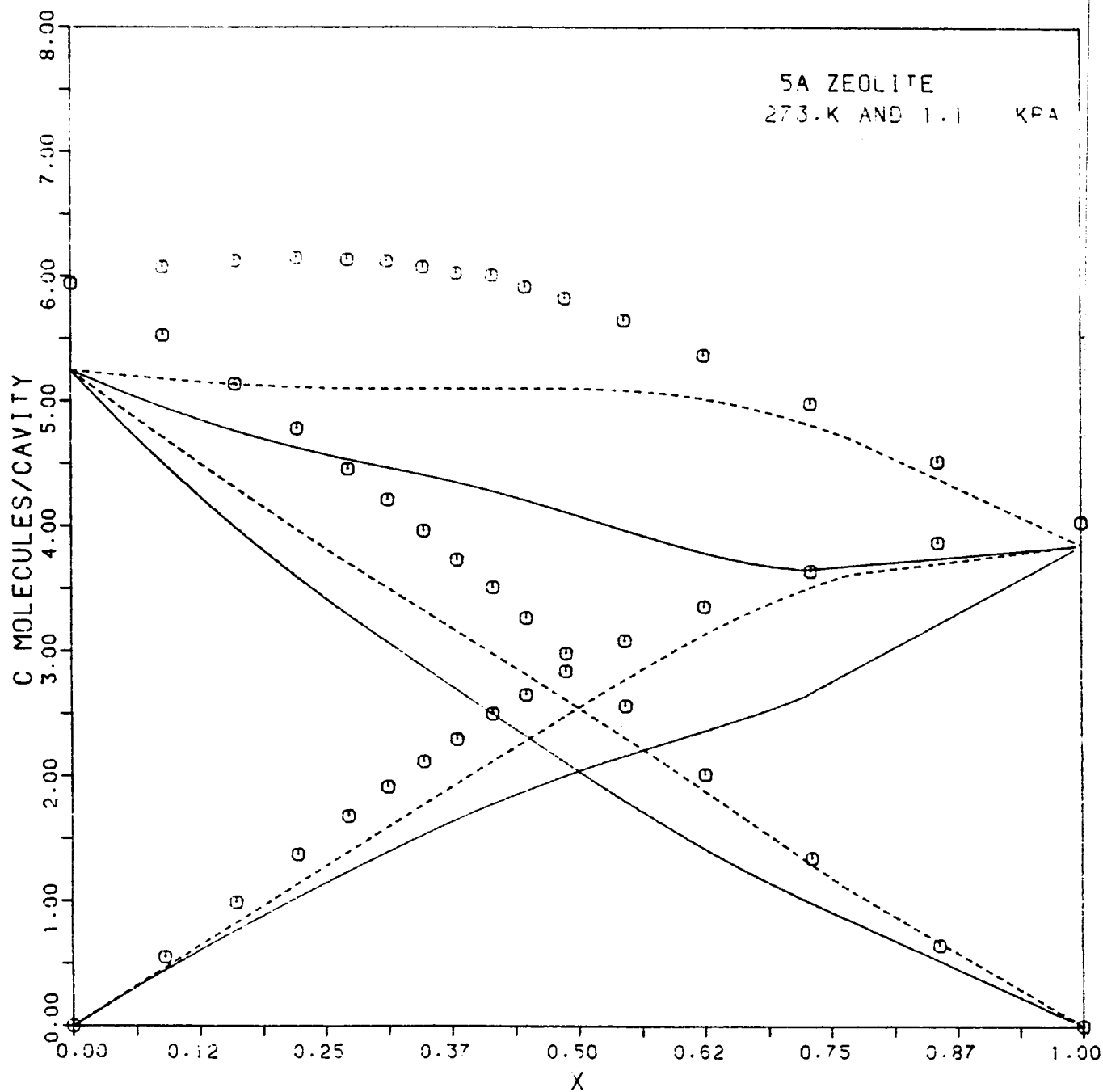


FIGURE A.12 Concentration curves for the sorption of ethylene-carbon dioxide binary mixture on 5A zeolite. Non-ideal solution

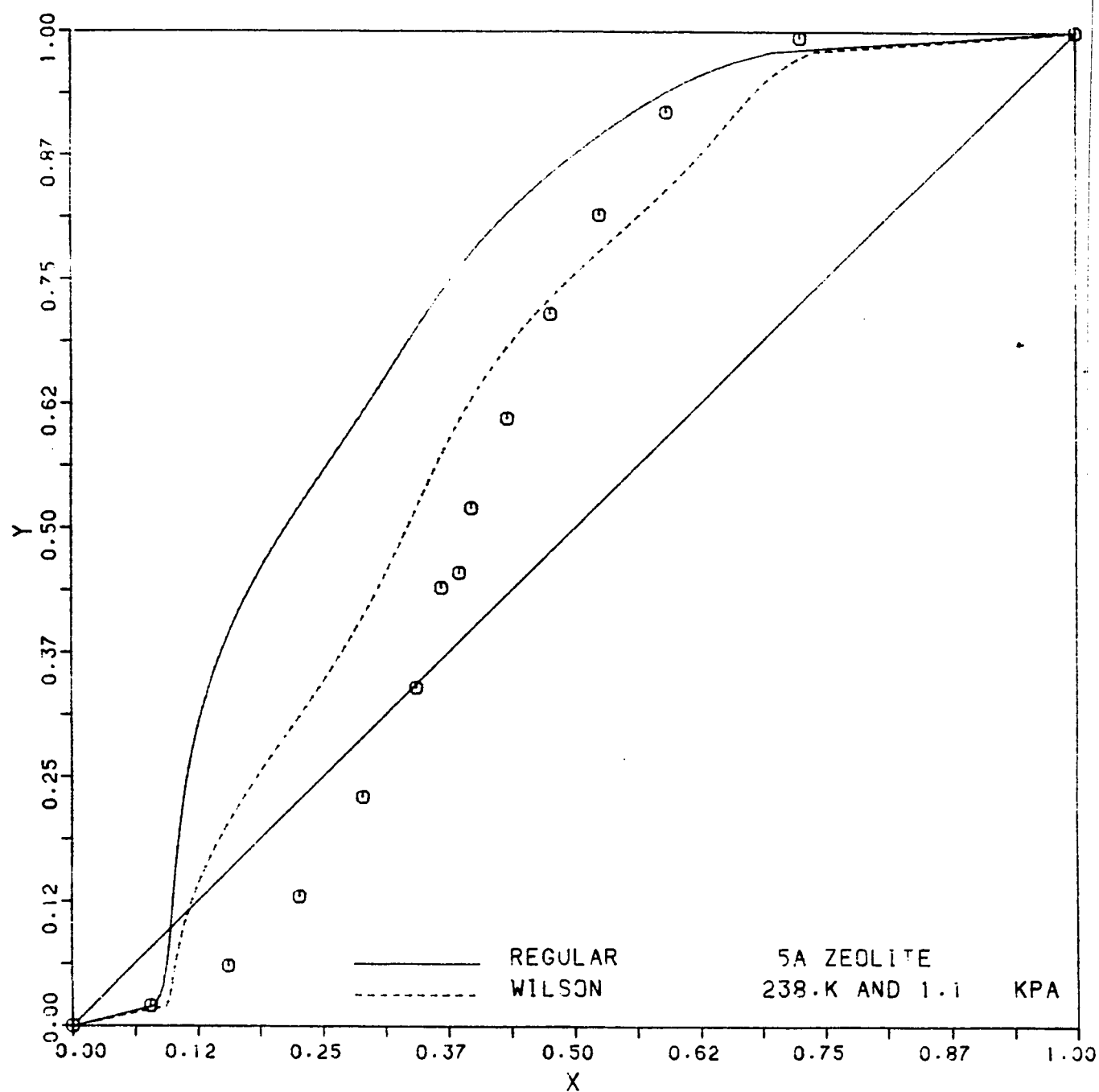


FIGURE A.13 X-Y diagram for the sorption of ethylene-carbon dioxide binary mixture on 5A zeolite. Non-ideal solution

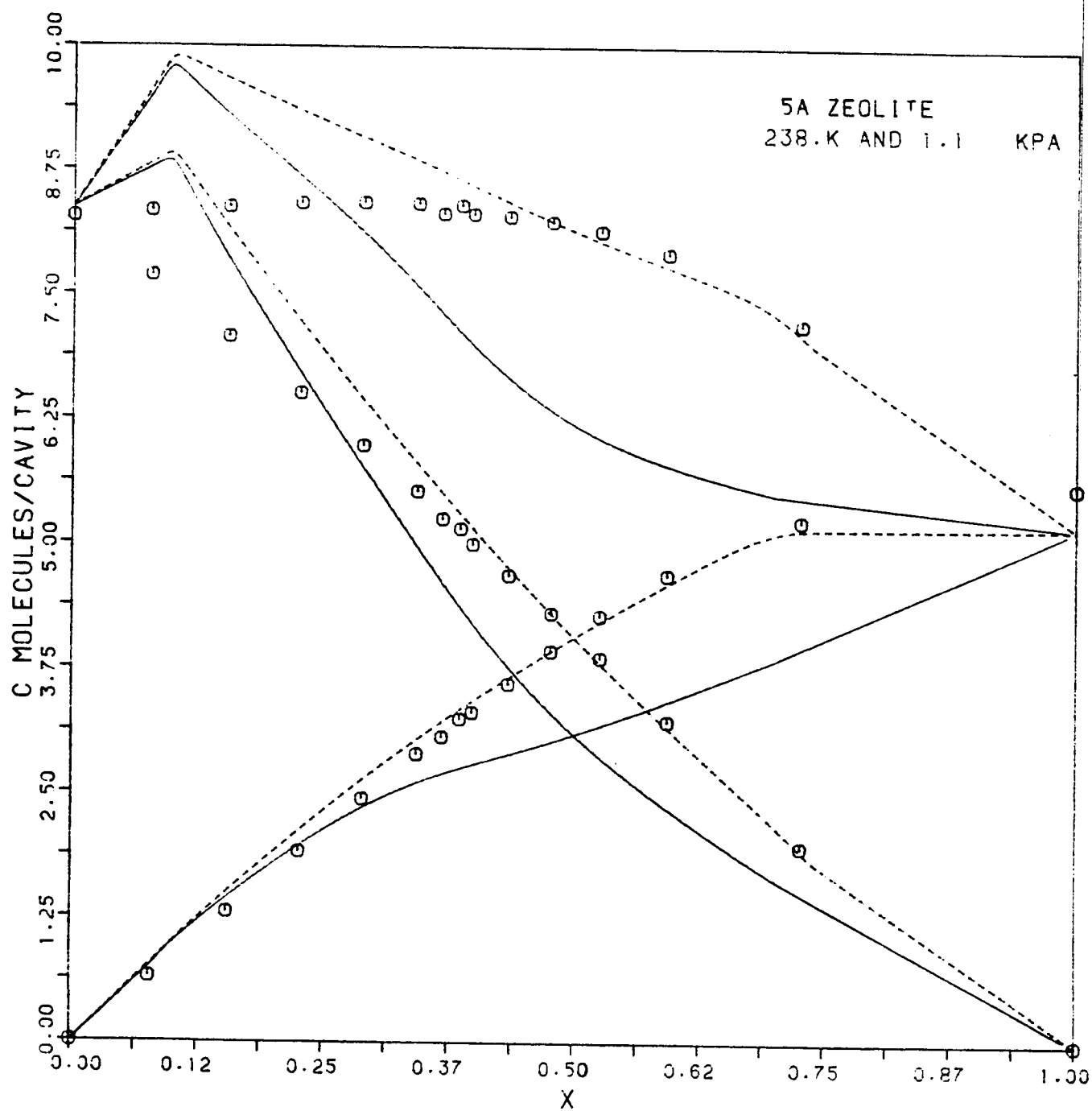


FIGURE A.14 Concentration curves for the sorption of ethylene-carbon dioxide binary mixture on 5A zeolite. Non-ideal solution

REFERENCES

1. Chao, K. C. and Greenkorn, R. A. "Thermodynamics of Fluids" , Marcel Dekker, Inc., New York. (1975)
2. Prigogine, I. and Defay, R. "Chemical Thermodynamics " , Longmans , London , (1973)
3. Smith, J. M. and Van Ness, H. C. "Introduction to Chemical Engineering Thermodynamics " , McGraw-Hill, Inc., New York, (1975)
4. Modell, M. and Reid, R. C. "Thermodynamics and its Applications" , Prentice-Hall, Inc., Englewood Cliffs, (1979)
5. Khvoshchev, V. E., Skazyvaev, V. E. and Vasiljeva, E. A. "Proceedings of the Fifth International Conference on Zeolites" , Naples, Heyden & Son Ltd. London, (1980)
6. Chien, C. H., Greenkorn, R. A. and Chao, K. C. AIChE J., 29 , 560, (1983)

APPENDIX B

EXPERIMENTAL DATA FOR SORPTION OF PROPANE AND N-BUTANE ON 5A AND 13X ZEOLITES

Conversion Factor

5A zeolite crystals : 1 mmole/gram = 1.78 molecules/cavity

13X zeolite crystals : 1 mmole/gram = 1.676 molecules/cavity

Propane on 5A zeolite
498. K

Pressure (kPa)	Concentration (molecules/cavity)
7.84	0.160
14.80	0.297
29.93	0.585
41.50	0.769
57.84	0.971
71.67	1.122
82.97	1.231
100.02	1.486
116.07	1.623
138.95	1.825

Propane on 5A zeolite
423. K

Pressure (kPa)	Concentration (molecules/cavity)
7.25	0.637
15.37	0.999
29.81	1.468
44.76	1.775
61.57	2.026
75.46	2.177
84.81	2.285
100.42	2.549
117.86	2.692
134.92	2.800

Propane on 5A zeolite
398. K

Pressure (kPa)	Concentration (molecules/cavity)
2.73	0.531
7.33	1.024
14.83	1.562
31.40	2.160
47.61	2.486
62.03	2.669
76.25	2.842
85.99	2.916
94.85	3.021
120.95	3.209

Propane on 5A zeolite
348. K

Pressure (kPa)	Concentration (molecules/cavity)
2.53	1.344
24.92	3.064
31.61	3.154
44.32	3.328
59.04	3.446
73.73	3.508
84.31	3.530
98.58	3.583
107.48	3.684
131.18	3.784

n-Butane on 5A zeolite
498. K

Pressure (kPa)	Concentration (molecules/cavity)
8.56	0.592
16.76	0.861
31.36	1.176
47.52	1.362
61.43	1.479
76.27	1.571
86.03	1.645
103.55	1.773
117.66	1.816
128.04	1.834

n-Butane on 5A zeolite
423. K

Pressure (kPa)	Concentration (molecules/cavity)
12.92	1.880
30.94	2.258
45.13	2.376
60.05	2.456
74.41	2.525
85.18	2.558
102.12	2.621
117.47	2.654
128.30	2.653

n-Butane on 5A zeolite
348. K

Pressure (kPa)	Concentration (molecules/cavity)
0.40	1.284
1.47	1.789
11.51	2.889
11.89	2.895
30.06	3.138
51.46	3.234
69.93	3.285
95.95	3.327
126.56	3.327

Propane on 13X zeolite
498. K

Pressure (kPa)	Concentration (molecules/cavity)
12.88	0.199
20.92	0.300
32.62	0.471
47.46	0.625
58.62	0.789
74.82	0.924
86.09	1.089
105.40	1.201
116.12	1.352
128.63	1.407

Propane on 13X zeolite
423. K

Pressure (kPa)	Concentration (molecules/cavity)
5.93	0.356
15.19	0.823
29.52	1.441
44.84	1.842
59.02	2.129
72.27	2.329
86.10	2.542
98.98	2.682
116.75	2.827
130.96	2.977

Propane on 13X zeolite
348. K

Pressure (kPa)	Concentration (molecules/cavity)
1.14	0.475
6.44	1.910
14.23	3.048
32.45	3.744
53.76	4.047
68.02	4.204
80.53	4.276
98.23	4.389
118.28	4.463
132.79	4.488

n-Butane on 13X zeolite
498. K

Pressure (kPa)	Concentration (molecules/cavity)
8.03	0.312
17.56	0.605
27.34	0.928
43.26	1.297
59.00	1.570
66.66	1.678
79.49	1.792
97.01	1.957
118.92	2.039
131.31	2.117
10.15	0.485
24.53	0.996
46.80	1.442
65.87	1.677
92.18	1.869
106.66	1.942
106.12	1.940
127.32	2.066
88.93	1.782

n-Butane on 13X zeolite
423. K

Pressure (kPa)	Concentration (molecules/cavity)
2.29	0.658
9.19	1.646
19.52	2.295
30.81	2.576
46.44	2.749
61.05	2.893
77.66	2.941
93.07	3.066
124.76	3.067
142.75	3.007
59.22	2.869
66.66	2.899
92.13	2.994
108.32	3.028
134.20	3.025
2.03	0.590
13.31	2.064
34.80	2.660
59.22	2.835
79.49	3.043
59.33	2.902

n-Butane on 13X zeolite
348. K

Pressure (kPa)	Concentration (molecules/cavity)
0.33	1.047
1.28	2.363
15.41	3.474
42.25	3.717
58.02	3.777
73.27	3.820
83.98	3.846
102.94	3.878
116.14	3.907
133.91	3.902
20.04	3.684
41.56	3.843
69.67	3.877
92.14	3.900
106.66	3.909
123.75	3.907
0.14	0.532
0.50	1.801
10.93	3.494
41.56	3.841

APPENDIX C

EXPERIMENTAL DATA FOR SORPTION OF PROPANE-N-BUTANE MIXTURE ON 5A AND 13X ZEOLITES

Conversion Factor

5A zeolite crystals : 1 mmole/gram = 1.78 molecules/cavity

13X zeolite crystals : 1 mmole/gram = 1.676 molecules/cavity

5A zeolite
 $T = 498. \text{ K} , P = 66.7 \text{ kPa}$

y_{propane}	x_{propane}	c_{total}^*	selectivity [#]
1.000	1.000	0.895	
0.954	0.826	0.967	0.226
0.769	0.455	1.142	0.251
0.677	0.355	1.227	0.262
0.561	0.249	1.287	0.259
0.481	0.188	1.332	0.250
0.000	0.000	1.615	
0.165	0.054	1.564	0.288
0.299	0.108	1.508	0.284
0.354	0.134	1.466	0.283
0.484	0.195	1.404	0.258
0.575	0.263	1.342	0.263

* c_{total} in molecules/cavity

selectivity coefficient for propane

5A zeolite
 $T = 423. \text{ K} , P = 66.7 \text{ kPa}$

y_{propane}	x_{propane}	c_{total}^*	selectivity
1.000	1.000	1.990	
0.912	0.645	2.217	0.175
0.841	0.493	2.236	0.184
0.733	0.355	2.238	0.200
0.616	0.240	2.266	0.197
0.000	0.000	2.489	
0.316	0.090	2.645	0.214
0.267	0.073	2.664	0.217
0.452	0.145	2.634	0.206
0.537	0.183	2.623	0.194
0.617	0.233	2.614	0.189

5A zeolite
 $T = 348. \text{ K}$, $P = 66.7 \text{ kPa}$

y_{propane}	x_{propane}	c_{total}^*	selectivity
1.000	1.000	3.461	
0.990	0.921	3.448	0.114
0.964	0.793	3.372	0.144
0.929	0.663	3.313	0.151
0.885	0.536	3.259	0.149
0.824	0.426	3.217	0.158
0.737	0.319	3.182	0.167
0.632	0.229	3.162	0.173
0.000	0.000	3.741	
0.089	0.008	3.633	0.078
0.200	0.029	3.614	0.119
0.321	0.051	3.563	0.115
0.448	0.065	3.548	0.086

5A zeolite
 $T = 498. \text{ K} , P = 106.7 \text{ kPa}$

y_{propane}	x_{propane}	c_{total}^*	selectivity
1.000	1.000	1.204	
0.913	0.701	1.369	0.224
0.809	0.524	1.450	0.259
0.707	0.393	1.512	0.269
0.593	0.290	1.566	0.280
0.509	0.227	1.595	0.283
0.300	0.130	1.640	0.350
0.000	0.000	1.874	
0.287	0.115	1.798	0.323
0.400	0.176	1.785	0.321
0.514	0.238	1.748	0.296
0.610	0.307	1.715	0.284

5A zeolite
 $T = 423. \text{ K} , P = 106.7 \text{ kPa}$

y_{propane}	x_{propane}	c_{total}^*	selectivity
1.000	1.000	2.499	
0.974	0.887	2.535	0.213
0.896	0.641	2.679	0.207
0.738	0.413	2.802	0.250
0.532	0.263	2.879	0.315
0.000	0.000	2.626	
0.199	0.065	2.685	0.278
0.295	0.107	2.676	0.284
0.420	0.162	2.688	0.266
0.525	0.215	2.705	0.248
0.621	0.286	2.716	0.244

5A zeolite
 $T = 348. \text{ K} , P = 106.7 \text{ kPa}$

y_{propane}	x_{propane}	c_{total}^*	selectivity
1.000	1.000	3.671	
0.966	0.806	3.620	0.145
0.908	0.601	3.571	0.153
0.818	0.412	3.624	0.157
0.683	0.267	3.710	0.169
0.524	0.168	3.724	0.183
0.353	0.110	3.745	0.226
0.000	0.000	3.421	
0.079	0.012	3.400	0.140
0.158	0.055	3.441	0.308

13X zeolite
 T = 498. K , P = 66.7 kPa

y_{propane}	x_{propane}	c_{total}^*	selectivity
1.000	1.000	0.858	
0.849	0.627	1.053	0.300
0.734	0.461	1.194	0.311
0.659	0.329	1.284	0.253
0.526	0.244	1.384	0.291
0.396	0.180	1.470	0.334
0.301	0.124	1.499	0.328
0.165	0.073	1.544	0.400
0.000	0.000	1.879	
0.222	0.083	1.752	0.316
0.313	0.120	1.752	0.298
0.370	0.163	1.681	0.331
0.500	0.216	1.586	0.275
0.591	0.280	1.516	0.269
0.181	0.076	1.720	0.373
0.352	0.160	1.620	0.351
0.473	0.233	1.476	0.339

13X zeolite
 T = 423. K , P = 66.7 kPa

y_{propane}	x_{propane}	c_{total}^*	selectivity
1.000	1.000	2.330	
0.973	0.842	2.431	0.147
0.943	0.734	2.470	0.167
0.902	0.581	2.590	0.151
0.843	0.458	2.597	0.157
0.699	0.318	2.666	0.202
0.616	0.243	2.689	0.201
0.527	0.183	2.663	0.201
0.000	0.000	3.068	
0.151	0.034	2.998	0.198
0.252	0.072	2.964	0.229
0.343	0.098	2.938	0.209
0.415	0.132	2.887	0.214
0.498	0.190	2.844	0.237

13X zeolite
 T = 348. K , P = 66.7 kPa

y_{propane}	x_{propane}	c_{total}^*	selectivity
1.000	1.000	4.301	
0.980	0.881	4.226	0.150
0.922	0.672	4.103	0.173
0.856	0.462	3.951	0.144
0.730	0.277	3.847	0.142
0.524	0.156	3.700	0.168
0.347	0.079	3.593	0.162
0.000	0.000	4.075	
0.202	0.059	4.085	0.247
0.323	0.098	4.103	0.228
0.460	0.151	4.128	0.209
0.541	0.200	4.159	0.213

13X zeolite
 $T = 498. \text{ K}$, $P = 106.7 \text{ kPa}$

y_{propane}	x_{propane}	c_{total}^*	selectivity
1.000	1.000	1.310	
0.858	0.679	1.548	0.351
0.833	0.617	1.625	0.322
0.743	0.499	1.750	0.344
0.652	0.394	1.875	0.347
0.557	0.308	1.974	0.354
0.000	0.000	2.138	
0.162	0.067	2.087	0.370
0.385	0.184	1.998	0.359
0.525	0.264	1.908	0.325
0.626	0.371	1.862	0.352
0.712	0.473	1.826	0.363

13X zeolite
 $T = 423. \text{ K}$, $P = 106.7 \text{ kPa}$

y_{propane}	x_{propane}	c_{total}^*	selectivity
1.000	1.000	2.814	
0.985	0.906	2.901	0.149
0.942	0.760	2.969	0.195
0.835	0.538	3.027	0.230
0.710	0.373	3.063	0.243
0.612	0.270	3.074	0.235
0.481	0.208	3.105	0.284
0.000	0.000	3.232	
0.195	0.066	3.211	0.295
0.321	0.116	3.216	0.278
0.511	0.209	3.204	0.252
0.609	0.278	3.205	0.247

13X zeolite
 $T = 348. \text{ K}$, $P = 106.7 \text{ kPa}$

y_{propane}	x_{propane}	c_{total}^*	selectivity
1.000	1.000	4.519	
0.908	0.634	4.383	0.176
0.779	0.351	4.215	0.154
0.528	0.181	4.103	0.197
0.296	0.101	4.075	0.267
0.170	0.056	4.012	0.289
0.099	0.031	4.022	0.290
0.986	0.944	4.531	0.244
0.956	0.799	4.465	0.182
0.903	0.641	4.383	0.192
0.823	0.484	4.337	0.201

APPENDIX D

COMPUTER PROGRAMS

CONC AND CONCB

These two programmes are written to calculate the concentration from raw data measured in the laboratory. Since the gas phase exhibits some non-ideality, two subroutines were included to account for this fact. Subroutine PVT which calculates the molar volume of the gas at a given temperature and pressure and PVTM which calculates the molar volume of a binary mixture of gases. In both subroutines the the COR equation of state was used and the constants in the subroutines are taken from reference [] in chapter four. Subroutine YCOMP used in CONCB finds the corresponding Y composition for a given area ratio. Lagrange interpolation is used. In CONCB the fact that the butane gas contains 1.0% of propane was taken into account. The data in appendices B and C are the output of these programs.

```

C   NAME :   CONC
C   THIS PROGRAM CALCULATES THE EXPERIMENTAL CONCENTRATION AT THE
C   EQUILIBRIUM PRESSURE FROM PVT DATA MEASURED IN THE LAB.
C
C       REAL NI,NZ,NG,AA(4,6)
c   R is the gas constant and A is the cross sectional area of the
c   manometer in cm2
      A=0.1963
      DO 20 N=1,100
C
C   INPUT THE ATMOSPHERIC AND THE INITIAL PRESSURES (in cm Hg)
C   IC=1 FOR PROPANE AND IC=2 FOR BUTANE
C
      READ,PA,P0,IC
      IF(PA.LT.0)STOP
C
C   INPUT  ROOM, SECTION TWO AND ZEOLITE TEMPERATURES ( in C )
C
      READ,TR,TM2,TZ
      PRINT,' T (C) = ',TZ
      TR=TR+273.
      TM2=TM2+273.
      TZ=TZ+273.
c
c   VG and VM are the volumes of the glass and metal parts of section two.
c   ( in cm3 ) WZ is the weight of zeolite with binder (in gm)
      WZ=121.9
      VM=741.0
      NI=P0*VG/(R*76.*TM2)
      DO 10 I=1,100
C
C   INPUT  THE INITIAL (I) AND THE FINAL (F) HEIGHTS (H) OF MERCURY IN
C   THE MANOMETER. ( L =LEFT, R=RIGHT). PG IS THE EQUILIBRIUM
C   IN SECTION TWO AND V IS THE VOLUME USED IN SECTION ONE.
C
      READ,HLI,HRI,HLF,HRF,PG,V
      IF(HLI.EQ.0)GOTO 20
      TL=HLI+HRI
      IF ( TL .GT. 94. .OR. TL .LT. 89. )GOTO 100
      TL=HLF+HRF
      IF ( TL .GT. 94. .OR. TL .LT. 89. )GOTO 100
      PI=(PA-HLI+HRI)/76.
      CALL PVT(IC,PI,TR,ZI)
      PF=(PA-HLF+HRF)/76.
      IF ( PF .GT. .2)THEN
        CALL PVT(IC,PF,TR,ZF)
      ELSE
        ZF=1.
      ENDIF
c
c   DN is the change in the number of moles in section two.
      DN=PI*(V-A*(HLI-44.8))/ZI

```

SSURE

```

&-PF*(V-A*(HLF-44.8))/ZF
DN=DN/(R*TR)
PG=PG/76.
  IF ( PG .GT. .2)THEN
    CALL PVT(IC,PG,TM2,ZM2)
    CALL PVT(IC,PG,TZ,ZZ)
  ELSE
    ZM1=ZZ=1.
  ENDIF
NG=PG/R*(VG/TM2/ZM2+VM/TZ/ZZ)
NZ=DN+NI-NG
C=NZ*1000./0.5965/(WZ*0.82)
NI=NI+DN
PRINT,I,PG*101.325,C
10 CONTINUE
20 PRINT,' _____
& _____
100 PRINT,' ERROR!!!! ',I
STOP
END
CCC
SUBROUTINE PVT(IC,P,T,Z)
REAL A(4,6),TS(2),C(2),V0(2)
DATA B0,B1,B2 /0.20095,0.019,-0.0632/
DATA TS(1),C(1),V0(1) /263.57,3.2,41.51/
DATA TS(2),C(2),V0(2) /293.25,4.4,52.24/
DATA A(1,1),A(1,2),A(1,3),A(1,4),A(1,5),A(1,6)/
&-9.04214,-125.11,525.415,-859.803,634.635,-167.336/
DATA A(2,1),A(2,2),A(2,3),A(2,4),A(2,5),A(2,6)/
&-1.12517,548.709,-2566.20,4471.80,-3402.75,939.226/
DATA A(3,1),A(3,2),A(3,3),A(3,4),A(3,5),A(3,6)/
&-0.809958,-838.503,4398.77,-8598.81,7409.90,-2365.34/
DATA A(4,1),A(4,2),A(4,3),A(4,4),A(4,5),A(4,6)/
&-0.672378,438.783,-2482.01,5289.80,-5017.09,1784.58/
V=82.05*T/P
TR=T/TS(IC)
DO 100 I=1,100
VR=V/V0(IC)
VRT=VR/0.7405
SUM=0.
DO 50 N=1,4
DO 50 M=1,6
SUM=SUM+M*A(N,M)/(TR**N*VR**M)
50 CONTINUE
C CALCULATE PV/NRT ,Z
Z=1.+( 4*VRT**2 -2*VRT )/(VRT-1.))**3
& +C(IC)/2.*0.078*(3*VRT**2+3.234*VRT-2.078)/(VRT-1.))**3
& +( 1.+C(IC)/2 *(B0+B1/TR+B2*TR) )*SUM
VN=Z*82.05*T/P
IF( ABS(V/VN-1.) .LT. .001)GOTO 120
V=VN
100 CONTINUE
PRINT,' PVT DOES NOT CONVERGE ???? '
120 RETURN

```

END

C Typical input data

c

75.44,0.010,2

23.,27.,225.

44.8,44.8,52.50,37.05,6.42

44.8,44.8,50.10,39.35,12.57

44.8,44.8,53.4,36.25,23.52

44.8,44.8,53.2,36.40,35.64

44.8,44.8,51.75,37.8,46.08

44.8,44.8,52.00,37.50,57.21

44.8,44.8,49.65,39.90,64.53

32.3,57.2,40.90,48.60,77.67

27.30,62.20,33.75,55.65,88.25

29.40,60.1,34.10,55.35,96.04

0.0000,0000,00000,00000,0000,00

-1,-1,-1,-1

```

C NAME : CONCB
C PURPOSE : TO CALCULATE THE BINARY ADSORPTION CONCENTRATION
C FROM PVT DATA MEASURED IN THE LAB.
C
      REAL NI,NG,NA,NB,NZA,NZB
      R=82.05
      A=0.1963
c XB is the ratio of propane in the butane gas
      XB=0.01
      DO 250 N=1,20
      NA=NB=0.

C
C INPUT THE ATMOSPHERIC, THE INITIAL AND THE TOTAL PRESSURES (in
C IC=1 FOR PROPANE AND IC=2 FOR BUTANE
C
      READ,PA,PI,PT,IC
      PT=PT/760.

C
C INPUT ROOM, SECTION TWO AND ZEOLITE TEMPERATURES ( in C)
C
      READ,TR,TG,TZ
      PRINT,' T(C)=' ,TZ
      PRINT,' P   =' ,PT*760.
      PRINT,'           XA           YA           CA
&           CB           CT'
      TR=TR+273
      TG=TG+273
      TZ=TZ+273
      W=140.0
      VG=1270.
      VM=741.
      NI=PI*VG/(R*TG)
      IF (IC.EQ.1) THEN
        NA=NI
      ELSE
        NB=NI
      ENDIF
      DO 200 I=1,100

C
C ID = -1 STOP
C ID = 0 START ANOTHER SET OF DATA AT DIFFERENT T AND/OR P
C ID = 1 GAS IS ADMITTED TO SECTION TWO, BUT DO NOT PRINT
C CALCULATIONS BECAUSE MORE GAS IS TO BE ADMITTED.
C ID = 2 GAS IS ADMITTED TO SECTION TWO, PRINT RESULTS.
C ID = 3 GAS IS TAKEN OUT FROM SECTION TWO.
C ID = 4 GAS IS TAKEN OUT FROM SECTION TWO. THE INITIAL PRESSURE

C SECTION TWO IS KNOWN.
C
      READ,ID
      IF (ID.EQ.-1) THEN
        STOP
      ELSE
        ENDIF
      IF (ID.EQ.0) GOTO250

```

IF (ID.EQ.1) THEN

C
C INPUT THE INITIAL (I) AND THE FINAL (F) HIGHTS (H) OF MERCURY IN
C THE LEFT(L) AND RIGHT(R) SIDES OF THE MANOMETER.
C V IS THE VOLUME USED IN SECTION ONE.

C
READ,IC,HLI,HRI,HLF,HRF,V
TL=HLI+HRI
IF(TL .GT. 940 .OR. TL .LT. 890)GOTO 300
TL=HLF+HRF
IF(TL .GT. 940 .OR. TL .LT. 890)GOTO 300
PI=(PA-HLI+HRI)/760.
CALL PVT(IC,PI,TR,ZI)
PF=(PA-HLF+HRF)/760.
IF (PF .GT. .2)THEN
CALL PVT(IC,PF,TR,ZF)
ELSE
ZF=1.
ENDIF
DN=PI*(V-A*(HLI-44.8))/ZI
&-PF*(V-A*(HLF-44.8))/ZF
DN=DN/(R*TR)
IF (IC.EQ.1)THEN
NA=NA+DN
ELSE
NB=NB+DN*(1.-XB)
NA=NA+DN*XB
ENDIF
ELSEIF (ID.EQ.2)THEN

C
C TG IS THE TEMPERATURE IN THE GLASS VOLUME OF SECTION TWO.
C AP IS THE AREA RATIO

READ,IC,HLI,HRI,HLF,HRF,V,TG,AP
TL=HLI+HRI
IF(TL .GT. 940 .OR. TL .LT. 890)GOTO 300
TL=HLF+HRF
IF(TL .GT. 940 .OR. TL .LT. 890)GOTO 300
TG=TG+273
PI=(PA-HLI+HRI)/760.
CALL PVT(IC,PI,TR,ZI)
PF=(PA-HLF+HRF)/760.
IF (PF .GT. .2)THEN
CALL PVT(IC,PF,TR,ZF)
ELSE
ZF=1.
ENDIF
DN=PI*(V-A*(HLI-44.8))/ZI
&-PF*(V-A*(HLF-44.8))/ZF
DN=DN/(R*TR)
IF (IC.EQ.1)THEN
NA=NA+DN
ELSE
NB=NB+DN*(1.-XB)
NA=NA+DN*XB


```

ENDIF
CALL YCOMP(AP, YA)
CALL PVTM(YA, PT, TG, ZG)
CALL PVTM(YA, PT, TZ, ZZ)
NG=PT/R*(VG/TG/ZG+VM/TZ/ZZ)
NZA=NA-NG*YA
NZB=NB-NG*(1.-YA)
XA=NZA/(NZA+NZB)
CA=NZA*1000.*1.78/(W*0.80)
CB=NZB*1000.*1.78/(W*0.80)
CT=CA+CB
PRINT11, XA, YA, CA, CB, CT
11  FORMAT(' ', 5(10X, F5.2) )
ELSEIF (ID .EQ. 3) THEN
    READ, HLI, HRI, HLF, HRF, V, TG, AP
    TG=TG+273
    TL=HLI+HRI
    IF( TL .GT. 940.OR. TL .LT. 890) GOTO 300
    TL=HLF+HRF
    IF( TL .GT. 940.OR. TL .LT. 890) GOTO 300
    PI=(PA-HLI+HRI)/760.
    CALL PVT(IC, PI, TR, ZI)
    PF=(PA-HLF+HRF)/760.
    IF ( PF .GT. .2) THEN
        CALL PVT(IC, PF, TR, ZF)
    ELSE
        ZF=1.
    ENDIF
    DN=PI*(V-A*(HLI-44.8))/ZI
    & -PF*(V-A*(HLF-44.8))/ZF
    DN=DN/(R*TR)
    CALL YCOMP(AP, YA)
    NA=NA+DN*YA
    NB=NB+DN*(1.-YA)
ELSE
    READ, PI, HLF, HRF, TG, AP
    TG=TG+273
    PI=PI/760.
    CALL PVT(IC, PI, TR, ZI)
    PF=(PA-HLF+HRF)/760.
    IF ( PF .GT. .2) THEN
        CALL PVT(IC, PF, TR, ZF)
    ELSE
        ZF=1.
    ENDIF
    DN=DN/(R*TR)
    DN=VG*(PF/ZF-PI/ZI)/(R*TG)
    CALL YCOMP(AP, YA)
    NA=NA+DN*YA
    NB=NB+DN*(1.-YA)
ENDIF
200 CONTINUE
250 PRINT,
& _____

```

```

300 PRINT, ' ERROR!!!! '
    PRINT, ' N=', I, ' TL = ', TL
    STOP
    END
CC
    SUBROUTINE YCOMP(AP, YA)
    REAL X(10), Y(10), L
    AP=AP/100.
    DATA X(1), X(2), X(3), X(4), X(5), X(6), X(7), X(8), X(9)/0.0, .062, .110,
&.313, .466, .589, .773, .878, 1.0/
    DATA Y(1), Y(2), Y(3), Y(4), Y(5), Y(6), Y(7), Y(8), Y(9)/0.0, .065, .117,
&.335, .504, .628, .800, .895, 1.0/
    N=9
    YA=0.
    DO 100 I=1, N
        L=1.
        DO 10 J=1, N
            IF(J.EQ.I)GOTO 10
            L=L*(AP-X(J))/(X(I)-X(J))
10        CONTINUE
        YA=YA+Y(I)*L
100    CONTINUE
    RETURN
    END
CCC
    SUBROUTINE PVT(IC, P, T, Z)
    REAL A(4,6), TS(2), V0(2), C(2)
    DATA B0, B1, B2 /0.20095, 0.019, -0.0632/
    DATA TS(1), C(1), V0(1) /263.57, 3.2, 41.51/
    DATA TS(2), C(2), V0(2) /293.25, 4.4, 52.24/
    DATA A(1,1), A(1,2), A(1,3), A(1,4), A(1,5), A(1,6)/
&-9.04214, -125.11, 525.415, -859.803, 634.635, -167.336/
    DATA A(2,1), A(2,2), A(2,3), A(2,4), A(2,5), A(2,6)/
&-1.12517, 548.709, -2566.20, 4471.80, -3402.75, 939.226/
    DATA A(3,1), A(3,2), A(3,3), A(3,4), A(3,5), A(3,6)/
&-0.809958, -838.503, 4398.77, -8598.81, 7409.90, -2365.34/
    DATA A(4,1), A(4,2), A(4,3), A(4,4), A(4,5), A(4,6)/
&-0.672378, 438.783, -2482.01, 5289.80, -5017.09, 1784.58/
    V=82.05*T/P
    TR=T/TS(IC)
    DO 100 I=1, 100
    VR=V/V0(IC)
    VRT=VR/0.7405
    SUM=0.
    DO 50 N=1, 4
        DO 50 M=1, 6
            SUM=SUM+M*A(N,M)/((TR**N*VR**M)
50    CONTINUE
C    CALCULATE PV/NRT , Z
    Z=1.+( 4*VRT**2 -2*VRT )/(VRT-1.)**3
&    +C(IC)/2.*0.078*(3*VRT**2+3.234*VRT-2.078)/(VRT-1.)**3
&    +( 1.+C(IC)/2 *(B0+B1/TR+B2*TR) )*SUM
C    PRINT, Z
    VN=Z*82.05*T/P

```

```

      IF( ABS(V/VN-1.) .LT. .001)GOTO 120
      V=VN
100  CONTINUE
      PRINT, '      PVT DOES NOT CONVERGE ????'
120  RETURN
      END
CCC
      SUBROUTINE PVTM(Y1,P,T,Z)
      REAL A(4,6),TR(3),UK(3),VR(3),TS(3),C(3),V0(3),K12
      DATA B0,B1,B2 /0.20095,0.019,-0.0632/
      DATA TS(1),C(1),V0(1) /263.57,3.2,41.51/
      DATA TS(2),C(2),V0(2) /293.25,4.4,52.24/
      DATA A(1,1),A(1,2),A(1,3),A(1,4),A(1,5),A(1,6)/
&-9.04214,-125.11,525.415,-859.803,634.635,-167.336/
      DATA A(2,1),A(2,2),A(2,3),A(2,4),A(2,5),A(2,6)/
&-1.12517,548.709,-2566.20,4471.80,-3402.75,939.226/
      DATA A(3,1),A(3,2),A(3,3),A(3,4),A(3,5),A(3,6)/
&-0.809958,-838.503,4398.77,-8598.81,7409.90,-2365.34/
      DATA A(4,1),A(4,2),A(4,3),A(4,4),A(4,5),A(4,6)/
&-0.672378,438.783,-2482.01,5289.80,-5017.09,1784.58/
      ZK=ABS(V0(1)-V0(2))/(V0(1)+V0(2))
      K12= 0.01008 - 0.03429*ZK + 0.3849*ZK**2 + 0.2823*ZK**3
      K12=0.01162
      Y2=1.-Y1
      V0(3)=Y1*V0(1)+Y2*V0(2)
      C(3)=Y1*C(1)+Y2*C(2)
      DO 30 J=1,2
          TR(J)=T/TS(J)
30      UK(J)=TS(J)*(1.+C(J)/2. *(B0+B1/TR(J)+B2*TR(J) ) )
      UK(3)=( Y1**2*UK(1)*V0(1) + Y1*Y2*(1.-K12)*SQRT(UK(1)*UK(2))*(V0
&(1)+V0(2)) + Y2**2 * UK(2)* V0(2) )/V0(3)
      TS(3)=(-(1.+B0*C(3)/2.)*SQRT( (1.+B0*C(3)/2. )**2 + 4.*B1*C(3)/2*(U
&K(3)/T-B2*C(3)/2) ) )/(C(3)*B1/T)
      TR3=T/TS(3)
      V=82.05*T/P
      DO 100 K=1,100
          VR3=V/V0(3)
          VRT3=VR3/0.7405
          SUM=0.
          DO 50 N=1,4
              DO 50 M=1,6
                  SUM=SUM+M*A(N,M)/(TR3**N*VR3**M)
50      CONTINUE
      C  CALCULATE PV/NRT ,Z
          Z=1.+( 4*VRT3**2 -2*VRT3 )/(VRT3-1. )**3
&      +C(3)/2.*0.078*(3*VRT3**2+3.234*VRT3-2.078)/(VRT3-1. )**3
&      +( 1.+C(3)/2 *(B0+B1/TR3+B2*TR3) )*SUM
      VN=Z*82.05*T/P
      IF( ABS(V/VN-1.) .LT. .001)GOTO 120
      V=VN
100  CONTINUE
      PRINT, '      PVTM DOES NOT CONVERGE ????'
120  RETURN
      END

```

C Typical input data

762.4, .02, 800., 1

23, 32, 225.

2

1, 203.0, 693.5, 419.0, 476.5, 5904.8, 31., 100.0

4

805., 587.8, 316.0, 30., 100.0

1

2, 247.0, 649.0, 429.2, 467.0, 1360.8

2

2, 367.8, 528.1, 384.7, 511.0, 1360.8, 30., 89.9

4

797., 591.0, 313.0, 30., 89.9

2

2, 214.0, 682.0, 379.2, 516.2, 1360.8, 29, 78.3

4

803., 588.0, 315.8, 29., 78.3

2

2, 220.0, 676.0, 377.8, 518.0, 1360.8, 29, 67.3

4

798., 609.0, 297.5, 29., 67.3

2

2, 210.0, 686.0, 378.5, 517.0, 1360.8, 29, 55.3

4

800., 575.0, 327.0, 29., 55.3

2

2, 225.0, 671.5, 358.0, 538.0, 1360.8, 29.0, 47.1

4

798., 797.0, 132.0, 29., 47.1

1

2, 211.5, 684.5, 443.5, 453.0, 1360.8

2

2, 295.0, 601.5, 380.5, 515.5, 1360.8, 29.0, 28.1

-1

LS

This is a general purpose program for optimizing the values of the parameters in non-linear multivariable functions. The original program was taken from ref [] in chapter four. The optimization is done in subroutine BSOLVE which is based on the Marquardt's algorithm. The equation or model to be fitted is provided by the user in subroutine FUNC. In this copy the vacancy solution model is used in FUNC.

Subroutine BCONST is added to apply the constraints described in chapter four on the parameters of Schirmer et al. model. It is not needed for other models. DERIV is a subroutine which contains the analytical derivatives of the model with respect to each independent variable. The user can let the program to calculate the derivatives numerically as done in this copy.

```

C NAME: LS
C PUTPOSE : TO PERFORM A LEAST SQUARES FIT FOR THE VARIOUS
C
  DIMENSION P(3000),A(30,30),AC(30,30),X(2,200),PL(2000),NP(10)
  DIMENSION B(30),Z(200),Y(200),BV(30),BMIN(30),BMAX(30)
  DIMENSION FV(30),DV(30),BE(20)
  EXTERNAL FUNC
  EXTERNAL DERIV
  COMMON X
  NI=5
  NO=6
C      MM = # OF INDEPENDENT VARIABLE
C      NN = # OF DATA POINTS
C      KK = # OF UNKNOWN COEFFICIENTS
C
  READ,MM, NN, KK
C
C*****
C B      INITIAL GUESSES OF COEFFICIENTS
C BMIN   MIN. VALUE OF EACH COEFFICIENT
C BMAX   MAX. VALUE OF EACH COEFFICIENT
C X(1,I) VALUES OF INDEPENDENT VARIABLE # 1
C X(2,I) VALUES OF INDEPENDENT VARIABLE # 2
C
C X(3,MM) VALUES OF INDEPENDENT VARIABLE # MM
C Y(I)   VALUES OF DEPENDENT VARIABLE
C*****
  READ,(B(J),J=1,KK)
  READ,(BMIN(J),J=1,KK)
  READ,(BMAX(J),J=1,KK)
C
C X(1,M) : TEMP.
C X(2,M) : CONC.
C Y(M)   : PRESSURE
C
C      ENTERING THE NUMBER OF SETS OF TEMPERATURES,NT
C
  NSS=0
  READ,NT
C
C      DO LOOP FOR ALL THE SETS
  DO 92 J=1,NT
C
C...  ENTERING THE TEMPERATURE,T.
C
  READ 96,X(1,1+NSS)
96  FORMAT(1X,F10.5)
  READ,X(1,1+NSS)
C
C...  DO LOOP TO READ THE WHOLE SET.
C
  NS=0
  DO 93 I=1,50
C

```

C ENTERING THE PRESSURE,P AND CONCENTRATION,C
C

```

      IF ( I+NSS .GT. NN) GOTO 99
      READ 91,Y(I+NSS),X(2,I+NSS)
      IF ( X(2,I+NSS).LE. 0.0) GOTO 94
      Y(I+NSS)=ALOG( Y(I+NSS)*0.133322 )
91  FORMAT(1X,F10.5,10X,F10.5)
      X(1,I+NSS)=X(1,I+NSS)
      NS=NS+1
93  CONTINUE
94  NSS=NSS+NS
      NP(J)=NS
92  CONTINUE
      NN=NSS
99  CONTINUE

```

C

C 019 FORMAT (7E10.5)

C 017 FORMAT (7E10.6)

```

      WRITE (NO,111) NN, KK
      WRITE(NO,1111) (B(J),J=1, KK)
      WRITE(NO,1111) (BMIN(J),J=1, KK)
      WRITE(NO,1111) (BMAX(J),J=1, KK)
      DO 18 M=1,MM

```

018 WRITE(NO,1112) (X(M,I),I=1,NN)

WRITE(NO,1112) (Y(I),I=1,NN)

111 FORMAT (2I10)

1111 FORMAT (10F12.4)

1112 FORMAT (10F12.5)

FNU=0.0

FLA= 0000.000

TAU=0.0

EPS=0.0

PHMIN=0.0

I=0

KD=KK

FV(1)=0.0

DO 100 J=1, KK

BV(J)=1

100 CONTINUE

ICON=KK

ITER=0

WRITE (NO,023)

023 FORMAT (1H1,10X,27HBSOLVE REGRESSION ALGORITHM)

200 CALL

BSOLVE(KK,B,NN,Z,Y,PH,FNU,FLA,TAU,EPS,PHMIN,I,ICON,FV,DV,BV,
&BMIN,BMAX,P,FUNC,DERIV,KD,A,AC,GAMM)

ITER=ITER+1

WRITE (NO,001) ICON,PH,ITER

001 FORMAT (/ ,2X,6HICON = ,I3,4X, 5HPH = ,F15.8,4X, 16HITERATION NO.

& ,I3)

IF(ICON) 10, 300, 200

10 IF(ICON+1) 20, 60 ,200

20 IF(ICON+2) 30, 70 ,200

30 IF(ICON+3) 40, 80 ,200

40 IF(ICON+4) 50, 90 ,200

```

50 GO TO 95
60 WRITE (NO,004)
004 FORMAT (//,2X,32HNO FUNCTION IMPROVEMENT POSSIBLE )
    GO TO 300
70 WRITE (NO,005)
005 FORMAT (//,2X, 28HMORE UNKNOWN THAN FUNCTIONS)
    GO TO 300
80 WRITE (NO,006)
006 FORMAT (//,2X, 24HTOTAL VARIABLES ARE ZERO)
    GO TO 300
90 WRITE (NO,007)
007 FORMAT (//,2X,79HCORRECTIONS SATISFY CONVERGENCE
REQUIREMENTS BUT
    &LAMDA          (FLA) STILL LARGE)
    GO TO 300
95 WRITE (NO,008)
008 FORMAT (//,2X,20HTHIS IS NOT POSSIBLE)
    GO TO 300
300 WRITE (NO,002)
002 FORMAT (//,2X,26HSOLUTIONS OF THE EQUATIONS)
    DO 400 J=1, KK
        WRITE (NO,003) J, B(J)
003 FORMAT (/ ,2X, 2HB(,I2,4H) = ,2F16.8)
400 CONTINUE
    CALL FUNC (KK,B,NN,Z,FV)
    WRITE (NO,401)
401 FORMAT (////,5X,19HEXPERIMENTAL VALUES,18X,17HREGRESSION
VALUES )

    DO 500 KK=1, NN
500 WRITE (NO,501) KK, Y(KK), KK, Z(KK), KK, X(1, KK), KK, X(2, KK)
501 FORMAT (/ ,2X, 2HY(, I3,4H) = ,F16.8, 10X, 5HYHAT(, I3,4H) = ,F16.8,
    &8X, 2HT(, I3,4H) = ,F16.8, 10X, 2HC(, I3,4H) = ,F16.8)
    SUMY=SNS=0.0
    DO 900 J=1, NN
C
C
        SNS=SNS+( Z(J)/Y(J)-1)**2
C
C
900 SUMY=SUMY+Y(J)
C
        PRINT, '          SUM OF SQUARS (Y TH /Y EXP. -1)**2 =

        YBAR=SUMY/FLOAT(NN)
        SUMST=0.0
        DO 950 J=1, NN
950 SUMST=SUMST+(Z(J)-YBAR)**2
        SUMSR=SUMST-PH
        RTEST=SUMSR/SUMST
        WRITE (NO,951) RTEST
951 FORMAT (' ',2X,' R**2 = ',F16.8)
1000 STOP
    END
C
C
    SUBROUTINE BCONST(M,BMAX,BMIN,BB,IEE)
    REAL BMAX(30),BMIN(30),BB(30)

```



```

      DO 10 I=2,M
C     IF (IEE .EQ. 0)GOTO10
C     BMAX(M+1)=BB(M+1-1)
10    BMAX(I)=BB(I-1)
      RETURN
      END

C
C
      SUBROUTINE FUNC (KK, B, NN, Z, FV)
      DIMENSION X(2,200), Z(200), B(30),FV(30),BE(20)
      COMMON X
      R=8.314
      DO 100 J=1,NN
C   HENRY CONSTANT
C     HK=B(1)*EXP(-B(2)/R/X(1,J) )
C   MAXIMUM CONC.
C     CC=B(1)*EXP(B(2)/X(1,J) )
C     CC=B(3)*EXP(B(4)/X(1,J) )
C   ALPHA
C     AA=B(3)*CC-1.
C     AA=B(5)*CC-1.
C     TH=X(2,J)/CC
C     Z(J)=-ALOG(HK) + ALOG( CC*TH/(1.-TH) )
C     & + AA**2*TH/(1.+AA*TH)
C     Z(J)= B(1) + B(2)/R/X(1,J) + ALOG( CC*TH/(1.-TH) )
C     & + AA**2*TH/(1.+AA*TH)
100   CONTINUE
      RETURN
      END

C
      SUBROUTINE DERIV (KK,B,NN,Z,PJ,FV,DV,J,JTEST)
      RETURN
      END

C
      SUBROUTINE BSOLVE (KK, B, NN, Z, Y, PH, FNU, FLA, TAU, EPS,
&      PHMIN, I, ICON, FV, DV, BV, BMIN, BMAX, P,
&      FUNC, DERIV, KD, A, AC, GAMM)
      DIMENSION B(30),Z(200),Y(200),BV(30),BMIN(30),BMAX(30),BB(30)
      DIMENSION P(3000),A(30,30),AC(30,30),X(2,200),FV(30),DV(30)
      K=KK
      N=NN
      KP1=K+1
      KP2=KP1+1
      KBI1=K*N
      KBI2=KBI1+K
      KZI=KBI2+K
      IF( FNU .LE. 0. ) FNU = 10.0
      IF( FLA .LE. 0. ) FLA = 0.01
      IF( TAU .LE. 0. ) TAU = 0.001
      IF( EPS .LE. 0. ) EPS = 0.00002
      IF(PHMIN.LE. 0.)PHMIN=0.
120  KE=0
130  DO 160 I1=1,K
160  IF( BV(I1) .NE. 0. ) KE=KE+1

```

```

      IF( KE .GT. 0 ) GO TO 170
162 ICON=-3
163 GOTO 2120
170 IF( N .GE. KE ) GOTO500
180 ICON=-2
190 GOTO 2120
500 I1=1
530 IF( I .GT. 0 ) GOTO 1530
550 DO 560 J1=1,K
      J2=KBI1+J1
      P(J2)=B(J1)
      J3=KBI2+J1
560 P(J3) = ABS(B(J1)) + 1.0E-02
      GO TO 1030
590 IF (PHMIN .GT. PH .AND. I .GT.1)GO TO 625
      DO 620 J1=1,K
      N1 = (J1-1)*N
      IF( BV(J1) ) 601,620,605
601 CALL DERIV (K, B, N, Z, P(N1+1), FV, DV, J1, JTEST)
      IF(JTEST .NE. (-1) ) GO TO 620
      BV(J1) = 1.0
605 DO 606 J2=1,K
      J3= KBI1 +J2
606 P(J3) =B(J2)
      J3= KBI1 +J1
      J4=KBI2+J1
      DEN = 0.001*AMAX1(P(J4),ABS(P(J3)))
      IF (P(J3) + DEN .LE. BMAX(J1)) GOTO 55
      P(J3) =P(J3)-DEN
      DEN  =-DEN
      GO TO 56
55 P(J3)=P(J3)+DEN
56 CALL FUNC(K,P(KBI1+1),N,P(N1+1),FV)
      DO 610 J2=1,N
      JB=J2+N1
610 P(JB)=(P(JB)-Z(J2))/DEN
620 CONTINUE
625 DO 725 J1=1,K
      N1=(J1-1)*N
      A(J1,KP1)=0.
      IF(BV(J1)) 630, 692,630
630 DO 640 J2=1,N
      N2=N1+J2
C 640 A(J1,KP1)= A(J1,KP1)+P(N2)*(Y(J2)-Z(J2))
640 A(J1,KP1)= A(J1,KP1)+P(N2)*(1.-Z(J2)/Y(J2))
650 DO 680 J2=1,K
660 A(J1,J2)=0.
665 N2=(J2-1)*N
670 DO 680 J3=1,N
672 N3=N1+J3
674 N4=N2+J3
680 A(J1,J2)=A(J1,J2)+P(N3)*P(N4)
      IF(A(J1,J1).GT.1E-20)GOTO 725
692 DO 694 J2=1,KP1

```

```

694 A(J1,J2)=0.
695 A(J1,J1)=1.
725 CONTINUE
    GN=0.
    DO 729 J1=1,K
729 GN=GN+A(J1,KP1)**2
    DO 726 J1=1,K
726 A(J1,KP2)=SQRT(A(J1,J1))
    DO 727 J1=1,K
        A(J1,KP1)=A(J1,KP1)/A(J1,KP2)
    DO 727 J2=1,K
727 A(J1,J2) = A(J1,J2)/(A(J1,KP2)*A(J2,KP2))
730 FL=FLA/FNU
    GOTO 810
800 FL = FNU*FL
810 DO 840 J1=1,K
820 DO 830 J2=1,KP1
830 AC(J1,J2)=A(J1,J2)
840 AC(J1,J1)=AC(J1,J1)+FL
    DO 930 L1=1,K
        L2=L1+1
    DO 910 L3=L2,KP1
910 AC(L1,L3)=AC(L1,L3)/AC(L1,L1)
    DO 930 L3=1,K
        IF(L1-L3)920,930,920
920 DO 925 L4=L2,KP1
925 AC(L3,L4)=AC(L3,L4)-AC(L1,L4)*AC(L3,L1)
930 CONTINUE
    DN=0.
    DG=0.
    DO 1028 J1=1,K
        AC(J1,KP2)=AC(J1,KP1)/A(J1,KP2)
        J2=KBI1+J1
        P(J2)=AMAX1(BMIN(J1),AMIN1(BMAX(J1),B(J1)+AC(J1,KP2)))
        DG=DG+AC(J1,KP2)*A(J1,KP1)*A(J1,KP2)
        DN=DN+AC(J1,KP2)*AC(J1,KP2)
1028 AC(J1,KP2)=P(J2)-B(J1)
        COSG=DG/SQRT(DN*GN)
        JGAM=0
        IF(COSG)1100,1110,1110
1100 JGAM=2
        COSG=-COSG
1110 CONTINUE
        COSG=AMIN1(COSG,1.0)
        GAMM=ARCOS(COSG)*180./(3.14159265)
        IF(JGAM .GT. 0 )GAMM=180.-GAMM
1030 CALL FUNC(K, P(KBI1+1), N, P(KZI+1), FV)
C
C
        IPR0=KBI1+1
        IPR1=IPR0+KK-1
        II=0
        DO 2000 IPR=IPR0 IPR1
            II=II+1

```

```

                BB(II)=P(IPR)
2000    CONTINUE
C
C
C
C
C
1500    PHI=0.
        DO 1520 J1=1,N
            J2=KZI+J1
1520    PHI=PHI+(P(J2)/Y(J1)-1.)*2
            IF(PHI .LT. 1.0E-10) GOTO 3000
            IF( I .GT. 0 )GOTO 1540
1521    ICON=K
            GOTO 2110
1540    IF( PHI .GE. PH)GO TO 1530
1200    ICON =0
            DO 1220 J1=1,K
                J2=KB11+J1
1220    IF( ABS(AC(J1,KP2))/(TAU +ABS(P(J2))) .GT. EPS ) ICON=ICON+1
            IF( ICON .EQ. 0 ) GOTO 1400
            IF ( FL .GT. 1.0 .AND. GAMM .GT. 90.0) ICON =-1
            GOTO 2105
1400    IF ( FL .GT. 1.0 .AND. GAMM .LE. 45.0) ICON =-4
            GOTO 2105
1530    IF(I1-2) 1531,1531,2310
1531    I1=I1+1
            GOTO (530,590,800),I1
2310    IF( FL .LT. 1.0E+8) GOTO 800
1320    ICON=-1
2105    FLA=FL
            DO 2091 J2=1,K
                J3=KB11+J2
2091    B(J2)=P(J3)
2110    DO 2050 J2=1,N
                J3=KZI+J2
2050    Z(J2)=P(J3)
            PH=PHI
            I=I+1
2120    RETURN
3000    ICON=0
            GOTO 2105
        END
C
FUNCTION ARCOS(Z)
X=Z
KEY=0
IF( X .LT. (-1.)) X=-1.
IF( X .GT. 1.) X=1.
IF( X .GE. (-1) .AND. X .LT. 0.) KEY=1
IF( X .LT. 0.) X=ABS(X)
IF( X .EQ. 0.) GOTO 10
ARCOS=ATAN (SORT(1.-X*X)/X)
IF( KEY .EQ. 1) ARCOS=3.14159265-ARCOS

```

GO TO 999

10 ARCOS=1.5707963

999 RETURN

END

2	200	5		
12.6	-38000	9.00	100.0	0.0001
9.0	-60000	7.25	000.	01.E-6
16.5	-10000	10.0	400.	100.

1

ETHYLENE ON LINDE 5A ZEOLITE

0023000000	
0002770000	0000637000
0004950000	0000659000
0006640000	0000671000
0007940000	0000680000
0009040000	0000685000
0009840000	0000689000
0010420000	0000691000
0012720000	0000698000
0014920000	0000705000
0016720000	0000708000
0018220000	0000712000
0023220000	0000723000
0019320000	0000714000
0016120000	0000707000
0013220000	0000700000
0011020000	0000694000
0009020000	0000685000
0007620000	0000678000
0006220000	0000673000
0005320000	0000664000
0004270000	0000657000
0003570000	0000651000
0002870000	0000644000
0002710000	0000639000
0002410000	0000627000
0002010000	0000616000
0001610000	0000603000
0001410000	0000586000
0000000000	0000000000

PLPR, PLVR AND PLB

These program were written to calculate the predictions of the pure component and binary models and plot them with the experimental values. PLPR perform the calculations for the Schirmer et al., Ruthven and vacancy solution models and PLVR for the virial model. PLB perform the calculation for the binary Schirmer et al., Ruthven et al., vacancy solution and IAST models. Each model is written in a separate subroutine. The output of these programs is sent to the CALCOMP plotter. It possible to get the output on the printer also by removing the comments from the write statements in the subroutines. YCOMP in PLB interpolates the entropy or the energy values for the pure component in Schirmer et al. model to be used in the binary calculations All the subroutine called from the main program and do not appear in the list of subroutines are CALCOMP subroutines.

```

C  NAME: PLPR
C
C  PURPOSE: TIS PROGRAM COMPUTES THE RESULTS OF THE SCHIRMER ET
C  RETHVEN AND VACANCY SOLUTION PURE COMPONENT MODELS. IT ALSO
C  PLOTS THE EXPERIMENTAL DATA AND THE THEORETICAL CURVES ON
C  CALCOMP PLOTTER.
      DIMENSION NAME(10)
      DIMENSION XC(50),XP(50)
      DIMENSION C(120),P(120),D1(2),D2(3)
      REAL M1,S(15),E(15)
      DATA D1(1),D1(2) / -0.1,0.1 /
      DATA D2(1),D2(2),D2(3) /-0.1,0.1,-0.3/
      COMMON FVALC,EC,FVALP,EP,FCV
      CALL PLOTS( 0, 0 ,1)
      DO 2000 KK=1,1
C  INPUT THE GAS AND ZEOLITES NAMES.
C
      READ(5,1) NAME(1),NAME(2),NAME(3),NAME(4)
      1  FORMAT(' ', 4A4 )
C  M IS THE MAXIMUM NUMBER OF MOLECULES A CAVITY CAN HOLD.
C  S AND E ARE THE ENTROPY AND ENERGY CONSTSANTS OF SCHIRMER
C  ET AL. MODEL
      READ(5,*) M
      READ(5,11) (S(J),J=1,M)
      READ(5,13) (E(J),J=1,M)
      11  FORMAT( 7F10.5)
      13  FORMAT( 7F10.7)
C
C  READ CONSTANTS FOR THE RUTHVEN MODEL
C  SR AND HR ARE THE PRE-EXPONENTIAL FACTOR AND HEAT OF
C  ADSORPTION IN THE HENRY CONSTANT FOR RUTHVEN MODEL.
C  BETA ( MOLECULAR VOLUME )= AA+ B*T
C  V IS THE VOLUME OF THE ZEOLITE CAVITY
C
      READ(5,*) SR,HR,AA,B,V
C
C  READ CONSTANTS FOR THE VACANCY SOLUTION MODEL
C  S0 AND H0 ARE THE PRE-EXPONENTIAL FACTOR AND HEAT OF
C  ADSORPTION IN THE HENRY CONSTANT FOR RUTHVEN MODEL.
C  CC8, R1 AND M1 ARE AS FOLLOWS
C  SATURATION CONCENTRATION = CC8 * EXP( R1/T )
C  ALPHA = M1*(SATURATION CONCENTRATION ) - 1
C
      READ(5,*) S0,H0,CC8,R1,M1
C
C  FVALC AND FVALP ARE THE INITIAL CONCENTRATION AND PRESSURE
C  VALUES ON THE AXIS, EC AND EP ARE THE END VALUES
C
      READ(5,*) FVALC,EC
      DVALC=EC/16.
      READ(5,*) FVALP,EP
      EP=ALOG10(EP/FVALP)
      DVALP=EP/16.
      IF( KK.EQ. 1)CALL PLOT(2.0,2.0,-3)

```

```

IF( KK .EQ. 2)CALL PLOT(0.0,32.0,-3)
CALL AXIS (0.0,0.0,'C MOLECULES/CAVITY', 19 ,16.0,90.,FVALC,
&          DVALC )
CALL LBAXS (0.0,0.0,'P KPA', -6 , 16.0 , 0. ,
& FVALP , DVALP )
CALL SYMBOL ( 0.5 ,15.5 ,.25,NAME(1),0.,14)

```

C
C NSET IS THE NUMBER OF ISOTHERMS TO BE CALCULATED AND PLOTTED
C

```

READ(5,*) NSET
WRITE(6,*) NSET
DO 1000 LL=1,NSET
  IF ( LL .EQ. 1 ) IS=1
  IF ( LL .EQ. 2 ) IS=4
  IF ( LL .EQ. 3 ) IS=10
  IF ( LL .EQ. 4 ) IS=11
  IF ( LL .EQ. 5 ) IS=0
  IF ( LL .EQ. 6 ) IS=12
  IF ( LL .EQ. 7 ) IS=5
  IF ( LL .EQ. 8 ) IS=6
  IF ( LL .EQ. 9 ) IS=7
  IF ( LL .EQ.10 ) IS=2

```

C
C N IS THE NUMBER OF DATA POINTS TO BE READ.
C T IS THE TEMPERATURE
C

```

READ(5,*) N,T
WRITE(6,*) N,T
DO 50 J=1,N

```

C
C XP(J)= THE EXPERIMENTAL PRESSURE
C XC(J)= THE EXPERIMENTAL CONCENTRATION
C

```

  READ(5,91) XP(J),XC(J)
91  FORMAT(1X,F10.5,10X,F10.5)
  XP(J)=XP(J)/760.*101.325
  WRITE(6,*) XP(J),XC(J)
50  CONTINUE
  XC(N+1)=FVALC
  XC(N+2)=DVALC
  XP(N+1)=FVALP
  XP(N+2)=DVALP
  CALL LGLIN ( XP(1),XC(1),N ,1,-1,IS , -1 )
  CALL SYMBOL ( .5,15.5 - 0.5*LL ,.25,IS ,0. , -1)
  CALL NUMBER ( 1.0,15.5 - 0.5*LL ,.25,T ,0. ,0 )
  CALL SYMBOL ( 1.5,15.5 - 0.5*LL ,.25,' K',0.,2 )
C  CALL SYMBOL ( 12.5, 0.5 + 0.5*LL ,.25,IS ,0. , -1)
C  CALL NUMBER ( 13.0, 0.5 + 0.5*LL ,.25,T ,0. ,0 )
C  CALL SYMBOL ( 14.0, 0.5 + 0.5*LL ,.25,' K',0.,2 )
  FCV=-EC/100.
  CALL VS (S0,H0,CC8,R1,M1,T,C,P,NT)
  C(NT+1)=FVALC
  C(NT+2)=DVALC
  P(NT+1)=FVALP

```



```

P(NT+2)=DVALP
CALL DASHS (D2,3)
CALL LGLIN ( P(1),C(1), NT ,1, 0,IS , -1 )
CALL SM (M,S,E,T,C,P,NT)
C(NT+1)=FVALC
C(NT+2)=DVALC
P(NT+1)=FVALP
P(NT+2)=DVALP
CALL DASHS (D1,0)
CALL LGLIN ( P(1),C(1), NT , 1, 0,IS , -1 )
CALL RV (M,SR,HR,AA,B,V,T,C,P,NT)
C(NT+1)=FVALC
C(NT+2)=DVALC
P(NT+1)=FVALP
P(NT+2)=DVALP
CALL DASHS (D1,2)
CALL LGLIN ( P(1),C(1), NT ,1, 0,IS , -1 )
1000 CONTINUE
CALL DASHS (D1,0)
CALL RECT ( 0.0,0.0,16.,16.,0., 3)
2000 CONTINUE
CALL PLOT(35.0,0.0,999)
STOP
END

c
c Schirmer et al. model
c
SUBROUTINE SM(M,S,E,T,C,P,NT)
REAL S(15),E(15),C(120),P(120)
DATA T0,P0,R /273.2,101.3,8.314/
COMMON FC,EC,FP,EP
PMP=10**EP*FP
DO 100 I=1,100
  C I)=FP * (PMP/FP)**((I-1)/100)
  SUM=0.
  SUMJ=0.
  DO 50 J=1,M
    A=(P(I)*T0/P0/T)**J*EXP( J*(S(J)*T-E(J) )/R/T )
    SUM=SUM+A
    SUMJ=SUMJ+A*J
50 CONTINUE
  C(I)=SUMJ/(1.+SUM)
  WRITE(6,*) I,P(I),C(I)
C NT=I
IF ( C(I)/EC .GT. .990) RETURN
100 CONTINUE
RETURN
END

c
c Ruthven model
c
SUBROUTINE RV(M,SR,HR,AA,B,V,T,C,P,NT)
REAL S(15),E(15),C(120),P(120),K
DATA R /8.314/

```

```

COMMON FC,EC,FP,EP
C PMP=10**EP*FP
  K=SR*EXP(-HR/R/T)
  BE=AA+B*T
  DO 100 I=1,NT
C   P(I)=FP * (PMP/FP)**((I-1)/100)
      SUM=0.
      SUMJ=0.
      DO 50 J=2,M
        A=(P(I)*K)**J/GAMMA(J*1.+1.)*( 1.-J*BE/V)**J
        SUM=SUM+A
        SUMJ=SUMJ+A*J
50    CONTINUE
55    C(I)=(K*P(I)+SUMJ) / (1.+K*P(I)+SUM)
C    NT=I
      IF ( C(I)/EC .GT. 0.990) RETURN
100  CONTINUE
      RETURN
      END

C
c  Vacancy solution model
C
  SUBROUTINE VS(S0,H0,CC8,R1,M1,T,C,P,NT)
  REAL K,C(120),P(120),M1
  DATA R /8.314/
  COMMON FC,EC,FP,EP,FCV
  PMP=10**EP*FP
  K=S0*EXP(-H0/R/T)
  CC=CC8*EXP(R1/T)
  A=M1*CC-1.
  DO 100 I=1,100
10    FCV=FCV+EC/100.*I
20    C(I)=FCV+EC/100.*I
      TH=C(I)/CC
      EX= A*A*TH/( 1.+ A*TH)
      P(I)=CC/K*TH/(1.-TH) * EXP( A*A*TH/( 1.+ A*TH) )
      IF ( P(I)/PMP .GT. .99 ) RETURN
      NT=I
100  CONTINUE
      RETURN
      END

C TYPICAL INPUT DATA
  BUTANE ON 5A
5
-56.32,-64.99,-72.39,-84.01,-118.19
-40819.,-40819.,-40819.,-40819.,-40819.
2.090E-6,-44266.,133.80,0.08927,776.
4.790E-6,-39747.,3.952,017.61,0.00753
0.0 4.0
0.150 3.00
3
10 498.0000000
      64.1999800 0.5918461
      125.6999000 0.3606819

```

	235.1999000	1.1761390	
	356.3999000	1.3618850	
	460.7998000	1.4791160	
	572.0998000	1.5705750	
	645.2998000	1.6447200	
	776.6997000	1.7730140	
	882.4992000	1.8164210	
	960.3991000	1.8336740	
9	423.0000000		
	96.8998800	1.8799780	
	232.1000000	2.2579890	
	338.5000000	2.3761400	
	450.3996000	2.4564920	
	558.0998000	2.5251890	
	638.8999000	2.5581220	
	765.9997000	2.6209010	
	881.0996000	2.6537160	
	962.2995000	2.6530790	
9	348.0000000		
	2.9999980	1.2838190	T=75
	10.9999900	1.7887360	
	86.2999400	2.8892770	
	89.1999200	2.8954370	
	225.4999000	3.1375050	
	386.0000000	3.2340730	
	524.4997000	3.2854460	
	719.6997000	3.3273570	
	949.2998000	3.3268510	

```

C NAME: PLVR
C
C PURPOSE : TIS PROGRAM COMPUTES THE RESULTS OF THE VIRIAL
C MODEL AND PLOTS THE EXPERIMENTAL DATA
C AND THE THEORETICAL CURVES ON CALCOMP PLOTTER IN A
C GENERALIZED FORM
  REAL K
  DIMENSION XC(25),XP(25),NAME(10)
  DIMENSION C(120),P(120),D(4)
  DATA D(1),D(2),D(3),D(4) / -0.4,0.1,-0.1,0.4 /
  DATA R /8.314/
  COMMON FVALC,EC,FVALP,EP
  CALL PLOTS( 0, 0 ,1)
  DO 2000 KK=1,1
C INPUT THE GAS AND ZEOLITES NAMES.
C
  READ(5,1) NAME(1),NAME(2),NAME(3),NAME(4)
1  FORMAT(' ', 4A4 )
C
C READ CONSTANTS FOR THE VIRIAL MODEL
C S0 AND Q0 ARE THE PRE-EXPONENTIAL FACTOR AND HEAT OF
C IN THE HENRY CONSTANT FOR RUTHVEN MODEL AND A1 AND A2 ARE
C COEFFICIENTS.
C
  READ(5,*) S0,Q0,A1,A2
  WRITE(6,*) S0,Q0,A1,A2
C
C ALL OTHER PARAMETERS ARE AS DESCRIBED IN "PLPR"
C
  READ(5,*) FVALC,EC
  DVALC=EC/16.
  READ(5,*) FVALP,EP
  EP=ALOG10(EP/FVALP)
  DVALP=EP/16.
  IF ( KK .EQ. 1)CALL PLOT(2.0,2.0,-3)
  IF ( KK .EQ. 2)CALL PLOT(0.0,32.0,-3)
  CALL AXIS (0.0,0.0, 'C MOLECULES/CAVITY', 19 ,16.0,90.,FVALC,
& DVALC )
  CALL LBAXS (0.0,0.0,'KP MOLECULES/CAVITY', -20 , 16.0 , 0. ,
& FVALP , DVALP )
  CALL SYMBOL ( 0.5 ,15.5 ,.25,NAME(1),0.,14)
  READ(5,*) NSET
  WRITE(6,*) NSET
  DO 1000 LL=1,NSET
    IF ( LL .EQ. 1 ) IS=1
    IF ( LL .EQ. 2 ) IS=4
    IF ( LL .EQ. 3 ) IS=10
    IF ( LL .EQ. 4 ) IS=11
    IF ( LL .EQ. 5 ) IS=0
    IF ( LL .EQ. 6 ) IS=12
    IF ( LL .EQ. 7 ) IS=5
    IF ( LL .EQ. 8 ) IS=6
    IF ( LL .EQ. 9 ) IS=7
  READ(5,*) N,T

```

SORPTION

E VIRIAL

```

WRITE(6,*) N,T
K=S0*EXP(-Q0/R/T)
DO 50 J=1,N
  READ(5,*) XP(J),XC(J)
  XP(J)=XP(J)/760.*101.325*K
50  CONTINUE
  XC(N+1)=FVALC
  XC(N+2)=DVALC
  XP(N+1)=FVALP
  XP(N+2)=DVALP
  CALL LGLIN ( XP(1),XC(1),N ,1,-1,IS , -1 )
  CALL SYMBOL ( .5,15.5 - 0.5*LL ,.25,IS ,0. , -1)
  CALL NUMBER ( 1.0,15.5 - 0.5*LL ,.25,T ,0. ,0 )
  CALL SYMBOL ( 1.5,15.5 - 0.5*LL ,.25,' K',0.,2 )
C  CALL SYMBOL ( 12.5, 0.5 + 0.5*LL ,.25,IS ,0. , -1)
C  CALL NUMBER ( 13.0, 0.5 + 0.5*LL ,.25,T ,0. ,0 )
C  CALL SYMBOL ( 14.0, 0.5 + 0.5*LL ,.25,' K',0.,2 )
1000 CONTINUE
  CALL VR (A1,A2,C,P,NT)
  C(NT+1)=FVALC
  C(NT+2)=DVALC
  P(NT+1)=FVALP
  P(NT+2)=DVALP
  CALL LGLIN ( P(1),C(1), NT ,1, 0,IS , -1 )
  CALL RECT ( 0.0,0.0,16.,16.,0., 3)
2000 CONTINUE
  CALL PLOT(35.0,0.0,999)
  STOP
  END

```

c
c Virial model
C

```

SUBROUTINE VR(A1,A2,C,P,NT)
REAL C(120),P(120)
DATA R /8.314/
COMMON FC,EC,FP,EP
PMP=10**EP*FP
FCV=EC/100.
DO 100 I=1,100
  GOTO 20
10  FCV=FCV+EC/100.*I
20  C(I)=FCV+EC/100.*I
  P(I)=C(I)*EXP(A1*C(I)+A2*C(I)**2)
  IF ( P(I) .LT. FP ) GOTO 10
  IF ( P(I)/PMP .GT. .99 ) RETURN
  NT=I
100 CONTINUE
  RETURN
  END

```

C TYPICAL INPUT DATA

BUTANE ON 5A
2.63E-6, -39533., -0.6139, 0.5204
3.50E-6, -44400., 1.2030, 0.1243
0.0 4.0

0.150 3.00

3

10 498.0000000

64.1999800

0.5918461

125.6999000

0.8606819

235.1999000

1.1761390

356.3999000

1.3618850

460.7998000

1.4791160

572.0998000

1.5705750

645.2998000

1.6447200

776.6997000

1.7730140

882.4992000

1.8164210

960.3991000

1.8336740

9 423.0000000

96.8998800

1.8799780

232.1000000

2.2579890

338.5000000

2.3761400

450.3996000

2.4564920

558.0998000

2.5251890

638.8999000

2.5581220

765.9997000

2.6209010

881.0996000

2.6537160

962.2995000

2.6530790

9 348.0000000

2.9999980

1.2838190

10.9999900

1.7887360

86.2999400

2.8892770

89.1999200

2.8954370

225.4999000

3.1375050

386.0000000

3.2340730

524.4997000

3.2854460

719.6997000

3.3273570

949.2998000

3.3268510

```

C  NAME: PLB
C
C  PURPOSE : TIS PROGRAM COMPUTES THE RESULTS OF THE SCHIRMER
C  ET AL., RUTHVEN ET AL., VACANCY SOLUTION AND IAST MODELS
C  AND PLOTS THE EXPERIMENTAL DATA AND THE THEORETICAL CURVES
C  ON THE CALCOMP PLOTTER.
      DIMENSION NAME(10)
      REAL S1(15),E1(15),M0(2),N0(2),N1(2),R0(2),Q(2),B0(2),NI(2)
      REAL S2(15),E2(15),SL(15,15),EL(15,15),BI(2)
      REAL X(120),Y(120),CA(120),CB(120),CT(120),X1(20),X2(20),Y1(20)
      REAL Y2(20),CA1(20),CA2(20),CB1(20),CB2(20),CT1(20),CT2(20)
      REAL KA,KB,D(2),D1(2),D2(2),SR(2),QR(2),AR(2),BR(2)
      DOUBLE PRECISION A(2)
      DATA D(1),D(2) / -0.1,0.1 /
      DATA D1(1),D1(2) / -0.4,0.1/
      DATA D2(1),D2(2) / -0.3,0.3/
      COMMON P,T,SL,EL
C  INPUT THE ZEOLITE NAME.
C
      READ(5,1) NAME(1),NAME(2),NAME(3)
1  FORMAT(3A4 )
C
C  READ CONSTANTS FOR THE SCHIRMER ET AL. MODEL FOR COMPONENTS 1
C  AND 2 M AND N ARE THE MAXIMUM NUMBER OF MOLECULES A CAVITY
C  HOLD. S AND E ARE THE ENTROPY AND ENERGY CONSTSANTS OF
C  ET AL. MODEL
      READ(5,*) M
      READ(5,*) (S1(I),I=1,M)
      READ(5,*) (E1(I),I=1,M)
      READ(5,*) N
      READ(5,*) (S2(J),J=1,N)
      READ(5,*) (E2(J),J=1,N)
C
C  READ CONSTANTS FOR THE VACANCY SOLUTION MODEL
C  B0 AND Q0 ARE THE PRE-EXPONENTIAL FACTOR AND HEAT OF
C  ADSORPTION IN THE HENRY CONSTANT.
C  CC8, R1 AND M1 ARE AS FOLLOWS
C  SATURATION CONCENTRATION = N0 * EXP( R0/T )
C  ALPHA = M0*(SATURATION CONCENTRATION ) - 1
C
      DO 10 I=1,2
10  READ(5,*) B0(I),Q(I),N0(I),R0(I),M0(I)
C
C  READ CONSTANTS FOR THE RUTHVEN MODEL
C  SR AND QR ARE THE PRE-EXPONENTIAL FACTOR AND HEAT OF
C  ADSORPTION
C  BETA ( MOLECULAR VOLUME )= AR+ BR*T
C  V IS THE VOLUME OF THE ZEOLITE CAVITY
C
      DO 17 I=1,2
17  READ(5,*) SR(I),QR(I),AR(I),BR(I),V
      R=8.31434
      P0=101.325
      T0=273.15

```

```

MM=M+1
NN=N+1
DO 40 II=1,MM
I=II-1
DO 30 JJ=1,NN
J=JJ-1
IF(1./M+1./N .GT. 1.)GOTO 40
L=I+J
IF(J .EQ. 0 .AND. I .EQ. 0)GOTO 28
IF(I .EQ. 0)GOTO 26
IF(J .EQ. 0)GOTO 24
TH=I*1./M + J*1./N
XM=TH*M
CALL YCOMP(M,S1,XM,SL1)
CALL YCOMP(M,E1,XM,EL1)
XN=TH*N
CALL YCOMP(N,S2,XN,SL2)
CALL YCOMP(N,E2,XN,EL2)
SL(I+1,J+1)= I*SL1+J*SL2+R*ALOG(GAMMA(L+1.)/(GAMMA(I+1.)*
& GAMMA(J+1.)))
EL(I+1,J+1)= I*EL1+J*EL2
GOTO 30
24 SL(I+1,J+1)=I*S1(I)
EL(I+1,J+1)=I*E1(I)
GOTO 30
26 SL(I+1,J+1)=J*S2(J)
EL(I+1,J+1)=J*E2(J)
GOTO 30
28 SL(I+1,J+1)=0.
EL(I+1,J+1)=0.
30 CONTINUE
40 CONTINUE
CALL PLOTS( 0, 0 ,1)

```

```

C
C NSET IS THE NUMBER OF SETS TO BE CALCULATED AND PLOTTED
C

```

```

READ(5,*) NSET
DO 1000 K=1,NSET

```

```

C
C T AND P ARE THE TEMPERATURE AND PRESSURE. NP1 AND NP2 ARE THE
NUMBER OF DATA POINTS SATRTING FROM Y=1 (NP1) AND FROM Y=0. (NP2)
C EC IS THE VALUE OF CONCENTRATION AT THE END OF THE
CONCENTRATION AXIS
C

```

```

READ(5,*) T,P,NP1,NP2,EC
DO 33 IP=1,NP1

```

```

C
C READ THE EXPERIMENTAL X, Y, AND CONCENTRATIONS FOR SIDES 1 AND

```

```

C
33 READ(5,*) X1(IP),Y1(IP),CA1(IP),CB1(IP),CT1(IP)
DO 44 IP=1,NP2
44 READ(5,*) X2(IP),Y2(IP),CA2(IP),CB2(IP),CT2(IP)
X1(NP1+1)=0.0
X1(NP1+2)=0.0625
Y1(NP1+1)=0.0

```



```

Y1(NP1+2)=0.0625
CA1(NP1+1)=0.0
CA1(NP1+2)=EC/16.
CB1(NP1+1)=0.0
CB1(NP1+2)=EC/16.
CT1(NP1+1)=0.0
CT1(NP1+2)=EC/16.
X2(NP2+1)=0.0
X2(NP2+2)=0.0625
Y2(NP2+1)=0.0
Y2(NP2+2)=0.0625
CA2(NP2+1)=0.0
CA2(NP2+2)=EC/16.
CB2(NP2+1)=0.0
CB2(NP2+2)=EC/16.
CT2(NP2+1)=0.0
CT2(NP2+2)=EC/16.
IF( K      . EQ. 1) CALL PLOT(2.0,2.0,-3)
IF( K      . EQ. 2) CALL PLOT(-24.99999,25.0,-3)
IF( K      . EQ. 3) CALL PLOT(-24.99999,25.0,-3)
CALL AXIS (0.0,0.0, 'X', -1 ,16.0, 0.,0.0,0.0625)
CALL AXIS (0.0,0.0, 'Y',  1 ,16.0,90.,0.0,0.0625)
CALL RECT  ( 0.0,0.0,16.,16.,0., 3)
CALL PLOT(0.0,0.0,3)
CALL PLOT(16.0,16.0,2)
CALL SYMBOL (11.0 ,1.0 ,.25,NAME(1),0.,12)
CALL SYMBOL ( 7.0,2.0 ,.25,'SCHIRMER',0.,8  )
CALL DASHS (D,0)
CALL PLOT(4.5,2.0,3)
CALL PLOT(6.5,2.0,2)
CALL SYMBOL ( 7.0,1.5 ,.25,'IAS',0.,3  )
CALL DASHS (D,2)
CALL PLOT(4.5,1.5,3)
CALL PLOT(6.5,1.5,2)
CALL SYMBOL ( 7.0,1.0 ,.25,'RUTHVEN',0.,7  )
CALL DASHS (D1,2)
CALL PLOT(4.5,1.0,3)
CALL PLOT(6.5,1.0,2)
CALL SYMBOL ( 7.0,0.5 ,.25,'VACANCY'      ,0.,7  )
CALL DASHS (D2,2)
CALL PLOT(4.5,0.5,3)
CALL PLOT(6.5,0.5,2)
CALL NUMBER ( 11.0,0.5 ,.25,T ,0. ,0 )
CALL SYMBOL ( 12.0,0.5 ,.25,'K AND',0.,5 )
CALL NUMBER ( 13.5,0.5 ,.25,P ,0. ,1 )
CALL SYMBOL ( 15.0,0.5 ,.25,'KPA',0.,3 )
CALL LINE  ( X1(1),Y1(1),NP1 ,1,-1,1  )
CALL LINE  ( X2(1),Y2(1),NP2 ,1,-1,4  )
CALL PLOT(25.0,00.0,-3)
CALL DASHS (D,0)
CALL AXIS (0.0,0.0, 'X', -1 ,16.0, 0.,0.0,0.0625)
CALL AXIS (0.0,0.0, 'C MOLECULES/CAVITY', 18,16.0,90.,
           0.0,EC/16.  )
CALL RECT  ( 0.0,0.0,16.,16.,0., 3)

```

```

CALL SYMBOL (11.0 ,15.0 ,.25,NAME(1),0.,12)
CALL NUMBER ( 11.0,14.5 ,.25,T ,0. ,0 )
CALL SYMBOL ( 12.0,14.5 ,.25,'K AND',0.,5 )
CALL NUMBER ( 13.5,14.5 ,.25,P ,0. ,1 )
CALL SYMBOL ( 15.0,14.5 ,.25,'KPA',0.,3 )
CALL LINE ( X1(1),CA1(1),NP1 ,1,-1,1 )
CALL LINE ( X1(1),CB1(1),NP1 ,1,-1,1 )
CALL LINE ( X1(1),CT1(1),NP1 ,1,-1,1 )
CALL LINE ( X2(1),CA2(1),NP2 ,1,-1,4 )
CALL LINE ( X2(1),CB2(1),NP2 ,1,-1,4 )
CALL LINE ( X2(1),CT2(1),NP2 ,1,-1,4 )
DO 20 I=1,2
  NI(I)=N0(I)*EXP(R0(I)/T)
  BI(I)=B0(I)*EXP(-Q(I)/(R*T))
  A(I)=M0(I)*NI(I)-1.
20 CONTINUE
  KA=SR(1)*EXP(-QR(1)/R/T)
  BA=AR(1)+BR(1)*T
  KB=SR(2)*EXP(-QR(2)/R/T)
  BB=AR(2)+BR(2)*T
  NP=99
  DO 500 KT=1,2
    IF (KT.NE. 1) GOTO 71
    CALL DASHS (D,0)
    CALL SM(M,N,Y,X,CA,CB,CT)
71 IF (KT.NE. 2) GOTO 73
    CALL DASHS (D,2)
    CALL IAS(S1,S2,E1,E2,N,M,X,Y,CA,CB,CT)
73 IF (KT.NE. 3) GOTO 76
    CALL DASHS (D1,2)
    CALL RV(N,M,KA,KB,BA,BB,V,X,Y,CA,CB,CT)
76 IF (KT.NE. 4) GOTO 79
    CALL DASHS (D2,2)
    CALL VSM(NI,BI,A,X,Y,CA,CB,CT)
79 X(NP+1)=0.0
    X(NP+2)=0.0625
    Y(NP+1)=0.0
    Y(NP+2)=0.0625
    CA(NP+1)=0.0
    CA(NP+2)=EC/16.
    CB(NP+1)=0.0
    CB(NP+2)=EC/16.
    CT(NP+1)=0.0
    CT(NP+2)=EC/16.
    CALL PLOT(-24.99999,000.0,-3)
    CALL LINE ( X(1),Y(1) ,NP ,1,0 ,4 )
    CALL PLOT(25.0,00.0,-3)
    CALL LINE ( X(1),CA(1),NP ,1,0 ,4 )
    CALL LINE ( X(1),CB(1),NP ,1,0 ,4 )
    CALL LINE ( X(1),CT(1),NP ,1,0 ,4 )
500 CONTINUE
    CALL DASHS (D,0)
1000 CONTINUE
    CALL PLOT(35.0,0.0,999)

```

STOP
END

CC

```

SUBROUTINE SM(M,N,Y,X,CA,CB,CT)
COMMON P,T,SL,EL
REAL SL(15,15),EL(15,15),X(120),Y(120),CA(120),CB(120),CT(120)
R=8.31434
P0=101.325
T0=273.15
MM=M+1
NN=N+1
DO 200 IP=1,99
Y(IP)=IP/100.
IF( IP .EQ. 1) Y(IP)=0.00001
IF( IP .EQ. 99) Y(IP)=0.99999
SUM1=0.
SUM2=0.
SUM=0.
DO 60 II=1,MM
I=II-1
DO 50 JJ=1,NN
J=JJ-1
IF(1.*I/M+1.*J/N .GT. 1.)GOTO 60
L=I+J
AA=(P*T0/(P0*T))**L* EXP((SL(I+1,J+1)*T
& -EL(I+1,J+1))/(R*T))
AL=AA*Y(IP)**I*(1.-Y(IP))**J
SUM1=SUM1+AL*I
SUM2=SUM2+AL*J
SUM=SUM+AL
50 CONTINUE
60 CONTINUE
CA(IP)=SUM1/SUM
CB(IP)=SUM2/SUM
CT(IP)=CA(IP)+CB(IP)
X(IP)=CA(IP)/CT(IP)
C WRITE(6,*) Y(IP),X(IP),CA(IP),CB(IP),CT(IP)
200 CONTINUE
RETURN
END

```

CCC

```

SUBROUTINE IAS(S1,S2,E1,E2,N,M,X,Y,CA,CB,CT)
REAL S1(15),S2(15),E1(15),E2(15),X(120),Y(120),CA(120),CB(120)
REAL CT(120)
COMMON P,T
P0=101.325
T0=273.15
R=8.31434
YY=0.01
DO 400 IP=1,99
X(IP)=IP/100.
IF( IP .EQ. 1) X(IP)=0.00001
IF( IP .EQ. 99) X(IP)=0.99999
DO 100 L=1,100

```

```

SUM1=0.
DSUM1=0.
DO 10 I=1,M
  AI=(P*T0*YY/(T*P0*X(IP)))*I*EXP(I*(S1(I)*T-E1(I))/(R*T))
  SUM1=SUM1+AI
  DSUM1=DSUM1+AI*I/YY
10 CONTINUE
SUM2=0.
DSUM2=0.
DO 20 J=1,N
  AJ=(P*T0*(1.-YY)/(T*P0*(1.-X(IP))))*J*EXP(J*(S2(J)*T-E2(J))
& /(R*T))
  SUM2=SUM2+AJ
  DSUM2=DSUM2-AJ*J/(1.-YY)
20 CONTINUE
YN=YY-(SUM1-SUM2)/(DSUM1-DSUM2)
IF( ABS(YN-YY) .LT. YY/100.)GOTO 120
YY=YN
100 CONTINUE
WRITE(6,11)
11 FORMAT( 20HIAS DOS NOT CONVERGE )
120 Y(IP)=YN
SUM1=0.
SUM2=0.
DO 220 I=1,M
  AI=(P*T0/(T*P0))*I *EXP(I*(S1(I)*T-E1(I))/(R*T))
  SUM1=SUM1+I*AI
  SUM2=SUM2+AI
220 CONTINUE
CA0=SUM1/(1.+SUM2)
SUM1=0.
SUM2=0.
DO 240 J=1,N
  AJ=(P*T0/(T*P0))*J *EXP(J*(S2(J)*T-E2(J))/(R*T))
  SUM1=SUM1+J*AJ
  SUM2=SUM2+AJ
240 CONTINUE
CB0=SUM1/(1.+SUM2)
CT(IP)=1./(X(IP)/CA0+(1.-X(IP))/CB0)
CA(IP)=X(IP)*CT(IP)
CB(IP)=CT(IP)-CA(IP)
400 CONTINUE
RETURN
END

C
SUBROUTINE YCOMP(NN,Y,XX,YY)
REAL X(15),Y(15),L
DO 5 I=1,NN
5 X(I)=I
YY=0.
DO 100 I=1,NN
L=1.
DO 10 J=1,NN
IF(J.EQ.I)GOTO 10

```

```

      L=L*(XX-X(J))/(X(I)-X(J))
10    CONTINUE
      YY=YY+Y(I)*L
100  CONTINUE
      RETURN
      END
CCC
      SUBROUTINE RV(N,M,KA,KB,BA,BB,V,X,Y,CA,CB,CT)
      REAL KA,KB,X(120),Y(120),CA(120),CB(120),CT(120)
      COMMON P,T
      R=8.31434
      DO 100 IP=1,99
      Y(IP)=IP/100.
      IF( IP .EQ. 1) Y(IP)=0.00001
      IF( IP .EQ. 99) Y(IP)=0.99999
      SUM=0.
      SUM2=0.
      SUM1=0.
      MM=M+1
      NN=N+1
      DO 60 II=1,MM
      I=II-1
      DO 50 JJ=1,NN
      J=JJ-1
      IF(I*BA + J*BB .GT. V )GOTO 50
      IF(I + J .LT. 2 )GOTO 50
      L=I+J
      AL=(KA*Y(IP))**I * (KB*(1.-Y(IP)))**J * (1.-I*BA/V-J*BB/V)**L
      & * P**L/GAMMA(I+1.)/GAMMA(J+1.)
      SUM1=SUM1+AL*I
      SUM2=SUM2+AL*J
      SUM=SUM+AL
50    CONTINUE
60    CONTINUE
      CA(IP)=(KA*Y(IP)*P+SUM1)/(1.+KA*Y(IP)*P+KB*(1.-Y(IP))*P+SUM)
      CB(IP)=(KB*(1.-Y(IP))*P+SUM2)/(1.+KA*Y(IP)*P+KB*(1.-Y(IP))*P+SUM)
      CT(IP)=CA(IP)+CB(IP)
      X(IP)=CA(IP)/CT(IP)
C    WRITE(6,*) IP,Y(IP),X(IP),CA(IP),CB(IP)
100  CONTINUE
      RETURN
      END
CC
      SUBROUTINE VSM(C8,HK,A,X,Y,CA,CB,CT)
      REAL HK(2),C8(2),X(120),Y(120),CA(120),CB(120),CT(120)
      DOUBLE PRECISION U(3),G(3),CTL,CTM,CTR,Z1,Z2,CTT,X1S,X2S,XVS
      DOUBLE PRECISION A(2),A12
      COMMON P,T
      A12=(A(1)+1.)/(A(2)+1.) -1.
      CTL=0.
      CTR=6.
      DO 200 I=1,99
      X(I)=I/100.
      IF( IP .EQ. 1) X(IP)=0.00001

```

IF(IP .EQ. 99) X(IP)=0.99999

212

X1=X(I)

X2=1.-X(I)

CT8=X1*C8(1)+X2*C8(2)

CTL=0.1

CTR=CT8

Z1=X1*C8(1)/CT8/HK(1)*DEXP(A(1))/(1.+A(1))

Z2=X2*C8(2)/CT8/HK(2)*DEXP(A(2))/(1.+A(2))

DO 150 J=1,100

CTM=(CTR+CTL)/2.

DO 80 J1=1,2

IF (J1 .EQ. 1)CTT=CTM

IF (J1 .EQ. 2)CTT=CTL

X1S=CTT*X1/CT8

X2S=CTT*X2/CT8

XVS=1.-CTT/CT8

U(1)=X1S + X2S/(1.+A12) + XVS/(1.+A(1))

U(2)=(1.+A12)*X1S + X2S + XVS/(1.+A(2))

U(3)=(1.+A(1))*X1S + (1.+A(2))*X2S + XVS

DO 50 J2=1,3

G(J2)=DEXP(1.-1./U(J2)) / U(J2)

50

CONTINUE

F =G(1) * Z1 *(G(3)*XVS)**((C8(1)-CT8-CTT)/CTT)

&

+G(2)* Z2 *(G(3)*XVS)**((C8(2)-CT8-CTT)/CTT)

F=F*CTT-P

IF(J1 .EQ. 1)FCTM=F

IF(J1 .EQ. 2)FCTL=F

80

CONTINUE

IF(FCTM*FCTL) 90, 100,110

90

CTR=CTM

GOTO 120

100

CTR=CTM

110

CTL=CTM

120

IF(DABS(CTL-CTR)/CTM .LT. 1.D-11) GOTO 160

150

CONTINUE

WRITE(6,11)

11

FORMAT (20HVSM DOS NOT CONVERGE)

RETURN

160

CT(I)=CTM

CA(I)=CTM*X1

CB(I)=CTM*X2

Y(I)=G(1)*Z1*(C8(1)-CT8-CTM) * DLOG(G(3)*XVS)/P

Y(I)=G(1)*Z1*CTM* (G(3)*XVS)**((C8(1)-CT8-CTM)/CTM)/P

C WRITE(6,*) Y(I),X(I),CA(I),CB(I),CT(I)

200 CONTINUE

RETURN

END

C TYPICAL INPUT DATA

5A ZEOLITE

6

-58.25, -64.39, -68.81, -75.60, -84.32, -93.21

-35400., -35400., -35400., -35400., -35400., -35400.

5

-63.48, -72.25, -80.28, -92.57, -130.00

-44400., -44400., -44400., -44400., -44400.

5.260E-6, -35400., 3.410, 145.40, 0.00274

3.500E-6, -44400., 3.374, 000.00, 1.154
 5.260E-6, -35400., 136.30, 0.00000, 776.
 3.500E-6, -44400., 129.00, 0.10060, 776.
 1

498., 66.7, 6, 6, 4.5

1.0000000	1.0000000	0.8947500	0.0000000	0.
0.8255203	0.9544593	0.7982341	0.1687126	0.
0.4552233	0.7692520	0.5196613	0.6218913	1.
0.3546033	0.6770908	0.4351440	0.7919852	1.
0.2489824	0.5611470	0.3205258	0.9668190	1.
0.1883579	0.4814525	0.2508512	1.0809270	1.
0.0000000	0.0000000	0.0000000	1.6147650	1.
0.0538318	0.1649207	0.0841675	1.4793590	1.
0.1079025	0.2985708	0.1626775	1.3449570	1.
0.1342038	0.3539268	0.1967875	1.2695460	1.
0.1948814	0.4836155	0.2736902	1.1307020	1.
0.2629542	0.5752342	0.3528062	0.9888962	1.

APPENDIX E

COR EQUATION OF STATE

The Chain-of-Rotators equation of state (COR) is derived based on perturbation theory of fluid state. Only three substance-specific parameters are required to be known for a fluid to be described by this equation. The equation is

$$\frac{pV}{nRT} = 1 + \frac{4\left(\frac{\bar{v}}{\tau}\right)^2 - 2\left(\frac{\bar{v}}{\tau}\right)}{\left(\frac{\bar{v}}{\tau} - 1\right)^3} + \frac{c}{2}(\alpha - 1) \frac{3\left(\frac{\bar{v}}{\tau}\right)^2 + 3\alpha\left(\frac{\bar{v}}{\tau}\right) - (\alpha + 1)}{\left(\frac{\bar{v}}{\tau} - 1\right)^3} + \left[1 + \frac{c}{2}\left(B_0 + B_1/\bar{T} + B_2\bar{T}\right)\right] \sum_{n,m} \frac{mA_{nm}}{\bar{T}^n \bar{v}^m}$$

where \bar{v} is the reduced volume defined as V/V_0 . V_0 is the closest packed volume and $\tau = \pi\sqrt{2}/6 = 0.7405$.

$$\alpha = 1.078.$$

B_i and $A_{n,m}$ are universal constants

The three fluid parameters are the characteristic temperature T^* , the rotational degrees of freedom c and the closest packed volume V_0 . The values of B_i and $A_{n,m}$ and the three parameters for propane and n-butane are included in subroutine PVT.

This equation is applied to mixtures with the use of Van der Waals one fluid mixing rules. For hydrocarbon + hydrocarbon mixtures the interaction parameter found from experimental is correlated with the core volumes as follows

$$Z = |V_{\alpha} - V_{\beta}| / (V_{\alpha} + V_{\beta})$$

$$k_f = 0.01008 - 0.03429Z + 0.3849Z^2 + 0.2823Z^3$$

APPENDIX F

METHODS OF CALCULATIONS

This appendix gives the methods for performing the calculations for the models used in this study.

Schirmer Model

Pure component isotherm

Eq 2.19 gives the pure component isotherm derived by Schirmer et. al.

$$C = \frac{\sum_{i=1}^m \left(\frac{P/P_0}{T/T_0} \right)^i \exp\left(i \frac{TS_i - E_i}{RT}\right)}{\sum_{i=0}^m \left(\frac{P/P_0}{T/T_0} \right)^i \exp\left(i \frac{TS_i - E_i}{RT}\right)}$$

In this equation P_0 , the reference pressure is taken to be 101.325 kPa and T_0 , the reference temperature is taken to be 273.15 K. The maximum number of molecules that can get in a cavity is found by dividing the volume of one cavity by the volume of one molecule as found from liquid density. This value, m is found to be approximately equal to six for propane on both 5A and 13X zeolites. The values of S_i and E_i are given in Table 4.4 . R is the universal gas constants.

Binary isotherm

Eq 2.20 gives the binary isotherm of Schirmer et. al. model.

$$C_A = \frac{\sum_{i=1}^m \sum_{j=0}^n \left(\frac{P_A/P_0}{T/T_0} \right)^i \left(\frac{P_B/P_0}{T/T_0} \right)^j \exp \left[l \frac{S_l T - E_l}{RT} \right]}{\sum_{i=0}^m \sum_{j=0}^n \left(\frac{P_A/P_0}{T/T_0} \right)^i \left(\frac{P_B/P_0}{T/T_0} \right)^j \exp \left[l \frac{S_l T - E_l}{RT} \right]}$$

$$E_C = \frac{1}{2} [i E_{A2} + j S_{B2} + \Delta E^E]$$

$$S_L = \frac{1}{L} [i S_{AL} + j S_{BL} + R \ln \frac{L!}{i! j!} + \Delta S^E]$$

The value of n (for n -butane) is found to be approximately five. The values of S_L and E_L are calculated from the pure components constants. For a cavity holding three propane molecules ($i=3$) and two n -butane molecules ($j=2$) the value of S_{AL} is the S -value of A at a coverage A molecules equivalent to 3 molecules of A and 2 molecules of B that is

$$\text{Equivalent molecules of } A = 6 \left(\frac{3}{6} + \frac{2}{5} \right) = 5.4 \text{ molecules of } A$$

$$\text{Equivalent molecules of } B = 5 \left(\frac{3}{6} + \frac{2}{5} \right) = 4.5 \text{ molecules of } B$$

These values are used to interpolate for the values of S_{AL} , E_{AL} , S_{BL} and E_{BL} . For example, if a linear interpolation is used then the value of S_{BL} will be in the middle between 84.01 (for four molecules) and 118.19 (for five molecules) or $S_{BL} = 101.1$

The values of P_A and P_B are found from the total pressure and the gas phase composition, y_a . For a total pressure of 106.7 kPa and $y_A = 0.2$ then

$$P_A = 106.7 \times 0.2 = 21.34 \text{ kPa}$$

$$P_B = 106.7 \times 0.8 = 85.36 \text{ kPa}$$

The value of c_A is obtained by substituting these values in Eq 2.20. The value of c_B is obtained by replacing the factor i by j and starting i from zero and j from one in the numerator of Eq 2.20. The composition of the adsorbed phase, x is found from

$$x = c_A / (c_A + c_B)$$

Ruthven Model

pure component isotherm

Eq 2.16 gives the pure component Ruthven isotherm.

$$C = \frac{K_P + \sum_{i=2}^m \frac{(K_P)^i}{(i-1)!} (1 - i\beta/V)^i}{1 + K_P + \sum_{i=2}^m \frac{(K_P)^i}{i!} (1 - i\beta/V)^i}$$

The value of Henry constant is evaluated at a given temperature from the constants in Table 4.5. For propane on 5A at $T = 423$ K Eq 4.4 gives

$$K = 5.09 \times 10^{-6} \exp(35957/(8.314 \times 423)) = 0.1403 \text{ molecules/cavity/kPa}$$

v is the volume of one cavity and m is the same as in Schirmer model.

The molecular volume, β is calculated from Eq 4.5

$$\beta = 0.1362 + 0.000 \times 423 = 0.1362 \text{ nm}^3$$

These values are substituted in Eq 2.16 to find the value of c .

Binary Isotherm

The binary form of Ruthven model is given in Eq 2.17

$$C_A = \frac{K_A P_A + \sum \sum \frac{(K_A P_A)^i (K_B P_B)^j}{(i-1)! j!} (1 - \frac{i\beta_A}{V} - \frac{j\beta_B}{V})^{i+j}}{1 + K_A P_A + K_B P_B + \sum \sum \frac{(K_A P_A)^i (K_B P_B)^j}{i! j!} (1 - \frac{i\beta_A}{V} - \frac{j\beta_B}{V})^{i+j}}$$

$$i + j \geq 2$$

$$\text{and } i\beta_A + j\beta_B \leq V$$

The parameters used here are the same for the pure component isotherm and P_A and P_B are the same as in the Schirmer model.

Vacancy Solution Theory

Pure Component Isotherm

The pure component isotherm is given in Eq 2.38

$$P = \frac{c^*}{K} \frac{\theta}{1-\theta} \exp \left[\frac{\alpha_{1v}^2 \theta}{1+\alpha_{1v} \theta} \right]$$

The values of α_{1v} , K and c^* are given in Table 4.6. This equation is implicit in c . Therefore, if the pressure and the temperature are given and it is desired to find c then a numerical solution of Eq 2.38 is required. If c and T are known then the pressure is found by direct substitution in Eq 2.38. $\theta = c/c^*$

Binary Isotherm

The mixture isotherm is given in Eq 2.40.

$$y_i P = \gamma_i^s x_i \frac{c_m}{c_m^*} \frac{c_i^*}{K_i} \frac{\exp \alpha_{iv}}{1 + \alpha_{iv}} \exp \left[\left(\frac{c_i^*}{c_m} - 1 \right) \ln \gamma_v^s x_v^s \right]$$

The calculations proceed as follows

1. Select the composition of the adsorbed phase, X_i .
2. Use Eq 2.34 to calculate c_m^* .
3. Calculate the mole fractions based on the vacancy solution, X_i^s from Eq 2.31
4. Use Eq 2.39 to calculate the activity coefficients. There exists one activity coefficient for each component including the vacancy.
5. Eq 2.40 is summed over the components to eliminate y_i . This results in one equation with one unknown which is c_m . Solve numerically for c_m .
6. Now the value of c_m is known, and hence the value of y_i is calculated from Eq 2.40 (for component i).

Virial model

There exists only a pure component isotherm for this model as given in Eq 4.3. The Henry constant is calculated from K_0 and q_0 as describe earlier and the values of A_1 and A_2 are given in Table 4.7. Direct substitution in Eq 4.3 will give the value of P knowing c . If T and P are given then the solution for c has to be done numerically.

$$P = c/K \exp(A_1 c + A_2 c^2 + A_3 c^3 + \dots)$$

IAST

This model does not provide a pure component isotherm. Therefore, to predict the binary behavior a pure component equation has to be substituted in Eq 2.29. In this work the Schirmer et al. model was used. The result of the integration is

$$\sum_{i=1}^m \left(\frac{P_A/P_O}{T/T_O} \right)^i \exp\left(i \frac{TS_i - E_i}{RT}\right) = \sum_{j=1}^n \left(\frac{P_B/P_O}{T/T_O} \right)^j \exp\left(j \frac{TS_j - E_j}{RT}\right)$$

This equation gives a relation between P , T , x_i and y_i . If three of them are specified then the fourth one can be calculated by solving the equation numerically.